EVALUATION OF SOME PLANT EXTRACTS AS CORROSION IN HIBITORS FOR Al – 7.0 % Si – 0.35 % Mg ALLOY IN 3.5 % NaCl AQUEOUS SOLUTION

BY

SANI MOHAMMED ADAMS

DEPARTMENT OF METALLURGICAL AND MATERIALS ENGINEERING,
AHMADU BELLO UNIVERSITY,
ZARIA, NIGERIA

FEBRUARY, 2017

EVALUATION OF SOME PLANT EXTRACTS AS CORROSION IN HIBITORS FOR Al – 7.0 % Si – 0.35 % Mg ALLOY IN 3.5 % NaCl AQUEOUS SOLUTION

BY

Sani Mohammed ADAMS B. ENG. (ABU) 1995, M.Sc. (ABU) 2012
Ph.D. / Eng /40570 /2012-2013

A THESIS SUBMITTED TO THE SCHOOL OF POSTGRADUATE STUDIES, AHMADU BELLO UNIVERSITY, ZARIA

IN PARTIAL FULFILLMENT OF THE REQUIREMENTS FOR THE AWARD OF DOCTOR OF PHILOSOPHY DEGREE IN METALLURGICAL AND MATERIALS ENGINEERING

DEPARTMENT OF METALLURGICAL AND MATERIALS ENGINEERING,
FACULTY OF ENGINEERING,
AHMADU BELLO UNIVERSITY,
ZARIA, NIGERIA

FEBRUARY, 2017

Declaration

I declare that the work in this thesis "Evaluation of some plant extracts as corrosion inhibitors for Al- 7.0 % Si – 0.35 % Mg Alloy in 3.5 wt % NaCl Aqueous Solution" has been conducted by me in the Department of Metallurgical and Materials Engineering under the supervision of Prof. S. A. Yaro, Dr. M. Abdulwahab and Prof. E. E. Oguzie. The information derived from the literature has been duly acknowledged in the text and a list of references provided. No part of this thesis was previously presented for another degree or diploma at this or any other institution.

Sani Mohammed ADAMS	_____	_____
Name of Student	Signature	Date

Certification

This thesis entitled "EVALUATION OF SOME PLANT EXTRACTS AS CORROSION INHIBITORS FOR Al – 7.0 % Si – 0.35 % Mg ALLOY IN 3.5 wt % NaCl AQUEOUS SOLUTION" by Sani Mohammed ADAMS meets the regulations governing the award of the degree of DOCTOR OF PHILOSOPHY of Ahmadu Bello University, and is approved for its contribution to knowledge and literary presentation.

Prof. S. A Yaro	_____	_____
Chairman, Supervisory Committee	Signature	Date
Dr. M. Abdulwahab	_____	_____
Member, Supervisory Committee	Signature	Date
Prof. E. E Oguzie	_____	_____
Member, Supervisory Committee	Signature	Date
Dr. A. Kasim	_____	_____
Head of Department	Signature	Date
Prof. S. Z. Abubakar	_____	_____
Dean, School of Postgraduate Studies	Signature	Date

Dedication

This thesis is dedicated to my entire family and friends for their patients during my course of study. It is also dedicated to my late lovely wife, Rasheedat Abdullahi. May Allah have mercy on her and blessed her with paradise.

Acknowledgement

My greatest thanks go to Almighty Allah who gave me the wisdom, strength and health in the course of this program. O Allah, my tongue cannot glorify you to meet the standard of glorification. Glory, Mighty, Power over all things are yours in this world and hereafter. Thank you.

I wish to express my profound appreciation to my supervisors Prof. S.A. Yaro, Dr. M. Abdulwahab , and Prof. E. E. Oguzie. Special thanks go to the Head of the Department, Dr. A. Kasim. I also thank Dr. Umar Shehu of Metallurgical and Materials Engineering Department and Prof. Idris Sulaiman of Chemistry Department for their useful advice and contributions during the course of study. May the Almighty Allah bless them all in their undertakings. I also thank the entire staff of the Department for their cooperation during my stay in the School.

I am indebted to Dr. A. Abubakar and Mallam Kabiru Ibrahim of the Department of Pharmacognosy and Drug Development, and Brother Abdulkareem Ismail of University Medical Centre, Ahmadu Bello University, Zaria. I recognize the assistance of Dr. Femi Awe of the Federal University, Dutsin-ma. My special gratitude goes to the Tertiary Educational Trust Fund (TETFUND), Kogi State Polytechnic, Lokoja for providing financial support for this work. I also thank Dr. Moses Shaibu, Dean of Academic Planning Unit of the Polytechnic, Engineer Yakubu Habib Muhammed, Dean of School of Engineering, Itakpe Campus. Finally, to my wives, children, relatives, friends, Mentors' club members, Ansarul Islam Society of Nigeria, Okene branch and other well-wishers too many to mention..

Abstract

In this study, the effects of methanolic leave extracts of *Combretum micrantum (CM), Combretum Glutinosum (CG), Ficus exasperate (FE) and Ficus platyphylla (FP)* on the corrosion of A356.0 type Al-Si-Mg alloy in 3.5 % NaCl aqueous solution were determined. It evaluated the inhibition efficiency of each of the inhibitors and determined their mechanism of inhibition. It also characterized the microstructures of the corroded surfaces. All these were done with a view to determining the inhibitive potentials of all the inhibitors with regards to the corrosivity of A356.0 Al-Si-Mg alloy in marine environment. Weight loss and electrochemical techniques were used for corrosion study of the alloy. Thin Layer Chromatography (TLC), Fourier Transform-Infrared Spectroscopy (FT-IR), Gas Chromatography-Mass Spectroscopy (GC-MS) were used to characterize the plant extracts in order to identify the chemical bonding and functional groups. Some physicochemical properties such as viscosity, solubility, density, pH value and Biodegradability tests of the plant extracts were also determined. The weight loss method of corrosion tests were carried out at 1, 2, 3, 4, and 5 hours of exposure time using various concentration of extracts (0.2, 0.4, 0.6, 0.8 and 1.0) v/v at different temperatures 30 ^{O}C, 50 ^{O}C, and 70 ^{O}C in a static solution. The effect of co-inhibition was also studied, and the surface morphology of the coupons before and after corrosion tests was characterized by Optical Microscope (OPM) and Scanning Electron Microscopy (SEM) techniques. A statistical design for the corrosion process was carried out to determine which parameters (Inhibitor concentration, exposure time and temperature) are statistically significant using ANOVA and F-test distribution at 95% confidence level.The phytochemical screening (Qualitative and Quantitative) and thin layer chromatography results revealed the presence of tannins, saponins, flavonoids and alkaloids in the plant extracts. The results of FT-IR and GC-MS analyses detected all organic species. Each peak area in the chromatogram was proportional to the amount of the organic compound(s) forming the peak. The plant extracts displayed high level of solubility in different solvents, low

densities and less viscous at the studied temperatures. From the result, the corrosion rates decreases with increase in inhibitor concentration for all the inhibitor types. The maximum inhibitor efficiency of the inhibitors are 94.44 % at 0.8 v/v for CM, 81.25 % at 0.4 v/v for CG, 84.62 % at 0.4 v/v for FE, 94.74 % at 1.0 v/v for FP and 94.64 % at 1.0 v/v for the Sodium chromate (control). The co-inhibitor shows that the best combination occurred at 1.0 v/v of CG and FE with 95.13 % IE and that of surfactant was at 1.0 v/v FE and TEA with 84.20 % IE. The potentiodynamic polarization results revealed a change in the anodic and cathodic regions for the corroded samples indicating a mixed type inhibitors. The percentage inhibition efficiency (IE%) of the linear polarization resistance (LPR) for the various plant extracts are 90.11 % CM, 91.01 % CG, 92.69 % FE, 91.34 % FP and 96.19 % Na_2CrO_4 with inhibitor concentration of 0.8, 1.0, 0.4, 0.8 and 1.0 v/v respectively. The kinetic and thermodynamic studies showed that activation energy (E_a) in the presence of inhibitor is greater than in the absence of inhibitor at all the temperatures studied. The mechanism of physical adsorption was proposed for the extracts as inhibitors with the temperature range investigated since the E_a and ΔG_{ads} values are lesser than 80 kJ/mol.and -20 kJ/mol, respectively. The surface morphology of some of the samples indicated that the alloy in the presence of the inhibitors had smooth surfaces compared to the alloy that has no inhibitor. The results of the ANOVA show that inhibitor concentration is the significant corrosion parameter.

List of Abbreviations, Notations and Symbols

ANOVA	Analysis of Variance
β_a	Anodic Tafel Slope (V)
β_c	Cathodic Tafel Slope (V)
CG	*Combretum glutinosum*
CM	*Combretum micranthum*
CR	Corrosion Rate
e^-	Electron
E_a	Activation Energy
E_{corr}	Corrosion Potential (V)
FE	*Ficus exasperata*
FP	*Ficus platyphylla*
FT-IR	Fourier Transform Infrared Spectroscopy
F	Faraday Constant (96500 coulomb)
V/V	Volume/Volume
GC-MS	Gas Chromatography Mass Spectroscopy
ΔG_{ads}	Free Energy Change adsorbed
ΔG	Free Energy Change
ΔH_{ads}	Enthalpy Change adsorbed
h	Planck Constant (6.6261×10^{-34} J/Sec)
I	Current density (A/cm^2)
I_{corr}	Corrosion Current density (A/cm^2)
IC	Inhibitor Concentration
IE	Inhibition Efficiency
mm/yr	Millimeter Per Year
N_A	Avogadro's Number (6.022×10^{23} mol.)

R	Universal Gas Constant (J/mol)
R_p	Polarization Resistance (Ωcm^2)
Sr	Strontium
ΔS_{ads}	Entropy Change adsorbed
SEM	Scanning Electron Microscope
TLC	Thin Layer Chromatography
T	Temperature
ϴ	Degree of Surface Coverage
-1	Low level
+1	High level

Table of Contents

List of Figures

List of Tables

List of Plates

List of Appendices

Appendix

CHAPTER ONE

1.0 INTRODUCTION

Aluminium and its alloys are widely used as engineering materials in the automotive, aviation and aerospace industries, in the making of household appliances, in ship building and military hardware (Lebe *et al.*,2011). They provide excellent physical and mechanical properties such as high strength-to-weight ratio, recyclability, castability, good machining properties, as well as outstanding resistance to corrosion.

Corrosion of materials is known to lower performance efficiency and lead to reduced service life. In severe cases it could serve as a precursor to catastrophic failures with attendant great losses (Alaneme, 2011). The corrosion resistance of aluminium and some of its alloys is attributable to the formation of a stable protective thin film of aluminium oxide when exposed to the atmosphere The protective oxide films are characterized to be amphoteric and easily dissolved in strong acidic and alkaline media leading to corrosion attack (Oguzie *et al.,* 2007).

Aluminium alloys consisting of Al-Si have being used in wide range of engineering application. They are characterized by a wide temperature range in the semi-solid region. Magnesium, when added to Al-Si, is the main solid solution strengthener to aluminium alloys and responsible to precipitation hardening to yield higher strength (Abdulwahab *et al.,* 2011). When exposed to the atmosphereand other aggressive media, the thin film that protects this alloy gives way. Additionally, the alloy is also susceptible to pitting and intergranular corrosion in seawater.

Over the years, various methods have been used for corrosion prevention. A lot of efforts have been put in developing strategies of mitigating corrosion through materials selection, changes in design philosophies and the adoption of varied prevention techniques. The use of

inhibitors has been well documented as an effective method of protecting metallic materials from corrosion in aqueous environments (Tosun and Ergun, 2006; Benali*et al*., 2012; Awe *et al*., 2015 and Asuke *et al.*, 2015).

Corrosion inhibitors are chemical substances which, when added to a corrosive system in optimum concentration, decreases the corrosion rate. The chemical substance modify electrochemical reactions by their action from the solution side of the metal/solution interface; and the increase in corrosion resistance can be measured by various parameters (Eddy, 2009). To be effective, an inhibitor must be able to interact with anodic and cathodic reaction sites to respectively retard the oxidation and reduction corrosion reactions, and prevent transportation of water and active corrosion species on the metal surface (Maqsood *et al.*, 2011).

Synthetic inorganic compounds used as inhibitors for corrosion prevention and control have been reported to have an excellent performance. However, their toxic effects do not only affect living organisms but also poison the environment, hence the need for green/eco-friendly corrosion inhibitors (Al-Sehaibani, 2000). Therefore, effort towards identifying potential eco-friendly and less expensive inhibitors remains the subject of focus in current research efforts of corrosion science and engineering. Over the years, several inhibitors have been synthesized or chosen from different compounds and it has been found that the best inhibitors are those that have centre for π electron donation usually enhanced by the presence of hetero atoms in aromatic compound (Eddy, 2008).

Natural products of plant origin containing different organic compounds (e.g alkaloids, tannins, saponins, steroids, terpenoids, flavonoids, phenols, oxalates, glycosides, pigments, organic, and amino acids) are known to have inhibitive action (Ebenso and Ekpe, 1994).They are generally eco-friendly, cheap, and easily available and have heteroatoms in

their aromatic or long carbon chain (Abiola *et al.,* 2007).Research by Obot *et al.* (2009) reported successful uses of extrude gum extract from natural plants as corrosion inhibitors of aluminium in alkaline media.

Avwiri and Igho (2003) reported that organic compounds having heteroatom O, N and S are found to have basicity and electron density thus assist in corrosion inhibitor. O, N and S are the active centers for the adsorption on the metal surface. When an H atom attached to the C in the hydrocarbon ring is replaced by a substituent group ($-NH_2$, $-NO_2$, -CHO, or COOH) it improves inhibition. The electron density in the metal at the point of attachment changes thereby resulting in the retardation of the anodic and cathodic reactions. Electrons are consumed at the cathode and furnished at the anode, thus, corrosion is retarded (Amitha and Bharathi, 2011).

Several authors have used different extracts of leaves, stems, roots, fruits, flowers, and seeds as inhibitors for aluminium and its alloys in different media (Babatunde *et al.,* 2012; Wan *et al.,* 2012; Ihebrodike *et al.,* 2010; Ajanaku *et al.,* 2012; Rajkiran *et al.,* 2010; Rajendran *et al.,* 2009; and Benali *et al.,* 2012).Due to economic importance of aluminium and its alloys, its protection against corrosion has attracted much attention (Yingchao *et al*., 2011; Zhenhua *et al*., 2011).

1.1 Research Problem

i. The Corrosion of Al-Si-Mg alloy in aggressive environments such as seawater does occur. The use of inhibitors is an option of protecting the alloys against corrosion.

ii. Inorganic inhibitors such as chromates are highly toxic; some of them have been reported to be carcinogenic. In view of these observations, there exists the need for development of eco-friendly, cheap and readily available/renewable corrosion inhibitors.

iii. Corrosion of materials occurs frequently and corresponding lives, materials and money have being loss. Therefore, there is the need to reduce losses caused by corrosion attack in order to save these losses.

1.2 Justification of the Study

The significance of the work is to explore the potential of developing environmentally/eco-friendly inhibitors that will serve as substitute for chromates, dichromates, nitrates, benzoates and hydrazine which are highly toxic and sometimes carcinogenic. Plant extracts are products of naturally occurring substance, they are cheap and can be readily produced and are available in our environment. This will add-up to the list of available eco-friendly inhibitors for aluminium alloys.

1.3 Aim and Objectives

The aim of the research is to determine the potential of using *Combretum micranthum, Combretum glutinosum, Ficus exasperata and Ficus platyphylla* as corrosion inhibitors for Al–Si–Mg alloy in 3.5 % NaCl solution (artificial seawater). The Specific objectives of the research are to:

i. Characterized the methanolic leave extracts if *Combretum micranthum, Combretum glutinosum, Ficus exasperate and Ficus platyphylla;*

ii. Determine the effects of the extracts in (i) on the corrosion of A356.0-type Al-Si-Mg alloy in 3.5 % NaCl solution;

iii. Determine the inhibition and co-inhibition efficiencies and mechanisms of inhibition by the in inhibitors; and

iv. Characterized the microstructures of all the corroded and uncorroded surfaces.

1.4 Contribution to Knowledge

The study established the following:

i. The plant extracts have been characterized through phytochemical screening, TLC, FT-IR, GC-MS and physic-chemical tests and were found to be good inhibitors for Al-Si-Mg alloy in 3.5 % NaCl aqueous solution. Hence, leave extracts of CM, CG, FE and FP can be used as corrosion inhibitors for the alloy haven obtained maximum inhibition efficiencies of 94.44 %, 81.25 %, 84.62 % and 94.74 % were obtained for CM, CG, FE and FP.

ii. That the mechanism of inhibition by the plant extracts on Al-Si-Mg alloy is of physical adsorption and the use of surfactants with the aim of improving the performance of the plant extract did not yield any favourable result.

iii. The plant extracts reduced the corrosion rates of the alloy with 0.0028, 0.0084, 0.0056 and 0.0028 mm/yr as the least corrosion rates for CM, CG, FE and FP as against 0.0504, 0.0448, 0.0392 and 0.0532 obtained from the control.

iv. The extracts will reduce the rates of usage of inorganic inhibitors and also reduce pollution.

CHAPTER TWO

2.0 LITERATURE REVIEW

2.1 Aluminium and Aluminium Alloys

Aluminum and its alloys are used in many engineering applications because of their combination of lightness with strength, high corrosion resistance, thermal and electrical conductivity, light reflectivity, and non-toxic qualities. The variety of forms in which they are available also enhances their utility (Shreir *et. al.*, 2000).

2.1.1 Cast aluminium

Sand casting, permanent mold casting, and die-casting are commonly casting techniques used for aluminum alloys. As a rule, heat treatable alloys are either sand or permanent mold cast. The following combinations of elements constitute the main families of cast aluminum alloys (Roberge, 1999). Casting compositions are described by a three-digit system followed by a decimal value. The decimal .0 in all cases refer to casting alloy limits. Decimals .1 and .2 concern ingot compositions. Table 2.1 shows the main families of cast Al alloys and their basic properties while Table 2.2 presents the classification of Al alloy base on their casting composition.

2.1.2 Al-Si alloys

Commercial cast Al-Si alloys are polyphase materials which composed of microstructure belonging to the Aluminium Association Classification series 3xx.x for aluminium – silicon plus copper and/or magnesium alloys and 4xx.x aluminium – silicon alloys. The use of this alloy as a structural material is determined by the physical properties (primarily influenced by the chemical composition of the alloy) and its mechanical properties (influenced by chemical composition and microstructure). The characteristic property of Al-Si alloys is relatively high tensile strength in relation to density when compared with that of other cast alloys, such as

Table 2.1: Main families of cast Al alloys and their basic properties

Alloy	Description
Pure Al	Rarely used in the cast condition. But special castings may be required for electrical applications.
Al-Si	Silicon is the principal element for conferring good castability on aluminium alloys.
Al-Si-Mg	Good casting alloys, which can be solution treated and age hardened to give good mechanical properties.
Al-Mg	Best combination of strength and toughness of all the aluminum casting alloys.
Al-Cu	Moderately high strength, medium or poor impact resistance, and fast casting properties; poorest corrosion resistance of aluminum alloys and age hardenable.
Al-Mn	A cheap, non-heat-treatable alloy of poor mechanical properties, fair castibility, but exceptional for non-load-bearing applications at temperatures of up to 500^0C (for instance, gas burners of domestics cookers).

Table 2.2: Classification of Al alloy base on their casting composition

Alloy group	Alloying elements
1xx.x	Controlled unalloyed (pure) composition especially for rotor manufacture.
2xx.x	Alloys in which copper is the principal alloying element.
3xx.x	Alloys in which silicon is the principal alloying element, but other alloying elements such as copper and magnesium are specified.
4xx.x	Alloys in which silicon is the principal alloying element.
5xx.x	Alloys in which magnesium is the principal alloying element.
6xx.x	Alloys in which silicon and magnesium are the principal alloying element.
7xx.x	Alloys in which zinc is the principal alloying element, but other alloying elements such as copper and magnesium may be specified
8xx.x	Alloys in which tin is the principal alloying element
9xx.x	Unused

ductile cast iron or cast steel. The high specific tensile strength of Al-Si alloys is strongly influenced by the composition ofpolyphase microstructure. The silicon content in standardized commercial cast Al-Si alloys is in the range of 5 to 23 wt. %. The structure of the alloys can be hypoeutectic, hypereutectic, or eutectic, as shown on Al-Si equilibrium phase diagram in Figure 2.1. Al–Si based cast alloys having a maximum solubility of silicon in aluminium at 1.65 wt.% and 577^{o}C are reported to have eutectic composition at 12.7 % Si. The hypoeutectic alloy has Silicon < 12.7% while the hypereutectic alloy has Silicon content > 12.7 % (Shi *et al*., 2013).

Al–Si alloys are important casting alloys because of high fluidity (large volume of Al–Si eutectic), high resistance to corrosion, good weldability and low co-efficient of thermal expansion. The properties of Al-Si alloys depend on the amount of Si present. The eutectic composition is best for casting. However, the higher the Si content the better the mechanical properties. Cooling and solidification of Al–Si alloy produces a very coarse microstructure in which the eutectic consists of large plates, or needles of Si in a continuous Al matrix. Al–Si–Mg, Al–Si–Cu and Al–Si–Cu–Mg are some of the important Al–Si alloys system (Srinivasa and Devaki, 2014). The properties of a specific alloy can be attributed to the individual physical properties of its main phase components (α - aluminium solid solution and silicon crystals) and to the volume fraction and morphology of these components.

2.1.3 Al–Si–Mg alloy and its applications

The 3xx.x alloy series is one of the most widely used because of the flexibility provided by the high silicon content and its contribution to fluidity plus response to heat treatment, which provides a variety of high-strength options. In addition, the 3xx.x series may be cast by a variety of techniques ranging from relatively simple sand or die casting to very

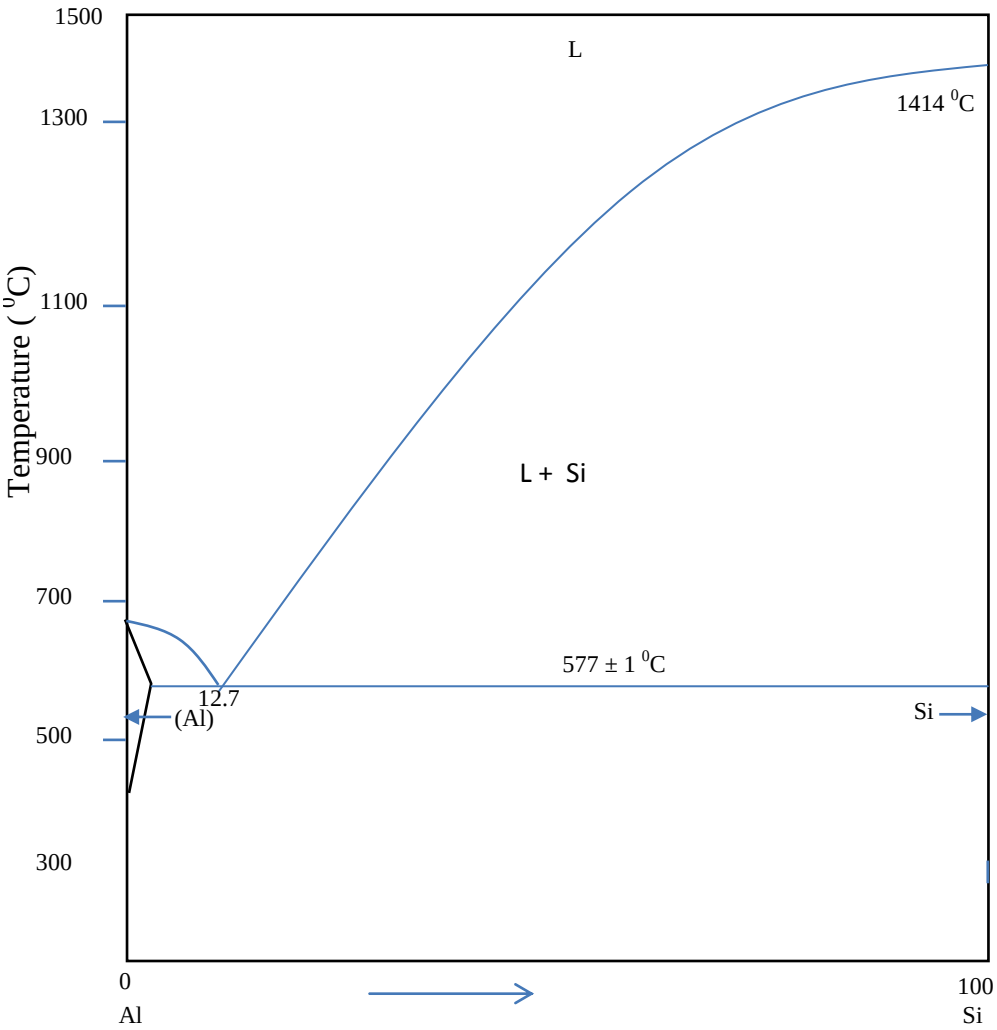

Figure 2.1: The Al – Si – binary phase diagram (ASM, 2004a)

intricate permanent moldinvestment castings, and the newer thixocasting and squeeze casting technologies (Dietrich, 1998).

A356.0 type Al-Si-Mg alloy is categorized as cast aluminium alloy. This alloy can be sand cast, chill cast; can as well be modified. The major alloying elements in A356.0 alloy is silicon while Mg or Cu are added as minors. Silicon imparts good castability, high wear resistance and hardness. Small addition of Mg improves solution treatment, increase coefficient of thermal expansion and electrical resistivity, strength, ductility and corrosion resistance. Introduction of copper increase strength, hardness, fatigue, creep resistance and machinability (Sarada *et al.*, 2013).

Alloy A356 is currently the workhorse of Al structural casting and the most popular alloy used in squeeze casting and semi-solid metal processing. The 356/A356 family of alloys are also used for a variety of commercial castings, electrical hardware, marine hardware, pumps bodies and many other components. The transportation industry, and in particular the automotive industry is working to seek light materials in the development of robust parts. Al – Si alloys have the potential to be used in internal combustion engines, plain bearing, compressor and refrigerator. It was concluded that Al–Si–Mg alloy with 3.67 % Si and 4.9 % Mg have the best wear resistance due to the precipitates of Al_4Si phase (Abdel-Jaber*et al*., 2010). The application of the alloy includes its use in radiator, fuel storage tank, and structural ship bodies, cooling system and body panels (Shi *at al.*, 2013). Figure 2.2 is the ternary phase diagram of Al-Si-Mg alloy.

2.1.4 Modification of Al-Si-Mg alloy

Modification is a process of changing shape of the second phase elements by enhancing its growth and the property of the alloy to bring about change in its shape. The percentage of these modified elements is very small but the effect is remarkable.

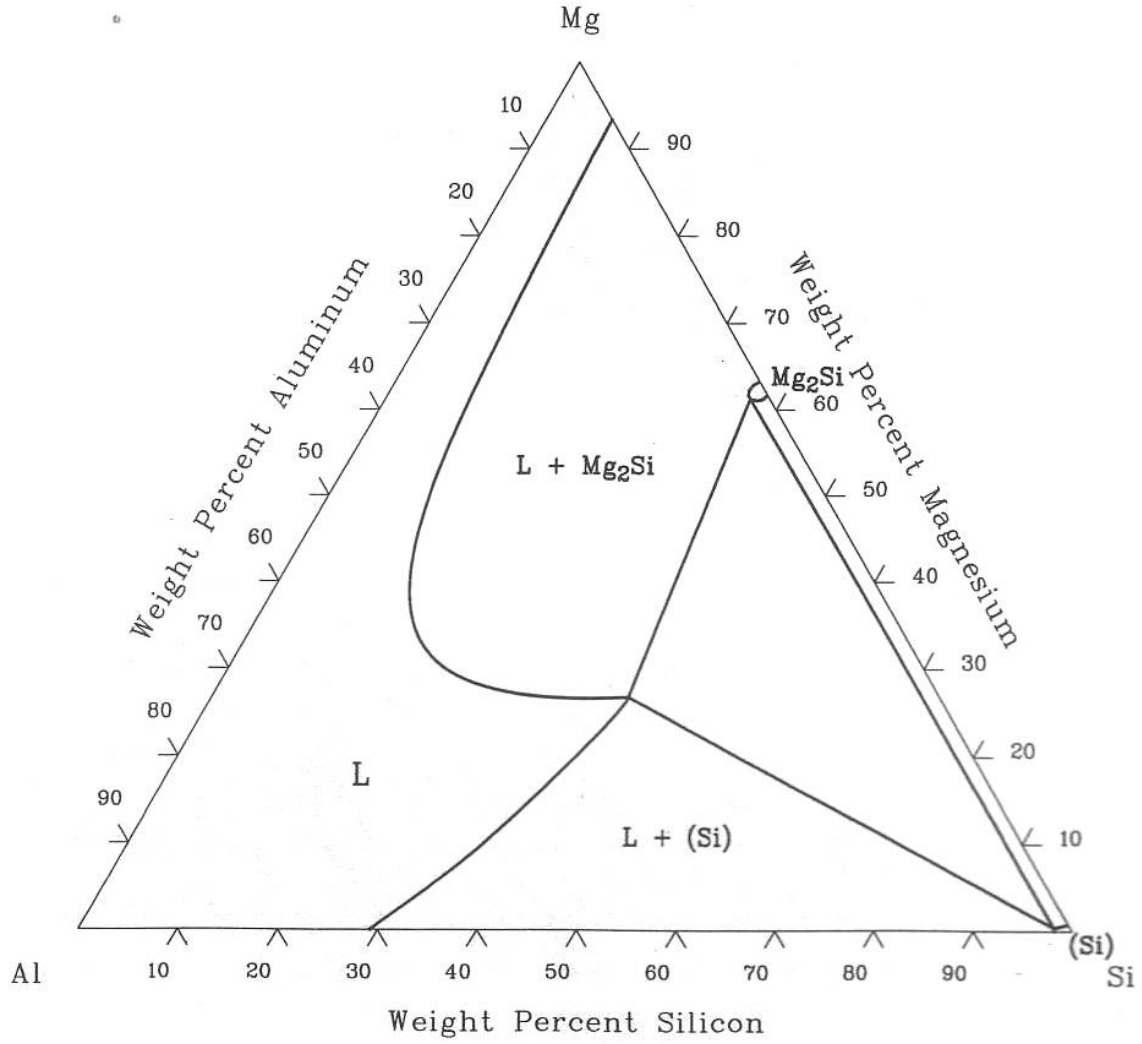

Fig. 2.2: Ternary Phase Diagram of Al-Si-Mg (ASM, 2004b)

Modification is carried out extensively in Al-Si alloys. Modification is one of the important melt treatments as it improves the mechanical properties by changing the microstructure of the material. Unmodified alloys contain silicon in the form of brittle flakes which leads to poor ductility of the material. The commonly used modifiers are strontium, sodium, calcium and antimony (Sarada e*t al.,* 2013).

These modifiers replace the coarse acicular Si crystals with a finer, more fibrous microstructure. The fundamental mechanism of modification is to increase, by orders of magnitude, the number of crystallographic twins formed on the Si crystal during solidification. The increased twinning of the Si enables the fibres to bend and split to produce a substantially finer microstructure than in the unmodified alloy. The amount of Sr level of the alloy, for example 0.01 %, 0.02 % by weight, is sufficient to modify alloy A356 which contains 7 % Si, while 0.04 % is needed for eutectic alloy which contains 12 % Si. The microstructural refinement of the modified alloy has been shown to produce higher ultimate tensile strength, ductility, impact strength, improved thermal shock properties and increase hot tearing resistance when compared to unmodified alloy. Sodium is a better modifier than strontium, but it can add hydrogen to the melt and tends to fade more quickly than strontium as its level in the melt decreases with time because of oxidation (John and Bernard, 1990).

Other ways of modifying Al-Si alloy structure include high cooling rate, mechanical modification which include high intensity shear, mechanical or electromagnetic stirring and ultrasonic vibration. Ultrasonic melt treatment helps to refine Al-Si alloy by the introduction of accoustic waves with a frequency greater than 17 kHz into the liquid metal. This results in cavitation of the melt and intense mixing through agitation (Zhang *at el.,* 2012).

2.2 Corrosion

With non-metallic materials, the term corrosion invariably refers to the deterioration from chemical causes, but a similar concept is not necessarily applicable to metals. Metallic corrosion embraces all interactions of a metal or alloy (solid or liquid) with its environment, irrespective of whether this is deliberate and beneficial or adventitious and deleterious. This definition of corrosion is for conveniences referred to as the transformation definition (Winston and Uhlig, 2008).

On the other hand, corrosion has been defined as the undesirable deterioration of a metal or alloy as a result of interaction of the metal with its environment that adversely affects those properties of the metal that are to be preserved. This definition will be referred to as the deterioration. It is also applicable to non-metallic materials such as glass, concrete.

Fontana and Staehle have stated that corrosion include the reaction of metals, glasses, ionic solids, polymeric solids and composites with environments that embrace liquid metals, gases, non-aqueous electrolytes and other non-aqueous solutions.

Vermilyea defined corrosion as a process in which atoms or molecules are removed one at at time, considers that evaporation of a metal into vacuum should come within the scope of the term, since atomically it is similar to other corrosion processes.

Evans considers that corrosion may be defined as that branch of chemical thermodynamics or kinetics, as the outcome of electron affinities of metals and non-metals, as short-circiuted electro-chemical cells, or as the demolition of the crystal structure of a metal. These considerations lead to the conclusion that there is probably a need for two definitions of corrosion, which depend upon the approach adopted:

1. Definition of corrosion in the contest of corrosion science: the reaction of a solid with its environment

2. Definition of corrosion in the context of Engineering: the reaction of an engineering constructional metal (materials) with its environment with a consequent deterioration in properties of the metal (materials).

2.2.1 Corrosion in aqueous solutions

Aqueous environment will range from thin condensed films of moisture to bulk solutions, and will include natural environments such as the atmosphere, natural waters, soils, body fluids, chemicals food products (Shreir *et al,* 2000). All corrosion reactions in aqueous solutions are characterized by the following features.

a. The electrified interface between the metal and the electrolyte solution (the metal surface may be film- free or partially or completely covered with films or corrosion products).
b. Transfer of positive charge from the metal to the solution with consequent oxidation of the metal to a higher valency state.
c. Transfer of positive charge from the solution to the metal with consequent reduction of a species in solution (an electron acceptor) to a lower state.
d. Transfer of charge through the solution and corroding metal.

It follows that corrosion is an electrochemical reaction in which the metal itself is a reactant and oxidized (loss of electrons) to a higher valency state, whilst another reactant, an electron acceptor, in solution is reduced (gain of electrons) to a lower valency state. This may be regarded as a concise expression of the electrochemical mechanism of corrosion (Winston and Uhlig, 2008)

2.2.2 Common methods of corrosion prevention

In most industrial processes, it is virtually impossible to prevent corrosion. The general strategy is to use measures that reduce the corrosion rate to an economically

sustainable level. The most important corrosion mitigation procedure involves selection of materials and design against corrosion, cathodic protection, anodic protection, protective coatings, change of environment and chemical inhibitors (Sastri, 1998; Danny, 2004)

i. Selection of materials and design against corrosion

Materials for a particular working environment (composition, temperature, velocity) are selected taking into account mechanical and physical properties, availability, method of fabrication and overall cost of component or structure. Geometrical configurations that facilitate corrosive conditions should be avoided which includes:

a. Features that trap dust, air and water
b. Designs with inaccessible areas that cannot be re-protected, e.g., by maintenance painting
c. Designs that lead to heterogeneity, in the metal or in the environment

Also, metal-metal or metal-nonmetallic contacting materials that facilitate corrosion such as bimetallic couples, a metal in contact with absorbent materials that maintain constantly wet conditions and contact with substances that give off corrosive vapours, should be avoided (Sastri, 1998; 2011).

ii. Protective coatings

Basically, a protective coating should provide a complete barrier and exclude the corrosive environment from having contact with the metal which it is design to protect. This can be achieved by the following techniques (Sastri, 1998; 2011):

a. Using inorganic coatings, e.g., vitreous enamel, glasses, ceramics
b. Application of organic coatings, e.g., paints, plastics, greases
c. Generating metallic coatings that form protective barriers (Ni, Cr) or protect the substrate by sacrificial action (Zn, Al, Cd on steel).

iii. Cathodic protection

Cathodic protection is achieved by lowering the potential of the metal being protected by connecting the metal to a corrosion cell were the protected metal forms the cathode and another anodic reaction (the oxidation) instead takes place away from the metal. two principal means are used to achieved such a corrosion cell; sacrificial anode and impressed current. Sacrificial anode utilizes a less noble metal electrically connected to the metal being protected to form a corrosion cell were the sacrificial anode corrodes preferentially thus protecting the cathode from corrosion. Impressed- current method instead uses an external power source to produce a corrosion cell were the metal being protected is connected as cathode (Sastri, 1998; 2011).

iv. Anodic protection

Anodic protection is achieved by raising the potential of the metal being protected. The higher potential alters the corrosion product formed to create a protective surface keeping the metal in a passive region where the corrosion current is reduced.

v. Chemical inhibition

Chemical corrosion inhibitors generally prevent corrosion by forming or promoting the formation of an adsorption layer on the metal surface thus separating the metal surface and the electrolyte containing water. The inhibitor can function either by limiting the anodic reaction (anodic inhibitor), the cathodic reaction (cathodic inhibitor) or both (mixed inhibitor) (Umoren *et* al., 2009; Eddy *etal*., 2010; Akalezi *etal*., 2012).

2.2.3 Classification of inhibitors

Inhibitors may be classified as shown in Figure 2.3. There are two major classes of inhibitors: inorganic and organic. The anodic type of inorganic inhibitors includes chromates, nitrites, molybdates and phosphates, while the cathodic type includes zinc and poly phosphate inhibitors. The film forming class is the major class of organic inhibitor as it includes amines,

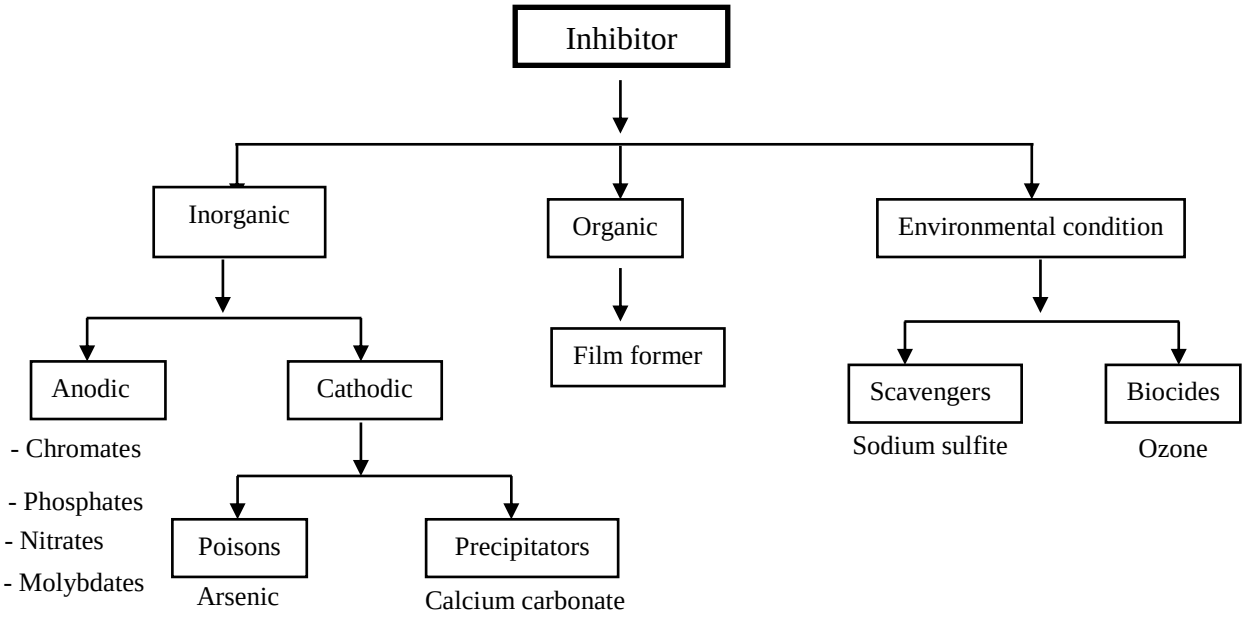

Figure 2.3 Classifications of inhibitors (Sastri, 2011)

amine salts, and imidazolines – sodium benzoate mercaptans, esters, amines and ammonia derivatives (Zaki, 2006)

Inhibitors are classified on the basis of their functions. For instance, chromates and nitrates are called passivating inhibitors because of their tendency to passivate the metal surface. Some inhibitors, such as silicates, inhibit both the anodic and cathodic reactions. Some types classified as near-neutral pH solutions are "safe" or "dangerous" inhibitors. The inhibitor must be present at an optimum concentration in order to be effective (Sastri, 2011).

It can also be classified as organic or inorganic depending on their constituent and their redox characteristics. However, according to Kelly *et al*; 2003, one of the most widely applied classification system for inhibitors based on three different forms are:

a. Adsorption inhibitors: These are inhibitors which are adsorbed on the metal surface and form protective barrier films. Adsorption inhibitors function by limiting the diffusion of oxygen to the corrosion surface, trapping the metal ion on the surface, stabilizing the double layer and reducing the rate of dissolution.
b. Passivation inhibitors: passivating inhibitors function by inducing and maintaining a passive film (consisting of metal oxide) on the surface.
c. Surface reaction product inhibitors: these are inhibitors that form sparingly soluble compounds other than an oxide layer. Surface reaction product inhibitors cannot form a protective oxide layer because they are not oxidizing agents but interact with metal on the surface to form insoluble compounds which plug in pores and inhibit corrosion.
d. Interphase inhibitors

   Interphase inhibitors function by facilitating the formation of a 3-D layer which acts as a barrier between the corroding substrate and the electrolyte. The protective film could be a solid film on the surface of the metal or a liquid film adjacent to it. The solid film may be an oxide layer, corrosion product, metallic or non-metallic

coating or inhibitor forming a porous layer or non-porous film (Mercer, 1990; Monika *et al.,* 2005). However, the liquid film is the electrolyte in the interphase which differs from the bulk of solution in its chemical or physical properties. Based on this model, the inhibition of metal corrosion is governed by properties of the layer such as its porosity and stabiliy.

e. Passivating or oxidizing inhibitors.

Pourbaix (1981) stated that iron polarizes anodically in the presence of oxidizing inhibitors and passivates as the open circuit potential shifts to more positive potential. It is also possible that the inhibitors are reduced and the reduction product is deposited on the weak points of the films to improve its protective effect. An oxidizing inhibitors function by inducing and maintaining a passive surface layer on the metal surface. These inhibitors are effective at certain concentrations (Critical concentration). At concentrations below the critical concentration, corrosion is enhanced but at very high concentrations of the inhibitor, increase in the anodic current density is observed.

f. Non-oxidizing inhibitors

Non-oxidizing inhibitors are also capable of passivating metals electrochemically, they include compounds such as NaOH and the salts of weak acids and strong bases such as Na_3PO_4, Na_2HPO_4, Na_2CO_3, $NaBO_3$, and $Na_2B_4O_7$ (Tarvassoli-Salardini, 2004):

g. Interface inhibitors

Interface inhibition occurs due to a strong interaction between the corroding metal and inhibitor. The adsorption of the inhibitor depends on the potential of the electrode as well as the charge on the adsorbate molecule. The protective film is a 2-D adsorbate, which can affect the corrosion reaction by one of the following mechanisms (Tarvassoli-Salardini, 2004)

a. Geometric blocking: In this case, an inert inhibitor blocks the surface of the metal at a high degree of coverage and forms a diffusion barrier which restricts the access of

reactants to the metal surface for example, inhibitors provided by proteins, polysaccharides or compounds with hydrocarbon chains.

b. Deactivation coverage: In this process, instead of the complete coverage of the metallic surface, only the active sites are covered by an inert adsorbate and the rates of the reactions (cathodic and anodic) are reduced in proportion to the extent of coverage of the reactive sites.

c. Reactive coverage: In this case, the adsorbate undergoes electrochemical reaction and primary or secondary inhibition occurs either by the adsorbate or its reaction product respectively.

Adsorption inhibition is observed when a bare metal is in contact with the adsorbate (inhibitor) and this is usually the case in acidic solutions where the condition is not favourable to oxide formation (Mansfeld, 1987). According to Tarvassolo-Salardini (2004), majority of the very effective interface inhibitors are organic compounds containing nitrogen, sulphur and oxygen. It has been found that some interface inhibitors after initial adsorption onto the metal surface, can be reduced and the reduction product may also posses some inhibitive properties.

2.2.4 Electrochemical aspect of corrosion

For metallic materials, the corrosion process is usually electro-chemical, that is, a chemical reaction in which there is transfer of electrons from one chemical species to another. Though the exact mechanisms governing corrosion of aluminium alloys in aqueous solution are not completely understood, it is thought that the corrosion of most aluminum alloys proceed through the following reactions (Kasim, 2013).

(A) Neutral/alkaline/basic medium

(i) At anode (oxidation)

$$Al \longrightarrow Al^{3+} + 3e \quad (2.1)$$

(ii) Atcathode (Reduction)

$$O_2 + 2H_2O + 4e^- \longrightarrow 4OH^- \quad (2.2)$$

(iii) Over all reaction

$$4Al + 3O_2 + 6H_2O \longrightarrow 4\,Al^{3+} + 12OH^- \quad (2.3)$$

(B) Acidic medium

(i) At anode (oxidation)

$$Al \longrightarrow Al^{3+} 3e \quad (2.4)$$

(ii) At cathode (Reduction)

$$2H^+ + 2e^- \longrightarrow H_2 \uparrow \quad (2.5)$$

(iii) Over all reaction

$$2Al + 6H^+ \longrightarrow 2Al^{3+} + 3H_2 \quad (2.6)$$

A general mechanism for the dissolution of aluminium metal in the presence of aqueous chloride solution has earlier been reported (Kasim, 2013).

$$Al(s) + H_2O \longrightarrow AlOH_{ads} + H^+ + e^- \quad (2.7)$$

$$AlOH_{ads} + 5H_2O + H^+ \longrightarrow Al^{3+} + 6H_2O + 2e^- \quad (2.8)$$

$$Al^{3+} + H_2O \longrightarrow [AlOH]^{2+} + H^+ \quad (2.9)$$

$$[AlOH]^{2+} + X\ [AlOHX]^+ \quad (2.10)$$

The controlling step in the metal dissolution is the complexation reaction between the hydrated cation and the anion (equation 2.10). In the presence of chloride ions, the reaction correspond to

$$[AlOH]^{2+} + Cl^-[AlOHCl]^+ \quad (2.11)$$

The soluble complex ion formed increases the metal dissolution rate which depends on the chloride concentration.

2.2.5. Pourbaix (Potential – pH) Diagram

i. Principle and purpose

Pourbaix (or potential–pH) diagrams, named after the inventor – Marcel Pourbaix, are graphical representations of thermodynamic information appropriate to electrochemical reactions. The presentation of information in this format facilitates its application to practical problems such as corrosion, electro deposition, geological processes, and hydrometallurgical extraction processes. A particular diagram for this purpose is usually called the pourbaix diagram for the iron-water system or thepourbaix diagram for the aluminium- water system (David and James, 1998). The diagram shows the relative stabilities of solid phases and soluble ions that are produced by reaction between a metal and an aqueous environment as functions of two parameters, the electrode potential, E, and the pH of the environment.The information needed to construct a pourbaixdiagram is the standard electrode potentials, E^{θ}, or the equilibrium constants, K, as appropriate, for all of the possible reactions considered.

ii. Pourbaix diagram of aluminium

The pourbaix diagram of aluminium indicates that hydrargilite, $A1_2O_3$. $3H_2O$ is the stable phase between about pH 4 and 9 (Winston, 2007). Indeed, this film is considered to be responsible for the successful use of aluminum in many structural applications. This diagram also predicts the amphoteric nature of aluminium corroding in highly acidic and alkaline conditions and its protection by an oxide film between about pH 4 and 9. As shown in Figure 2.4, line(a) in the diagram is the hydrogen line below which water is no longer stable and decomposes into hydrogen and OH^-(alkalization). Line (b) is the oxygen line above which water decomposes into hydrogen, oxygen and H^+(acidification). Between regions (a) and (b),

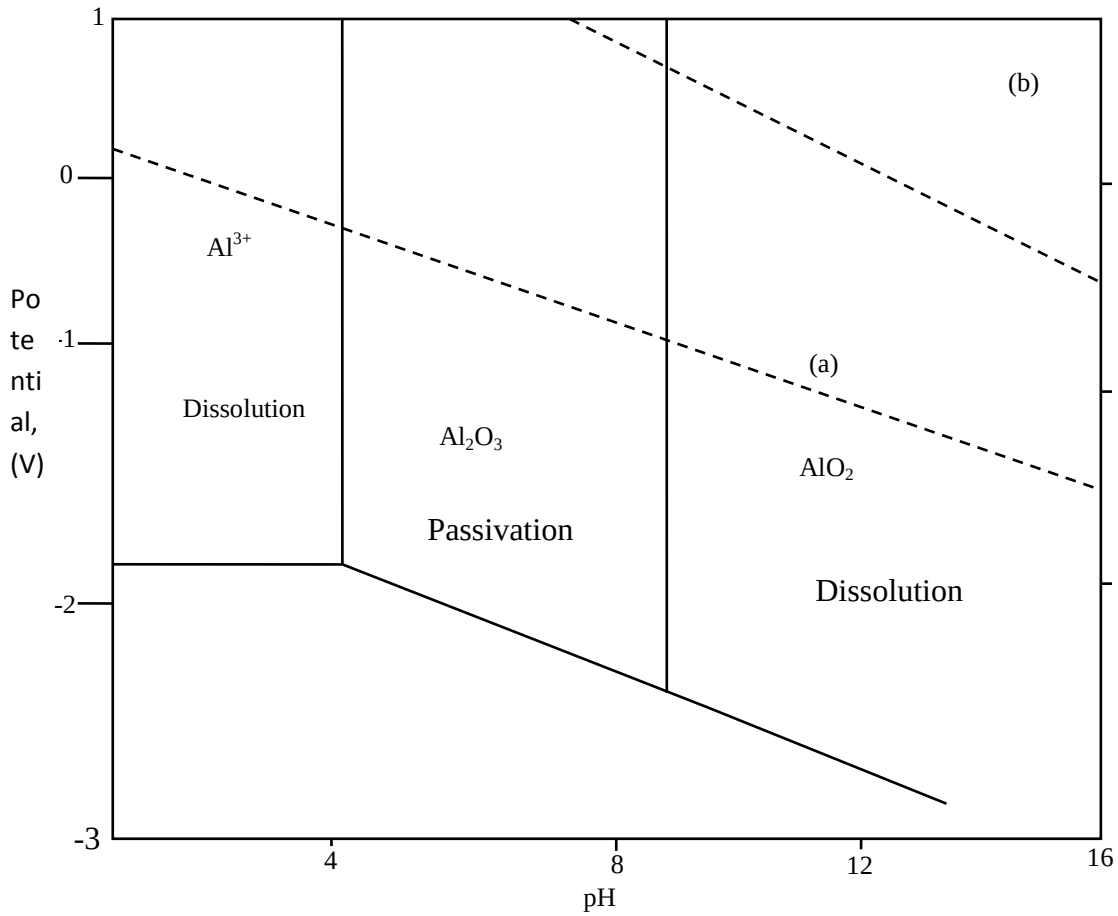

Figure 2.4: Pourbaix diagram for the Al- H_2O system at 25^oC (Winston, 2007)

water is stable. In acidic media, Al dissolves as Al^{3+}, in neutral solutions (4 – 8 pH), the hydroxide is insoluble which makes Al surface passive.

The pourbaix diagram for Al identifies the various region where the species Al (solid), Al_2O_3 (solid), Al^{3+} ions, and AlO_2^- ions are each stable. When the stable species is a dissolved ion, the region on the pourbaix is labelled as a region of "corrosion". When it is either solid oxide or hydroxide, the region is labeled "passivity", in which the metal is protected by a surface film of an oxide or a hydroxide. When the stable species is the unreacted metal species itself, the region is labeled as a region of "immunity" (Mc Cafferty, 2010).

2.2.6. Kinetics of Corrosion

Pourbaix diagram is a very useful thermodynamic tool for understanding the corrosion behavior of different systems. It gives information on spontaneity of reaction(s), but it does not give information about the rates of corrosion processes. The study of kinetic of corrosion processes gives us information about, the rates at which such reactions take place. This, in turn, will furnish us with crucial information pertaining to the life time of the material.

The rate of any transformation is controlled by the magnitude of one or more energy barriers that every particulate entity e.g., an atom or an ion must surmount to transform in to. These peaks are the energy maxima of intermediate transition states through which the entity must pass in transforming and the energy that must be acquired is the activation energy, ΔG. An expression for reaction rate that applies to many reactions over moderate temperature ranges is Arrhenius' equation (David and James, 1998).

$$r = K \exp - \Delta G^* / RT \qquad (2.12)$$

where r is the reaction rate, ΔG^* is the standard Gibb's free energy , R is the universal gas constant, T is the absolute temperature and K is a constant.

To apply the equation to an electrode process, it must be restated in electrical terms. Ions transported across an electrode carry electric charge, so that the reaction rate, r in the above equation (2.12), can be replaced by an electric current, i.

The energy of the process is the product of the charge and the potential drop, E, through which it is carried. Thermodynamic quantities are expressed per mole of substance and because the charge on a mole of singly charged ions is the faraday, F = 96490 coulombs, the free energy change, ΔG of an electrode process is (David and James, 1998):

$$\Delta G = - zFE \qquad (2.13)$$

where z is the charge on a particular ion species transferred in the process, e.g z is 1 for H^+ or Cl^-, 2 for $Fe^{2+,}$ 3 for Fe^{3+} or Al^{3+} etc.

Substituting equation (2.13) in to equation (2.12) in the Arrhenius equation, equation (2.12) become as thus

$$r = K \exp \frac{-\Delta G^*}{RT} = K \exp. \frac{zFE}{RT} \qquad (2.14)$$

2.3 Corrosion Inhibitors

Over the years, considerable efforts have been deployed to find suitable corrosion inhibitors of organic origin in various corrosive media (Amitha and Bharthi, 2011). In acid media, nitrogen – based materials and their derivatives, sulphur – containing compounds, aldehydes, thioaldehydes, acetylenic compounds and various alkaloids, for example, papaverine, strychnine, quinine, and nicotine are used as inhibitors. In neutral media, benzoate, nitrite, chromate, and phosphate act as good inhibitors. Generally, inhibitors

decrease or prevent the corrosion reaction, in essence; they are negative catalysts. They reduce the corrosion rate by one or combination of the following:

i. Adsorption of ions/molecules onto metal surfaces.
ii. Increasing or decreasing the anodic and/or cathodic reaction.
iii. Decreasing the diffusion rate of ions to the surface of the metal.
iv. Decreasing the electrical resistance of the metal surface (Amitha and Bharthi, 2011).

Several factors such as cost, quantity, availability and most importantly, safety of the environment are among the factors to be considered when choosing an inhibitor.

2.3.1 Organic inhibitors

Organic inhibitors generally known to have heteroatoms, O, N, and S are found to have higher basicity and electron density and thus act as corrosion inhibitors. O, N, and S are the active centers for the process of adsorption onto the metal surface. The order of sequence in the performance of compounds having these heteroatoms is as follows $O < N < S < P$ (Amitha and Bharthi, 2011).

The crucial property of the plant extracts is because they contains phytochemical compounds such as alkaloids, tannins, flavonoids, saponins, amino acids, phenolic acids, pigments, resins, triterpenoids, with molecular electronic structures close to conventional corrosion inhibitors (Awe *et al.,* 2015). Organic inhibitors are used in the oil industry to control oil and gas well corrosion. Most common types are long chain (C_{18}) hydrogen and nitrogen containing compounds, they are neither anodic nor catholic, but can inhibit both the anodic and catholic sites to varying degrees depending on the type of inhibition (Zaki, 2006).

The polar nitrogen groups attached to a hydrocarbon chain donate electrons to the metal surface and form a strong chemiadsorbtive bond. The strength of protection is dependent on this bond. The hydrocarbon portion of the inhibitor is oil soluble and it is water repellent. The large hydrocarbon chain orientates towards the solution and forms a hydrophobic network (repels water from the metal surface). The water molecules are desorbed and replaced by organic molecules through the following reaction:

[organic (solution) + NH_2O (adsorbed) $\rightarrow$ organic (adsorbed.) + nH_2O (solution)] (2.15)

Water molecules, which are the main source of corrosion, are thus eliminated. Figure 2.5 present a simplified mechanism of this process.

2.3.2 Performance of an organic inhibitor

The performance of an organic inhibitor is related to the chemical structure and physicochemical properties of the compound like functional groups, electron density at the donor atom, p-orbital character, and the electronic structure of the molecule. Inhibition could be due to:

(i) adsorption of the molecules or its ions on anodic and/or cathodic sites.

(ii) increase in cathodic and/or anodic over voltage, and

(iii) the formation of a protective barrier film (Amitha and Bharthi, 2011).

Some of the factors that contribute to the action of inhibitors are chain length, size of the molecule and bonding, and aromatic/conjugate, strength of bonding to the substrate, cross-linking ability, and solubility in the environment.

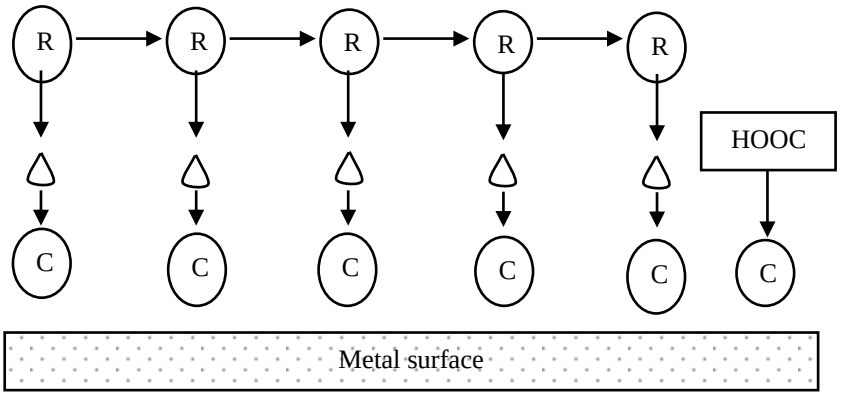

R – Non-polar group

CH_2 HOOC – polar group

– Oil droplets

C – Chemisorbed layer

Figure 2.5:Mechanism of corrosion inhibition by poly phosphates (Zaki, 2006)

2.3.3 Adsorption

The two types of adsorption of an organic inhibitor on a metal surface are physical or electrostatic and chemisorption. Adsorption of organic compounds depends upon the charge and the nature of the metal surface, electronic characteristics of the metal surface, ionic species, temperature of the corrosion reaction and the electrochemical potential at the metal – solution interface. The adsorption process oforganic substances involves two types of possible interaction with the metal surface. The first one is weak undirected interaction due to the electrostatic attraction between inhibiting organic ions ordipole and the electrically charged surface of the metal. This interaction is termed physicaladsorption. The second type of interaction occurs when there is interaction between the adsorbate and absorbent. This type of interaction involves charge sharing or charge transfer from adsorbate to the atoms of the metal surface in order to form a coordinate type of bond and the interaction is termed chemical adsorption (Stephen *et al.,* 2014).The various types of adsorption isotherms along with the verification plots are given below (Sastri, 2011).

2.3.4 Physical adsorption (physisorption)

It is due to electrostatic attraction between inhibiting ions or dipoles and the electrically charged metal surface. The forces involved in electrostatic (physical) adsorption are generally weak. Inhibitor adsorbed onto the metal due to electrostatic force can be desorbed easily. The main feature of electrostatic adsorption is that the adsorbed ions are not in direct physical contact with the metal. A layer of solvent molecules separates the metal from the ions. The physical adsorption process has low activation energy and is relatively independent of temperature (Sastri, 2011).

2.3.5 Chemical adsorption (chemisorption)

This is the most important type of interaction between the metal surface and an inhibitor molecule. Here, the adsorbed inhibitor is in direct contact with the metal surface. Chemisorption process is slower than electrostatic sorption and requires higher activation energy. Unlike electrostatic adsorption, chemisorption is specific for certain metals and is not completely reversible (Sastri, 2011).

2.3.6 Adsorption isotherms

The adsorption of inhibitors on the metal surface is governed by the residual change on the metal and the chemical structure of the inhibitor. Adsorption isotherms are often used to demonstrate the performance of organic adsorbent-type-inhibitors, and the surface coverage rates determined by capacitance measurements give a good correlation with the adsorption isotherm plot. The absorption characteristics of inhibitors can be predicted by fitting the dependence of surface coverage (θ), on inhibitor concentration into adsorption models (Babatunde *et al.,* 2012).The adsorption isotherms provide important clues regarding the nature of the metal- inhibitor interaction. Inhibitor molecules adsorb on the metal surface if the interaction between molecules and metal surface is higher than that of the water molecule and the surface (Ating *et al*., 2010).

2.3.7 Langmuir adsorption isotherm

The Langmuir model, developed to account for monolayer coverage on uniform surfaces, can be expressed in the form given in equation (2.16).

$$\frac{c}{\theta} = \frac{1}{K} + c \qquad (2.16)$$

where c is the inhibitor concentration and K is the adsorption equilibrium constant representing the degree of adsorption and θ is the degree of surface coverage (Obot *et al*.,

2011).The Langmuir adsorption isotherm results if the adsorbent is energetically homogeneous (all adsorption sites are equivalent) so that the heat of adsorption of the inhibitor is independent of coverage.

2.3.8 Temkin adsorption isotherm

The Temkin adsorption isotherm model is given as

$$\exp^{(2a\theta)} = KC \tag{2.17}$$

$$K_{ads}C = \frac{\exp(a\Theta) - 1}{1 - \exp^{\Theta - 1}} \tag{2.18}$$

where *a* is the attraction constant. The constant of adsorption equilibrium, K is found from the free energy of adsorption.

$$K_{ads} = \exp.\left(\frac{-\Delta\sigma}{RT}\right) \tag{2.19}$$

Where σ is the interfacial tension and R is the gas constant which can be calculated from the degree of surface coverage. A plot of θ against Log C gives a linear plot (Eddy and Ebenso, 2010; Adejo *et al.*, 2012).

2.3.9 Frumkin Adsorption Isotherm

This model is represented by the expression:

$$\text{Log}\left(\frac{\theta}{1-\theta}\right) = 2.303 \text{ Log K} + 2\alpha\Theta \tag{2.20}$$

where K = adsorption equilibrium constant, α = the lateral interaction term describing the molecular interaction in the adsorbed layer. α is a parameter which indicates the attractive behavior of the surface of the metal (Eddy and Odiongenyi, 2010).

The adsorptional equilibrium constant $K_{ads}$is related to the free energy of adsorption, ΔG_{ads} according to equation

$$K = \frac{1}{55.5EXP^{(\frac{-\Delta G}{RT})}} \quad (2.21)$$

where R = gas constant, T = absolute temperature, 55.5 = Concentration of water in solution. Generally, ΔG_{ads} values with magnitude much < 40 kJ/Mol. have typically been correlated with the electrostatic interactions between organic molecules and charged metal surface (Physiosorption), whilst those of magnitude in the order of 40 kJ/Mol. and above are associated with charge sharing or transfer from the organic molecules to the metal surface, i.e chemisorption (Eddy and Ita, 2010). Apart from the aforementioned adsorption isotherms, there exist other isotherms such as Freundlich, El-Awady, Flory-Huggins, Dhar-Flory Huggins, Hill de boer, Parsons and Bockris- Swinkels' isotherms. All these isotherms follow a general expression as given by equation (2.22)

$$f(\Theta, X) \exp(-2\alpha\Theta) = KC \quad (2.22)$$

where (f (Θ, X) is a configuration factor which depends upon the physical model and assumption underlying the derivation of the isotherm, Θ is the surface coverage, C is the inhibitor concentration, X is the size ratio, α is the molecular interaction parameter and K is the equilibrium constant of adsorption process which is temperature dependent and is related to the free energy of adsorption by equation (2.23)

$$\Delta G_{ads} = -2.303RT \text{ Log } (55.5K) \quad (2.23)$$

where $K = [\Theta / (1-\Theta) C]$

2.3.10 Mechanism of corrosion inhibition

Corrosion inhibition in acid solution can be achieved by halides, carbon monoxide and organic compounds containing heteroatoms such as nitrogen, phosphorus, oxygen, sulphur and selenium, organic with multiple bonds, proteins, polysaccharides, glue, bitumen and natural plant products such as chlorophyll and anthocyanins

The structure of the inhibitor, especially in the case of organic inhibitor, plays a very important role in corrosion inhibition of metals. Organic inhibitors such as amines (aliphatic amines, pyridines, imidazoles) and thiazoles form a coordinate bond with metals such as iron, copper and zinc. Corrosion inhibition of metals by organic inhibitors containing electron donor atoms such as oxygen, nitrogen, sulphur and selenium increased with decreasing electronegativity in the order O < N < S < Se (Makrides and Hackerman, 1954). The metal - inhibitor bond is also formed with inhibitors containing the electrons associated with triple bonds or aromatic rings. The introduction of a double bond in a compound appears to increase the degree of corrosion inhibition.

The adsorption of inhibitors onto the metal surfaces can be studied electrochemically by determination of the anodic cathodic polarization curves of the corroding metal. A displacement of the polarization curve without a change in Tafel slope upon addition of an inhibitor indicates that the adsorbed inhibitor is blocking active sites and inhibiting the reaction without affecting the mechanism of the corrosion process. An increase in the Tafel Slope of the polarization curve upon addition of the inhibitor indicates the effect of the inhibitor on the corrosion reaction mechanism(Sastri, 2011).

2.4 Surfactants

A class of compounds called surface-active compounds (or surfactants) decrease prominently, the interfacial tension or interfacial free energy of the interfaces. The molecules are amphiphilic in character, i.e., they possess hydrophilic and hydrophobic regions having a

long hydrocarbon tail and a relatively small ionic or polar head group. Amphiphiles can be ionic (cationic, anionic), zwitterionic, or nonionic depending on the nature of their head groups. The surfactants have a tendency to accumulate at the interface of immiscible fluids with a marked influence resulting in decrease in free energy which is reflected in a corresponding lowering of interfacial tension that facilitates emulsification of the immiscible fluids and hence such compounds are also known as emulsifiers. A schematic diagram of typical surfactants is shown in Figure 2.6. Research on surfactants is rapidly developing due to their booming applications in many important practical and fundamental sciences like petroleum oil recovery, corrosion inhibition, water and environmental pollutions, understanding the mysterious role of biological membranes, biotechnology, and other systems. The behavior of surfactants in solution are subject of considerable interest because of its wide applications in different industries, medical sciences, life sciences, analytical chemistry, pollution control and even in the fields of physics and engineering (Maqsood *et al.,* 2011).

2.4.1 Classification of surfactants

Surfactants are classified according to the composition of their head: non-ionic, anionic, cationic, amphoteric. Most commonly, surfactants are classified according to polar head group. A non-ionic surfactant has no charge group in its head. The head of an ionic surfactant carries a net charge. If the charge is negative, the surfactant is more specifically called anionic; if the charge is positive, it is called cationic. If a surfactant contains a head with two oppositely charged groups, it is termed zwitterionic (Maqsood *et al.*,2011).

2.4.2 Mechanism of inhibition of surfactants

The mechanism of Corrosion inhibition by surfactants involves the formation of mono or multi- dimensional protective layers onto the metal surface. The protective nature of the surface layer

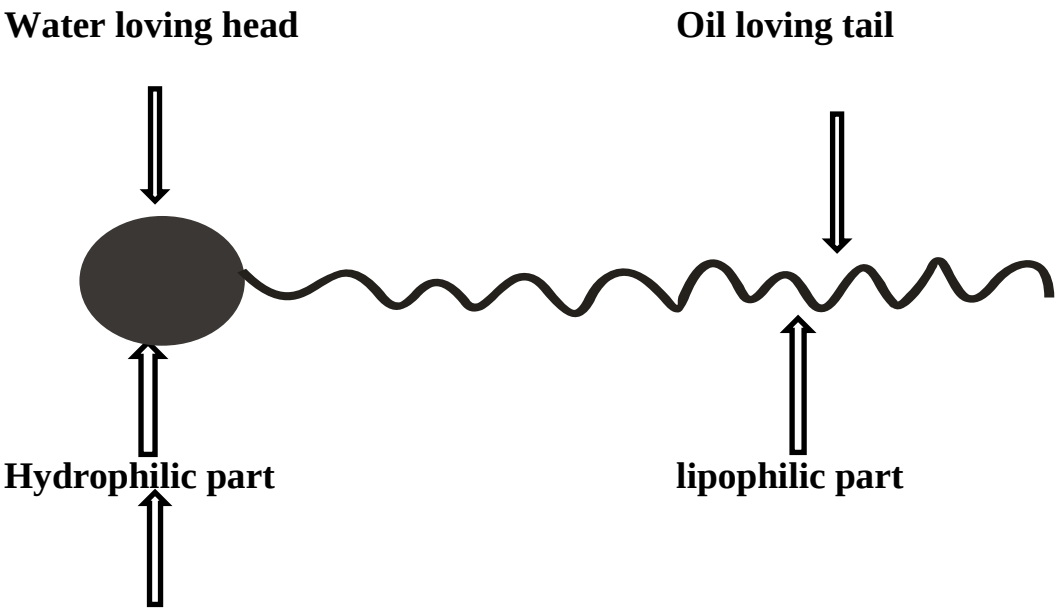

Figure 2.6: Schematic diagram of surface-active molecule (Source: Maqsood *et al.*, 2011)

depends on many factors; interaction between inhibitors and substrate, incorporation of the inhibitor in the surface layer, chemical reactions, electrode potentials, concentration of the inhibitor, temperature and properties of the corresponding surface, etc. The first stage in the action of the surfactants as corrosion inhibitors in aggressive media is adsorption of the surfactant molecules on to the metal surface. The adsorption process is influenced by the nature and the surface charge of the metal, the chemical structure of the surfactant, and the nature of the aggressive electrolyte. Adsorption of the surfactant molecules on the metal surface can be expressed according to the following equation:

$$\text{Surfactant}_{(\text{solution.})} + n\text{H}_2\text{O}_{(\text{adsorbed.})} = \text{Surfactant}_{(\text{adsorbed.})} + n\text{H}_2\text{O}_{(\text{solution.})} \qquad (2.24)$$

where n is the number of water molecules removed from the metal surface for each molecule of surfactant adsorbed.

It is clear that the value of n depends on the cross sectional area of the surfactant molecule with respect to that of the water molecule. Adsorption of the surfactant molecules occurs because the interaction energy between the surfactant molecules and the metal surface is higher than that between water molecules and the metal surface. Hence, the inhibition effect by surfactants is attributed to the adsorption of the surfactant molecules via their functional groups onto the metal surface. The adsorption rate is usually rapid and hence the reactive metal is shielded from the aggressive environment. Corrosion inhibition depends on the adsorption ability of the surfactant molecules on the corroding surface, which is directly related to the capacity of the surfactant to aggregate to form cluster (micelles).

The critical micelle concentration, CMC, is a key factor in determining the effectiveness of a corrosion inhibitor. Below CMC, as the surfactant concentration increases, the molecules tend to aggregate at the interface, and this interfacial aggregation reduces the surface tension. Above CMC, the metal surface is covered with a monolayer of surfactant molecules and the additional molecules combine to form micelles or multiple layers.

This,consequently, does not alter the surface tension and the corrosion rate (Maqsood *et al*., 2011).

2.4.3 Monoethylamine and triethylamine as surfactants

Monoethylamine (MEA) and triethylamine (TEA) can be regarded as derivatives of ammonia (NH_3) in which one, or three hydrogen atoms have been replaced by a CH_2CH_2OH group. MEA and TEA are viscous, colourless, clear, hygroscopic liquids at room temperature; Dimethylamine (DEA) is a crystalline solid. All ethanolamines absorb water and carbon dioxide from the air and are infinitely miscible with water and alcohols. Ethanolamines are used widely as intermediates in the production of surfactants which have become commercially important as detergents, textile and leather chemicals, emulsifiers, and as protective coatings. MEA and TEA are applied as admixtures with corrosion inhibitors, particularly in coolants for automobile engines, as well as in drilling and cutting oils. They are also employed as additives in lubricants (Kohl and Nielsen, 1997).

2.4.4 Co- inhibitors

It is very rare that a single inhibitor is used alone in systems such as cooling water systems. More often, a combination of inhibitors (anodic and cathodic) is used to obtain better corrosion protection properties. The blends which are produced by mixing of multi-inhibitors are called synergistic blends if the inhibitive potentials of the blend is greater than the sum of their individual potentials. Examples include chromate-phosphates, polyphosphate-silicate, zinc-tannins, zinc-phosphates (Zaki, 2006). The synergism parameters were calculated using the relationship given by Aramaki and Hackerman as reported by Obot *et al.,* (2011)

$$S_1 = \frac{1 - I_{1+2}}{1 - I'_{1+2}} \quad (2.25)$$

where $I_{1+2} = (I_1 + I_2)$; I_1 = inhibition efficiency of inhibitor A : I_2 = inhibition efficiency of inhibitor B. I'_{1+2} = measured inhibition efficiency for the inhibitor A in combination with inhibitor B. S_1

approaches 1 when no interaction between the inhibitor compounds exists, while $S_1 > 1$ points to a synergistic effect. In the case $S_1 < 1$, the antagonistic interaction prevails, which may be attributed to competitive adsorption. Similarly, another equation commonly used to further determine whether synergistic inhibition effects do occurred is defined thus:

$$S = \frac{1-\theta_A-\theta_B+\theta_A\theta_B}{1-\theta_{AB}} \quad (2.26)$$

where Θ_A and Θ_B are the surface coverage of compound A and B respectively acting alone, and Θ_{AB} is that of the mixture. When no interaction between the two inhibitive compounds exists, the value of S is equal to unity. Otherwise, the S □ 1 and S □ 1 correspond to synergistic effect and antagonistic effect respectively (Umoren *et al*., 2008).

2.5 Previous Studies on Plant Extracts as Inhibitors

The study of corrosion of aluminium which is a light weight material is of most important and of tremendous theoretical and practical concern and has gain a considerable amount of interest in the global world. Several attempts have been made to solve the corrosion problems associated with aluminium and one of which was the use of corrosion inhibitors. Plant extracts (leaves, barks, stems, roots, and fruits) and oil extracts have been used by various authors as corrosion inhibitors, alone or as co-inhibitors at various temperatures, different media and exposure time for ferrous and non-ferrous materials. Naturally occurring substance as corrosion inhibitors of acid cleaning process has continued to receive attention as replacement for synthetic organic inhibitors. Recent literature has shown that plant materials such as *Azadirachta indica, ocimum viridis, Hibiscus Sabdariffa extract, olives leaves, prosopis cineraria, Aloe vera extract, Datura Stramonium and Phyllantus amarus* extracts are effective inhibitors for metal in aggressive solutions (Obot *et al.*, 2011).

Awe *et al* (2015) study the inhibitive and adsorptive effect of *Parinari polyandra* on mild steel corrosion in aqueous sulphuric acid. The study was carried out at different temperatures

using weight loss technique and linear.polarization method. The inhibition efficiency increased with a corresponding increase in the concentration of the inhibitor. The adsorption of the inhibitor on mild steel surface was found to be exothermic, spontaneous and was best described by Freundlich and Temkin adsorption models.

Idawu (2013) investigated on evaluation of plant extracts as corrosion inhibitors for mild steel in acidic environment. The feasibility of using extracts of *Acacia senagalensis* (gum arabic tree) *Acacia tortilis* (umbrella thorn tree) and *Grewa venusta* (wildjute tree) as corrosion inhibitors for mild steel in 0.5 M H_2SO_4 was studied using gravimetric and electrochemical techniques. The inhibition efficiencies were 94.16% AS, 93.19% AT and 86.4% GV at 6, 10 and 10% v/v inhibitor concentration compare to the control (Sodium benzoate) which has 93.60% at 10% v/v optimum inhibitor concentration. ThePotentiodynamic polarization results revealed a change in the anodic and cathodic regions for the corroded sample indicating a mixed type inhibitors.

Inhibitive effects of natural *Cyperus esculentus L.* oil was studied on the corrosion of A356.0 types Al-Si-Mg alloy in simulated sea water environment (Mohammed *et al*, 2013). The corrosion study was conducted using gravimetric method and different concentrations of *Cyperus esculentus L*. oil (0.2, 0.4, 0.6 and 0.8g/v) was used at 30^0C, 50^0C, and 70^0C respectively. The results revealed that *Cyperus esculentus L*. oil in 3.5 % NaCl solution decrease the corrosion rate at various concentration and exposure time considered. The maximum inhibition efficiency obtained was 69.99% at 30^0C with 0.8 g/v of inhibitor concentration. The results demonstrated that *Cyperus esculentus L.* adsorbed on the surface of Al-Si-Mg alloy and obeyed Langmuir adsorption isotherm.

Ajanaku*et al*., (2012) investigated into the corrosion inhibition effect of *Vernonia amygdalina* extract on aluminium in 0.5M HCl solution using gravimetric method at 40^0C. The concentrations used were 0.4, 0.5, 0.6, 0.7, 0.8, 0.9 and 1.0 g/l at interval of 30 minutes

progressively for 150 minutes. The results showed that *Vernonia amygdalina* could be used as an ecofriendly corrosion inhibitor for aluminium in HCl solution. The corrosion inhibition efficiency of the extract increase with concentrations in the corrosion media. The surface coverage of the extract obeyed Langmuir adsorption isotherm.

The inhibitive effect of *Irvingia gabonensis* extract on the corrosion of aluminium in 2 M HCl solution was also examined (Babatunde *et al*, 2012). The inhibition efficiency for the extract increase with increasing concentration of the extract and decrease with increase in temperature. The temperature of study was at 30, 35 and 40^0C and the adsorption of the inhibitor molecules on aluminium surface was found to obey Langmuir adsorption isotherm. The phenomenon of physical adsorption was proposed based on the thermodynamic data governing the process.

Okafor *et al*., (2012) investigated the action of ethanol, acid and toluene extracts from *Artemisia annua* and *Artemisinim* on mild steel corrosion in H_2SO_4 solutions using gravimetric and gasometric techniques. The extracts functioned as good inhibitors and their inhibition efficiencies followed the trend EEAA > AEAA > TEAA. Inhibition efficiency was found to increase with increase in inhibitor concentration and decreased with increase in temperature. The adsorption of the inhibitors was consistent with Langmuir isotherm. Uwah *et al*., (2013) also investigated the inhibitive performance of ethanol extracts of *Andrographis paniculata* (King bitter) EEAP and *Vernonia amygdalina* (bitter leaf), EEVA on the corrosion of mild steel in 2 M HCl solution at 30, 40, 50 and 60 ^{O}C using weight loss and hydrogen evolution techniques. The results indicated that both plant extracts inhibit the corrosion of mild steel in the acid solution by adsorption, EEAP exhibited higher maximum inhibition efficiency 89.7 % than EEVA 76.9 % at 4.0 g/l. Inhibition efficiency was found to increase with temperature and the adsorption of both plant extracts on the mild steel coupon was found to obey Langmuir adsorption isotherm.

Niamien *et al*., (2011) studied the inhibitive action of hexadecyl trimethyl ammonium bromide (HDTAB) on aluminium alloy (AA3003) corrosion in 1M HCl acid medium by weight loss method. The temperature was varied from 25, 35, 45 and 55 ^{O}C and also the concentration was varied from 0.002, 0.004 0.006, 0.008 and 0.010 M. Adsorption of the inhibitor molecule on to the surface of the aluminium alloy was according to Langmuir isotherm. The inhibition efficiency decreases with increasing temperature. The adsorption free energies and apparent activation energies indicated that the process is spontaneous and that the trend follows physical adsorption.

Sangeetha *et al*., (2012) investigated on ecofriendly extract of Banana peel as corrosion inhibitor for carbon steel in seawater. The study involves weight loss and linear polarization methods and the surface morphology was analysed by FT-IR and atomic force microscopy, AFM. Protection film formed on the metal surface is confirmed by using Potentiodynamic polarization and AC impedance techniques. Polarization study reveals the system function as mixed type of inhibitor.

2.5.1 Inhibitors used

i. Sodium chromate

Sodium chromate has a molecular formula (Na_2CrO_4) and molecular weight of 161.97g. It is a yellow, translucent crystals, efflorescent, odourless. It is widely used as corrosion inhibitors in industries, but the use of it in cooling tower water has been prohibited in Califonia due to its adverse effect on ecosystem (Chowdhury and Miltra, 1995).

ii. *Combretum micranthum*

Combretum micranthum (combretaceae) is a savannah plant found in dry sites, sand stones, clay, laterite, crystalline rocks and skeletal soils. It is a small tree, shrub or liana of 4m high (attaining up to 10m underfavourable conditions). It may reach a height/length of 20m by twining around the branches of nearby trees. The bark is grey and fibrous, with orange to

brown-red slash, and hairy and scaly red brown stems. It is native to West Africa, distributed from Senegal, Mauritania, Niger to Nigeria, and is called Geeza, in Hausa. It is believed to possess antibacterial properties and is used traditionally for the treatment of several infections. The whole plant is densely covered with red scales. Leaves are variable, oblong-ethiptic 5 – 10cm long and 2.5 – 5.0 cm wide and are alternate, shining light green when young; typically rust coloured when matured, in the dry season. Leaves, roots and barks have many medicinal usages (McGraw*et al*., 2001; MSBP, 2008).

iii. *Combretum glutinosum*

Combretum glutinosum is a shrub species of the genus *combretum* found in the Sahel belt in parts of Senegal, Burkina Faso, Ghana, Mali, The Gambia, Niger, Nigeria, Cameroon and across parts of Sudan. It is known popularly as dooki in Pulaar, Kankara/Tarauniya in Hausa. It tends to grow in savannah forests, in several soil types but is best suited to sandy and free draining soils. It is drought resistant and grows in areas of annual rainfall of 200 – 700 mm; its growth is fast and profuse. As a bushy shrub, the plant grows up to 12m with an open crown with low branches that droop down, and is deciduous. The trunk is usually twisted and low branched, with grey-black rough bark. The thick, leathery, green leaves have a gummy feel to them and are glutinous when young. The plant's bark, leaves and roots are extracted for treating various ailments like influenza, Rheumatism, syphilis and sexual issues (Yahya *et al.*, 2012).

iv. *Ficus platyphylla*

Ficus platyphylla Delile (family – moraceae) commonly called "gamji" in Hausa and "ogbagba" in Yoruba, is a savannah treeof about 18m high, 6m in girth, with large widely spreading branches and broad crown. The bark is rusty red, flaking off in scattered patches

and greys beneath; slash pink. The leaves, barks, seeds have been used traditionally in combination to promote fertility. It grows widely in the Northern part of Nigeria up to 5 m high. Leaves are 7 – 40cm long by 10 – 28cm broad, mostly broadly elliptic, round or blunt at the apex and narrowly cordite; thick finely velvety or glabrous (Irvine, 1961).

v. *Ficus exasperata*

Ficus exasperata is widely distributed in tropical Africa, from Senegal eastward to Ethiopia and Djibout and southward to Mozambique and Angola. It also occurs in Yemen, India and Srilanka. Nigerian forests are replete with over 45 different species of *Ficus*. It is found in the savannah, rain forest, beside rivers and streams. Among its vernacular names include forest sand paper tree, white fig tree, Ewe ipin (Yoruba),Opoto (Calaba), Anwulinwa (Igbo), Ihariha (Ebira). Ficus exasperate occurs from sea level up to 2300meters altitude in forest, often at edges, in secondary vegetation, in rocky places, and along rivers, some times persisting in cleared land. It is also found in abandoned fields and along roads. Root decoctions are taken for the treatment of urinary tract ailments, gonorrhea, asthma and tuberculosis (Chinedu, 2012).

2.6 Determination of Corrosion Rates

Corrosion rates for metals undergoing uniform corrosion can be determined by any of the following methods

a- Weight loss

b- Weight grain

c- Chemical analysis

d- Gasometric techniques (when one of the chemical products is a gas)

e- Thickness measurements

f- Electrical resistance probes

g- Inert marker method

h- Electrochemical techniques

i. Weight loss method (gravimetric)

This method consist of removing previously weighed metal samples from the solution or the environment at various timed intervals (exposure time), and the loss in weight due to metallic corrosion is determined (per unit area of the sample). For this method to be accurate, any solid corrosion products must be removed from the metal surface. If the corrosion products are closed and non - adherent they can be removed by mechanical means.

ii. Weight gain method

This method is use to in oxidation where oxide filing or products are more adherent and generally not useful in aqueous corrosion studies. It is done in such a way that the weight gain measurements in dry environments have the feature of being measured continuously and without removal of the specimen from the environment (Mc Cafferty, 2010).

iii. Chemical analysis of solute

A useful method for chemical analysis of solute is atomic absorption spectrophotometry (AAS). The sample size need for this method is very small (typically about 10 mg). The sample is accurately weighed and then sprayed into the flame of the instrument and atomized. Light of a suitable wavelength for a particular element is directed through the flame, and some of this light is absorbed by the atoms of the sample. The amount of light absorbed is proportional to the conclusion of the element in the solution. The method is sensitive to trace elements down to the parts per million levels (Williams and Bause, 1996).

iv. Thickness measurements

Measurement of the thickness of a metal as a function of time is a method used to monitor the corrosion behavior of a system (Jaske *et al.,* 2002). This method is used to survey the practical corrosion behavior of a system in service, rather than as a laboratory technique, and has been used to track the progress of corrosion in railroad hopper cars, storage tanks, and

pipelines. The thickness measurements are based on the response of a specimen to an ultrasonic or a magnetic signal.

v. Electrochemical techniques

All the aforementioned methods has an application in either the laboratory or the field and none of them above can provide insights into the underlying mechanism of corrosion. Electrochemical techniques have this capability and in addition offer the possibility of mitigating corrosion by controlling the electrode potential. Among the various methods of determining the corrosion rate by electrochemical techniques includes:

- Direct current (DC) polarization method and its offshoots
- Alternating current (AC) techniques, which are very powerful in determining corrosion and in monitoring the progress of corrosion

2.6.1Applications of the linear polarization

This method has been used in a variety of applications (Jaske *et. al.,* 2002). Some examples include the evaluation of corrosion inhibitors, the behavior of protective zinc coatings, atmospheric corrosion monitors, the oil industry, pipelines, chemical process industries, in pulp and paper plants, in water treatment applications, the corrosion of steel-reinforcing bars in chloride contaminated concrete, the corrosion behavior of biomedical implant alloys in simulated body fluids, and the corrosion of aluminium alloys in beverages or liquid foods, or of aluminium alloys in crevices

2.6.2 Linear polarization (instrumentation and procedures)

The electrochemical cells arrangement used for polarization measurements has three electrodes (the working, reference, and auxiliary electrodes). Graphite auxiliary electrodes can be used if platinum electrode is not available. Modern potentiostats (constant potential

devices) has computer control and a wide variety of software packages. These devices can be operated either in the potentiostatic or the galvanostatic mode. In the potentiostatic mode, the electrode potential is held constant and the resulting current is recorded. In the galvanostatic mode, the current is held constant and the resulting electrode potential is recorded. Either mode can be used unless there is an active-passive transition. In such cases, the galvanostatic mode, which determines potential, E, as a function, of current, I, will not detect the "nose" in the anodic polarization curve.

Polarization curve can be determined by the potential step or the potential sweep method. In the potential step method, the electrode potential is changed abruptly from one discrete value to another, and the resulting current is then recorded as a function of time until the current reaches a steady-state value which either is invariant with time or changes only minimally with time. The process is then repeated, potential by potential, until the entire polarization curve is determined. The potential step method is sometimes tedious but ensures that steady state polarization curves are obtained (McCafferty, 2010).

In the potential sweep method, the electrode potential is ramped continuously with time, and the resulting current is simultaneously recorded along with the applied potential. Care must be taken that the sweep rate is sufficiently slow so that the steady state is approximately by the sweep. Sweep rates of 10-100 mV/min. are commonly used.

CHAPTER THREE

3.0 MATERIALS AND METHODS

3.1 Materials

The following materials were used during this research work:

Four (4) plant extracts *(Combretum micranthum, Combretum glutinosum, Ficus exasperata and Ficus platyphylla)* as inhibitors, monoethylamine (MEA) and triethylamine (TEA) as surfactants, polishing powder, sodium chromate salt, desiccators, thread, distilled water, sodium chloride salt and methanol.

3.2 Equipment

Crucible furnace, Polishing machine, digital weighing balance, thermostated water bath, Potentiostat Corrosion Kit, Optical Metallurgical Microscope (OPM), Scanning Electron Microscopy (SEM) Machine, Fourier Transform Infrared spectroscopy (FTIR) Machine, Gas Chromatography Mass Spectroscopy (GCMS) and Viscometer Machines. Beakers, measuring cylinder, conical flask, brush, grinding papers with different grades (size), and lathe machine.

3.3 Methods

3.3.1 Production of Al-Si-Mg alloy

A356.0 type Al-Si-Mg alloy was produced through sand casting technique. The composition of the alloy shown in Table 3.1 was charged in to the crucible furnace for melting. The pure aluminium wire were first melted which was allowed to heat to a temperature of 750^{o}C before the crucible was removed. Silicon powder and copper ligand and zinc were added, which was stirred and then returned back. Thereafter, the temperature of the melt was allowed to reach 800^{o}C for super heating process to take place. The melt was

Table 3.1: Composition of A356.0 type Al-Si-Mg alloy used

Element	**Al**	**Si**	**Mg**	**Cu**	**Zn**
Weight %	92.35	7.0	0.35	0.20	0.10

Source: ASM, 1992.

removed and magnesium chips and strontium were equally added to the ladle and stirred thoroughly before pouring in to the mold cavity.

The alloy was sand cast cylindrical bars of dimension 22x 300 mm and machined to standard specification for weight loss and electrochemical corrosion test samples, respectively.

3.3.2 Preparation of plant extracts

The four plants used in this work were*Combretum micranthum,(CM), Combretum glutinosum,(CG), Ficus exasperate, (FE) and Ficus platyphylla, (FP).*The leaves of three plants (CM, CG and FP) were obtained from Malumfashi in Katsina State and that of FE was obtained from Okene in Kogi State. The plants were shade-dried and pulverized to powderusing motar. The Cold extraction method was used according to the method reported by Lebrini *et al.*(2011). About 500 g of dried leaves of each plant were poured into four different separating funnels and 1000 ml of methanol was added to them, a cotton wool was placed at the exit of the funnel to serve as a filter. The whole set up were left for five days for proper soaking to take place. After the soaking the solution (solvent + extract) were poured in to a round bottom flask which rotate inside the heating water bath. As a result of heating, the solvent got evaporated in to a condensing chamber which was surrounded with ice block externally. At the condenser, the solvent (methanol) was collected inside the second round bottom flask, cooled and leaving the plant extract only in the first round bottom flask. The stock of the extract so obtained were used in preparing different concentrations of the extract by dissolving 0.2, 0.4, 0.6, 0.8, and 1.0 g of the extracts in 250 ml of various concentration of the NaCl solution (Arora *et al*., 2007; Eddy and Odoemelam, 2009).

3.3.3 Phytochemical screening

The Phytochemical screening of the extracts for the detection of tannins, saponins, flavonoids and alkaloids was performed according to standard laboratory procedures (Lakshman, 2012).

a. Tannins- To a portion of the extract, 3 drops of ferric chloride solution were added.

b. Saponins- About 10 ml of distilled water was added to a portion of the extract and was shakenvigorously for 30 seconds. The tube was allowed to stand in a vertical position and was observed for 30 minutes.

c. Flavonoids- A few drops of 10 % NaOH were added to the extract.

d. Alkaloids- Few drops of Wagner's reagent were added to a portion of the extract.

Thin layer chromatography (TLC) was further used also to characterize the plant extract by identifying the presence of tannins, saponins, flavonoids, and alkaloid. The procedure consists of marking a base line with point at intervals of 1cm for spotting of the extracts on a thin layer plate (Silica gel coated on alumiunium or glass). The spotted samples were allowed to dry for10 minutes. A solvent system (mobile phase) usually ethyl acetate: methanol: water in the ratio 10:1:1 were mixed together to form the solvent system which was poured inside a glass tank. The thin plate was immersed inside the tank for 20 minutes to develop. . By capillary action the unknown compounds rose through the column in the plate, and then removed from the tank, dried, sprayed, specific sprayers were used for different compounds.

3.3.4 Fourier transform- infra red spectrum (FT-IR)

FTIR Spectrophotometer, model FT-IR-8400S Shimadzu was used for the determination of functional groups in the plant extracts. About 1.0 g of plant extracts were mixed with potassium bromide. A solid mass was made into pellets. The FT-IR absorption spectrums were recorded as peak, and each peak represent a frequency corresponding to a particular band assignment which translate to the type of functional group present in that peak.

3.3.5 Gas chromatography- mass spectroscopy (GC-MS)

The machine model GC-MS- QP2010 PLUS Shimadzu was used for the identification of an unknown compounds present in plant extracts. About 1.0 g of the extract was added to

2ml of methanol (solvent) and was shaken vigorously for 30 minutes and filtered. The filtrate extract was used for the analysis. About 1.5ml of the filtrate was placed in a sample vialand was placed in to the GC-MS machine to run the analysis for about 28 minutes. The Chromatogram and corresponding mass spectrum of the extract showing the peak of the compounds were recorded from the GC-MS machine. The number of peaks, compound names, molecular formula and molecular weight for a particular extract were indicated.

3.3.6 Physico-Chemical test

The Physico-chemical parameters such as pH and solubility were determined in accordance with the standard procedure set by Association of Analytical Chemists (1990). Density and viscosity were determined in accordance with the ATM D1298 and Newtonian method, respectively.

i. Solubility test

The solubility of the plant extracts was determined in distilled water, butanol and Hydrochloric acid. About 1.0 g of the extracts was added to 5 ml of the respective solvents at 30 ^{O}C and left over for 15 minutes. The temperature was then raised to 50 ^{O}C and 70 ^{O}C by heating the solvent on hot plate. It was then removed from the hot plate for grading various classes as insoluble, soluble, partial soluble and highly soluble respectively.

ii. pH test

The pH of the extracts was determined by shaking 1.0 g of the extracts in 5 ml of water for three hours and the pH was measured using a pre-calibrated digital pH meter (model AP71). The electrode of the pH meter was immersed in the dissolved solution and the pH value was read directly through a digital read out system.

iii. Viscosity test

The viscosity of the extracts was determined using viscometer (model RBT and serial no. 43320). 40 ml of the extracts (liquid) was poured into a small beaker of capacity 50 ml

while the spindle was connected to the viscometer. The spindle was immersed in the solution of the extract and three revolutions of the spindle were used to determine the viscosity of each extract at various temperatures (30 ^{O}C, 50 ^{O}C, and 70 ^{O}C). The viscosity value was read directly from the viscometer.

iv. Density test

The density of each extract was determined by weighing an empty bottle, M_1 and then 50 ml of each extracts was weighed including the bottle as M_2 , and the density, d, was calculated using the formula

$$d = \frac{M_2 - M_1}{V} \qquad (3.1)$$

where V is the total volume of sample used (50 ml).

v. Biodegradability test

The biodegradation tests were carried out in accordance with OECD 306 Marine BOD (2005) model adopting the Azide modification of the Winkler method. Standard tests solutions of each inhibitor were prepared by dissolving 0.5 g of the extract in100 ml of distilled water, and used for BOD test. The Biochemical Oxygen Demand (BOD) of each inhibitor was calculated using the relationship in equation (3.2)

$$\text{BOD (ppm)} = \left(\frac{DO_1 - DO_2}{P}\right) \qquad (3.2)$$

DO_1 = Dissolved Oxygen (mg/L) of diluted sample immediately after preparation

DO_2 = Dissolved Oxygen (mg/L) of diluted sample after incubation period at 20 ^{O}C

p = dilution factor (1:10)

3.4 Corrosion Rates Determination

3.4.1 Gravimetric mass-based loss

The test samples were mechanically cut into corrosion coupons of dimension 10 x10mm. Prior to weight loss and electrochemical measurement, the surface of the specimens

were ground using grit papers (grades 220, 320, 400 and 600) and polished using alumina powder. The samples were washed with distilled water, dried and kept in a desiccator before use. The initial weight of the samples were recorded before suspending them with thread in to 250ml of 3.5 wt% NaCl solution (artificial seawater) without and with addition of different concentrations of inhibitors and surfactants 0.2, 0.4, 0.6, 0.8 and 1.0 v/v at various temperatures 30^{O}C, 50^{O}C and 70^{O}C over an exposure time of 1, 2, 3, 4, and 5 hours respectively.The samples were removed from the medium after the exposure time, washed, dried and reweighed. From the weight loss, the corrosion rateswere calculated using equation 3.2 as reported (William, 2007).

$$\text{CR} = \frac{87.6W}{DAT} \text{ (mm/yr)} \qquad (3.2)$$

where W = weight loss in mg. D = density g/cm^3, A = area in cm^2 and T = exposure time in hours. The inhibition efficiency, (IE %) was also calculated using the equation (3.3) as reported (Yuli *etal.*, 2014).

$$\text{IE \%} = \frac{CR_o - CR}{CR_o} \text{ x } 100 \qquad (3.3)$$

where CR_O = corrosion rate in the absence of an inhibitor,CR= corrosion rate in the presence of an inhibition and the degree of surface coverage, Θ, was calculated (Ihebrodike *et al.*, 2010).

$$\Theta = \frac{CR_o - CR}{CR_o} \qquad (3.4)$$

3.4.2 Electrochemical method

The polarization studies were carried out using (Metrohm Autolab AUT50280). The set-up consists of three electrode cells consisting of Al-Si-Mg alloy as the working electrode (WE), a platinum foil as the counter electrode (CE), and saturated calomel electrode (SCE) was used as the reference electrode (RE). The volume of the cell was 250 ml and the medium

was 3.5 wt% NaCl artificial seawater and all the tests were performed at room temperature. The experiments were carried out using the inhibitors at various concentrations 0.2, 0.4, 0.6, 0.8 and 1.0 g/v. The potentiodynamic polarization measurements were performed in the potential range of -1500 mV to 1500 mV at a scan rate of 0.012v/s. The polarization curves were automatically recorded for each experiment. The corrosion parameters such as polarization resistance (R_P), corrosion potential (E_{corr}), corrosion current (i_{corr}), and Tafel slopes (βa and βc) were obtained. The inhibition efficiencies (IE %) were calculated using the equation :

$$IE\% = \frac{i_{corr} - i'_{corr}}{i_{corr}} \times 100\% \quad (3.5)$$

i_{corr} and i'_{corr} are the current densities of Al-Si-Mg alloy in the absence and presence of the inhibitor, respectively.

3.5 Microstructural Analysis

3.5.1 Optical Microscope

The surface morphology of some samples before and after corrosion test were examined using Optical Microscopy (OPM) (model NJS 120-A). The microstructures obtained were captured with an in-built ocular.

3.5.2 Scanning Electron Microscopy (SEM)

The SEM was carried on machine Model Pheom Prox, manufactured by phenomworld, Eindhoven to examine the corroded and un-corroded surface morphology. Some of the samples from weight loss and LPR tests were taken and placed on the sample holder which was then examined. The samples were then scanned with an electron beam and the reflected (or back –scattered) beam of electrons were collected, displayed at the same scanning rate on a cathode ray tube.

3.6 Statistical Design Analysis

The Statistical Design Analysis and Development of Mathematical equations were conductedusing statistical design expert 6.0 with model (SPSS version 20, US). A full factorial design experiment of the type $X^n$was used to investigate whichcorrosion control parameters significantly affects the corrosion rate of the inhibitors and the independently controllable process parameters considered for the investigation. Where n is the number of factors and X is the number of levels. In this research, n = 3 (temperature, inhibitor concentration and time) and X = 2 (lower and upper levels) for each variable.

Two levels of each of the three factors were used for the statistical analysis. The levels for the three factors were entered and the treatment combinations for the two levels and three factors were tabulated in Table 3.2 and the treatment combination in Table 3.3. The mathematical equation was obtained by representing the corrosion rate value by CR, the response function can be expressed by equation 3.6.

$$CR = f(A, B, C) \quad (3.6)$$

where A is the temperature, B is the inhibitor concentration and C is the exposure time. The mathematical equation selected includes the effects of main variables first order and second-order interactions of all variables. Hence the general equation is written as reported (Oloche *et al.,* 2009; Aigbodion *et al.,* 2010).

$$CR = \beta_0+\beta_1A_+ \beta_2B_+ \beta_3C_+ \beta_4AB_+\beta_5AC_+ \beta_6BC_+\beta_7ABC \quad (3.7)$$

where β_0 is average response of CR and $\beta_1, \beta_2, \beta_3, \beta_4, \beta_5, \beta_6, \beta_7$ are coefficients associated with each of the variables A, B, C and interactions.

The test results were recorded against the standard order of sequence. The sum of squares for main and interaction effects was calculated using Yates algorithm. The significant factors

Table 3.2: Statistical Design of the Corrosion Process

Factors	**Low level**	**High level**
Temperature (A)	$30^{O}C$	$70^{O}C$
Inhibitor concentration (B)	0	1.0 v/v
Exposure Time (C)	60 minutes	300 minutes

Table 3.3: Factorial Design of the Corrosion Process Showing Treatment Combination

Experimental number	**Temperature level**	**Concentration level**	**Time Level**
1	-1	-1	-1
A	+1	-1	-1
B	-1	+1	-1
C	-1	-1	+1
AB	+1	+1	-1
AC	+1	-1	+1
BC	-1	+1	+1
ABC	+1	+1	+1

Coded = -1 (low level), +1(upper level or high)

(main and interaction) were identified by analysis of variance (ANOVA) technique (Miller and Freund, 2001).

CHAPTER FOUR

4.0 RESULTS AND DISCUSSION

4.1 Characterization of the Plant Extracts

4.1.1 Phytochemical screening

Phytochemical screening of the plant extracts (CM, CG, FE, and FP) was carried out to identify the presence of the chemical constituents present in these plants. It was found that the plant constituents contain tannins, saponins, flavonoids and alkaloids. Flavonoids contribute to the inhibition efficiency of the inhibitors possibly due to being a cyclic compounds with O atoms attached to it (Helen *et.al*., 2014). The qualitative and quantitative phytochemical screening results are as shown in Tables 4.1 and 4.2. The extracts gave prominent colours for the outcome of the flavonoid and saponins in regard to CM and FP while colours are weak for other plants. There was an agreement between quantitative and qualitative result of the screening in which saponins, flavonoids are higher in CM and FP than others. These chemical constituents might have adsorbed on to the surface of the sample thereby blocking the active corrosion site. (Idawu, 2013).

4.1.2 Fourier Transform Infrared Spectroscopy

Earlier researchers have confirmed that FT-IR spectrometer is a powerful instrument that can be used to determine the type of bonding for organic inhibitors adsorbed on the metal or alloy surfaces (Sangeetha *et al.,* 2012). A FT-IR spectrum was used to further characterize the chemical constituents that contribute to the corrosion inhibition of the extracts and were found to have specific functional groups. Figures 4.1 – 4.4 show the FT- IR absorption spectrum of CM, CG, FP and FE. Appendices I - IV show the band frequencies of CM, CG, FE and FP while bands around 411.82, 596.99, 1041.60, 2930.93, 3402.54 and 3994.71 cm^{-1} for CM

Table 4.1: Phytochemical screening (Qualitative) result of the plant extracts

Plant extract	Tannins	Saponin	Flavonoids	Alkaloids
CM	+	++	++	+
CG	+	+	+	+
FE	+	+	+	+
FP	+	+	++	+

Where (+) means the presence of the chemical constituent and (++) means the presence of more chemical constituent.

Table 4.2: Phytochemical screening (Quantitative) result of the plant extracts

Plant extract	Tannins	Saponin	Flavonoids	Alkaloids
C.M	1.51%	23.30%	22.50%	4.78%
C.G	1.30%	8.90%	13.46%	2.10%
F.E	1.50%	9.10%	11.62%	6.60%
F.P	1.45%	10.96%	24.28%	8.84%

.

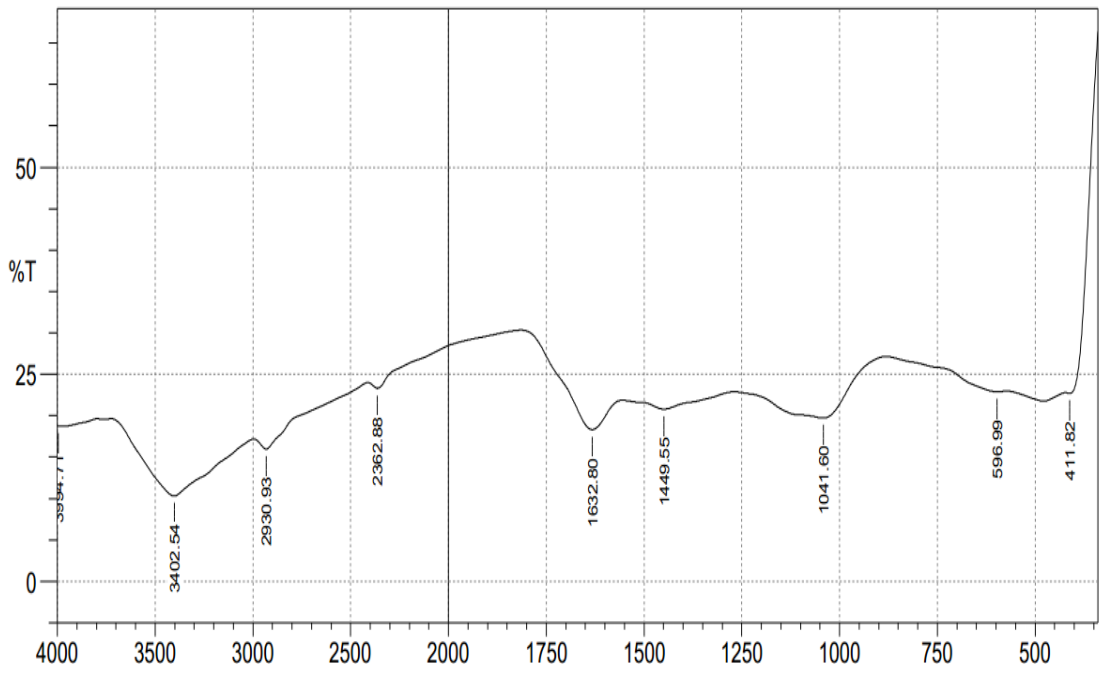

Figure 4.1: FT-IR absorption spectrum of CM extract

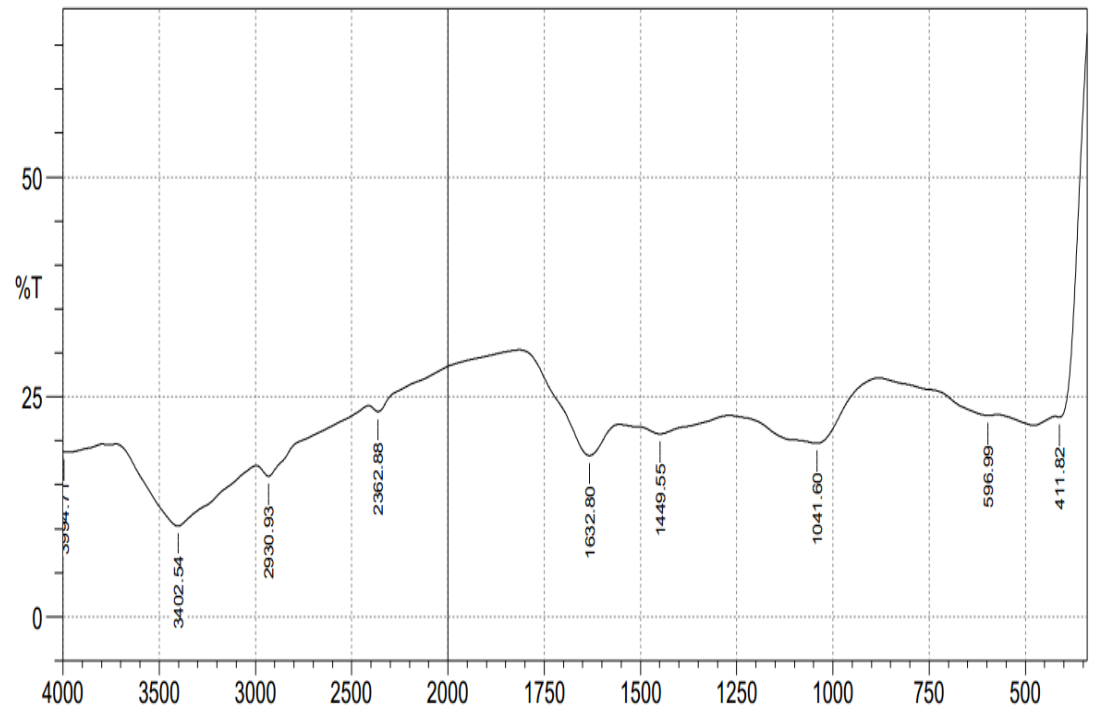

Figure 4.2: FT-IR absorption spectrum of CG extract

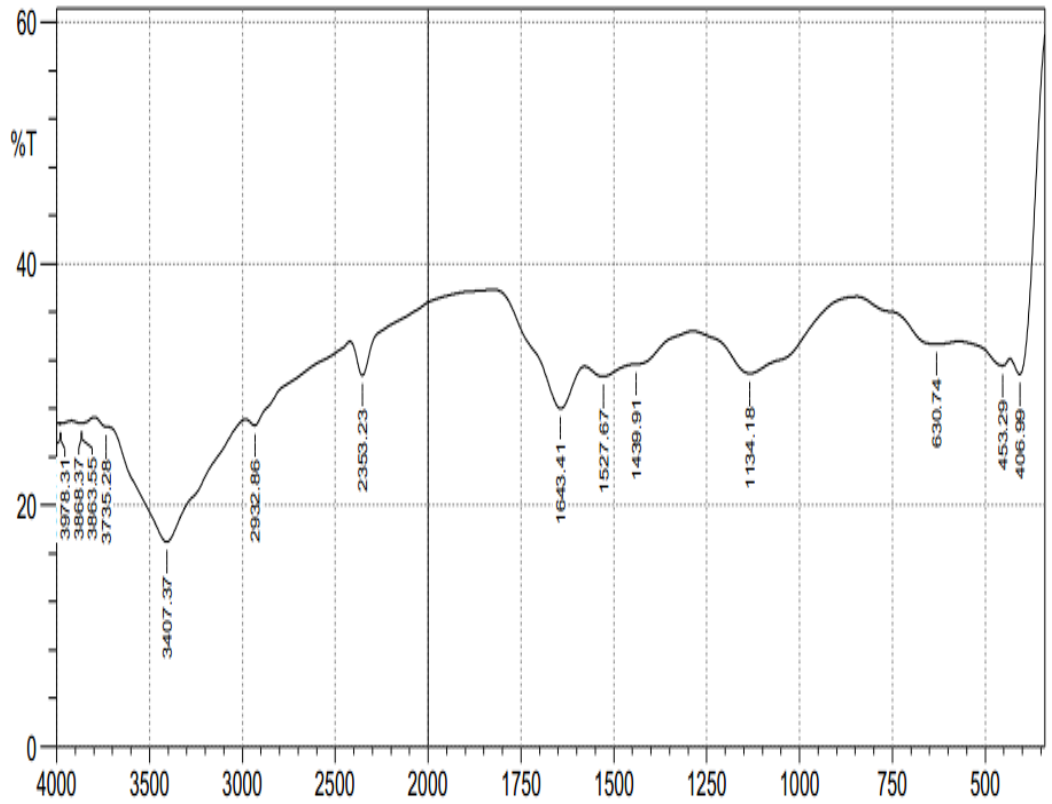

Figure 4.3: FT-IR absorption spectrum of FE extract

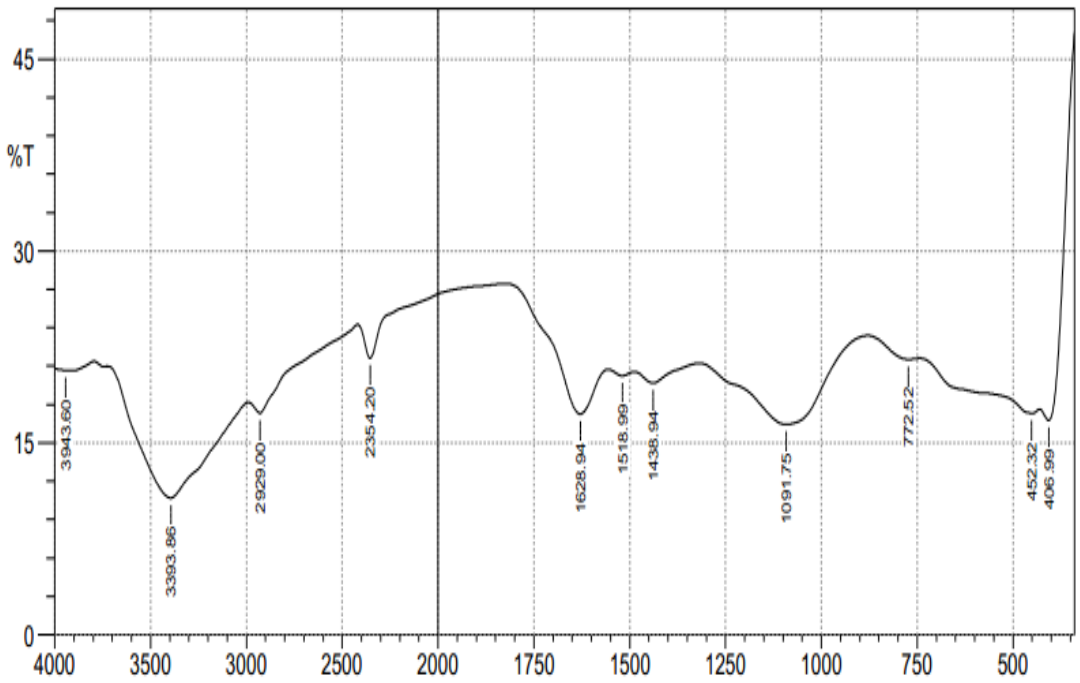

Figure 4.4: FT-IR absorption spectrum of FP extract

and this indicate the presence of the following functional groups: C-I, C-Br, C= C, CH_2, OH, C-H, and N-H for which the library assignment from the FT-IR are alkyl halides, alkanes, alkenes, alcohol aromatic compounds and amides. The FT-IR spectrum of CG has frequency bands around 406.99, 519.83, 655.82, 1041.60, 1452.45, 1509.35 and 1640.51. These indicate the presence of C-I, C-Br, = C-H, C= C-CH_2 – OH, C-H, C=C, C= O, respectively.

The FE spectrum shows the presence of functional groups from the following frequency bands: 406.99, 772.52, 1091.75, 1518.99, 1628.94, 2929.00 and 3393.86 cm^{-1} indicating the presence of C-I, C-H, C-O, N-H, O-H. The FT-IR bands of FP are 406.99, 453.29, 630.74, 1134.18, 1527.67, 1643.41 and 3407.37cm^{-1} which indicate C-I, C-O, N-H, C=O. The extracts were found to contain many functional groups such as alkyl halides, Amides, Amines, alcohols, alkenes and alkyls, aromatic compounds. From the FT-IR Spectrum, the plant extracts may be considered to have chemical constituents that are features of good green inhibitors (Helen *et al.*, 2014 and Sangeetha *et al*., 2012).

4.1.3 Gas Chromatography - Mass Spectrometry (GC-MS) analysis of the extracts

i.*Combretum micranthum*: GC-MS spectra of CM plant extract is shown in Figure 4.5. It detected all organic species present and each peak area in the chromatogram was proportional to the amount of the organic compound(s) forming that peak. The analyses of CM extract by GC-MS show ten components, as presented in Appendix V. These include the retention time, compound names, molecular formula and molecular weight.

ii. *Combretum Glutinosum*: The GC-MS Spectra of methanol extract of CG leaves and its various compounds are presented in Figure 4.6. The analysis of CG extracts by GC-MS show eleven components, as shown in Appendix VI. These include the retention time, compound names, molecular formula and molecular weight.

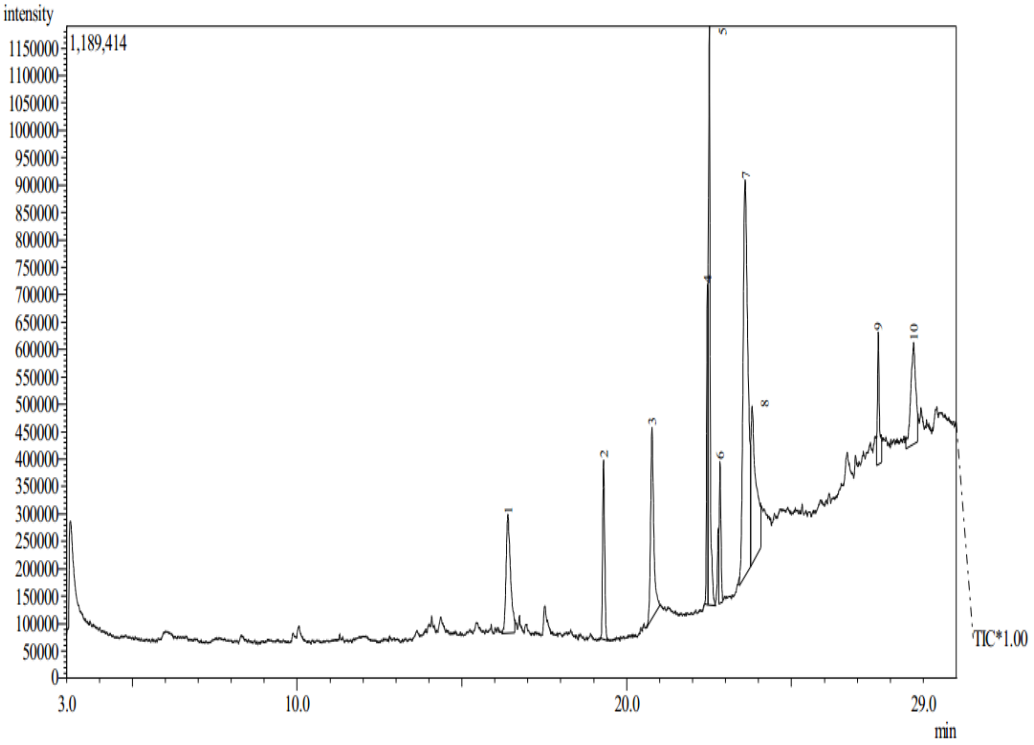

Figure 4.5: Chromatogram and Corresponding Mass Spectra of CM extract

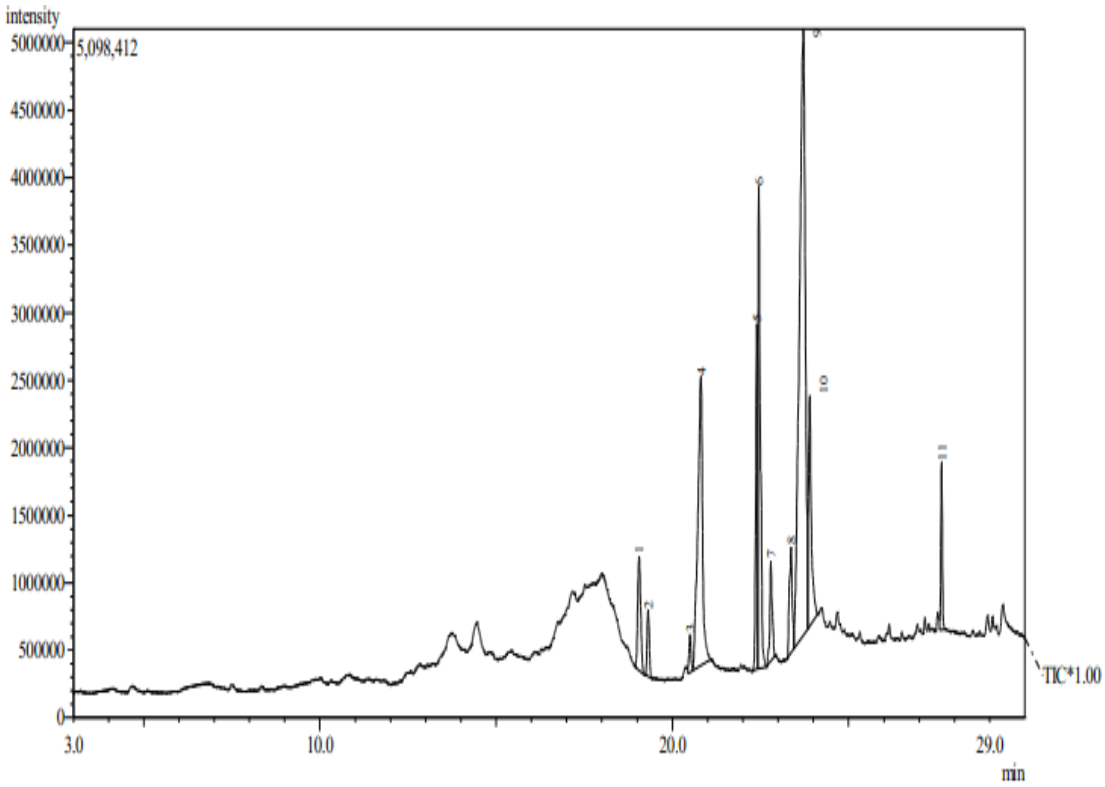

Figure 4.6: Chromatogram and Corresponding Mass Spectra of CG extract.

iii. *Ficus Exasperata*

The GC-MS Spectra of methanol extract of *Ficus Exasperata* is presented in Figure 4.7.The analysis of FE extract by GC-MS shows fourtheen components, as presented in Appendix VII.

iv.*Ficus Platyphylla*

The Spectra in Figure 4.8 shows the GC-MS of FP extract and the analysis shows seven components, as shown in Appendix VIII. The results obtained from the GC-MS revealed that the plant extract has functional groups having N, O, P, S atoms in them. The inhibitive effect of the extracts could be attributed to the presence of these phytochemical constituents in the plant extracts which are the centers of adsorption which may likely make these extract good corrosion inhibitors. Similar result has been reported by (Ambrish *et al.*, 2010., Johnsisrani *et al*., 2012). The constituent of CM, CG, FE and FP extracts having multiple bonds in them through which they get adsorbed onto the metal surface. The high performance of these extracts could also be due to large size of constituent's molecule which covers wide areas on the metal surface and thus retarding the corrosion. This agreed with the report elsewhere (Ambrish, *et al*., 2010).

4.1.4 Physico-chemical analysis of the plant extracts

The physico-chemical results of the plant extracts such as pH, density, solubility, viscosity and biodegradability tests are presented in Table 4.1

i. pH value

From the results, the pH values of the extracts were all in the acidic region but near neutral. CM has a pH value of 4.24, CG (5.25), FE (6.32) and FP (6.47) which are slightly acidic which is not bad to be used as inhibitor.

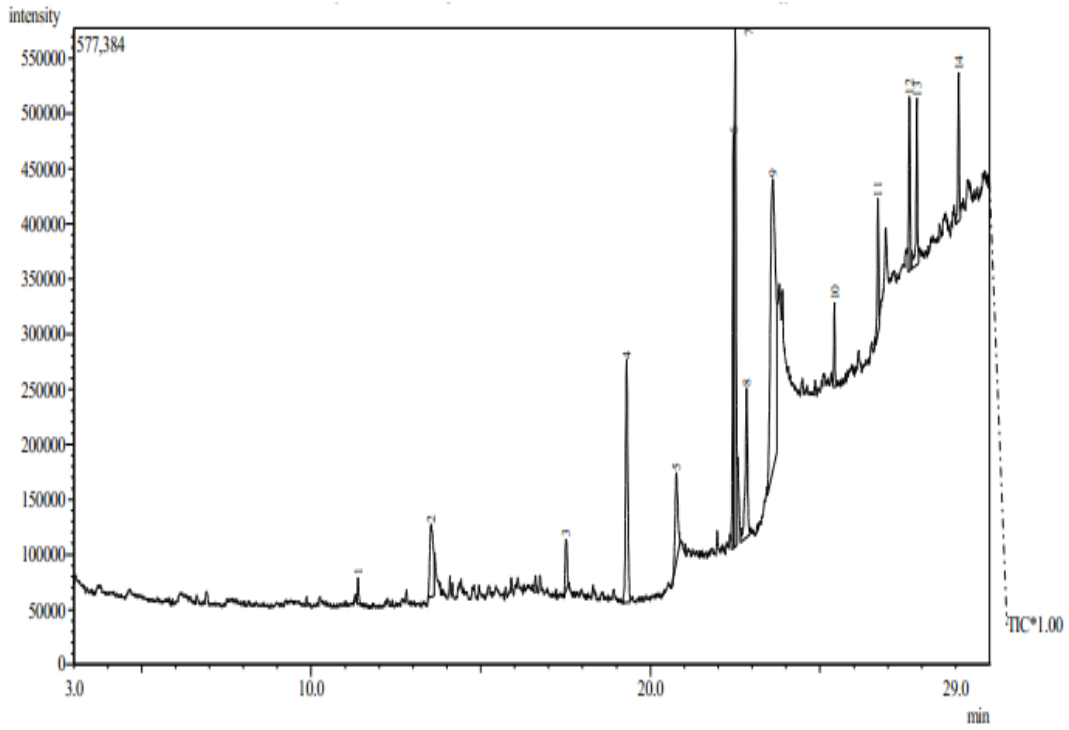

Figure 4.7: Chromatogram and Corresponding Mass Spectra of FE extract .

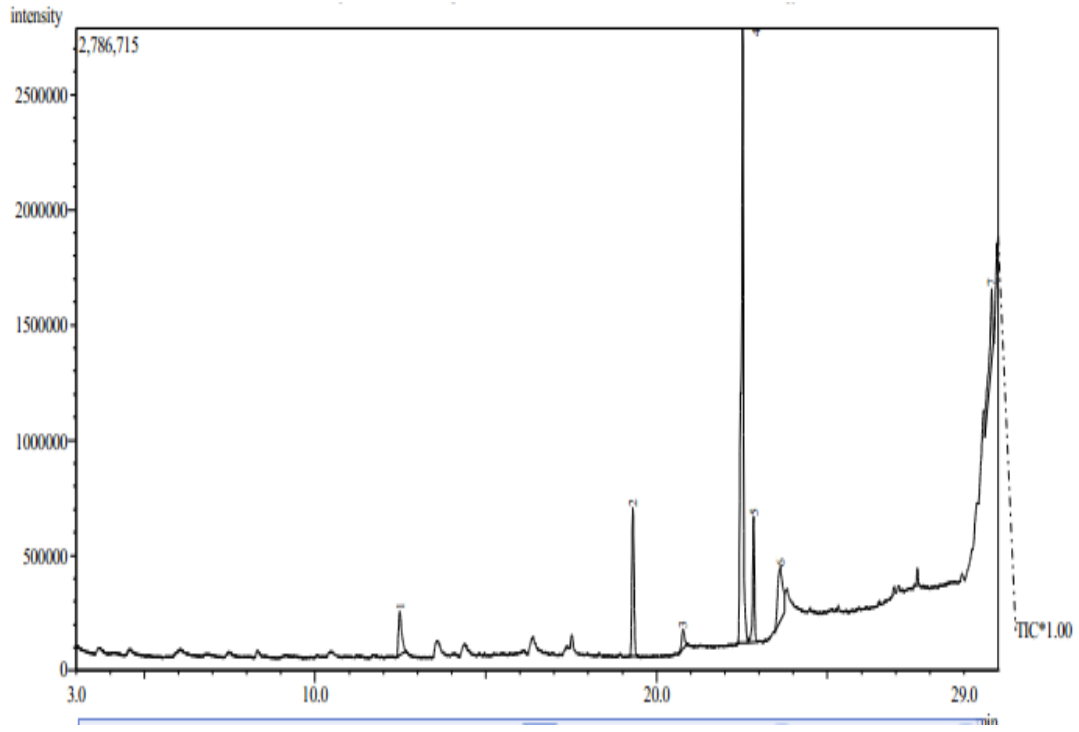

Figure 4.8: Chromatogram and Corresponding Mass Spectra of FP extract.

ii. Density

The density of the extracts differs slightly from one another as CM has a density of 0.9906 g/cm^3, CG (0.8930 g/cm^3), FE (0.9356 g/cm^3) and FP (0.9490 g/cm^3). There is a slight difference in density value obtained which might be due to the original nature of the extracts as indicated during phytochemical screening.

iii. Solubility

The values obtained from the solubility test show that the extracts are more soluble in butanol and hydrochloric acid than in distilled water. This is an indication of the solvent absorption characteristics of plant extracts as a result of increase in the degree of solvent molecule interaction. Generally, it can be established from the test that the extracts are soluble in butanol, hydrochloric acid and distilled water at 30 ^{O}C, 50 ^{O}C and 70 ^{O}C.

iv. Viscosity

The viscosity result of the plant extracts show that the plants are more viscous at 30^{O}C and their viscosity level decreases as temperature increases. CM and CG that fall in the same family of plant (Combratacea) happen to have the same viscosity while FE and FP of the same plant family (Moracea) also have the same viscosity. It is established that the viscosity of the extracts will not resist the flow while used as admixture coating for the alloy. Similar result was reported. The result is presented in Table 4.1.

v. Biodegradability Test

Biodegradability provides an indication of the persistence of any particular substance in the environment and is the yardstick for assessing the eco friendliness of substances. BOD data are widely used in environmental engineering practice especially in determining the strengths of both domestic and industrial wastes. It is a test that gives a measure of the amount of

Table 4.1: Physicochemical analysis test

Parameters	**CM**	**CG**	**FE**	**FP**
pH (30 ^{0}c)	4.24	5.25	6.32	6.47
Density (g/cm^3)	0.9906	0.9490	0.8930	0.9356
Viscosity (mPaS)				
• 30 ^{0}C	2.89	2.65	2.30	2,49
• 50 ^{0}C	2.30	2.20	2.01	2.08
• 70 ^{0}C	1.80	1.76	1.61	1.65
BOD^5 (mg/L)	70	90	100	60
Solubility (% w/v)				
➢ Distilled H_2O				
• 30 ^{0}C	PS	PS	PS	PS
• 50 ^{0}C	PS	PS	PS	PS
• 70 ^{0}C	PS	PS	PS	PS
➢ Butanol				
• 30 ^{0}C	S	S	HS	HS
• 50 ^{0}C	S	S	HS	HS
• 70 ^{0}C	S	S	HS	HS
➢ HCl				
• 30 ^{0}C	S	S	HS	HS
• 50 ^{0}C	S	S	HS	HS
• 70 ^{0}C	S	S	HS	HS

Keys: S = Soluble, PS = partially Soluble, HS = Highly Soluble

biologically, oxidisable organic matter present that can be used to determine the rates at which oxidation will occur. The BOD of FP extract was found to be least with a value of 70 mg/l while FE has the highest with a value of 100 mg/l. This indicates the level of oxygen dissolving in the plant in solution and hence also signals biodegradation since oxygen is required for such and is a pre-requisite for corrosion to occur. However, the level of BOD is very low in oxygen intake which is not a threat to the plant extracts to be used as inhibitor (Emmanuel *et al*., 2009).

4.2 Gravimetric mass-based loss measurements

4.2.1 Effect of inhibitor concentration on the corrosion rates of the alloy in 3.5% NaCl solution

The corrosion inhibitor efficiency of the plant extracts was determined in a test solution of 3.5 % NaCl solution on the alloy at various temperatures, concentrations and exposure time. Figures 4.9 – 4.11 are the variations of the corrosion rates against inhibitor concentration of Al-Si-Mg alloy in the presence and absence of CM extract in the aqueous medium. Figures 4.12 – 4.14 are for CG with optimum concentrations at 0.4 v/v. Figures 4.15 – 4.17 are for FE having optimum at 0.4 v/v and Figures 4.18 - 4.20 v/v are for FP with optimum concentrations at 1.0 v/v, while Figures 4.21 – 4.23 show Sodium chromate with optimum concentrations of 1.0 v/v.

The results obtained show that the corrosion rates decreased in the presence of the extracts compared with un-inhibited samples. The results are presented in Appendices IX - XXVIII. The decrease in corrosion rates with increase in concentration of the extracts depicts their inhibitive potentials in the medium. However, the corrosion rates increased with increase in temperature as expected since rate of reaction increase with increase in temperature and similar results have been reported (Adejo *et al.*, 2013; Awe, 2015; Kasim, 2013). The decrease in corrosion rates could be due to the formation of protective thin films

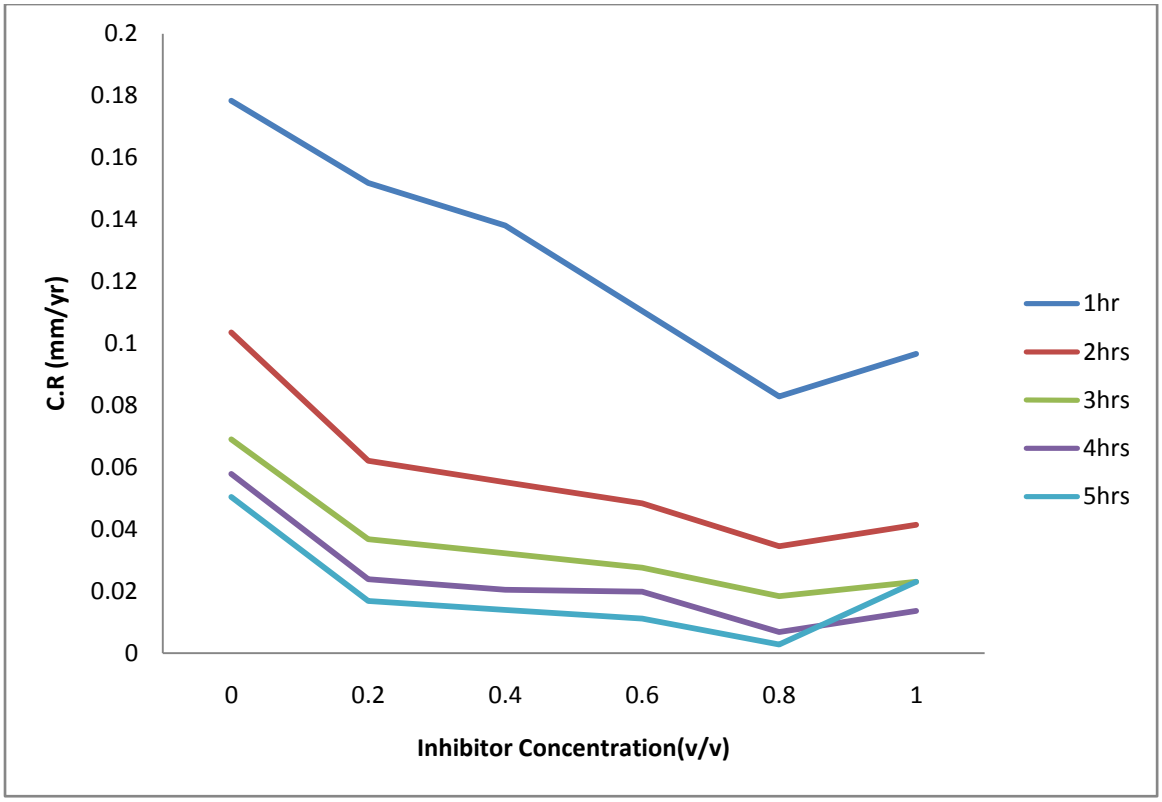

Figure 4.9: Variations of Corrosion Rates with Inhibitor Concentration of CM at 30^0C

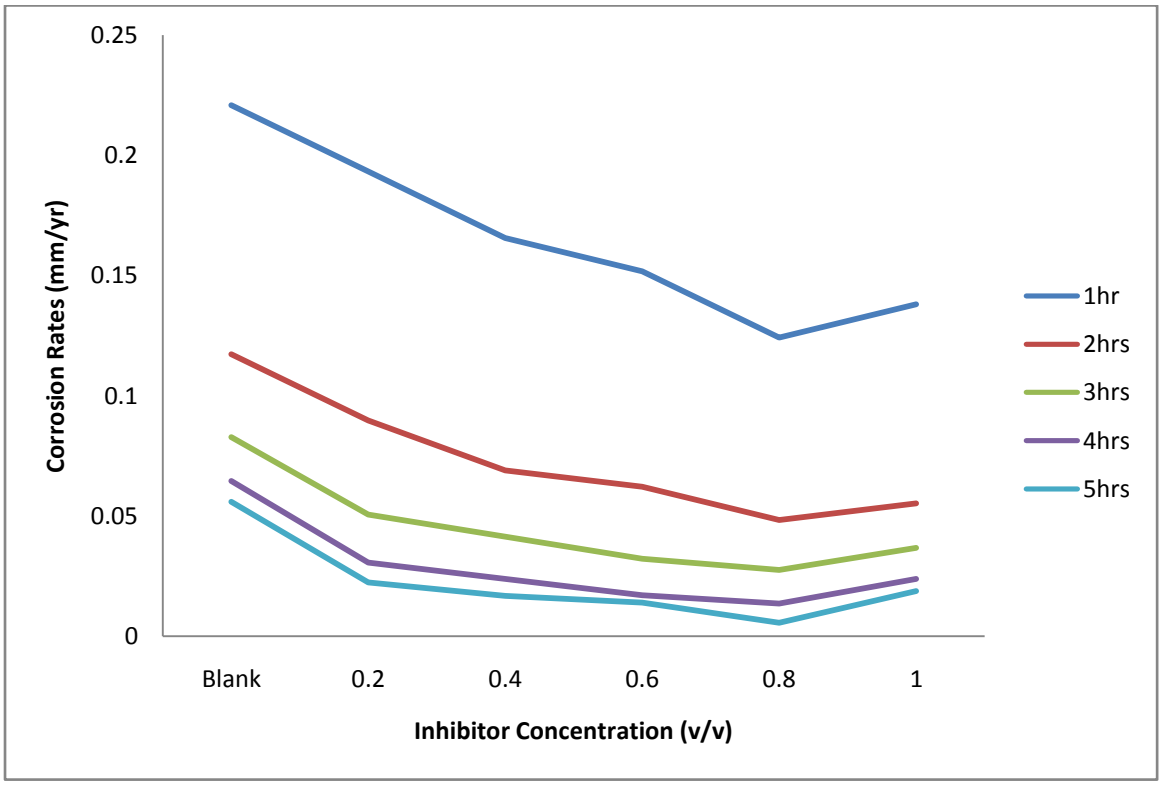

Figure 4.10: Variations of Corrosion Rates with Inhibitor Concentration of CM at 50^0C

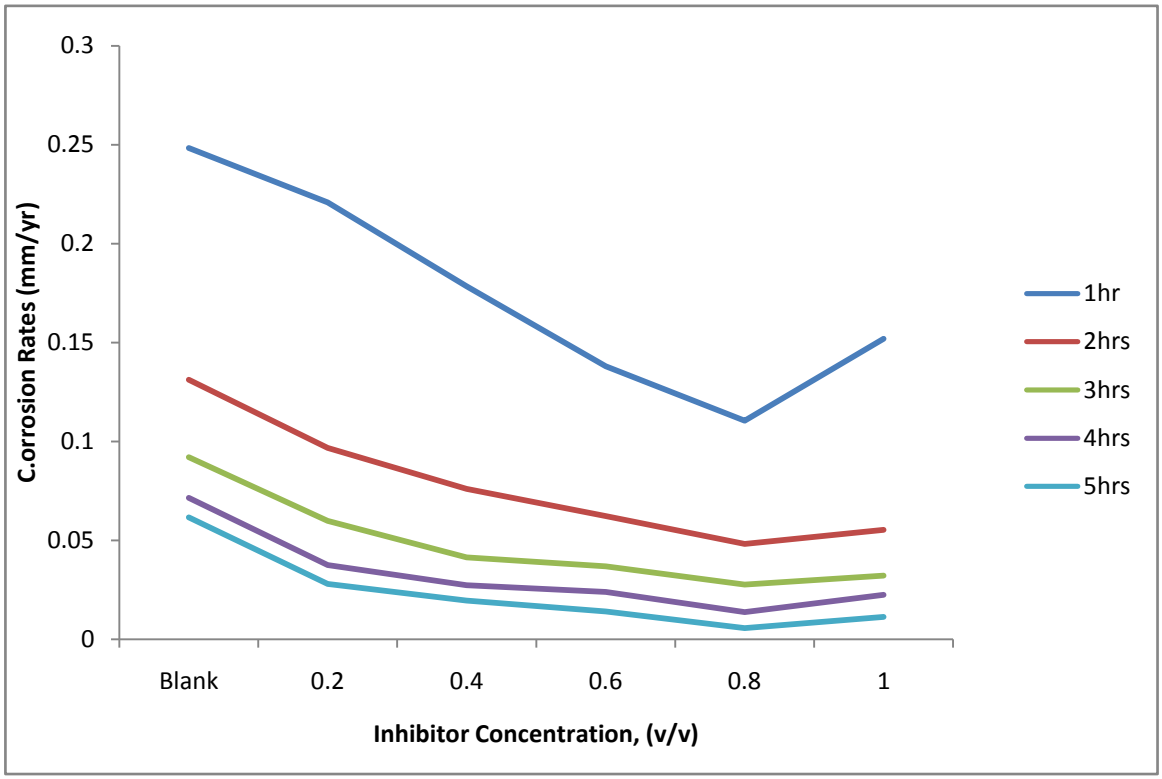

Figure 4.11: Variations of Corrosion Rates with Inhibitor Concentration of CM at 70^0C

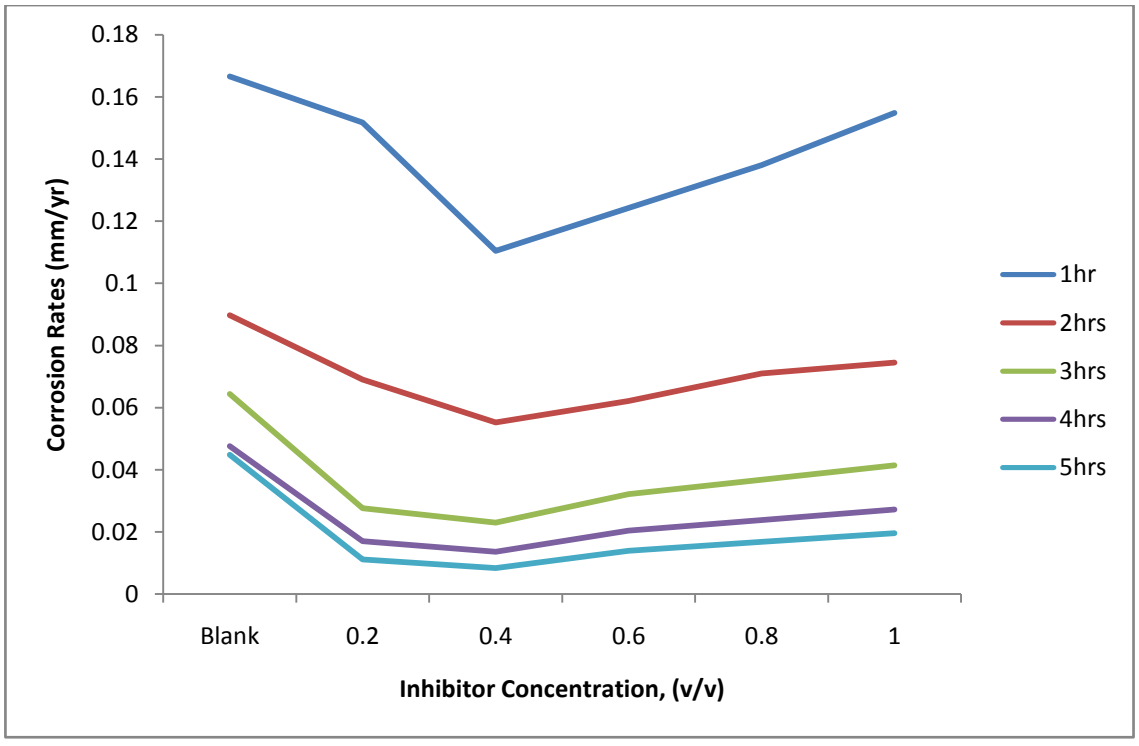

Figure 4.12: Variations of Corrosion Rates with Inhibitor Concentration of CG at 30^0

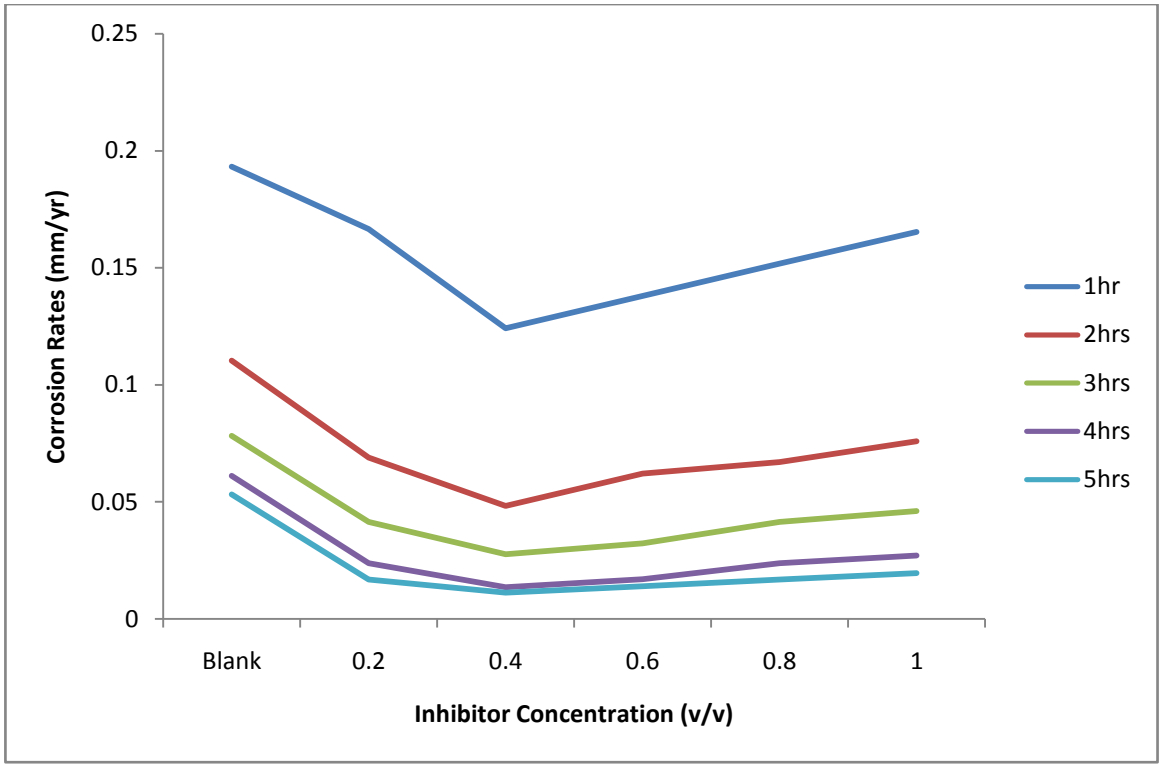

Figure 4.13: Variations of Corrosion Rates with Inhibitor Concentration of CG at 50^0C

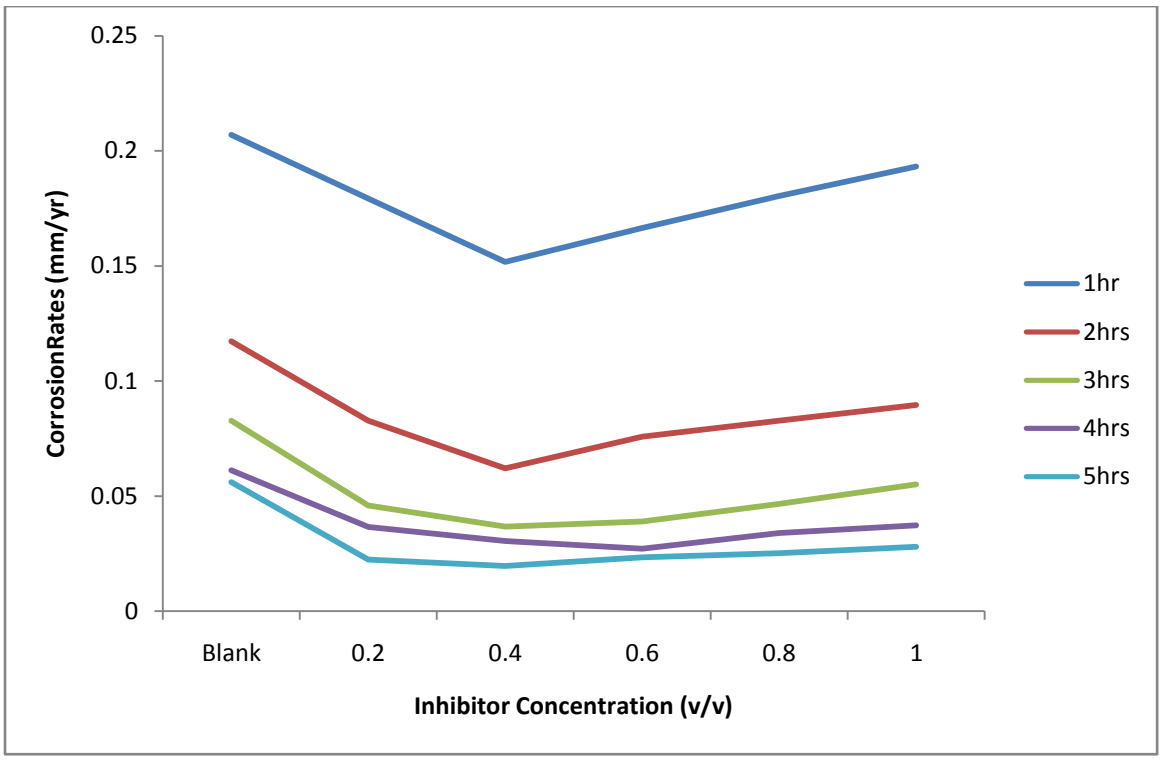

Figure 4.14: Variations of Corrosion Rates with Inhibitor Concentration of CG at 70^0C

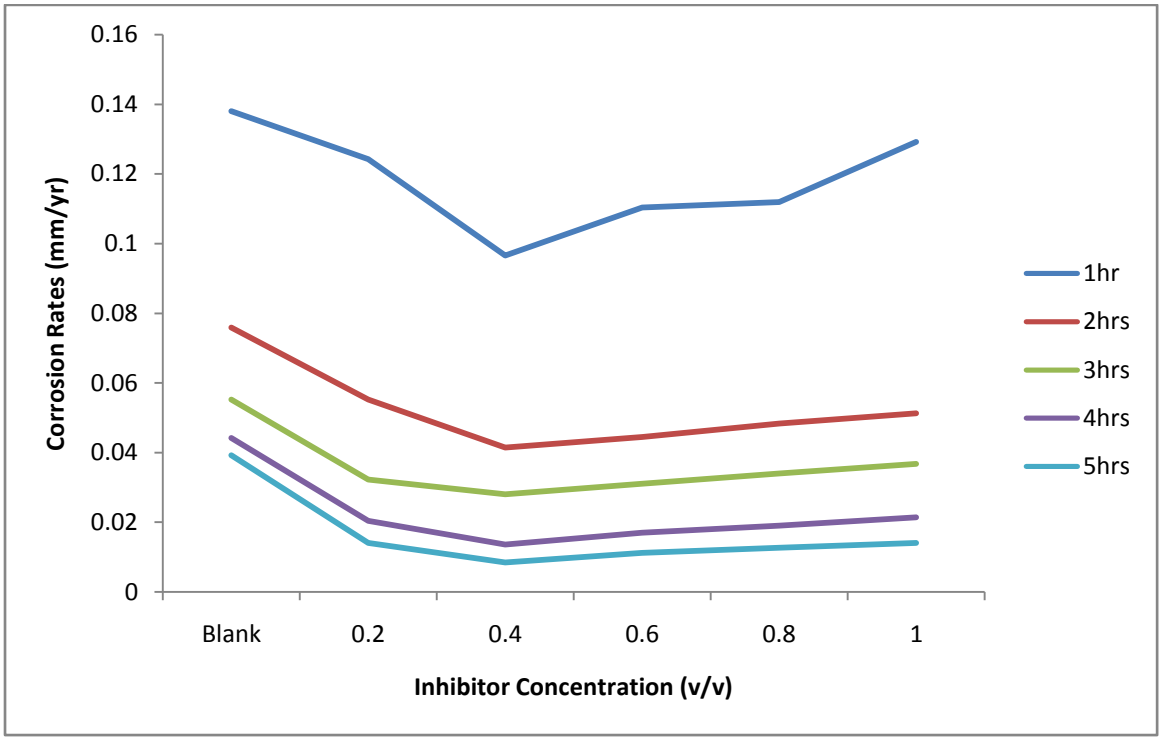

Figure 4.15: Variations of Corrosion Rates with Inhibitor Concentration of FE at 30^0C

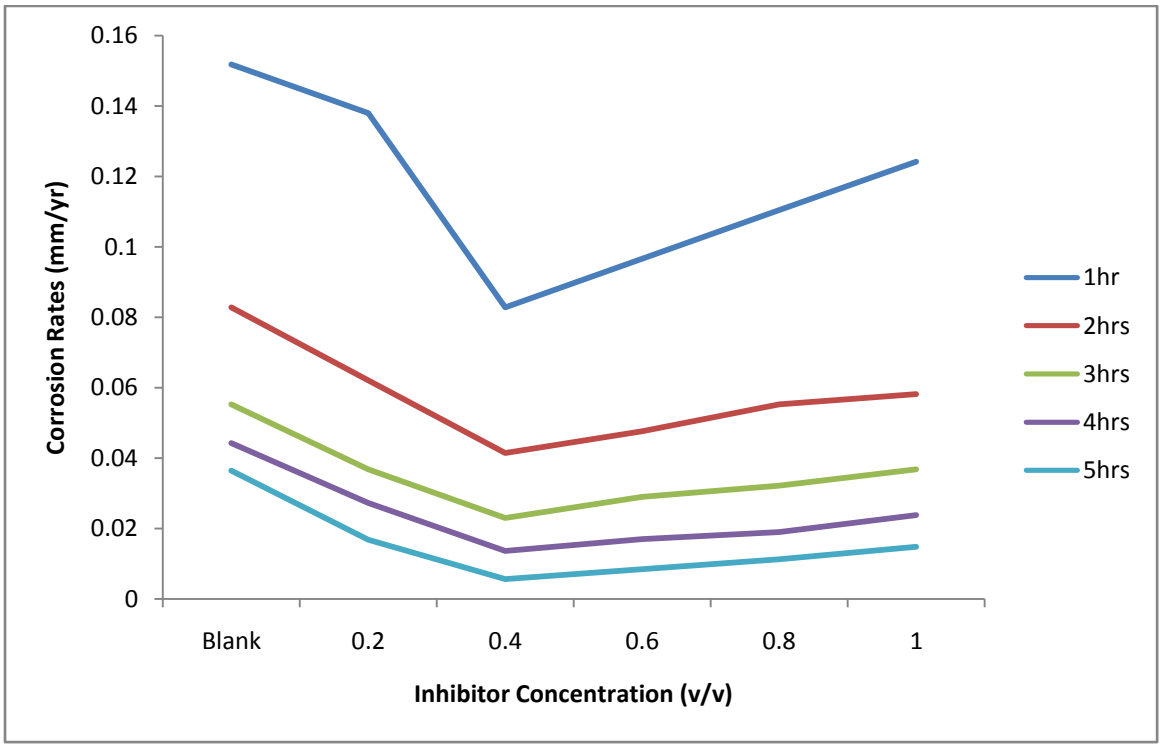

Figure 4.16: Variations of Corrosion Rateswith Inhibitor Concentration of FE at 50^0C

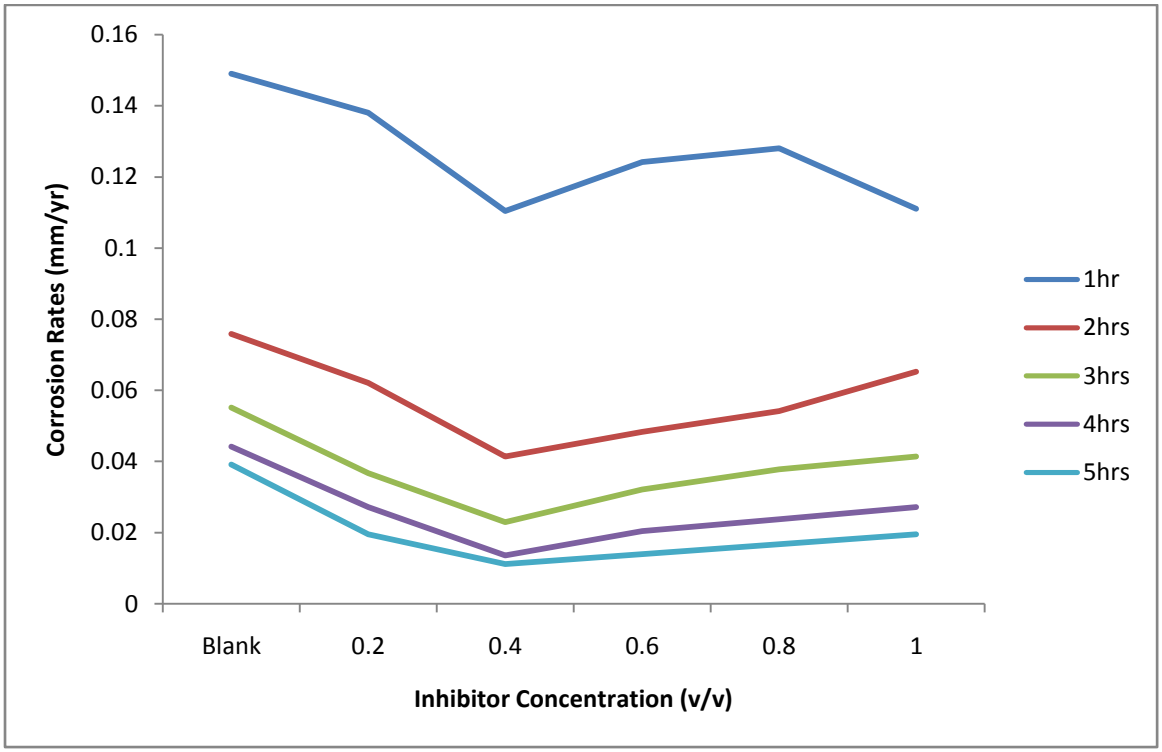

Figure 4.17: Variations of Corrosion Rates with Inhibitor Concentration of FE at 70^0C

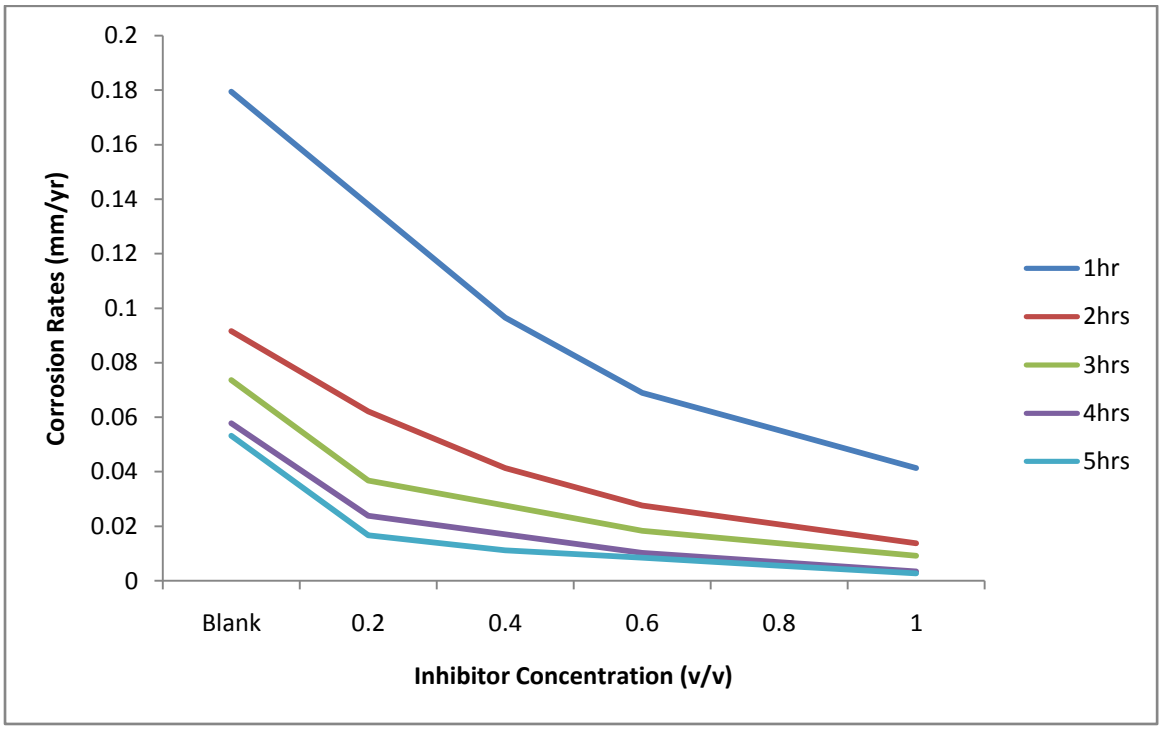

Figure 4.18: Variations of Corrosion Rates with Inhibitor Concentration of FP at 30^0C

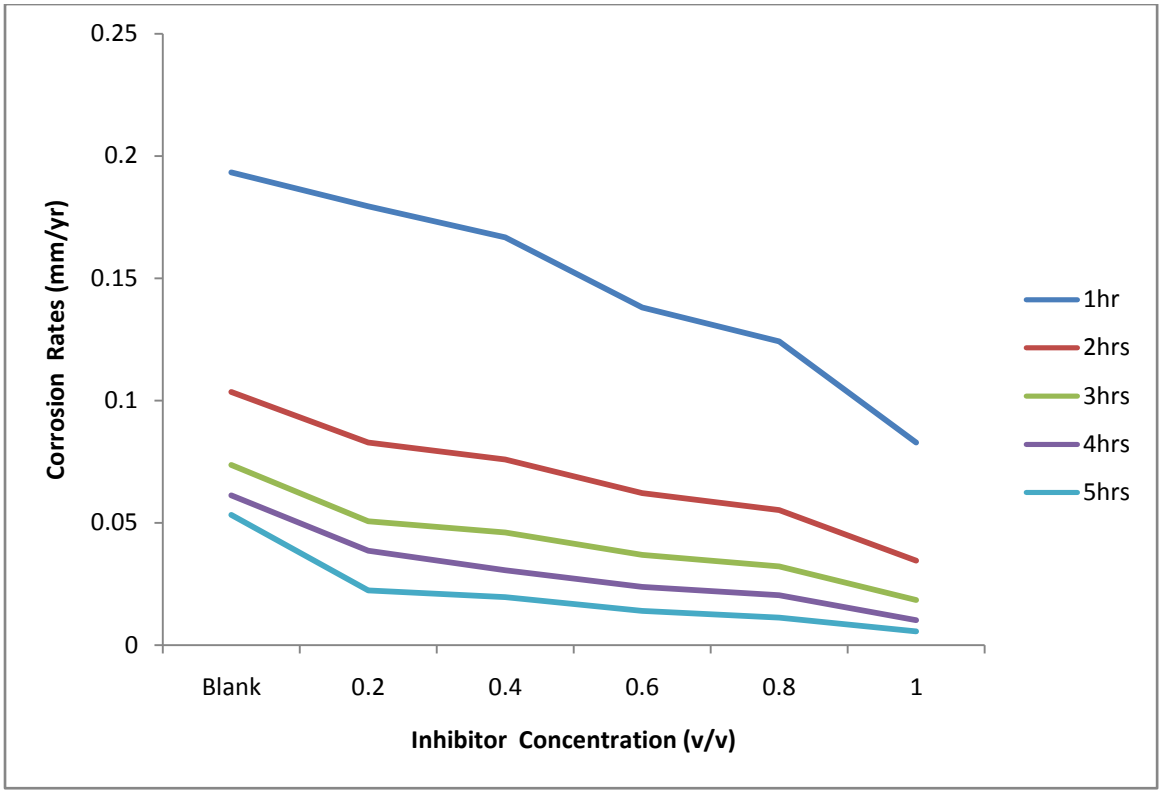

Figure 4.19: Variations of Corrosion Rates with Inhibitor Concentration of FP at 50^0C

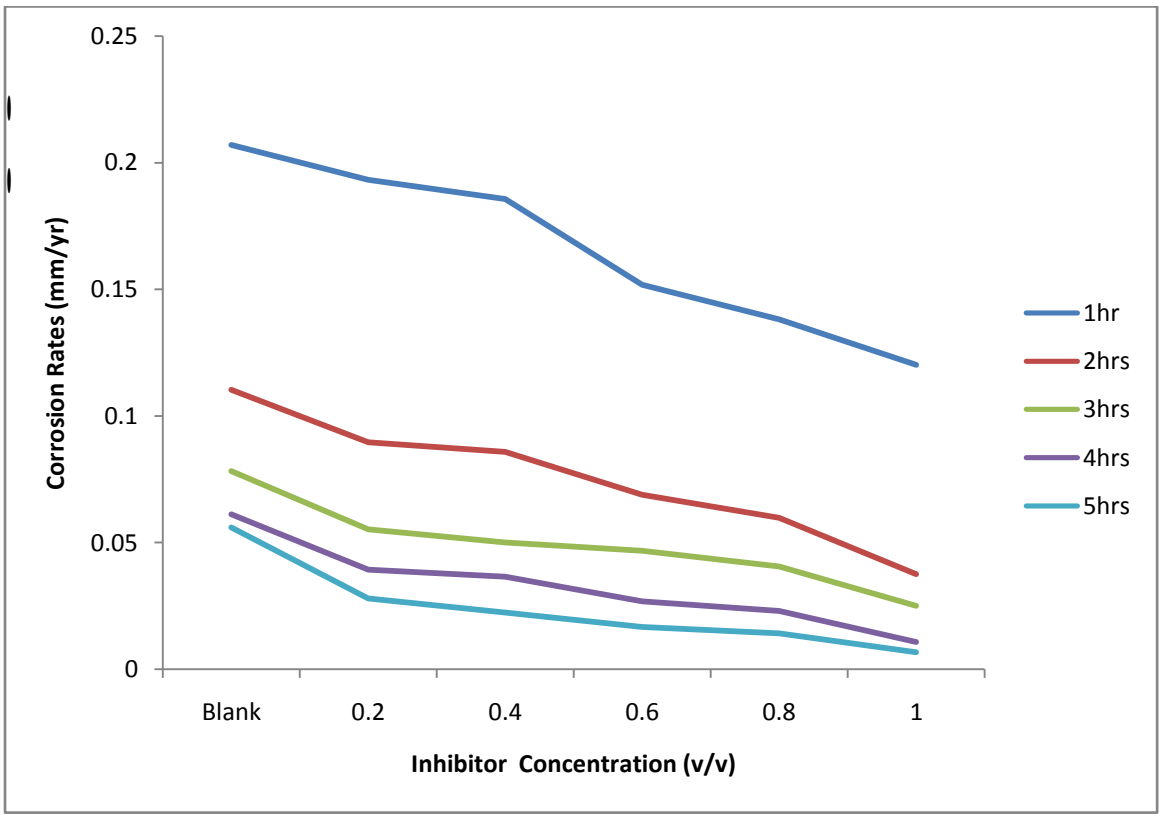

Figure 4.20: Variations of Corrosion Rates with Inhibitor Concentration of FP at 70^0C

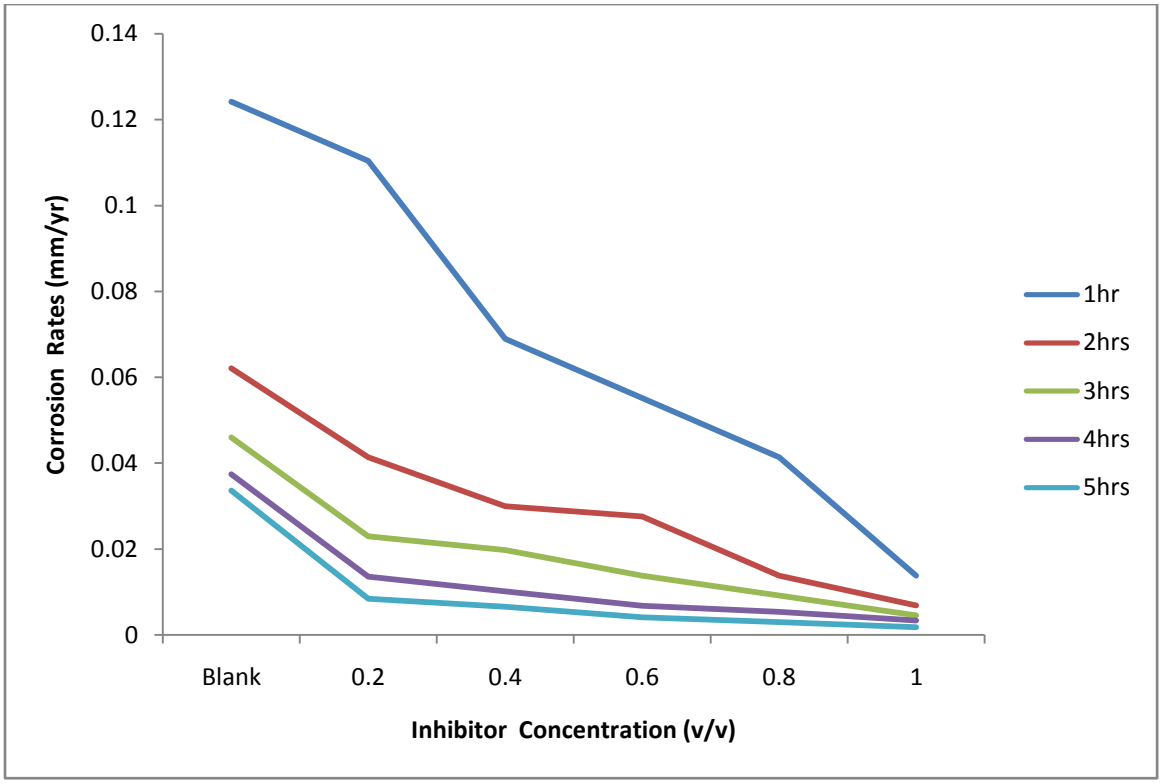

Figure 4.21: Variations of Corrosion Rates with Inhibitor Concentration of Sodium Chromate at 30^0C

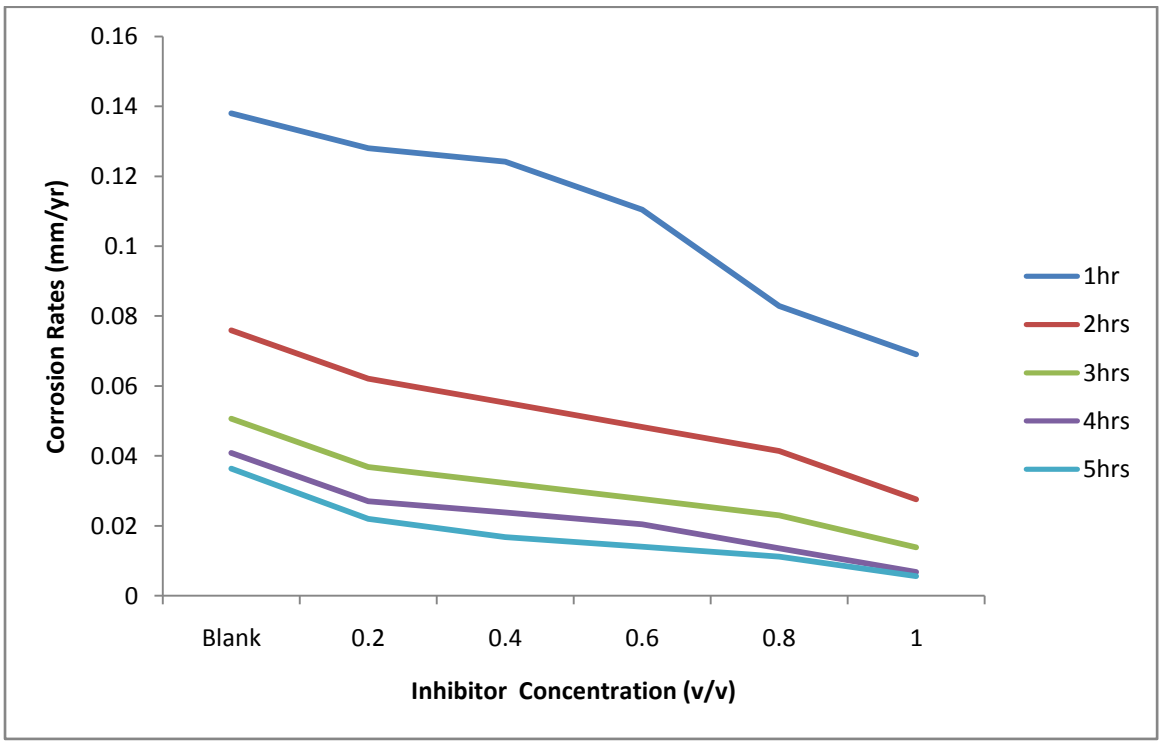

Figure 4.22: Variations of Corrosion Rates with Inhibitor Concentration of Sodium Chromate at 50^0C

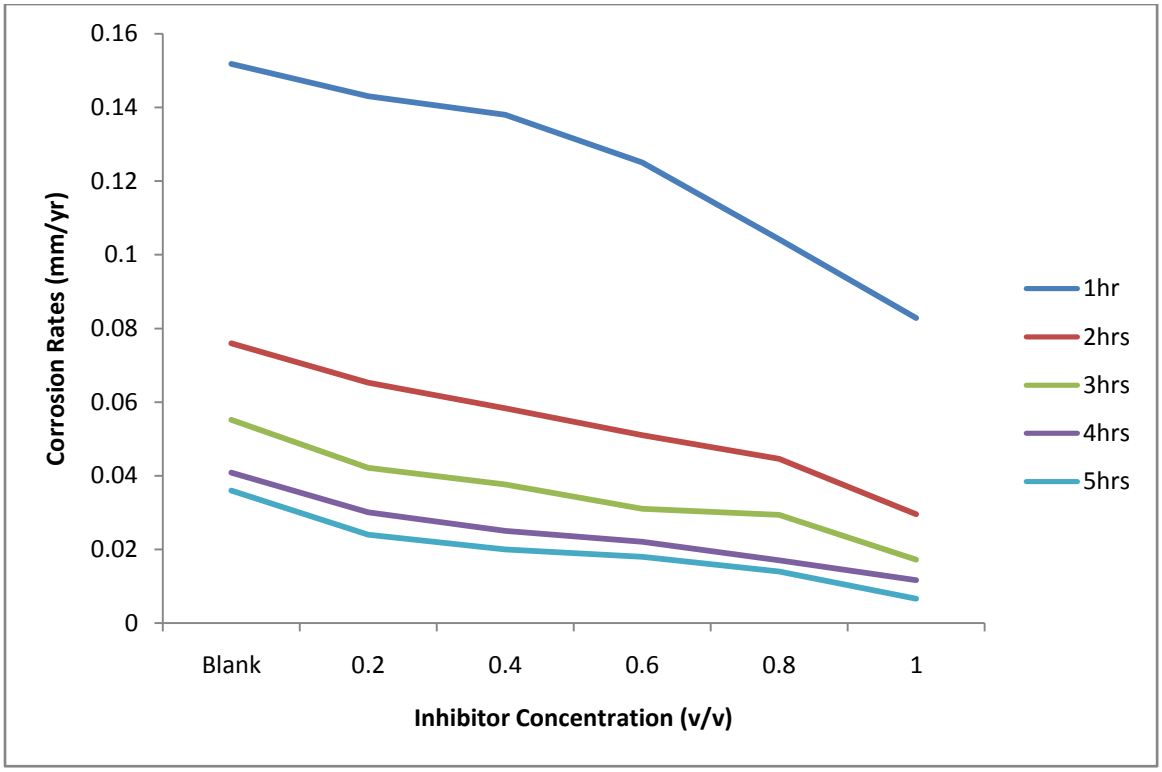

Figure 4.23: Variations of Corrosion Rates with Inhibitor Concentration of Sodium Chromate at 70^0C.

by the inhibitor molecules on the aluminum surface and signifying inhibitive action of the extract. It was equally found that generally, the corrosion rate decreases with increase in exposure time for the four plants studied.

When co-inhibition was considered by combining two different plants extracts together, similar results were obtained, that is the corrosion rate decreased with increase in inhibitor concentrations and exposure time. Since surfactants were believed to enhance the performance of an inhibitor, it was also co-inhibited with the extract. These results are shown in Figures 4.24 – 4.28 and Appendices XXII - XXVIII for different co-inhibition considered. The corrosion rates of the co-inhibited plants were significant. The result obtained when surfactants were added does not improve compare to the extract alone. The performance was in the order as thus: CR of two extracts > CR of single extract > CR of extract with surfactant. The surfactants might have transferred water from the metal surface, interact with the anodic or cathodic reaction sites to retard the oxidation and reduction corrosion reactions and prevent transportation of water and corrosion-active species on the metal surface as reported (Maqsood *et al.*, 2011)

4.2.2 Effect of inhibitors concentrations on exposure time

The effect of inhibitors concentrations on the exposure time is presented in Figures 4.29 – 4.43 and Appendices VIII – XXVIII. Generally, the corrosion rates were found to decrease with increase in the exposure time for all the extracts considered. This was because the performance of the extracts spread over time on to the surface of the alloy and promote inhibition process. Similar results have been reported (Idawu, 2013; Asuke *et al*., 2014; Awe *et al*., 2015).

.

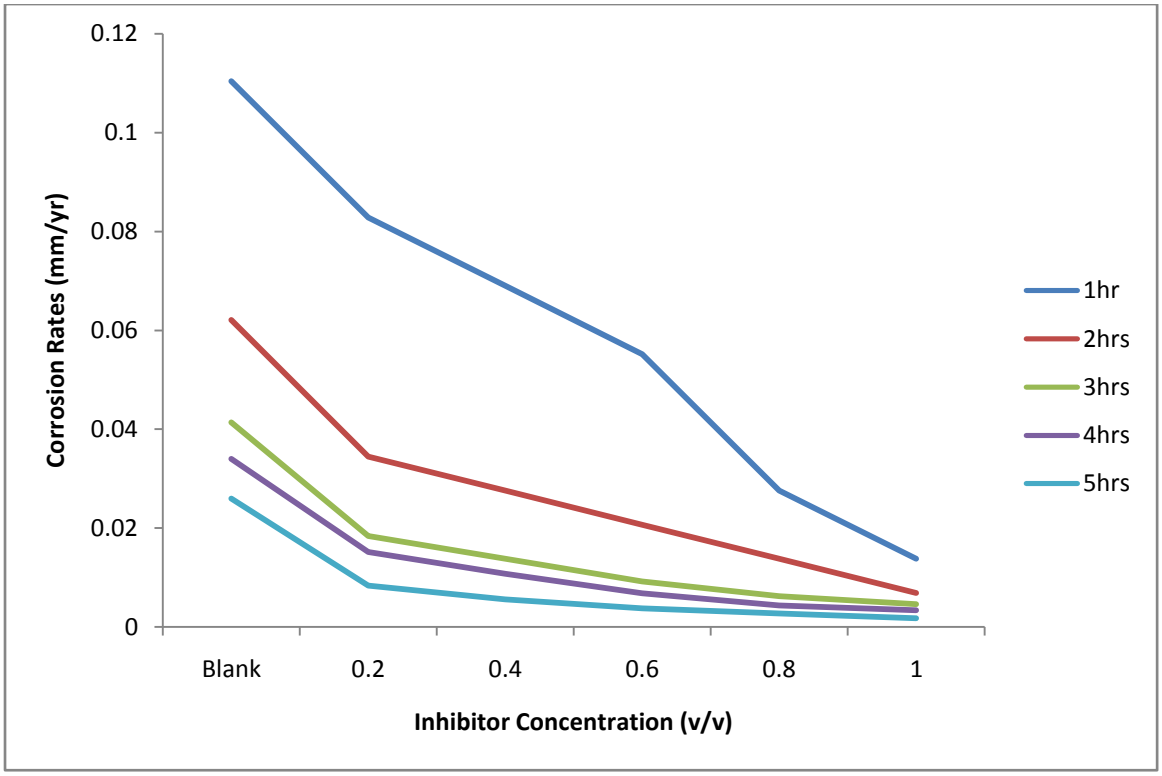

Figure 4.24: Variations of Corrosion Rates with InhibitorConcentration of co-inhibitor (CM with CG) at 30^0C

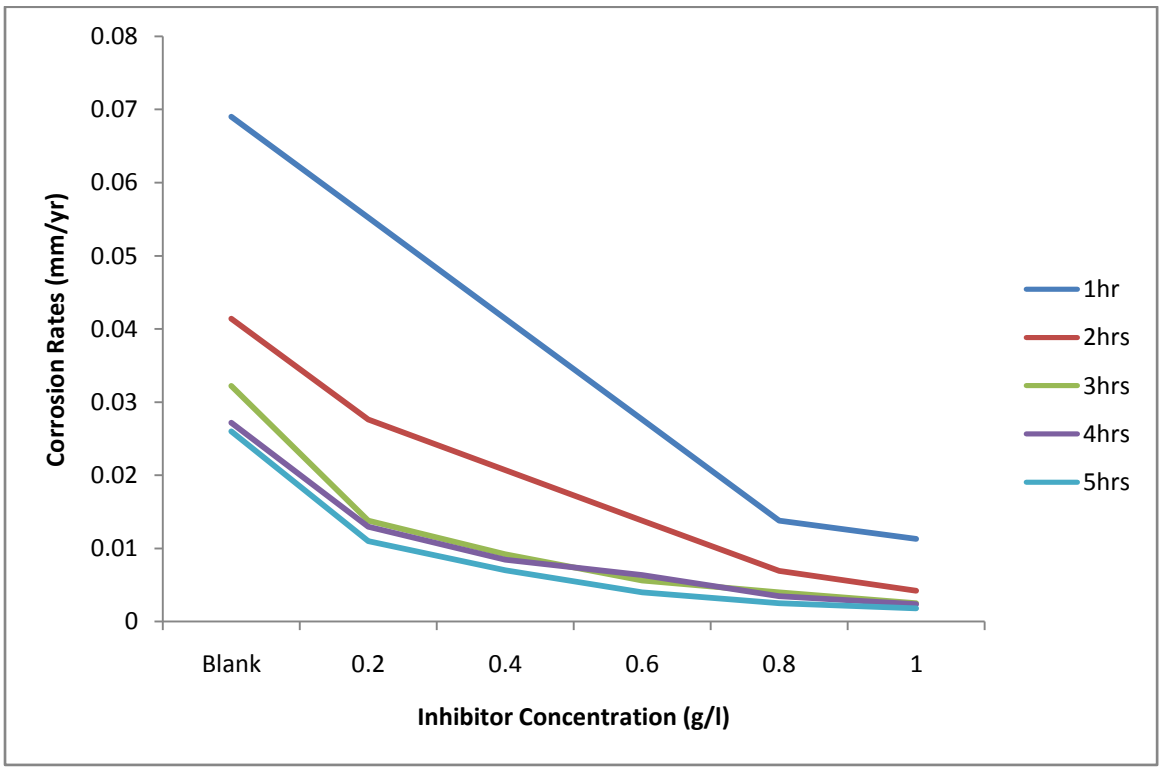

Figure 4.25: Variations of Corrosion Rates with Inhibitor Concentration of Synergy (CM with FP) at 30^0C

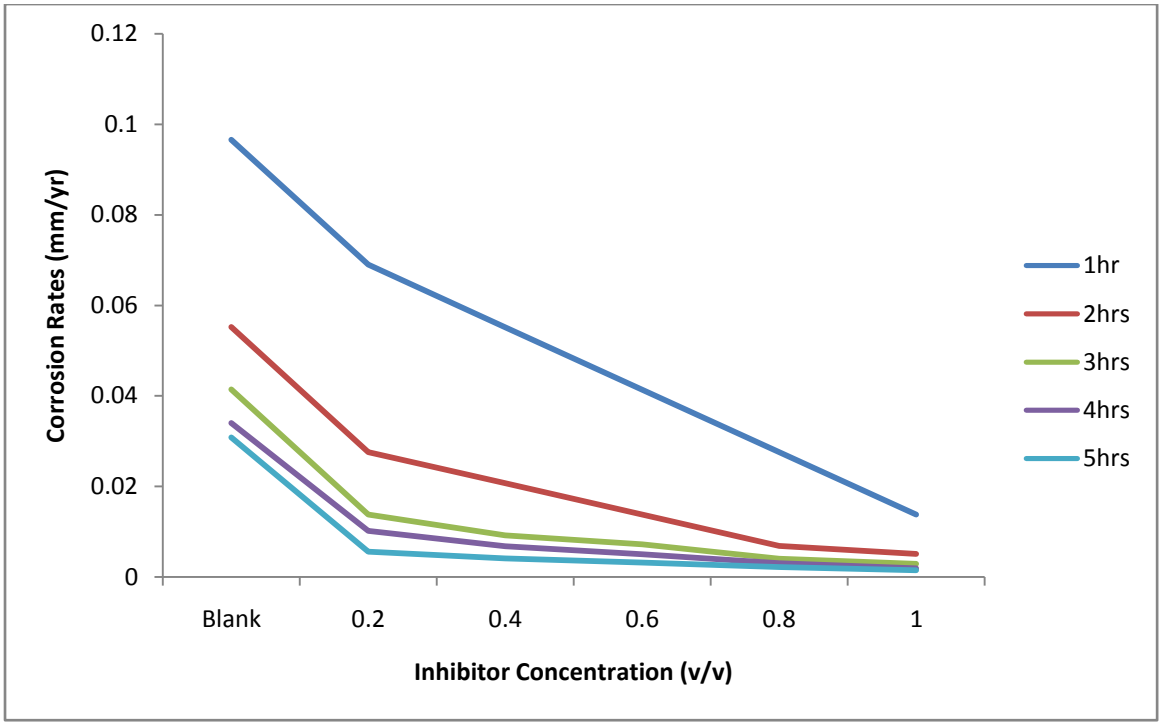

Figure 4.26: Variations of Corrosion Rates with Inhibitor Concentration of Synergy (CG with FE) at 30^0C

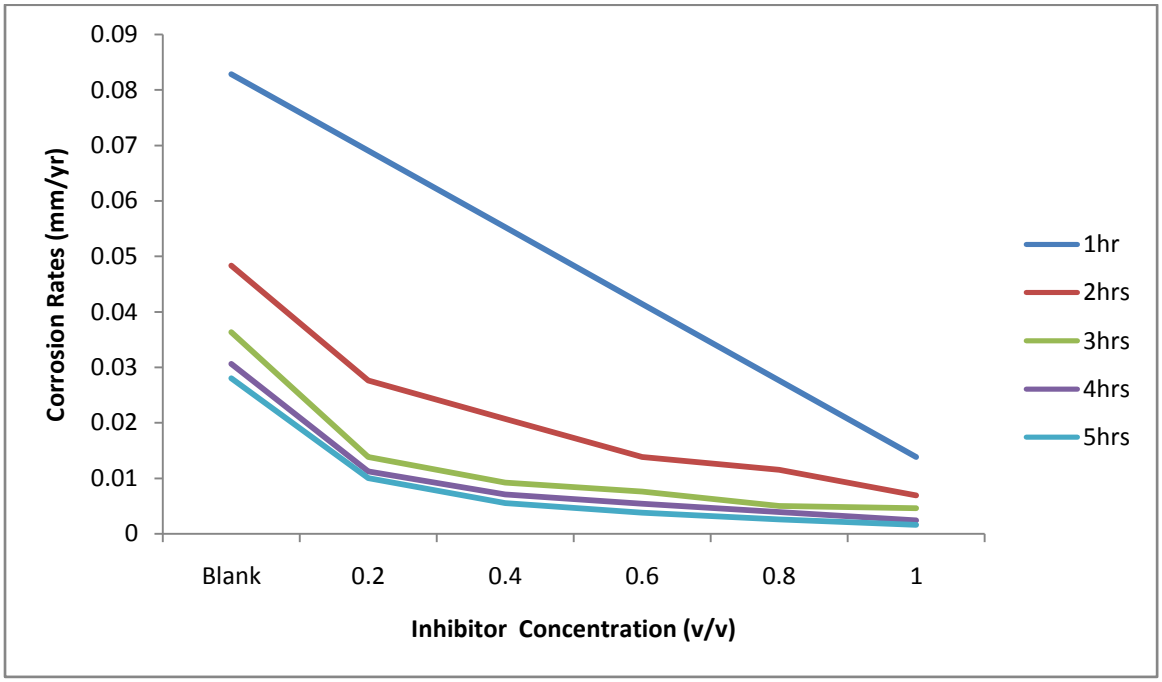

Figure 4.27: Variations of Corrosion Rates with Inhibitor Concentration of Synergy (FE with FP) at 30^0C

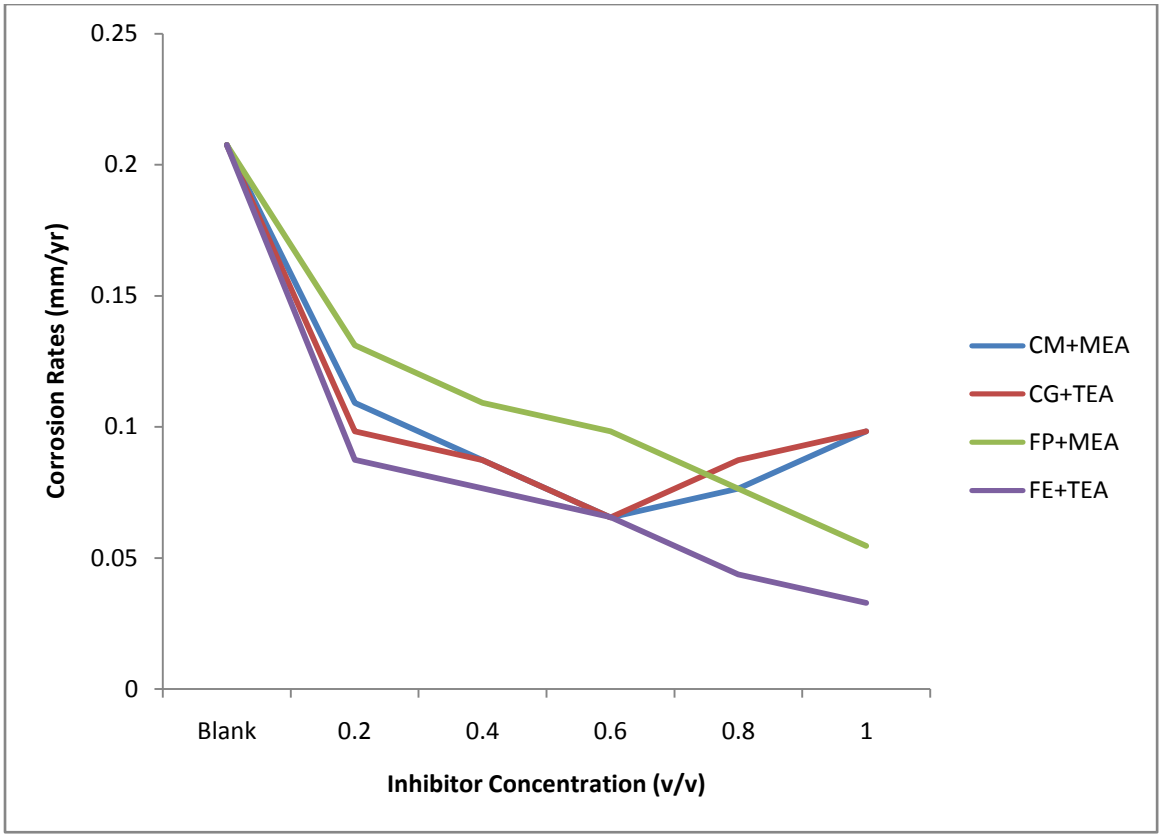

Figure 4.28: Variations of Corrosion Rates with Inhibitor Concentration of extracts with surfactant at 30^0C

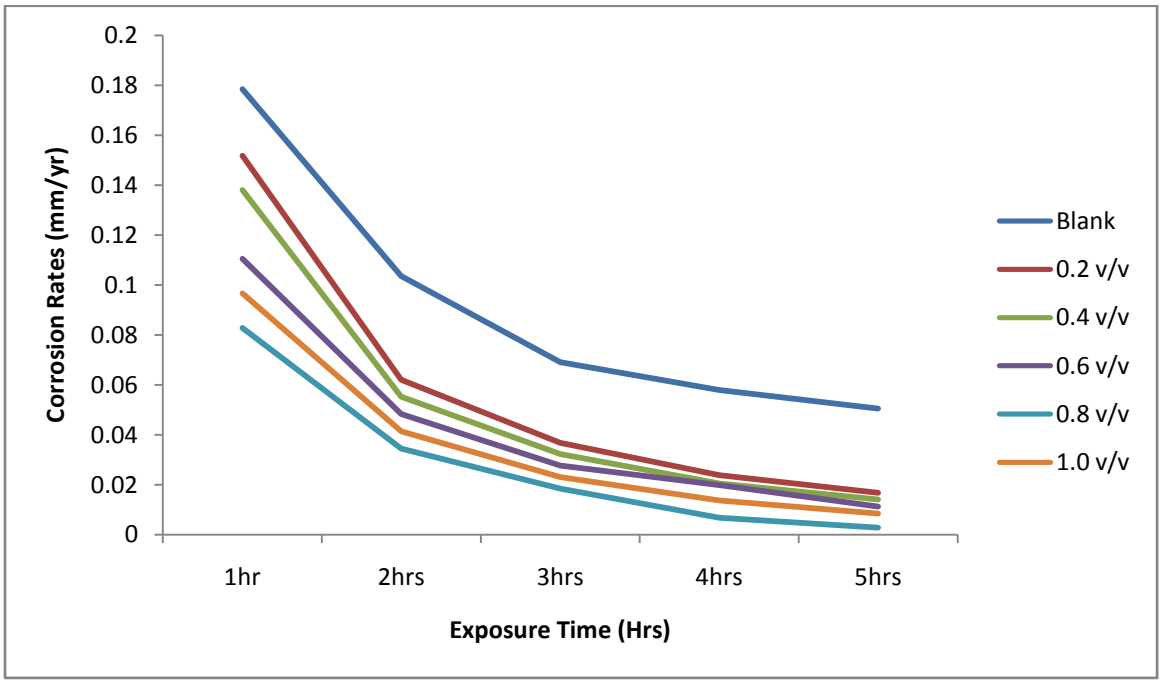

Figure 4.29: Corrosion Rates with Exposure Time of CM at 30 ^{O}C

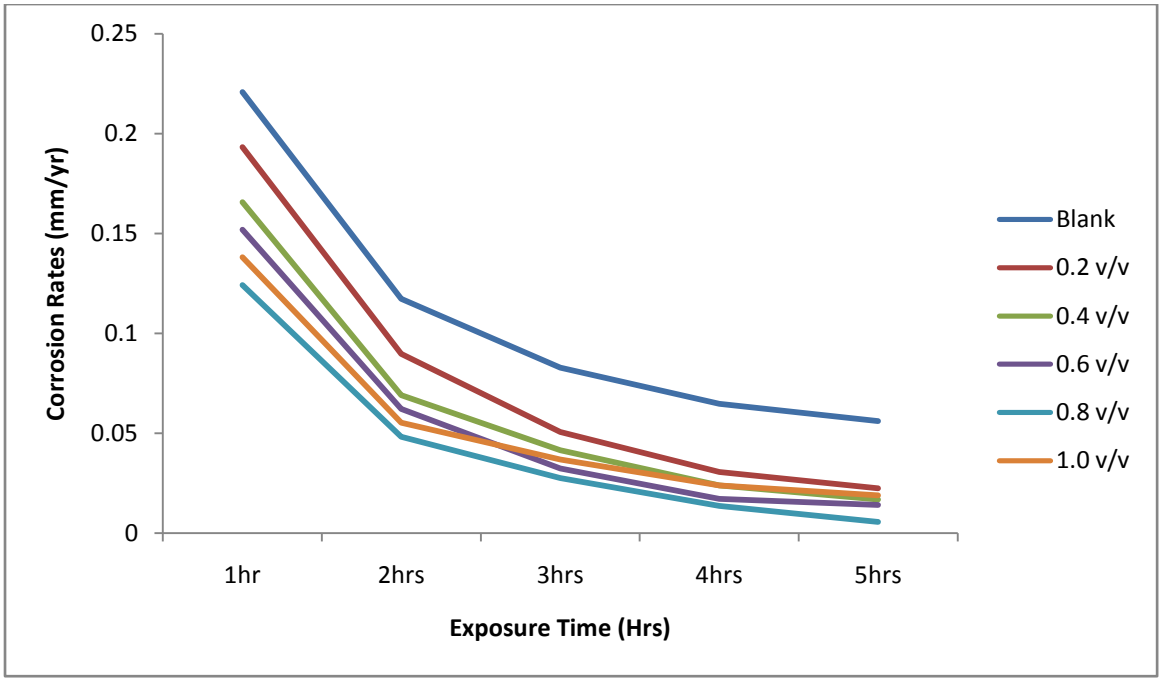

Figure 4.30: Corrosion Rates with Exposure Time of CM at $50^{O}C$

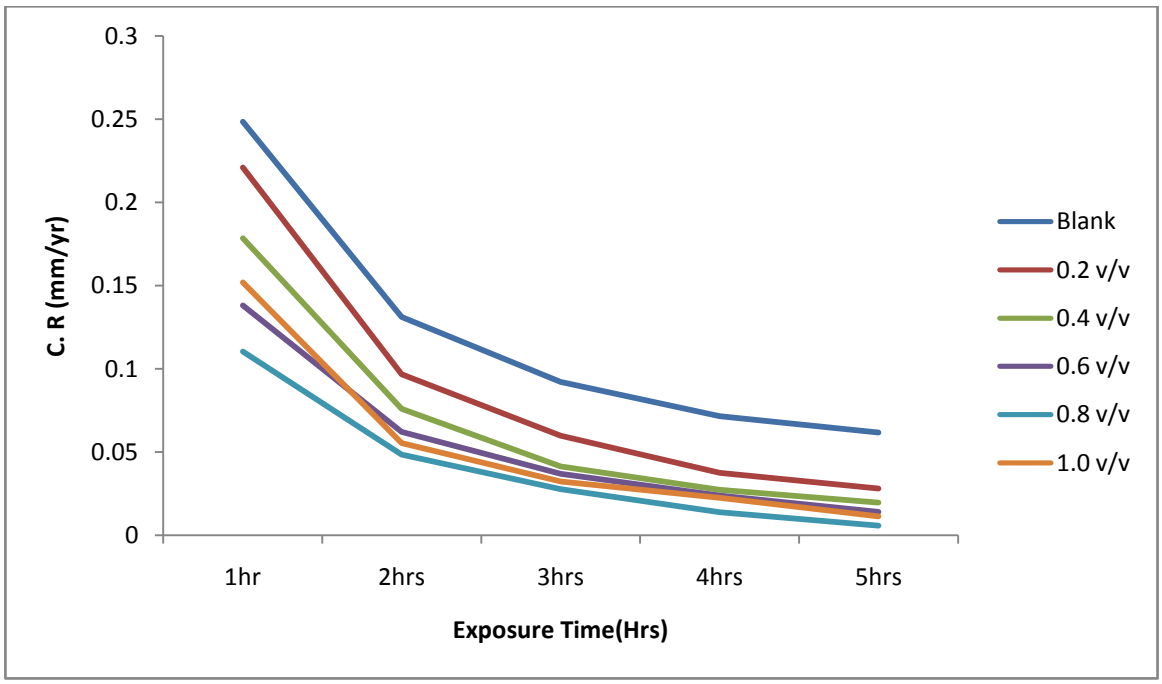

Figure 4.31: Corrosion Rates with Exposure Time of CM at $70^{O}C$

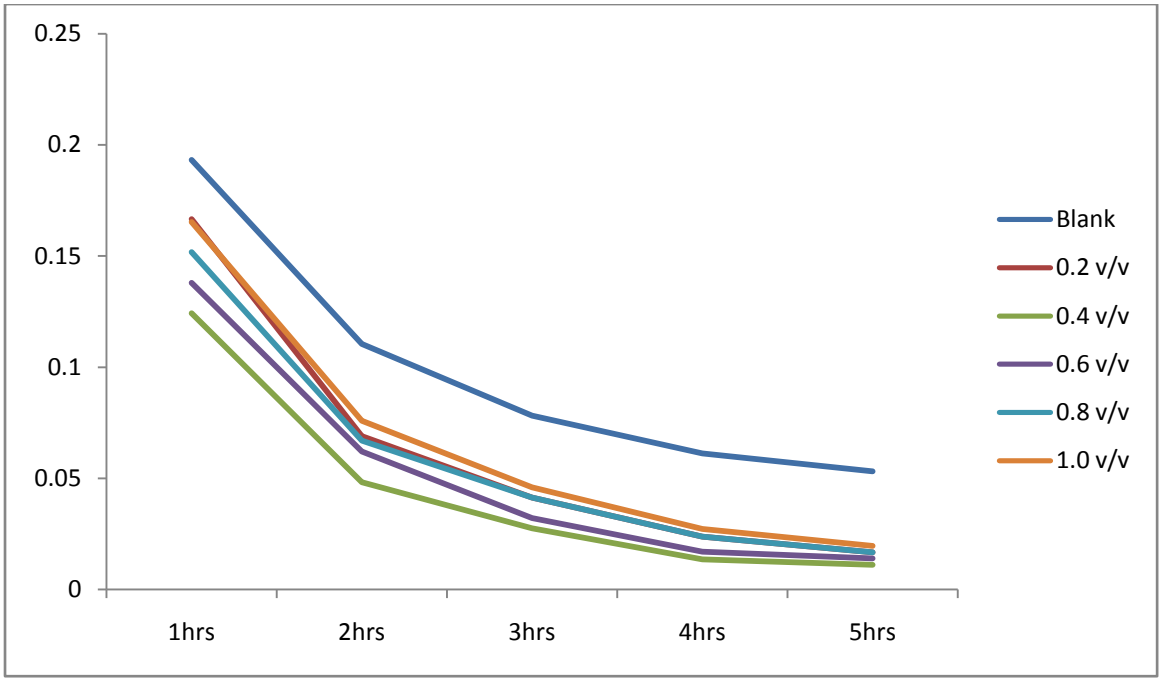

Figure 4.32: Corrosion Rates with Exposure Time of CG at 30^{O}C

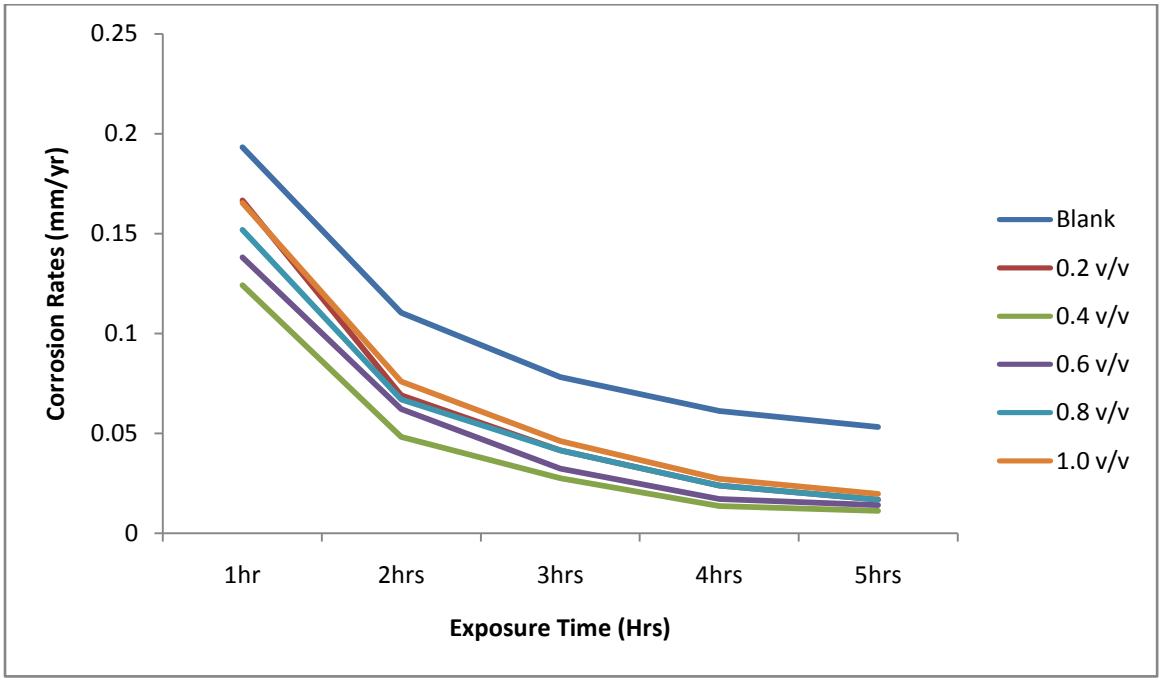

Figure 4.33: Corrosion Rates with Exposure Time of CG at 50^{O}C

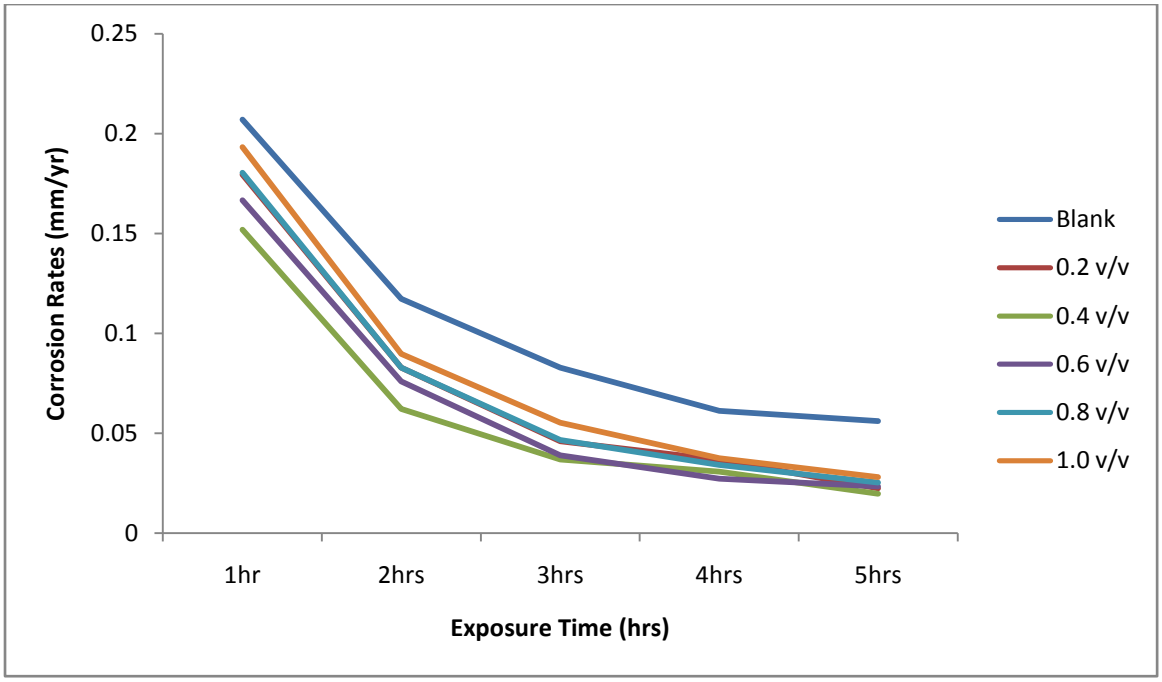

Figure 4.34: Corrosion Rates with Exposure Time of CG at $70^{O}C$

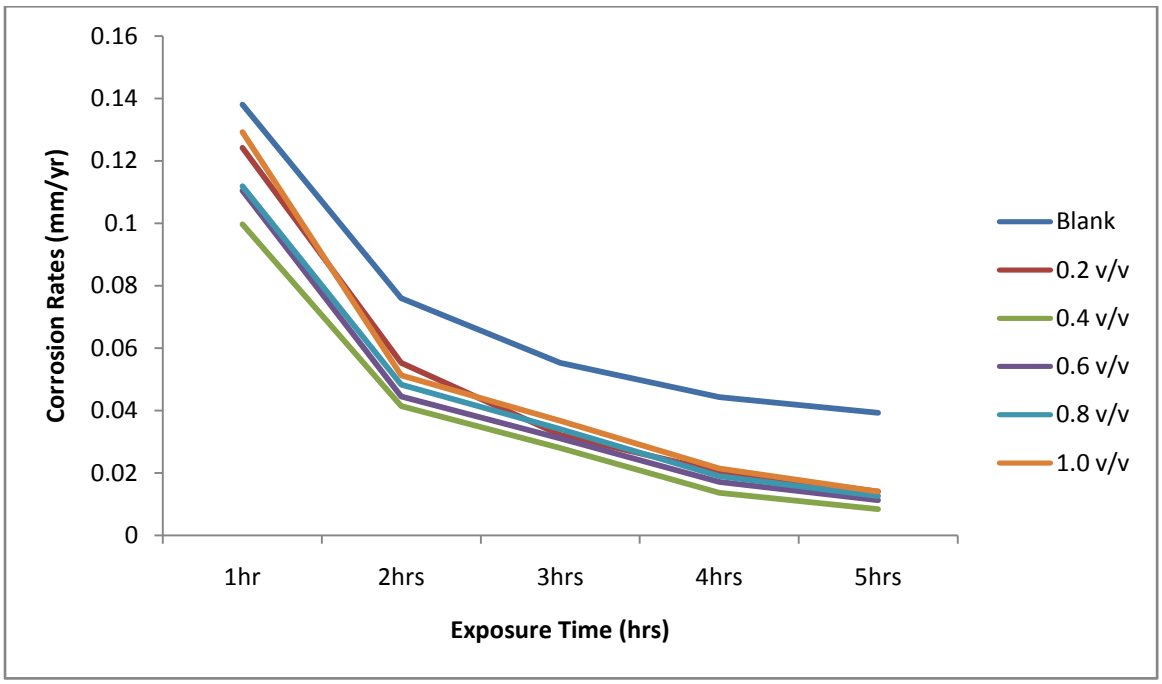

Figure 4.35: Corrosion Rates with Exposure Time of FE at $30^{O}C$

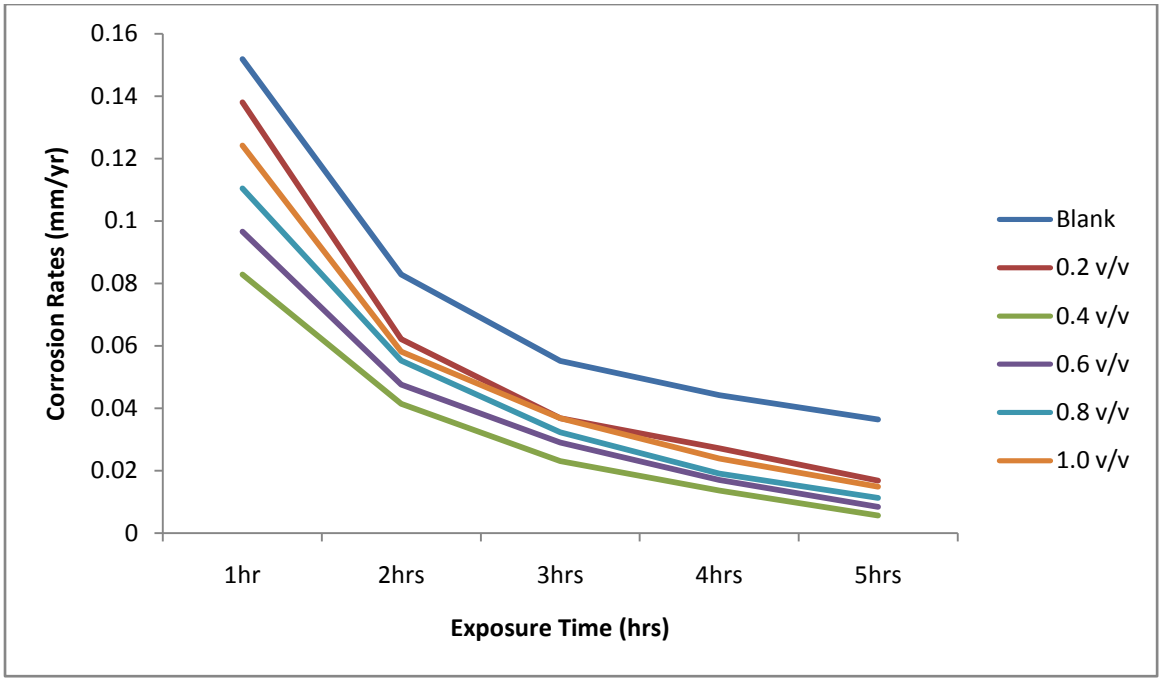

Figure 4.36: Corrosion Rates with Exposure Time of FE at $50^{O}C$

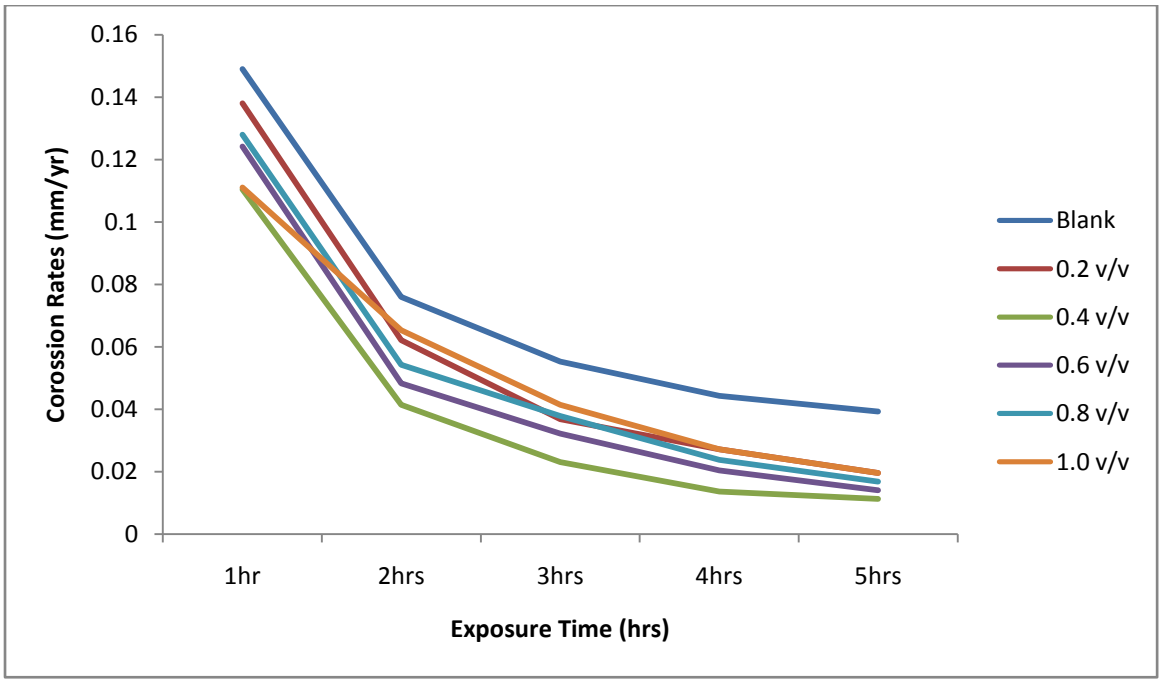

Figure 4.37: Corrosion Rates with Exposure Time of FE at $70^{O}C$

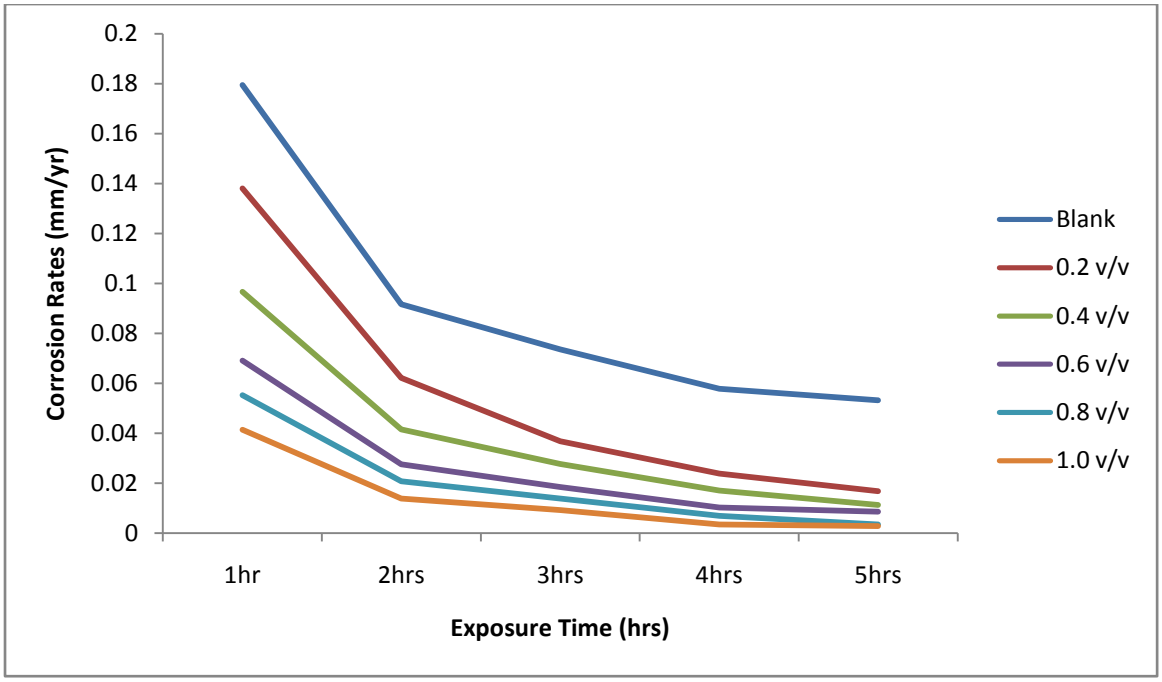

Figure 4.38: Corrosion Rates with Exposure Time of FP at 30^{O}C

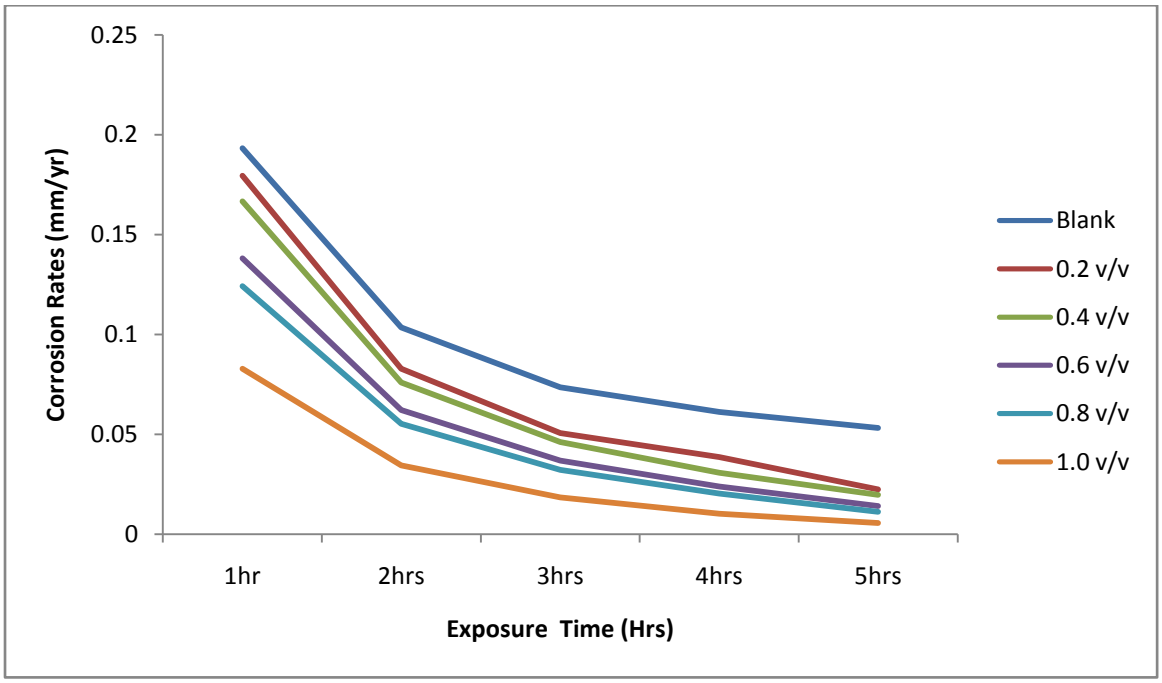

Figure 4.39: Corrosion Rates with Exposure Time of FP at 50^{O}C

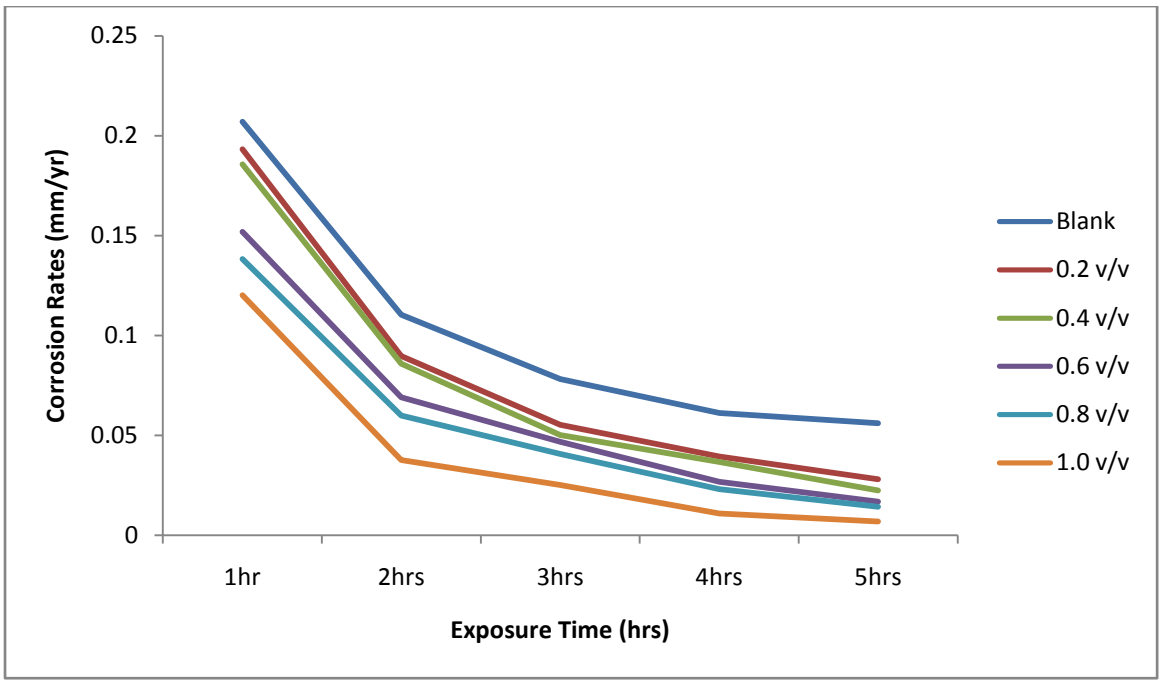

Figure 4.40: Corrosion Rates with Exposure Time of FP at $70^{O}C$

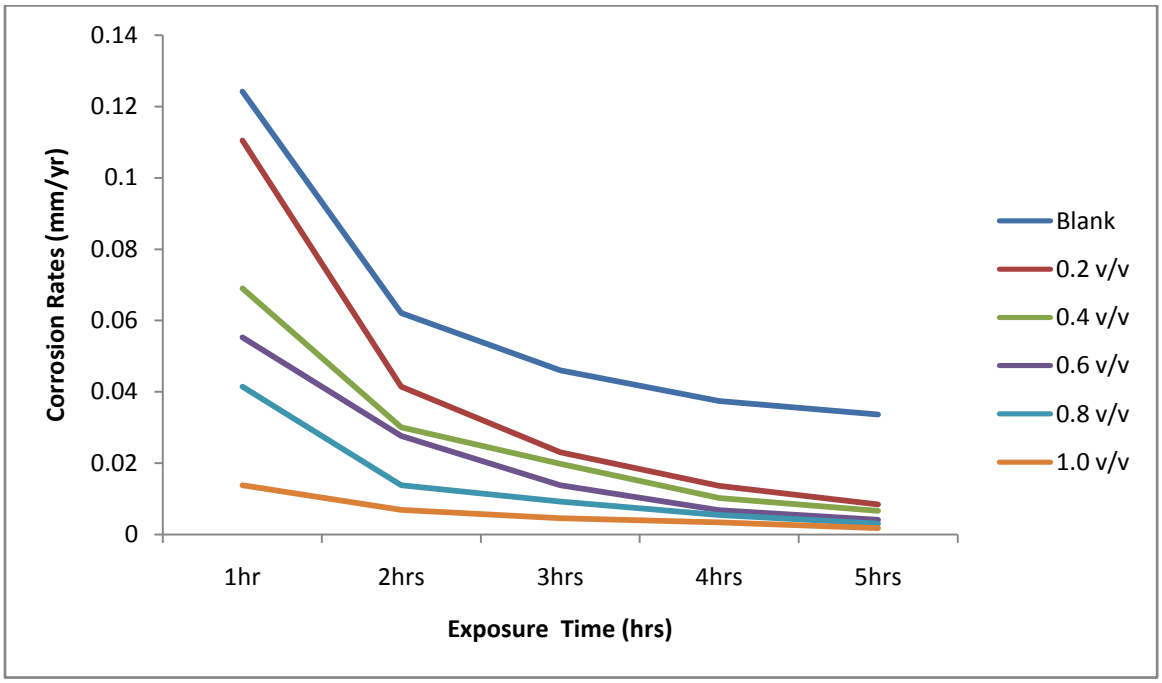

Figure 4.41: Corrosion Rates with Exposure Time of Sodium Chromate at $30^{O}C$

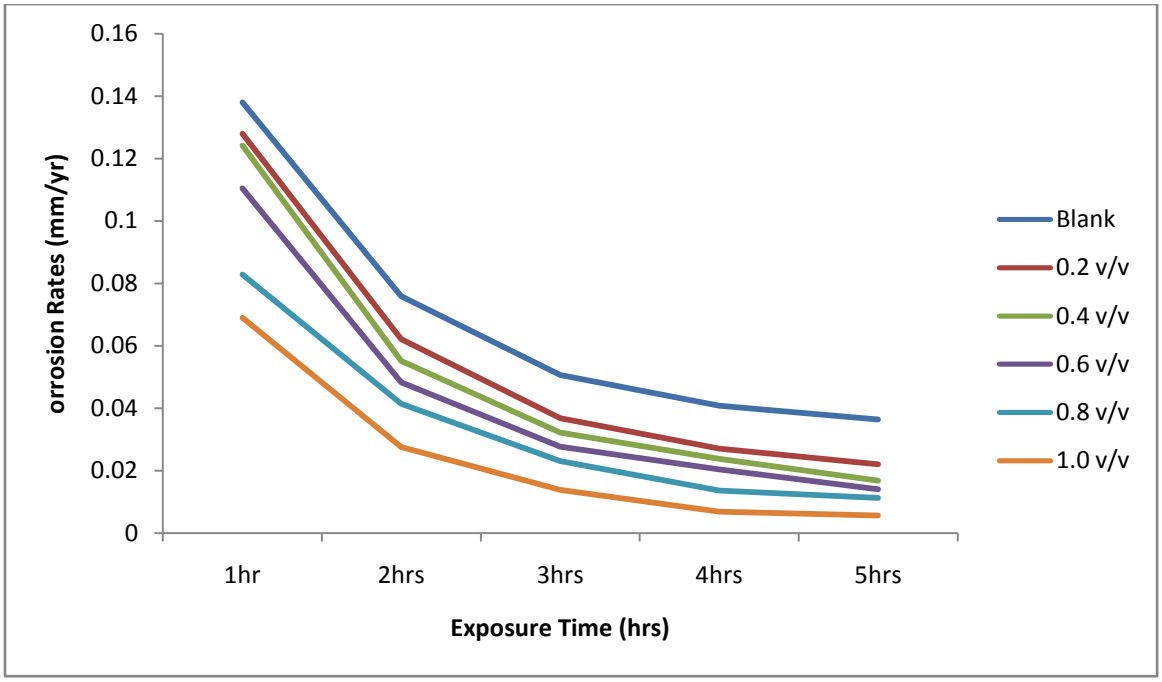

Figure 4.42: Corrosion Rates withExposure Time of Sodium Chromate at $50^{O}C$

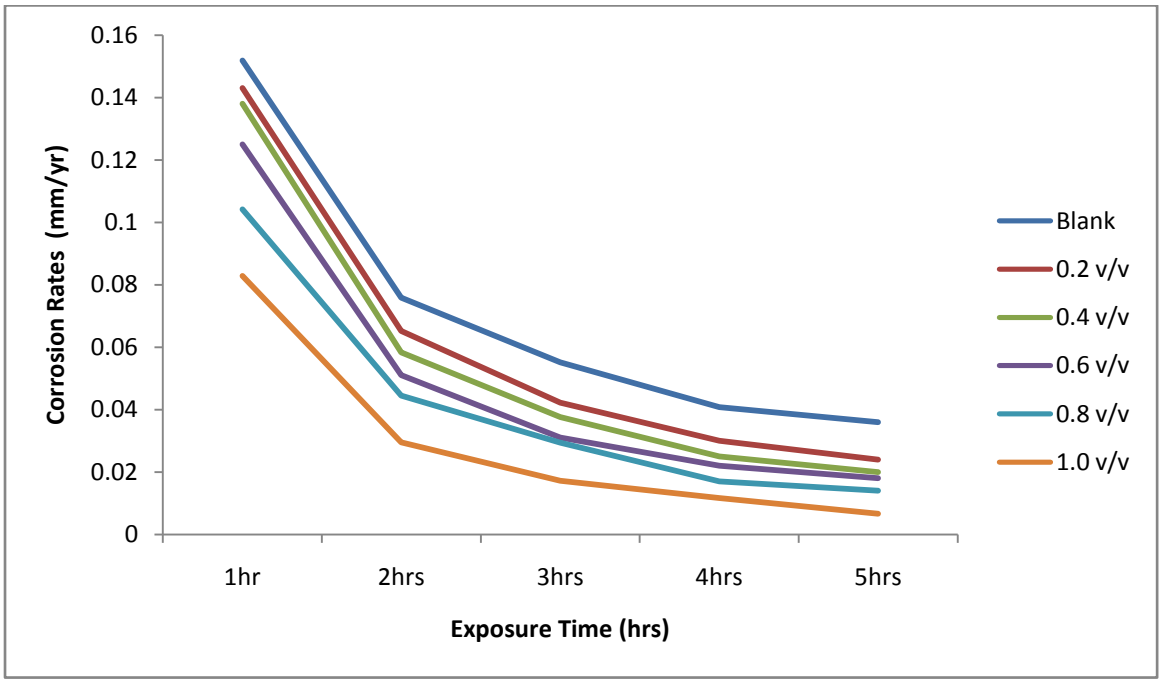

Figure 4.43: Corrosion Rates with Exposure Time of Sodium Chromate at $70^{O}C$

4.2.3 Effect of inhibitor concentrations on inhibition efficiencies

In order to assess the stability of the adsorbed inhibitors film at the alloy's surface with time, inhibition efficiency was calculated as shown in Appendices XXIX – XLIII. These tables present the inhibition efficiencies of the extracts only, while Appendices XLIV - XLVIII show the inhibition efficiencies of co-inhibited extracts. The percentage inhibition efficiency (IE %) increased with increase in inhibitors concentrations but decreased with increase in temperature. Figures 4.44 – 4.58 depict the inhibition efficiencies against inhibitor concentrations for all the plant extracts at 30 ^{0}C, 50 ^{0}C and 70 ^{0}C with the control sodium chromates.The decrease in inhibition efficiency with increase in temperature from 30 ^{0}C to 70 ^{0}C can be explained in terms of physical adsorption of inhibitive molecule on metal surface. This occurrence is in line with other work (Umoren and Ebenso, 2008). Figure 4.59 - 4.63 show the inhibition efficiency of co-inhibitors. The maximum inhibition efficiencies obtained from each extract and co-inhibition are presented in Appendices XLIX – L. The results show that a higher efficiency was obtained with combination of CG and FE (95.13 %) and that of a single extract was 94.74 % for FP. Table 4.4 shows maximum inhibition comparison obtained from gravimetric and linear polarization. The results are in agreement as the values are very close though that of electrochemical are higher than gravimetric.

4.2.4 Effect of Temperature

To evaluate the adsorption of plant extracts in the medium and activation parameters of the corrosion process of the alloy, mass loss measurement were investigated in the temperature range 30 ^{O}C, 50 ^{O}C and 70 ^{O}C. The effects of variation of temperature on inhibition efficiency and inhibitor concentration of each inhibitor are presented in Figures 4.65 - 4.69. As the temperature of the medium increases, the inhibition efficiency decreases. The corrosion rates decreased and inhibition efficiency increased with increasing inhibitor concentration which suggests that the inhibitor molecules acted by adsorption onto the metal

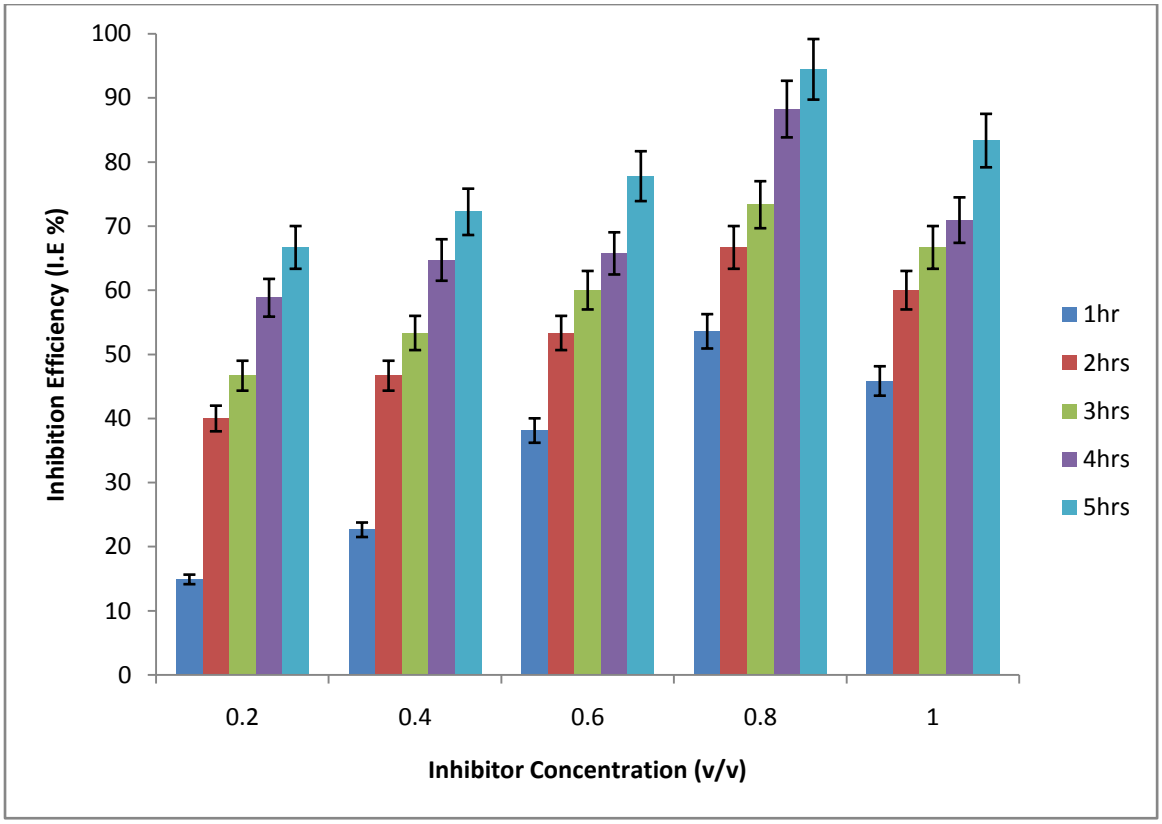

Figure 4.44: Variations of Inhibition Efficiency with Inhibitor Concentration of CM at 30^{O}C

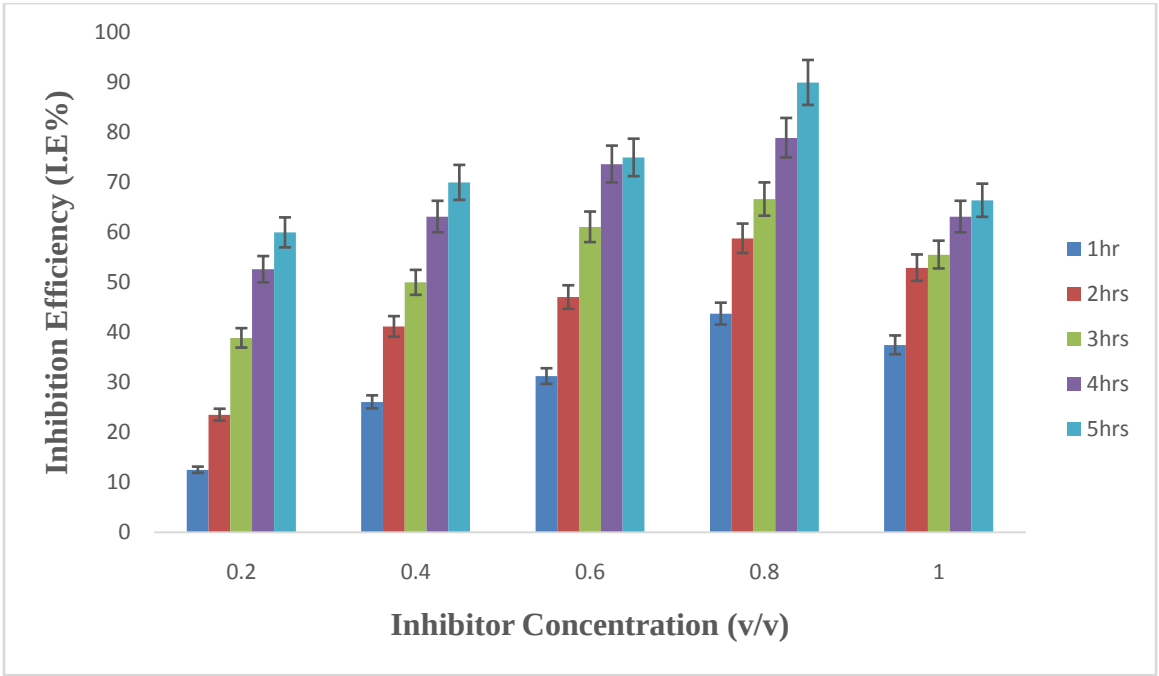

Figure 4.45: Variations of Inhibition Efficiency with Inhibitor Concentration of CM at 50 ^{O}C

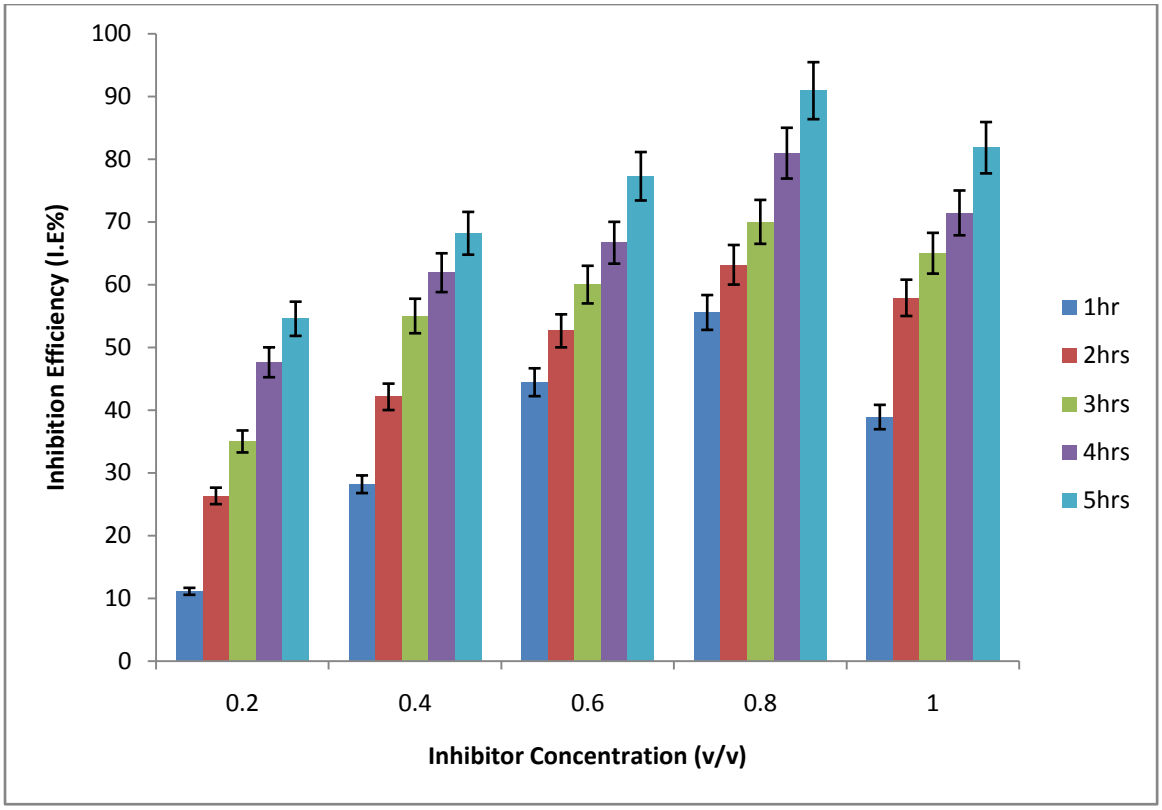

Figure 4.46: Variations of Inhibition Efficiency with Inhibitor Concentration of CM at 70 ^{O}C

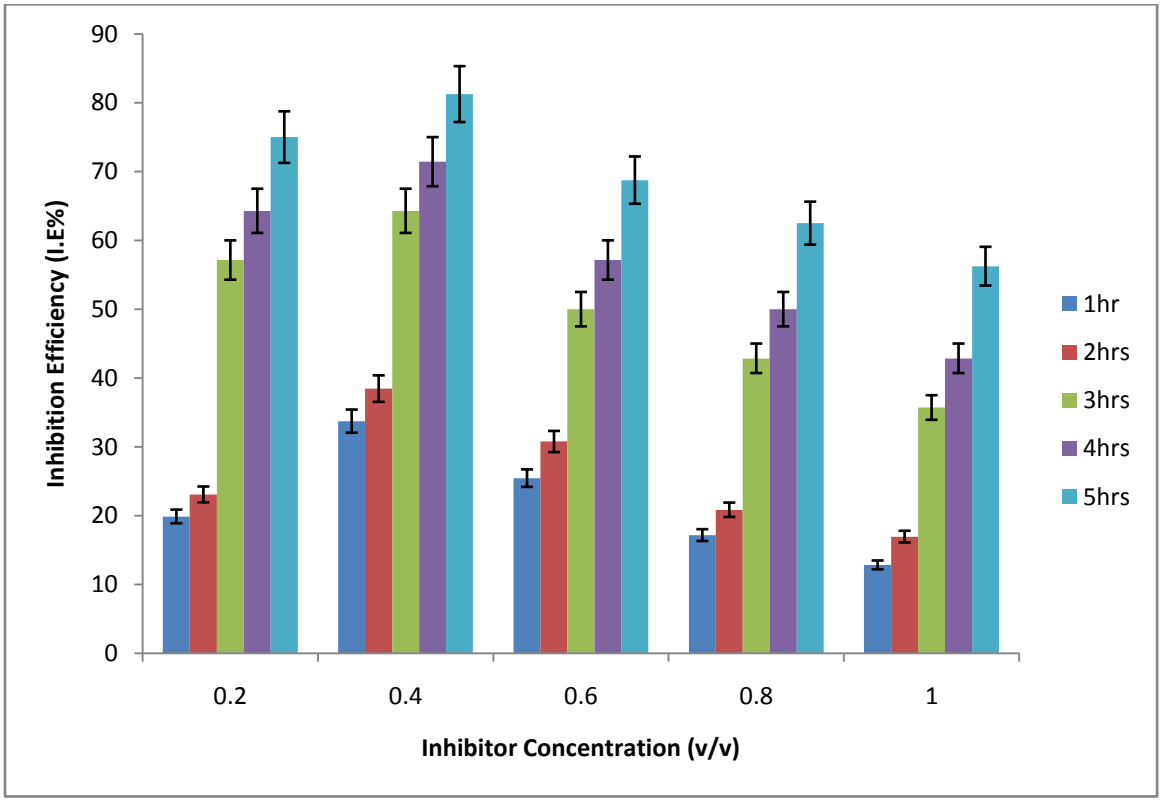

Figure 4.47 Variations of Inhibition Efficiency against Inhibitor Concentration of CG at 30 ^{O}C

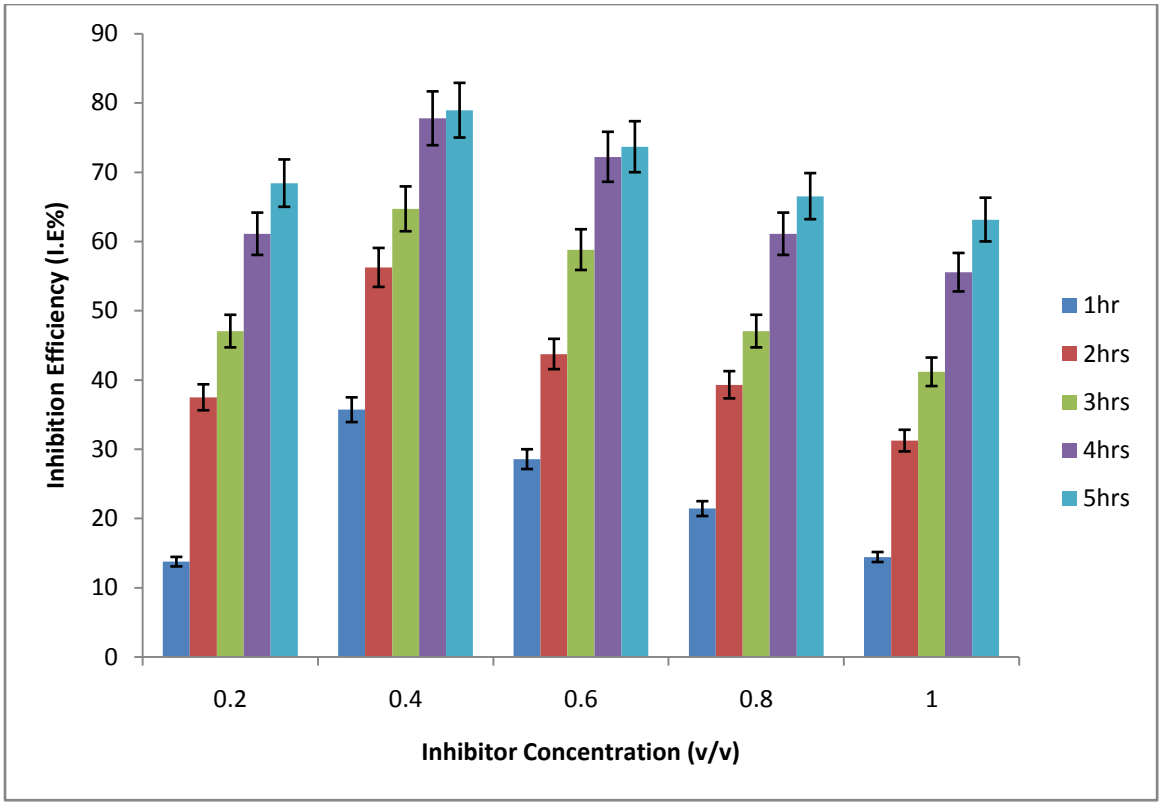

Figure 4.48: Variations of Inhibition Efficiency with Inhibitor Concentration of CG at $50^{O}C$

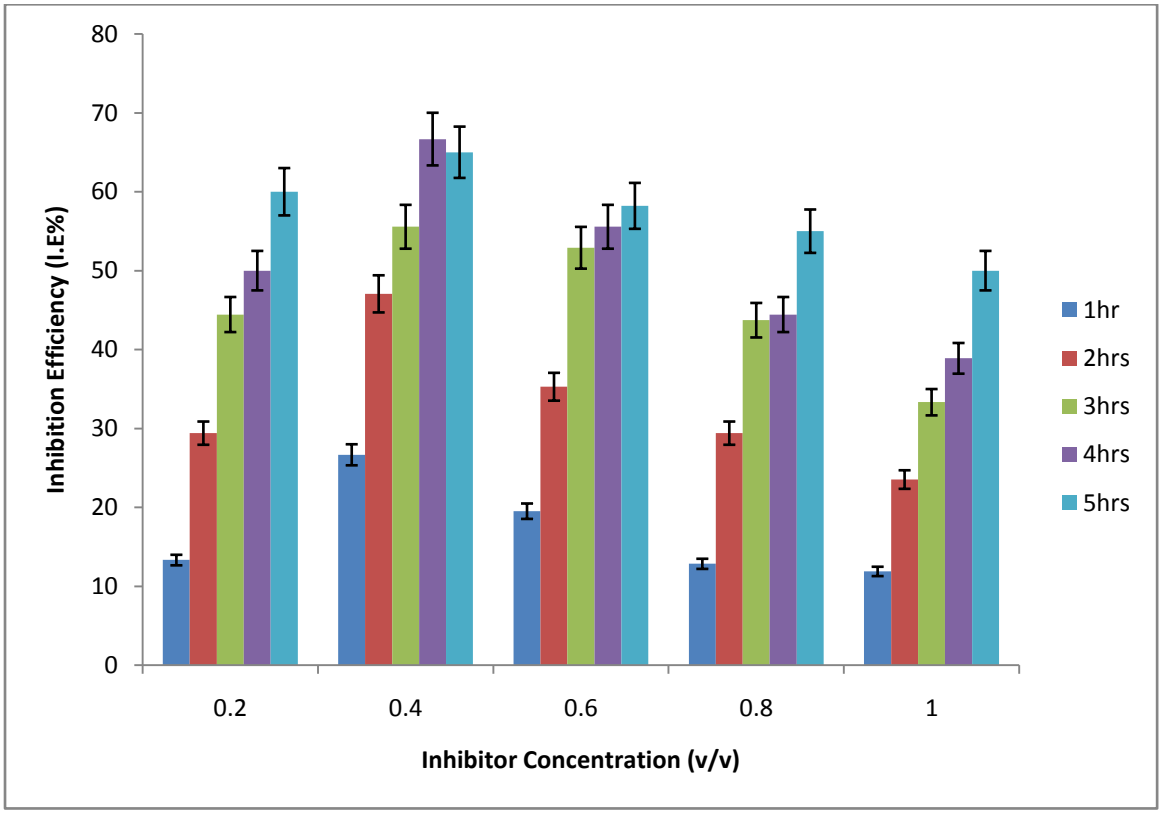

Figure 4.49: Variationsof Inhibition Efficiencywith Inhibitor Concentration of CG at$70^{O}C$

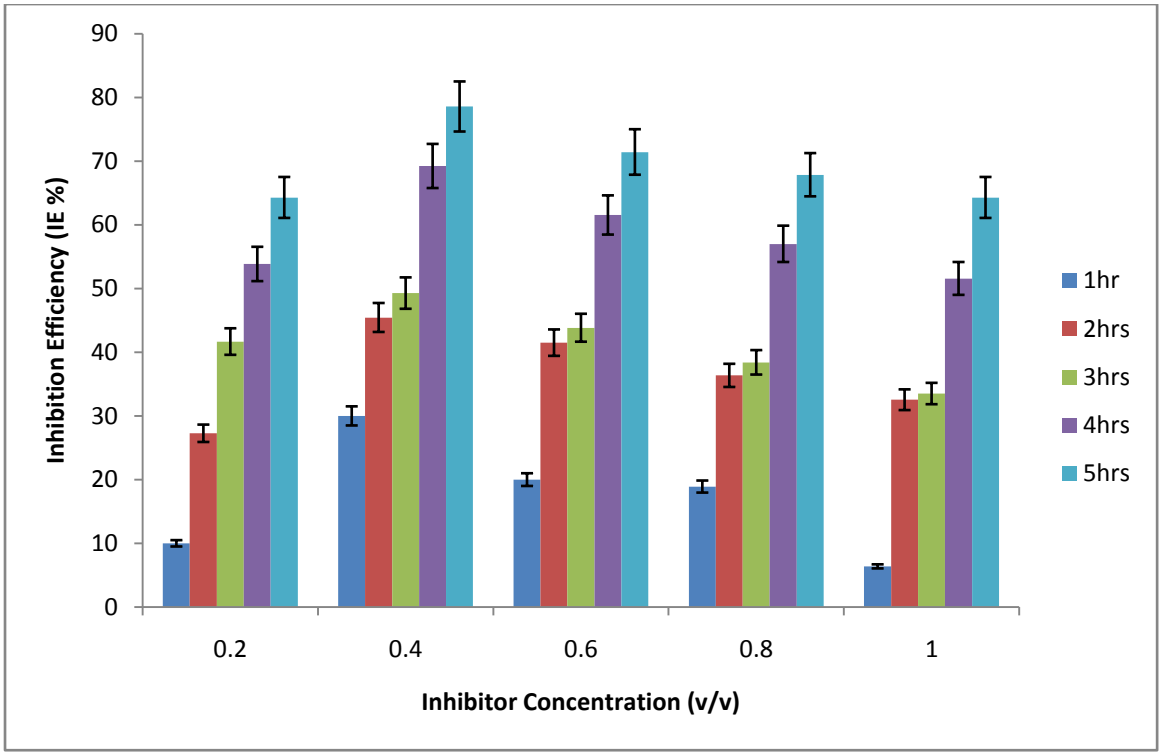

Figure 4.50: Variationsof Inhibition Efficiency with Inhibitor Concentration of FE at 30^{O}C

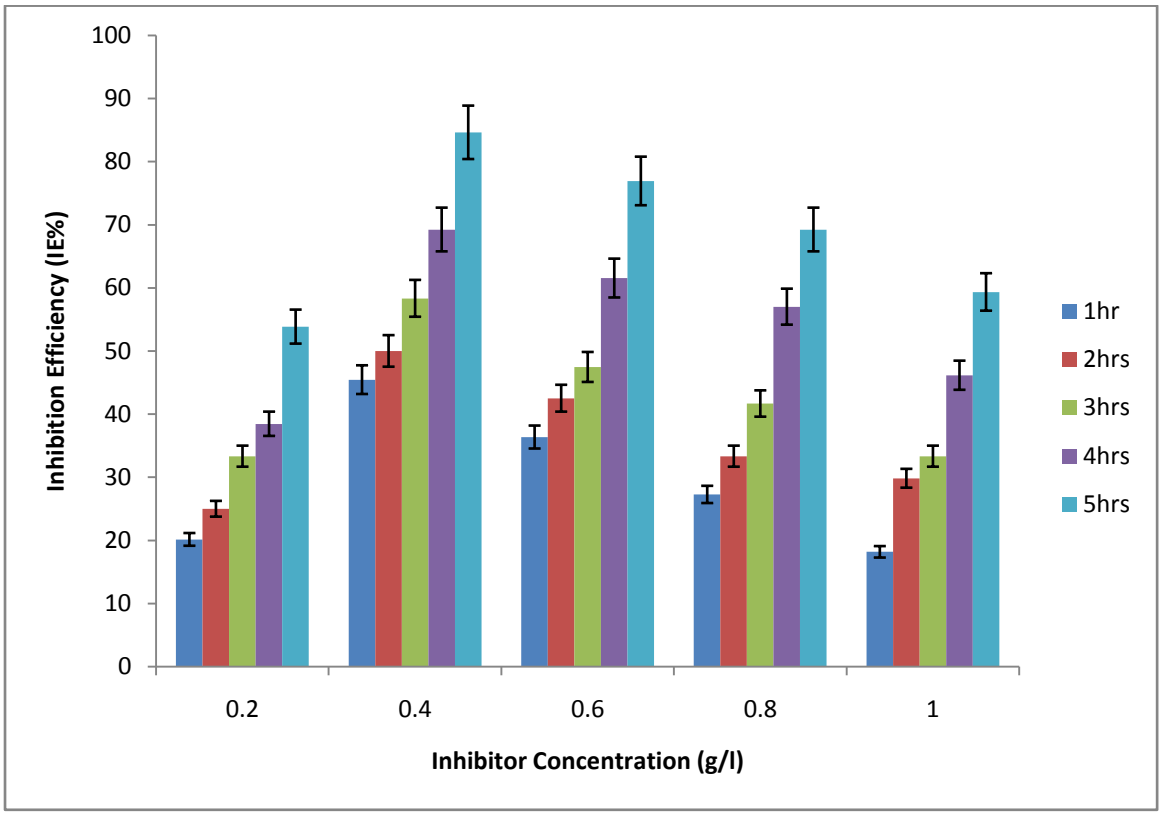

Figure 4.51: Variationsof Inhibition Efficiency with Inhibitor Concentration of FE at 50^{O}C

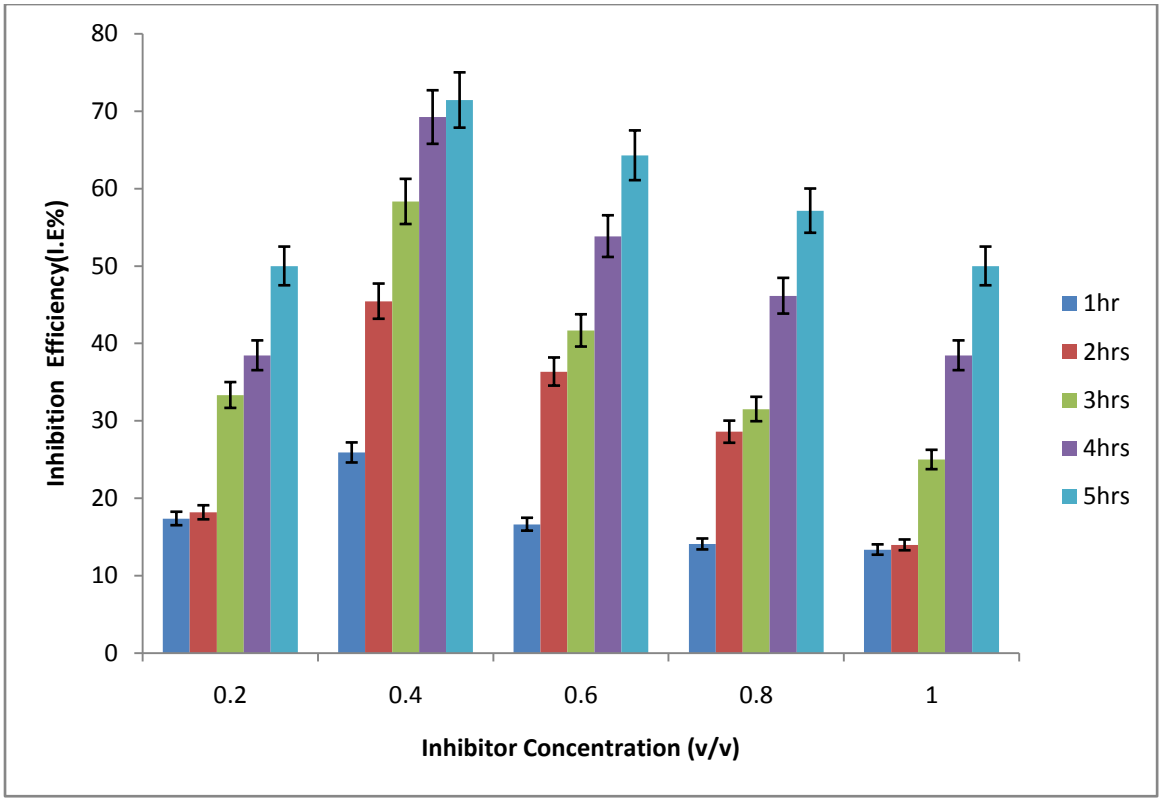

Figure 4.52: Variations of Inhibition Efficiency with Inhibitor Concentration of FE at70^{O}C

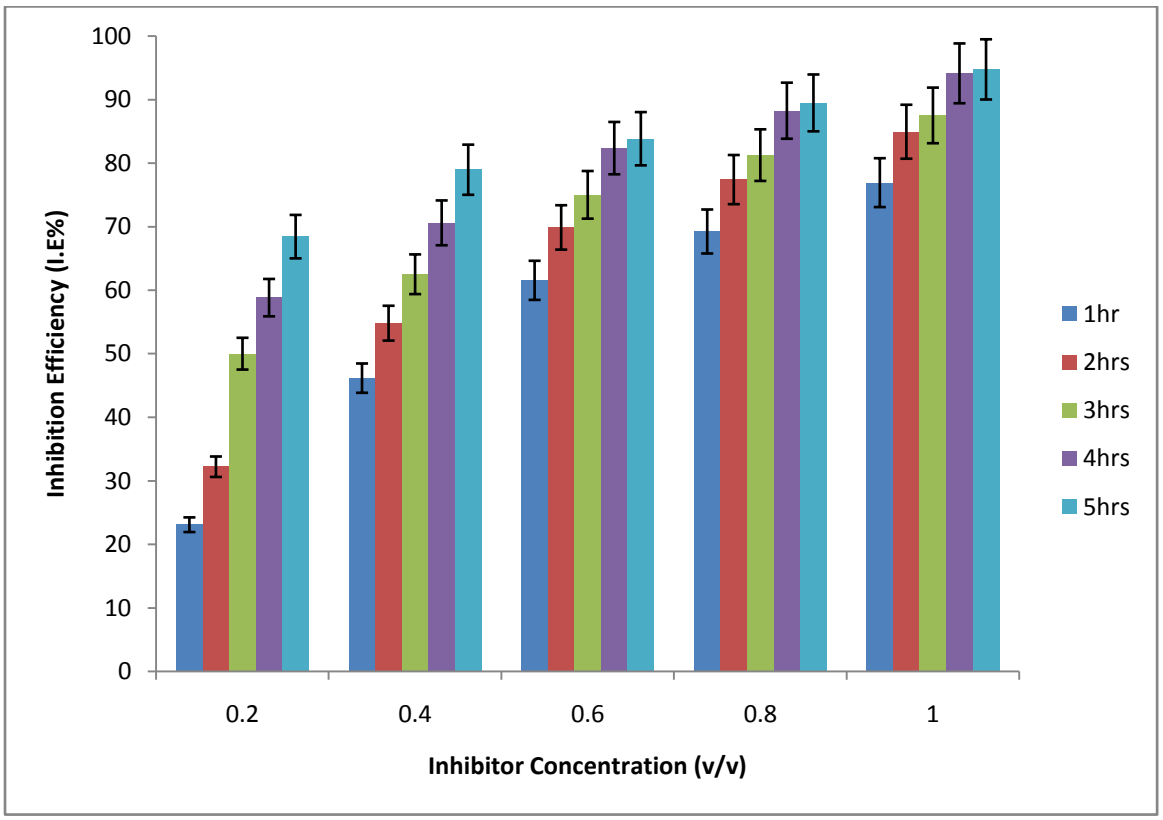

Figure 4.53: Variations of Inhibition Efficiency with Inhibitor Concentration of FP at 30 ^{O}C

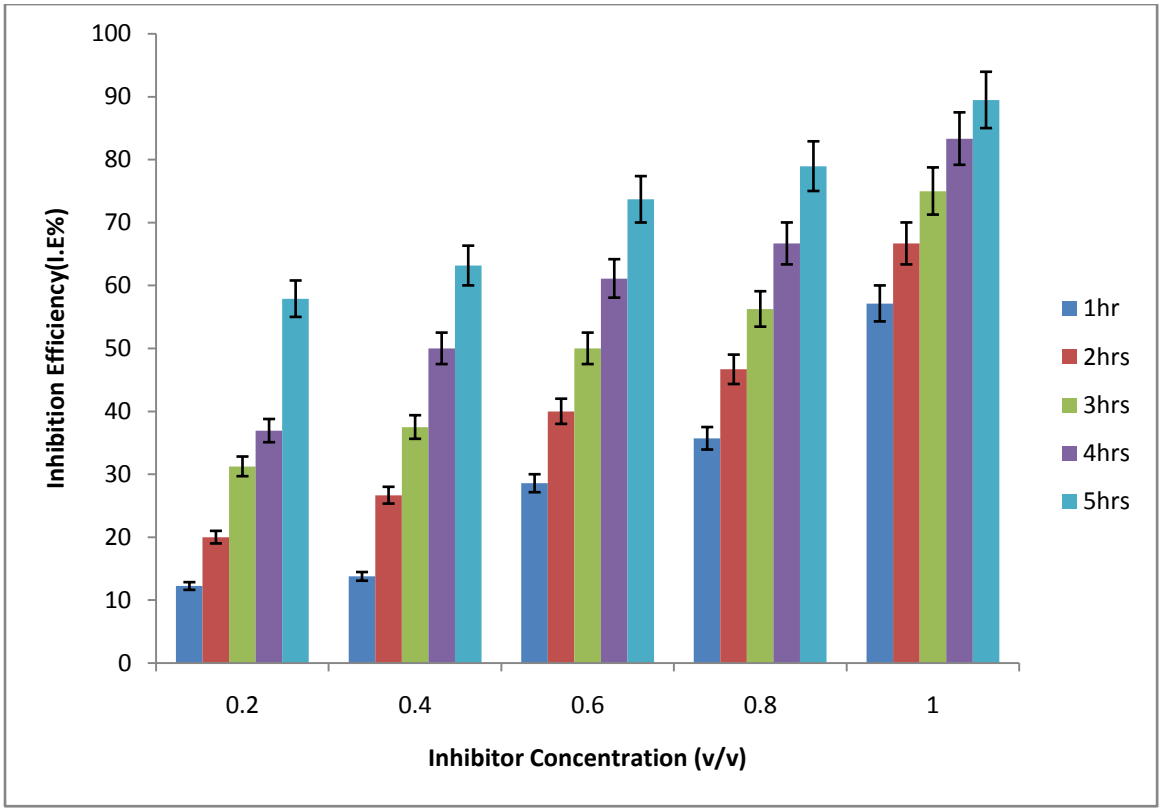

Figure 4.54:Variations of Inhibition Efficiency with Inhibitor Concentration of FP at $50^{O}C$

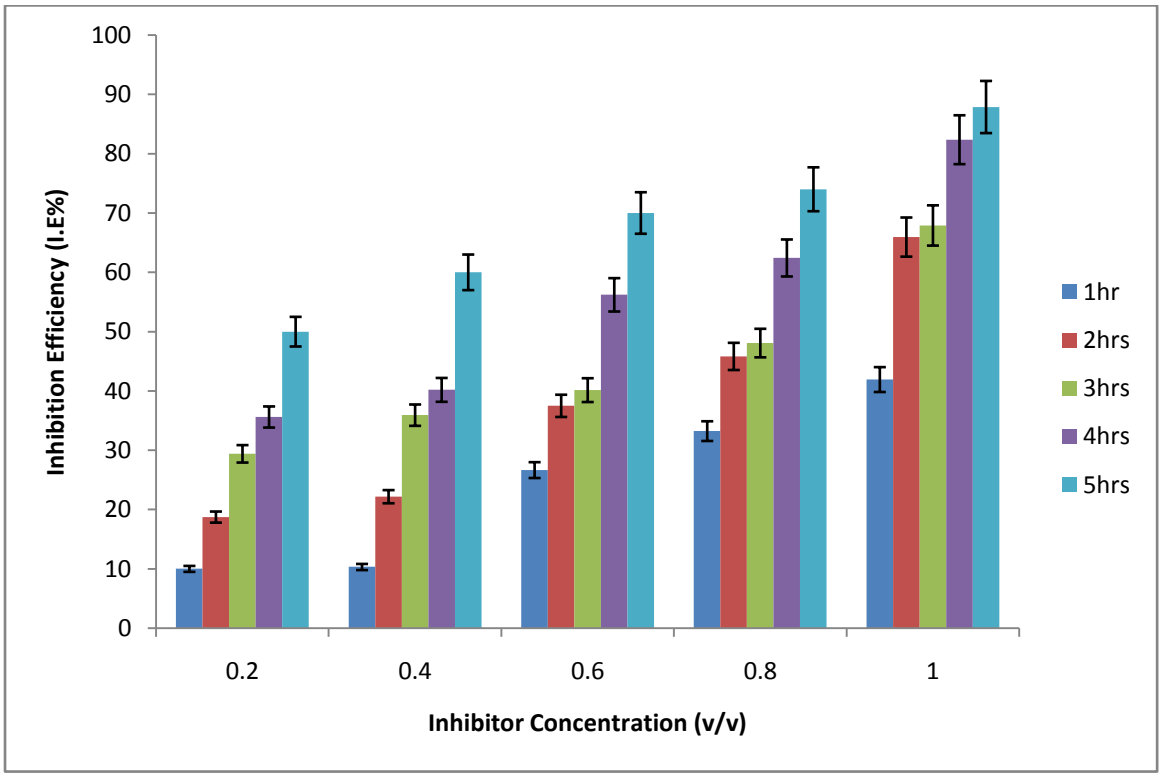

Figure 4.55: Variations of InhibitionEfficiency with Inhibitor Concentration of FP at$70^{O}C$

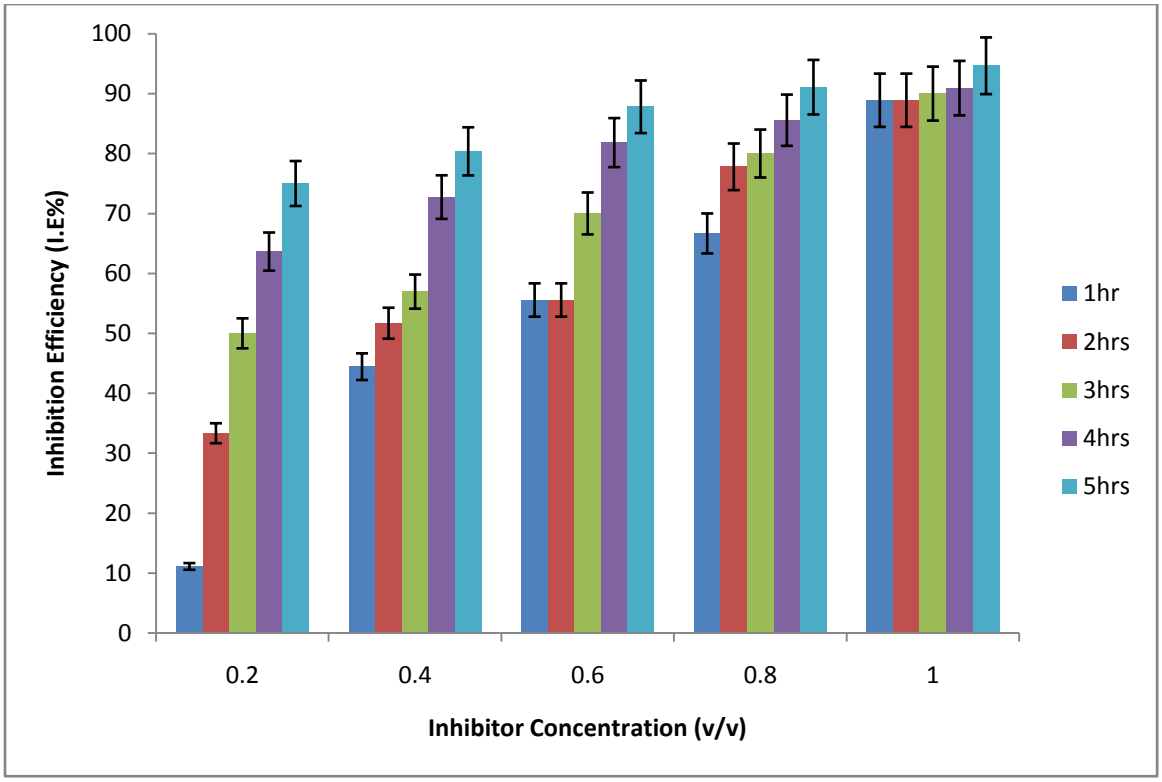

Figure 4.56: Variations of Inhibition Efficiency with Inhibitor Concentration of Sodium Chromate at 30^{O}C.

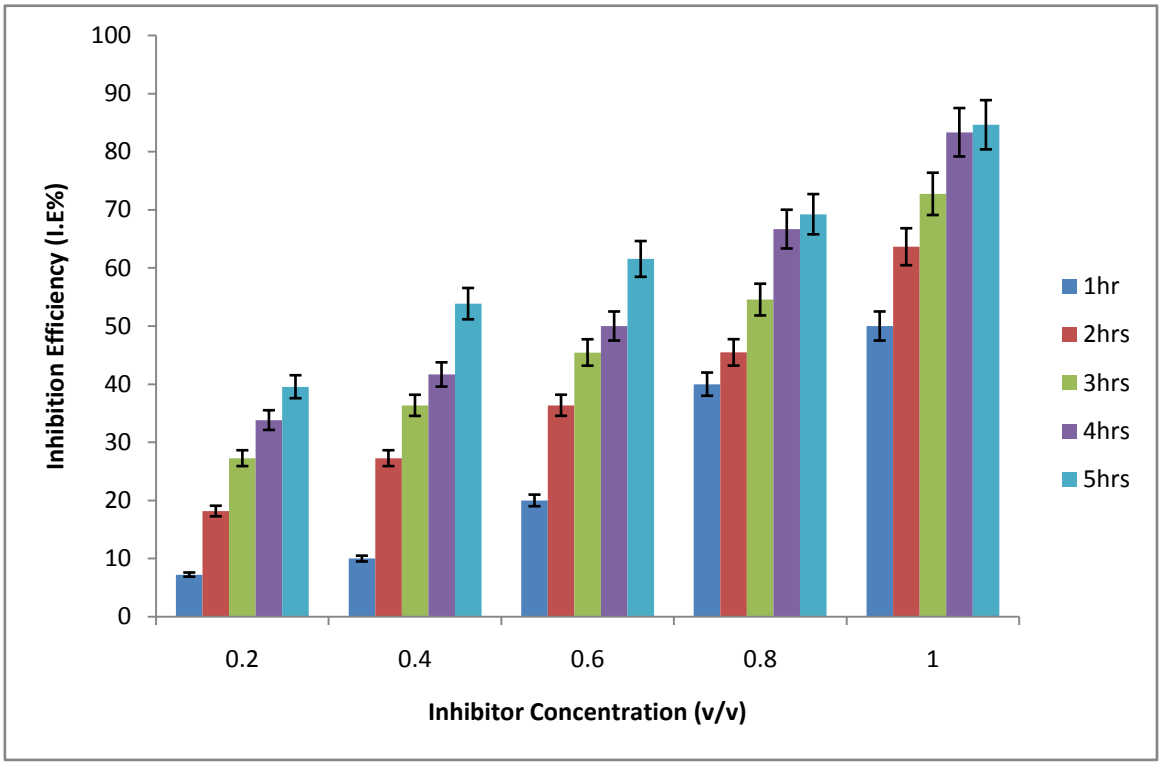

Figure 4.57: Variations of Inhibition Efficiency with Inhibitor Concentration of Sodium Chromate at 50 ^{O}C

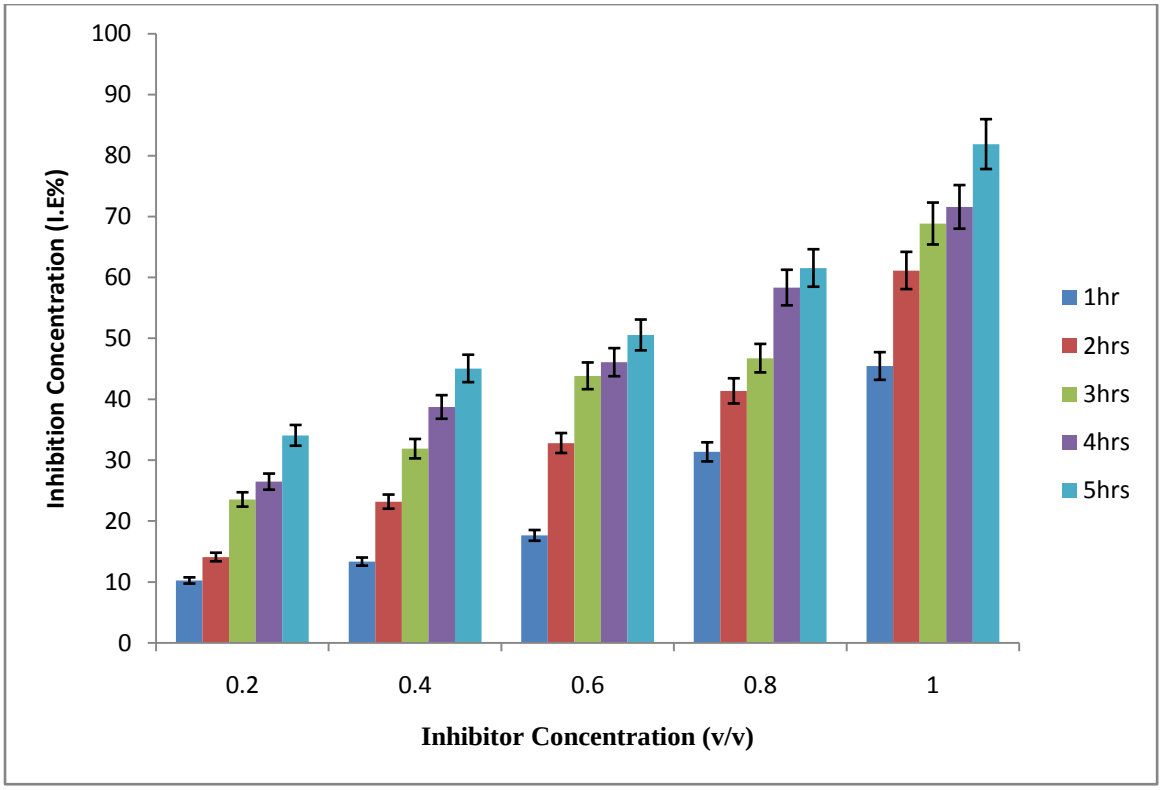

Figure 4.58: Variations of Inhibition Efficiency with Inhibitor Concentration of Sodium Chromates at $70^{O}C$

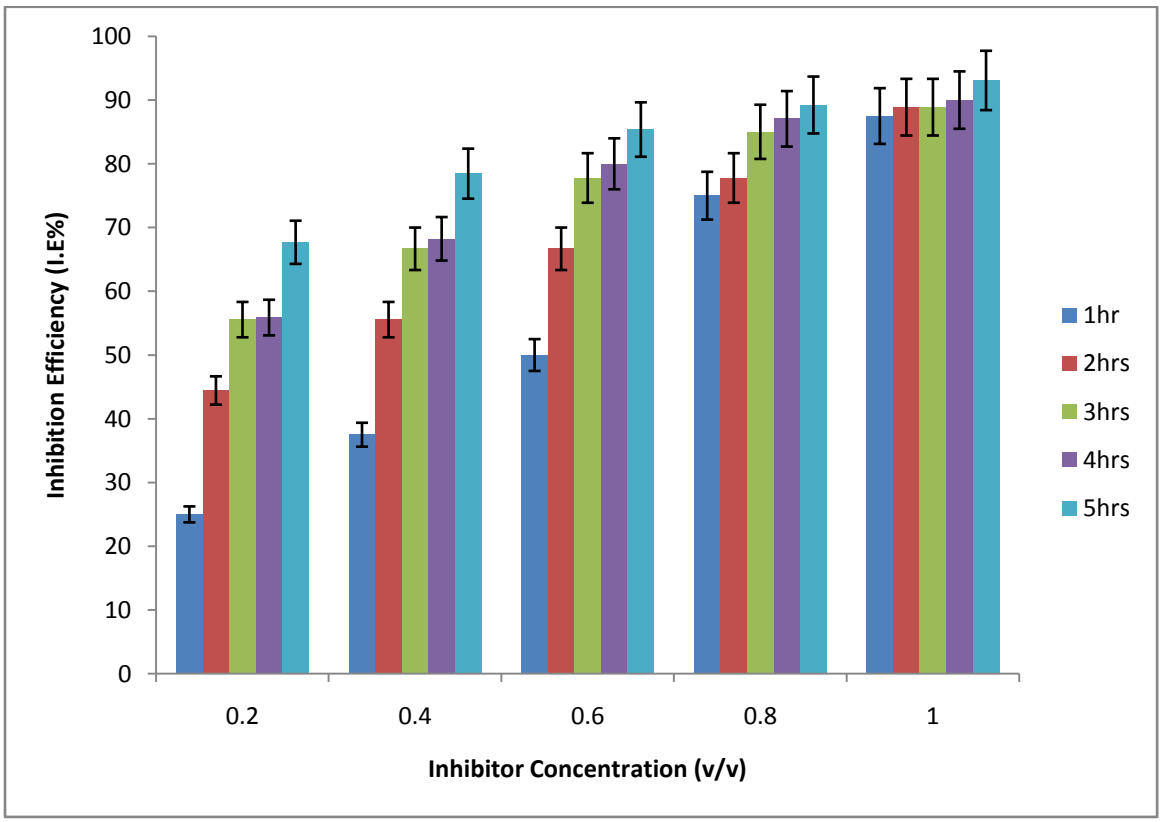

Figure 4.59: Variation of Inhibition Efficiency with Inhibitor Concentration of CM with CG at $30^{O}C$

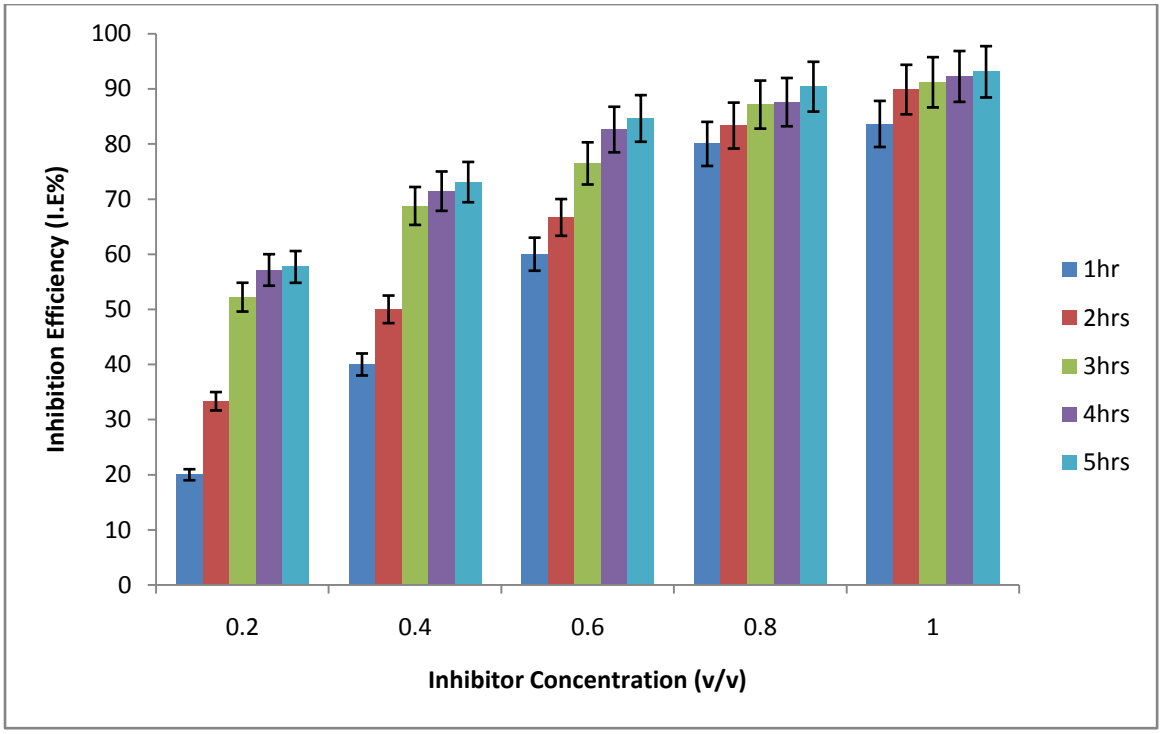

Figure 4.60: Variation of Inhibition Efficiency with Inhibitor Concentration of CM with FP at $30^{O}C$

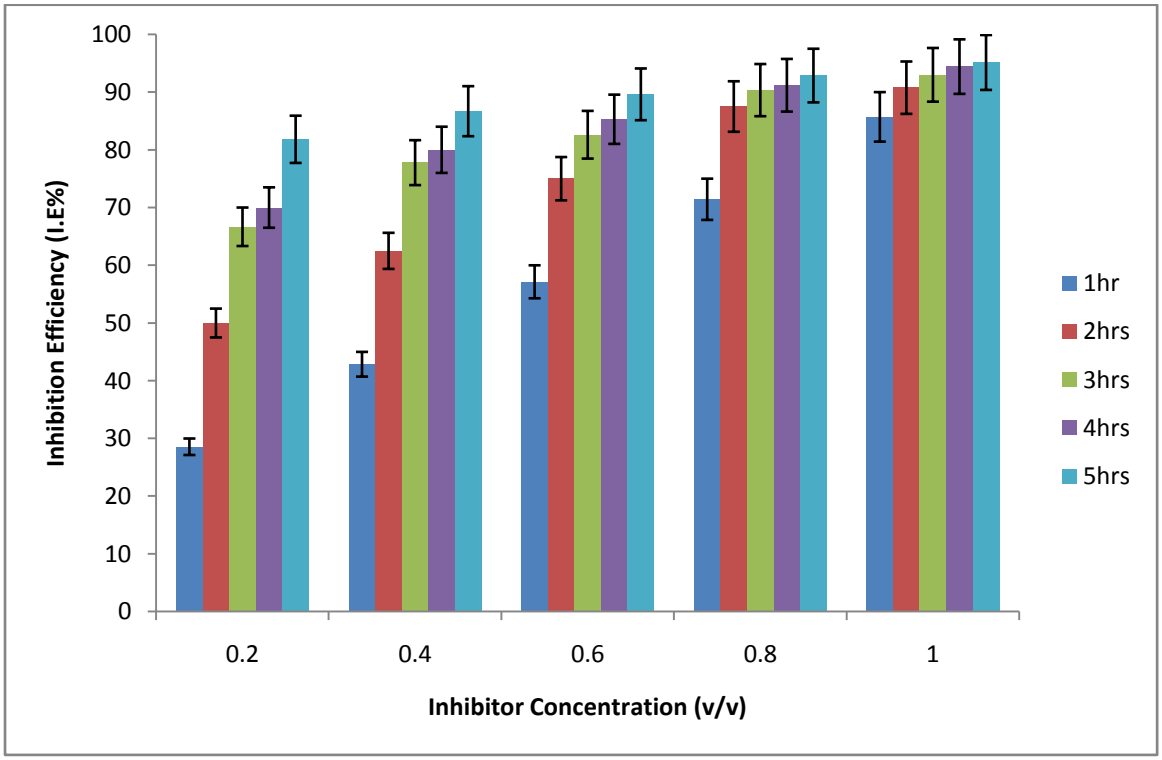

Figure 4.61: Variations of Inhibition Efficiency against Inhibitor Concentration of CG with FE at $30\ ^{0}C$

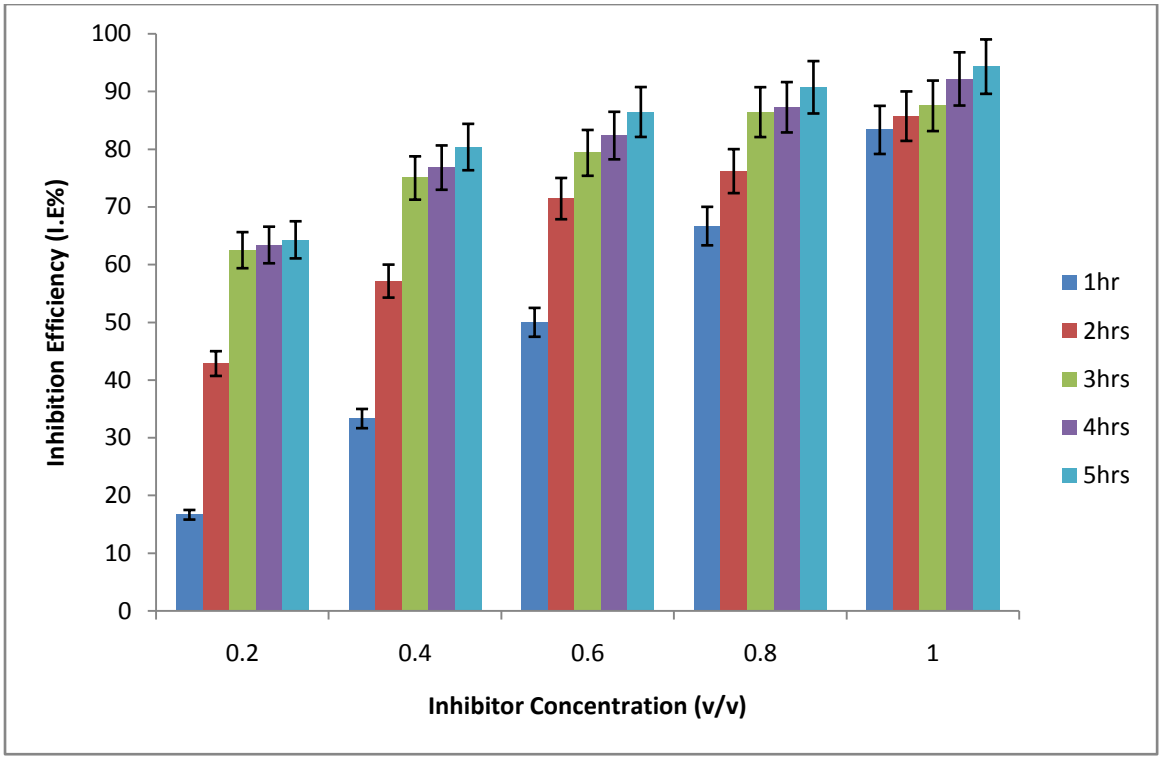

Figure 4.62: Variations of Inhibition Efficiency against Inhibitor Concentration of FE with FP at 30 ^{0}C

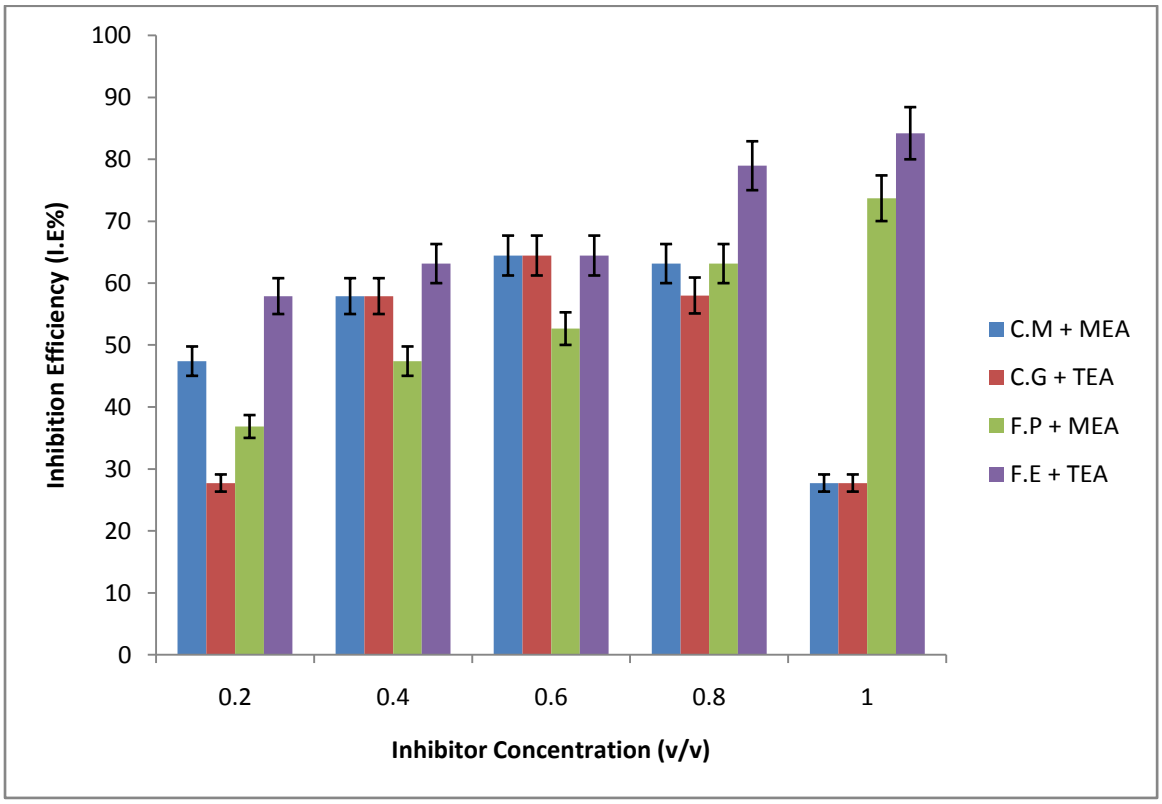

Figure 4.63: Variations of Inhibition Efficiency with Inhibitor Concentration of Extracts with Surfactants at 30 ^{0}C

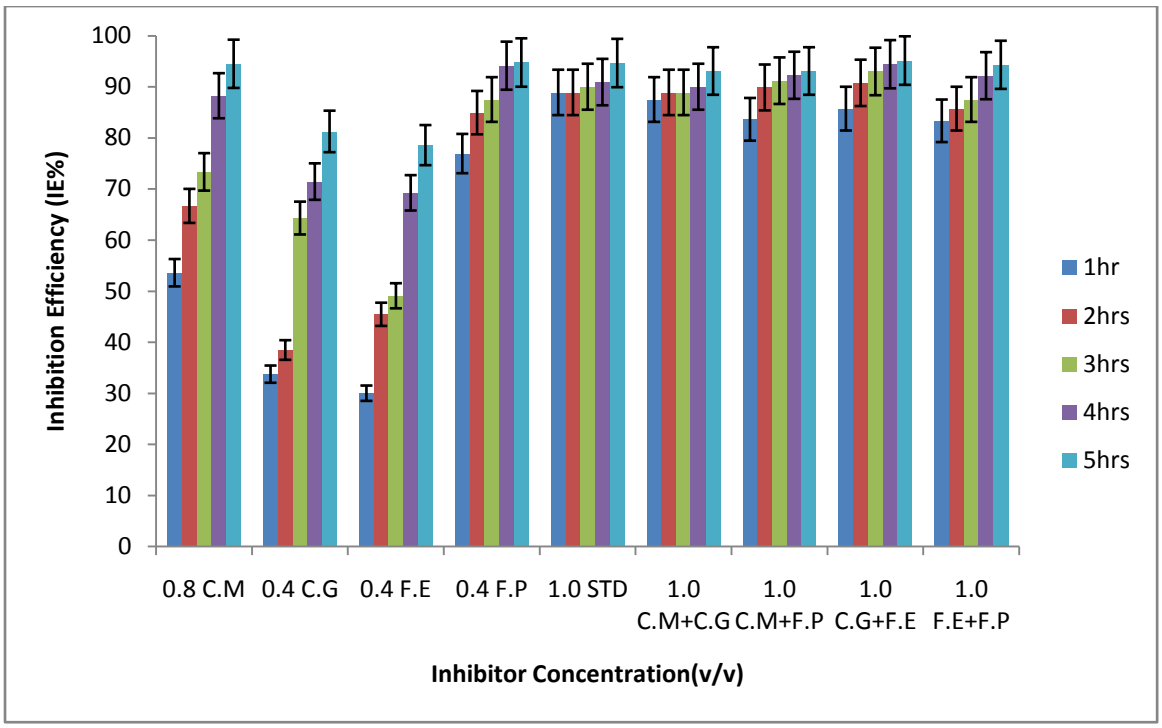

Figure 4.64: Comparing maximum inhibition efficiency of all extracts, sodium chromates and co-inhibition at 30 ^{0}C

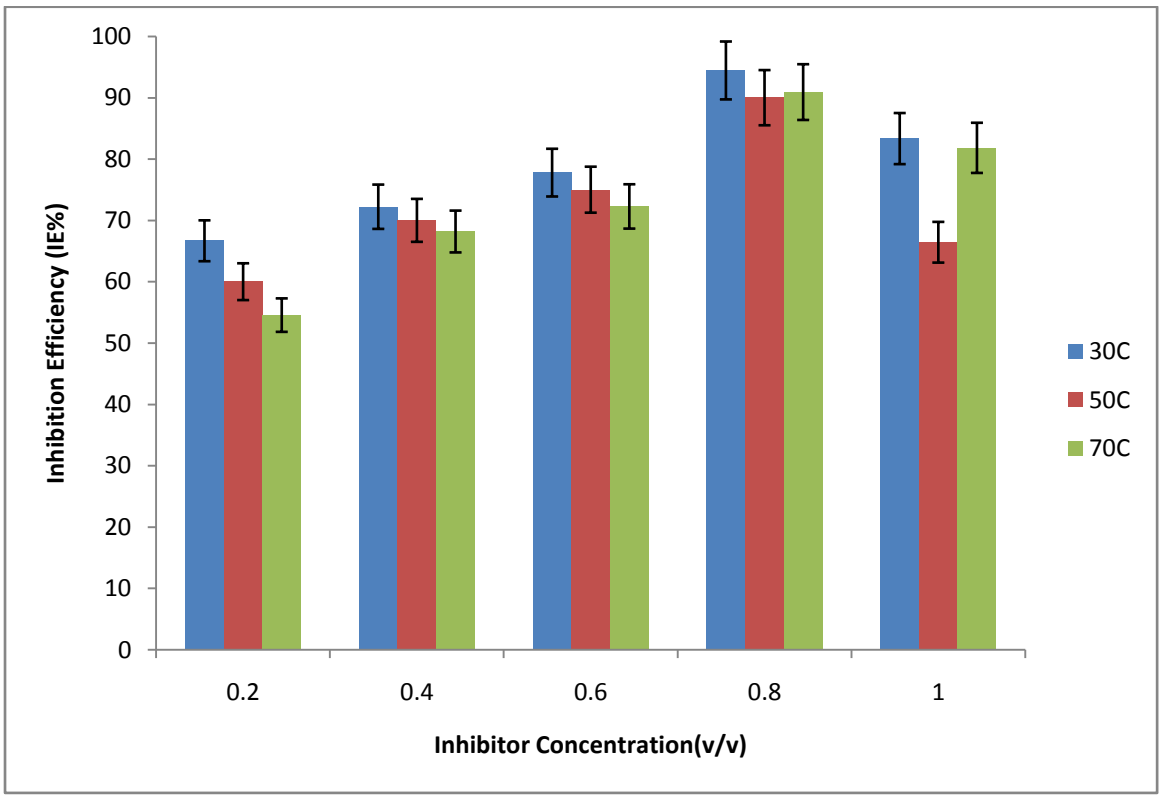

Figure 4.65: Variations of Inhibition Efficiencies (IE %) of CM with Inhibitor Concentrations at different temperatures in 3.5 wt% NaCl Solution.

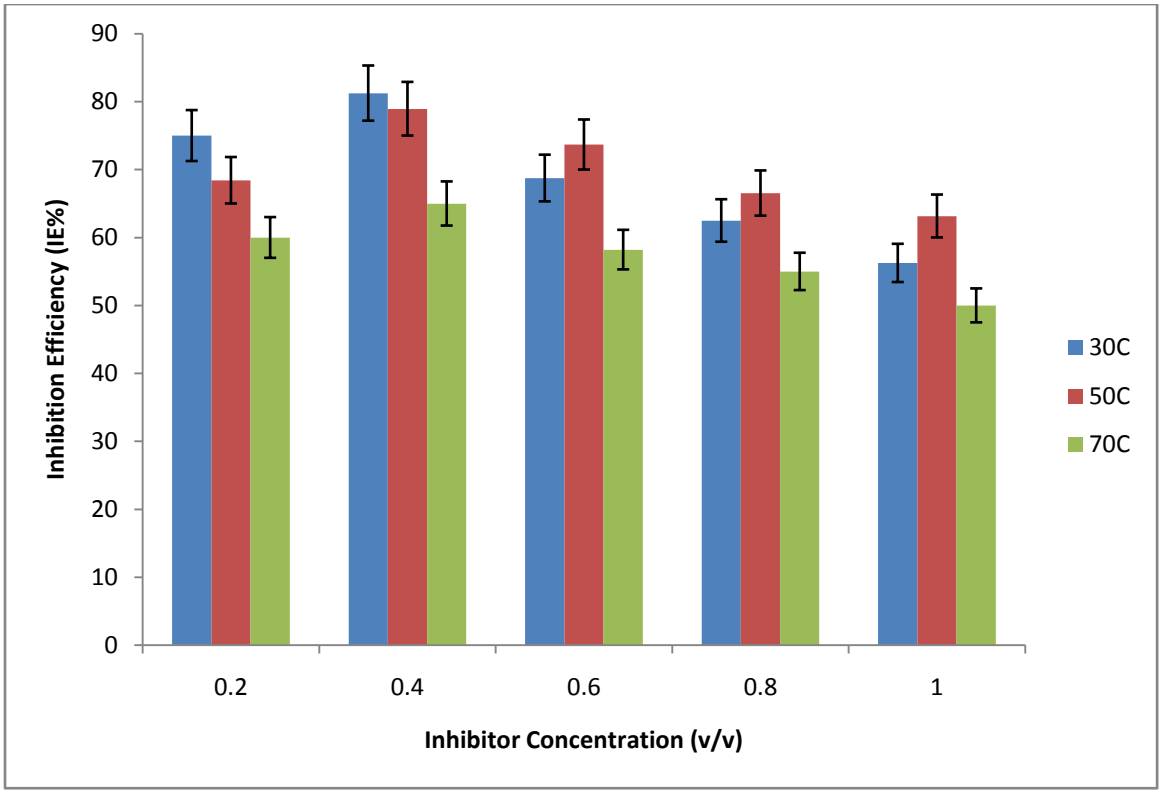

Figure 4.66: Variations of Inhibition Efficiencies (IE %) of CG with Inhibitor Concentrations at different temperatures in 3.5wt.% NaCl Solution.

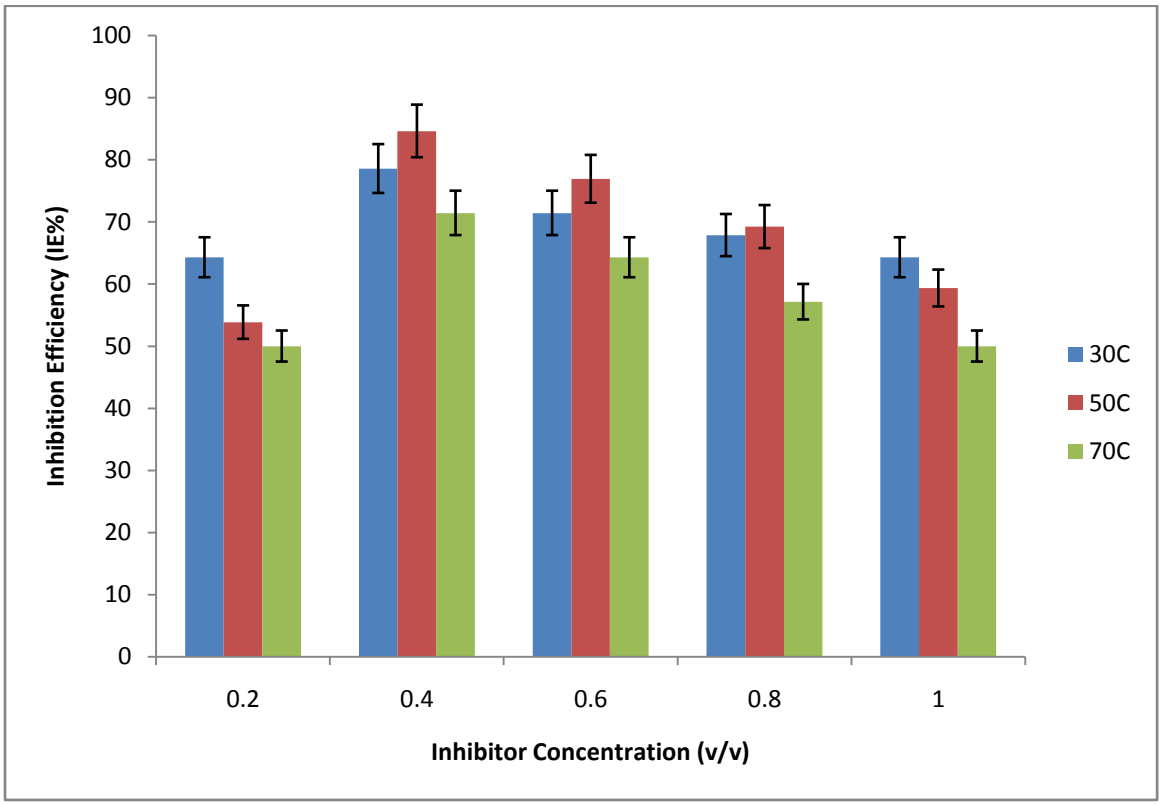

Figure 4.67: Variations of Inhibition Efficiencies (IE %) of FE with Inhibitor Concentrations at different temperatures in 3.5 wt. % NaCl Solution.

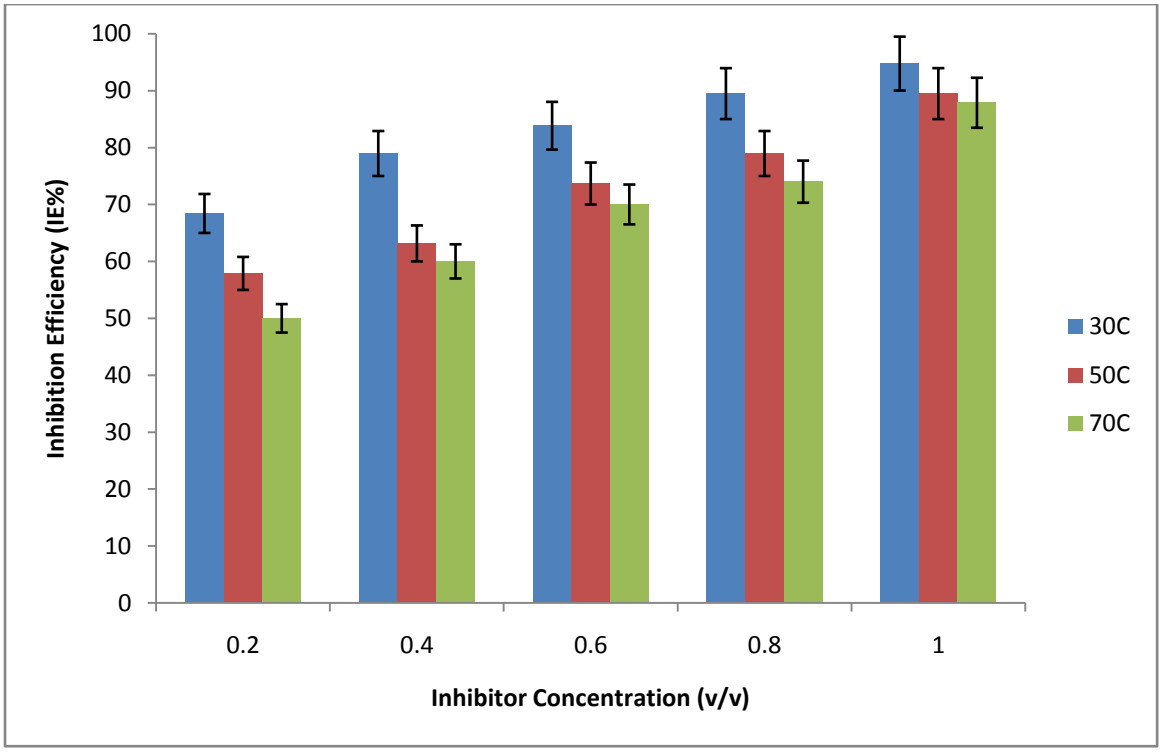

Figure 4.68: Variations of Inhibition Efficiencies (IE %) of FP with Inhibitor Concentrations at different temperatures in 3.5wt.% NaCl Solution.

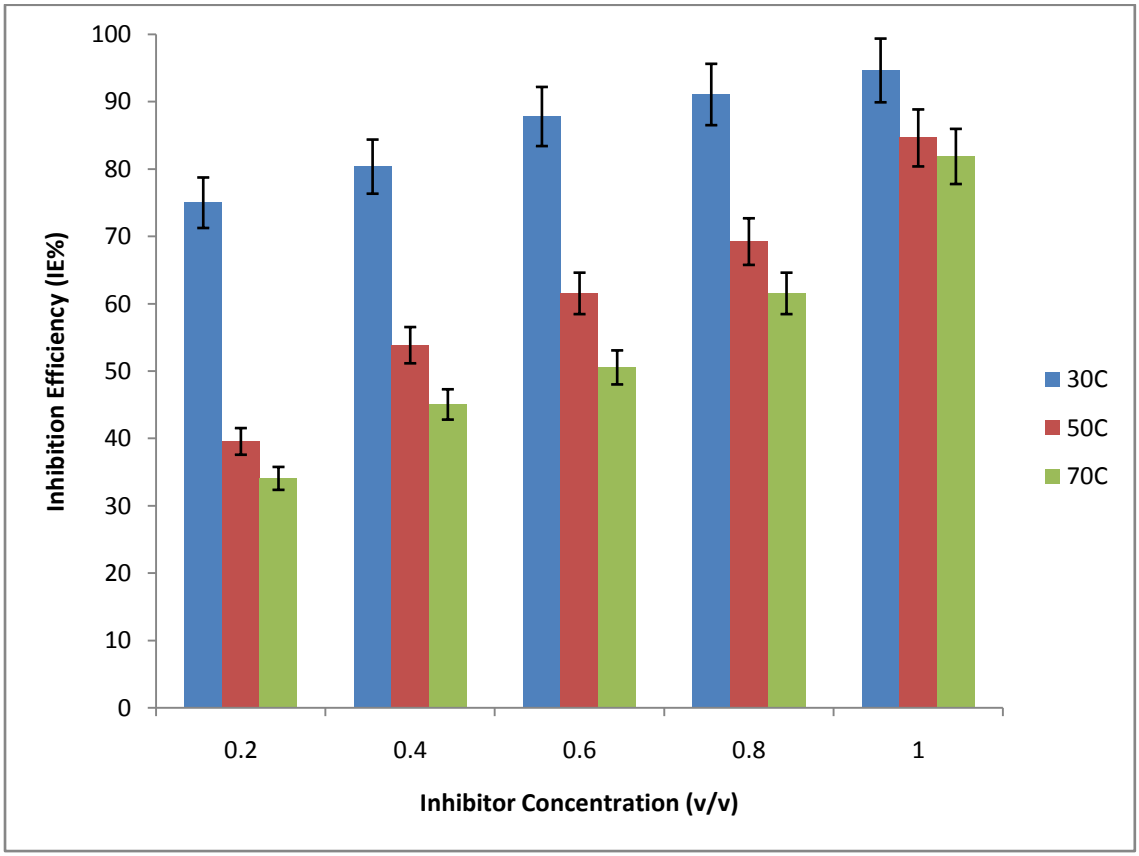

Figure 4.69: Variations of Inhibition Efficiencies (IE %) of Sodium Chromates with InhibitorConcentrations atdifferent temperatures in 3.5wt.%NaClSolution.

Table 4.4: Comparing maximum inhibition efficiencies of gravimetric and linear polarization

Inhibitor Concentration (v/v)	Gravimetric IE %		Linear Polarization IE %	
0.8	94.44	CM	96.15	CM
0.4	81.25	CG	96.83	CG
0.4	84.62	FE	97.50	FE
1.0	94.74	FP	97.43	FP
1.0	94.64	Sodium chromates	98.99	Sodium chromates

surface. Consequently, the increase in the inhibitor efficiency was ascribed to the large surface coverage. The decrease in the protective properties of the inhibitor with increase in temperature may be attributed to two reasons, a certain drawing of adsorption – desorption equilibrium towards desorption (meaning that the strength of adsorption process decreases at higher temperatures) and roughening of the metal surface which results from enhanced corrosion. These results suggested that the adsorption was of physicaladsorption on Al- Si-Mg alloy which is in line with earlier reports by other authors. (Sastri, 1998; Obot *et al*., 2010 and Obot *et al.*, 2014).

4.2.5 Adsorption isotherm determination for consideration of mechanism of inhibition

Surface coverage data play an important role in assessment of inhibitor characteristics and are useful for fitting experimental data into adsorption isotherms which in turn give an insight into the mechanism of inhibition. The results of Langmuir adsorption isotherms are presented in Figures 4.70 – 4.72 at various temperatures for all the plant extracts and sodium chromates. Figure 4.73 shows the result of adsorption isotherm of the co-inhibition of extracts while Figures 4.74 – 4.78 are the Freundlich adsorption isotherm and Figures 4.79 – 4.83 are for El- Awady isotherm. Table 4.5 shows the Langmuir adsorption parameters of the extracts for all the various adsorption isotherms considered. The plots of θ/C against C gave a straight line with some correlations obtained suggesting that it follows Langmuir adsorption isotherm. The adsorption isotherm is said to be a monolayer in nature. The fitness of the adsorption isotherm models was determined by the closeness of linear correlation coefficient (R^2) value to unity. The best fitted models with R^2 closest to unity were then picked to describe the mechanism of adsorption. The ΔG_{ads} values for the extracts range from (-7.66) to (-11.07) kJ/mol suggesting that adsorption mechanism of the inhibitors on the alloy is mainly physisorption. K_{ads} represents the strength of adsorption between adsorbate and

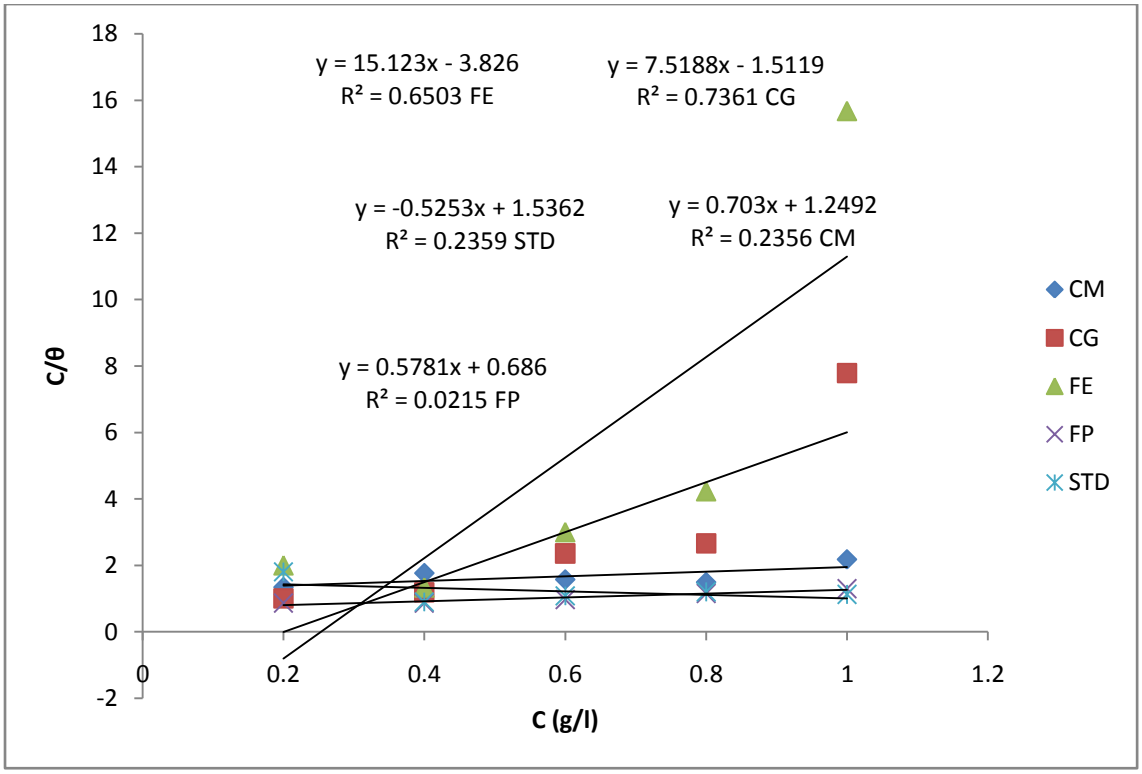

Figure 4.70: Langmuir Isotherm Plots of CM, CG, FE, FP, STD at 1hr, 30^{O}C

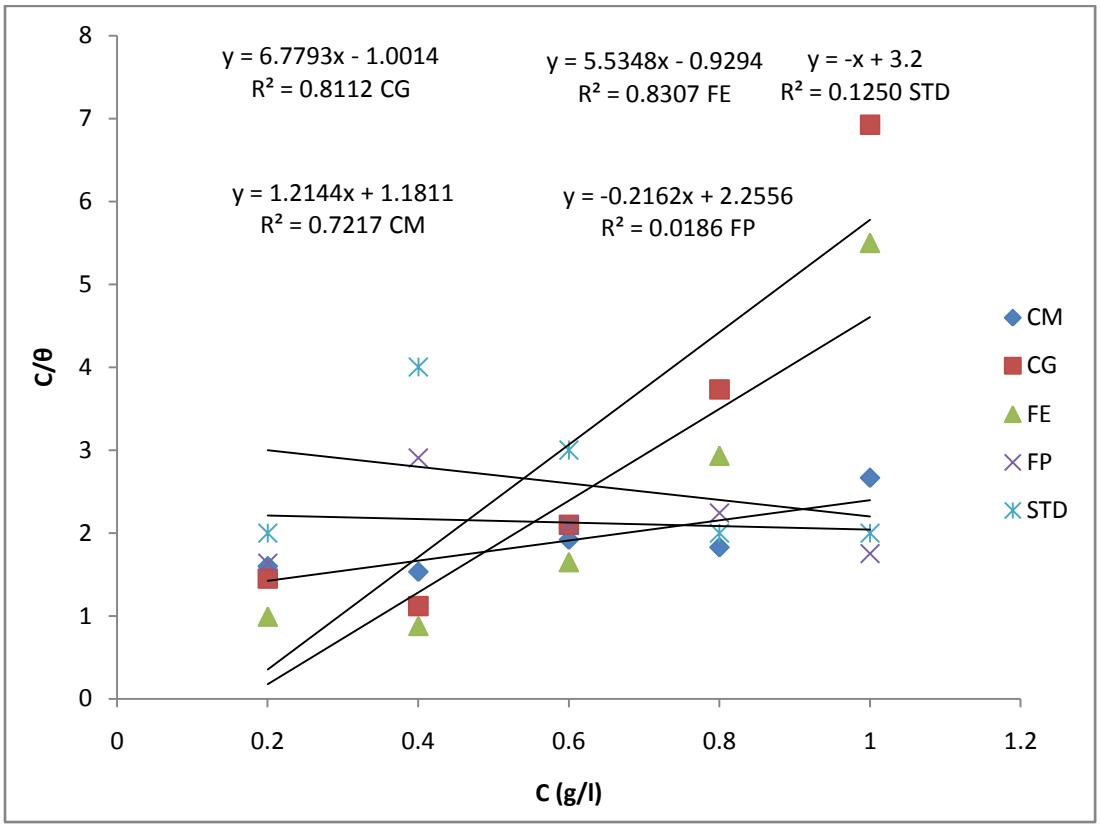

Figure 4.71: Langmuir Isotherm Plots of CM, CG, FE, FP, STD at 1hr, 50^{O}C

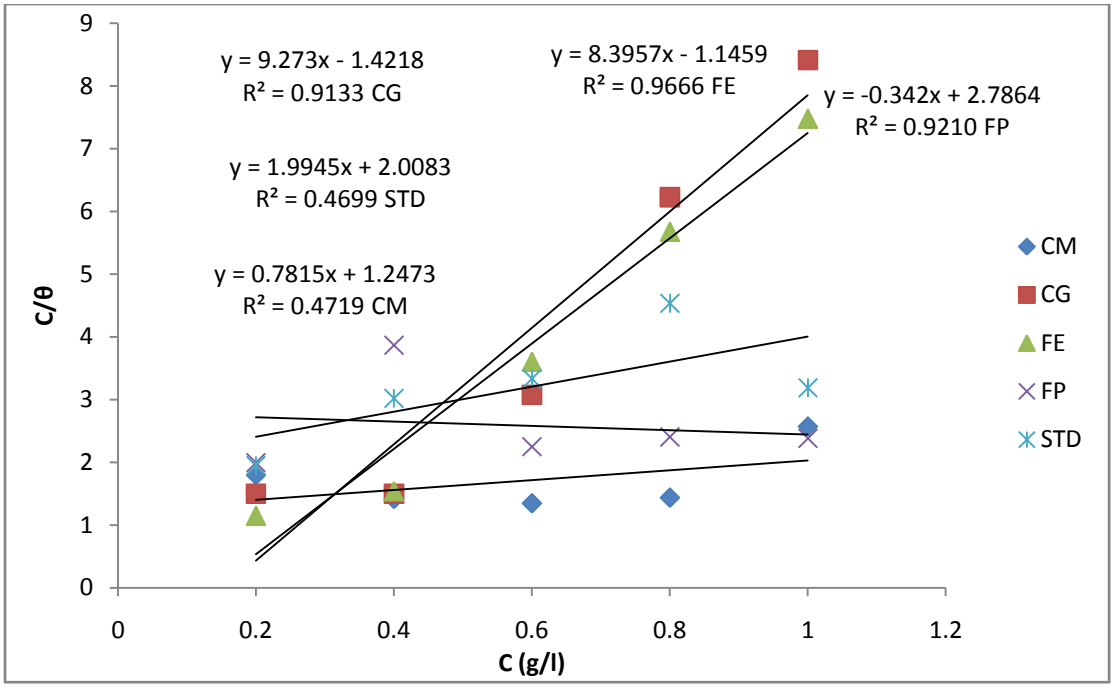

Figure 4.72: Langmuir Isotherm Plots of CM, CG, FE, FP, STD at 1hr, 70^{O}C

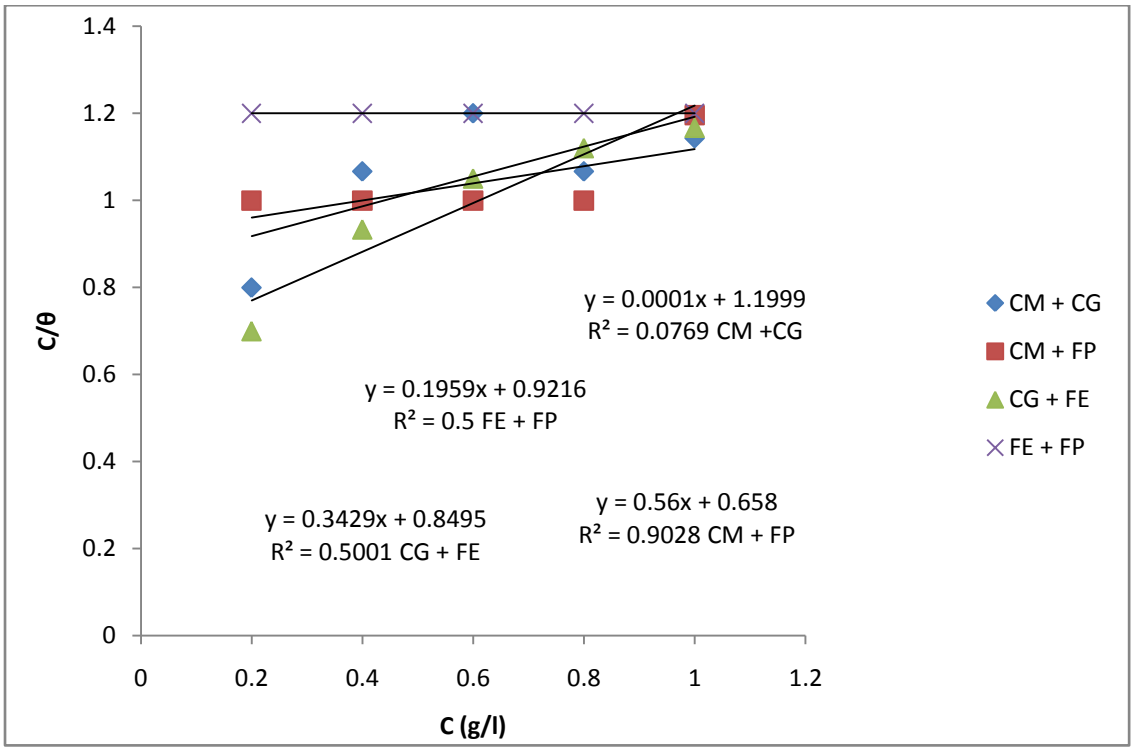

Figure 4.73: Langmuir Isotherm Plots of CM with CG, CM with FP, CG with FE, FE with FP, at 1hr, 30^{O}C

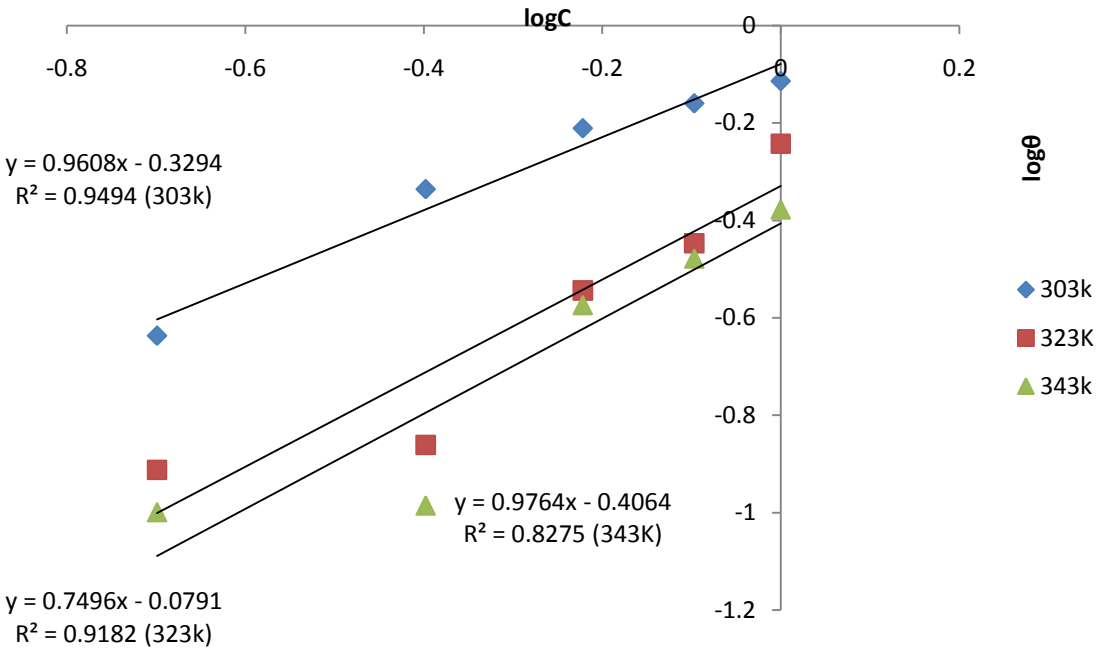

Figure 4.74: Freundlich Isotherm Plots of CM, 1hr. of exposure time, at 30^0C

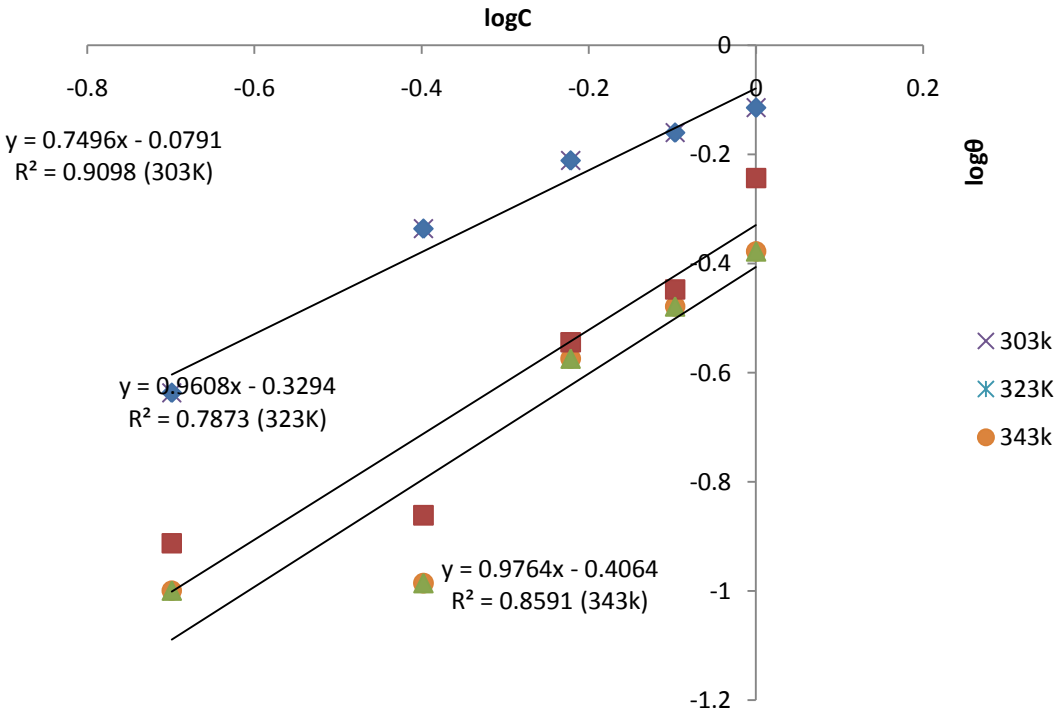

Figure 4.75: Freundlich Isotherm Plots of CG, 1hr. of exposure time, at 30 ^{O}C

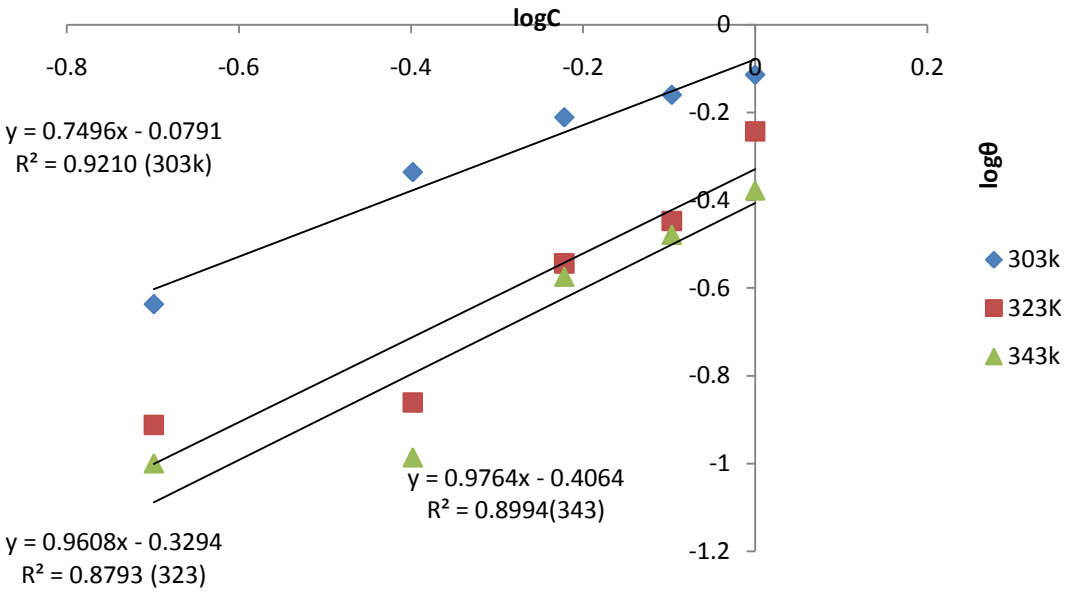

Figure 4.76: Freundlich Isotherm Plots of FE, 1hr. of exposure time, at 30^0C

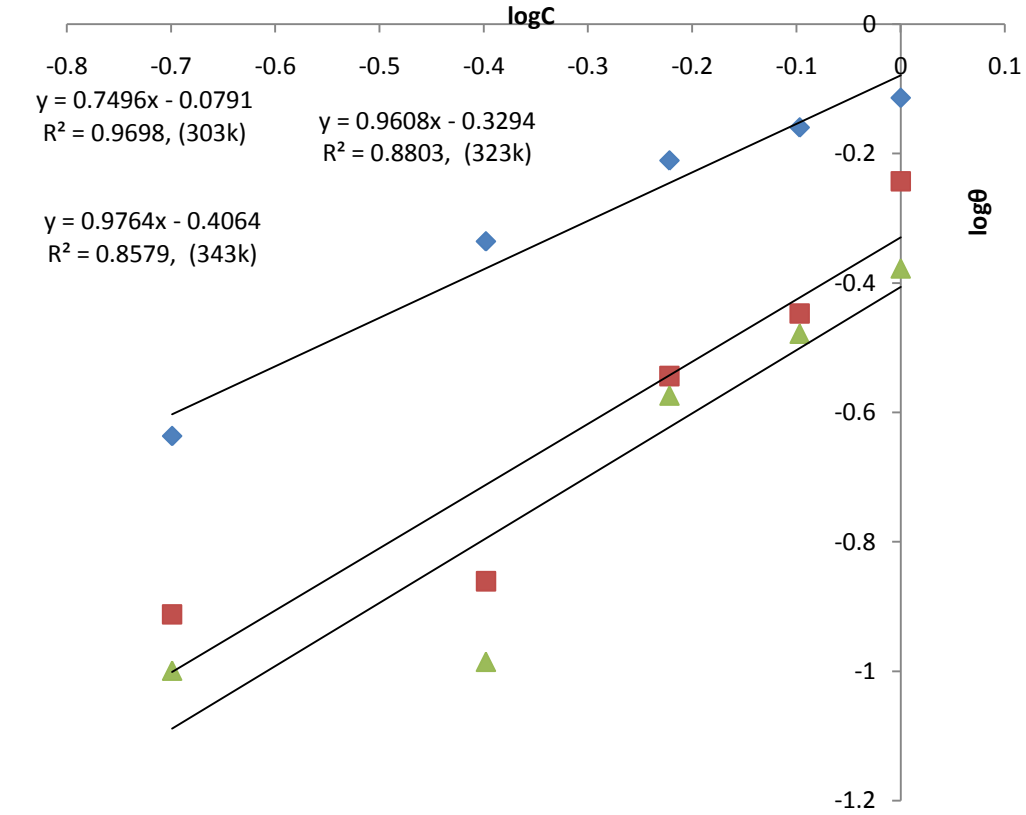

Figure 4.77: Freundlich Isotherm Plots of FP, 1hr. of exposure time, at 30 ^{0}C

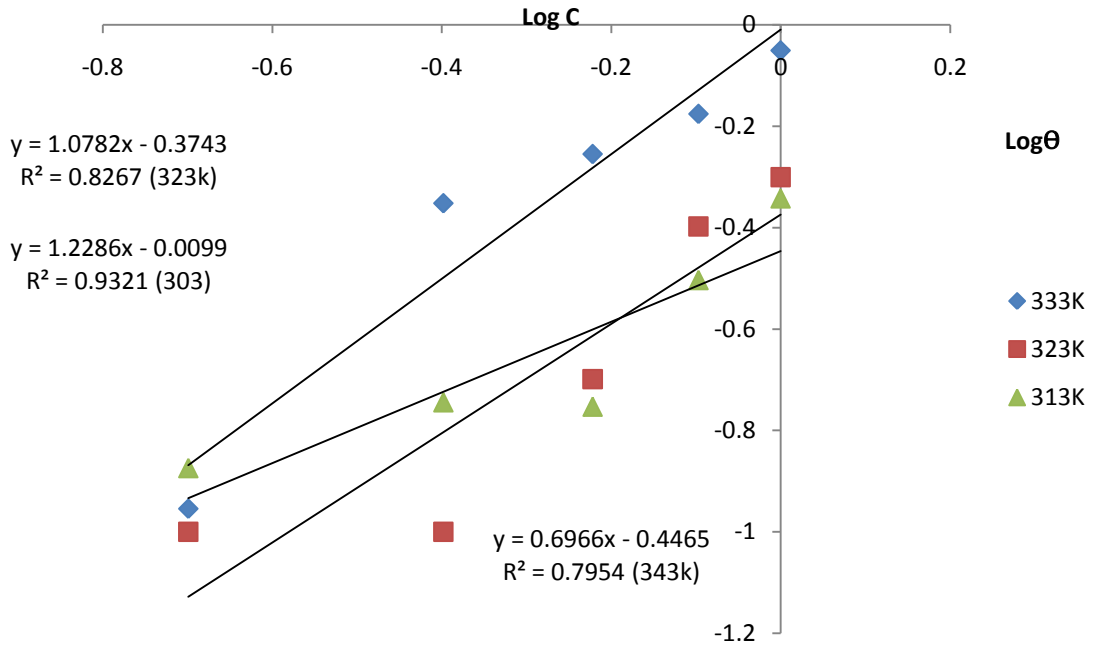

Figure 4.78: Freundlich Isotherm Plots of Sodium Chromate, 1hr. of exposure time, at 30^0C

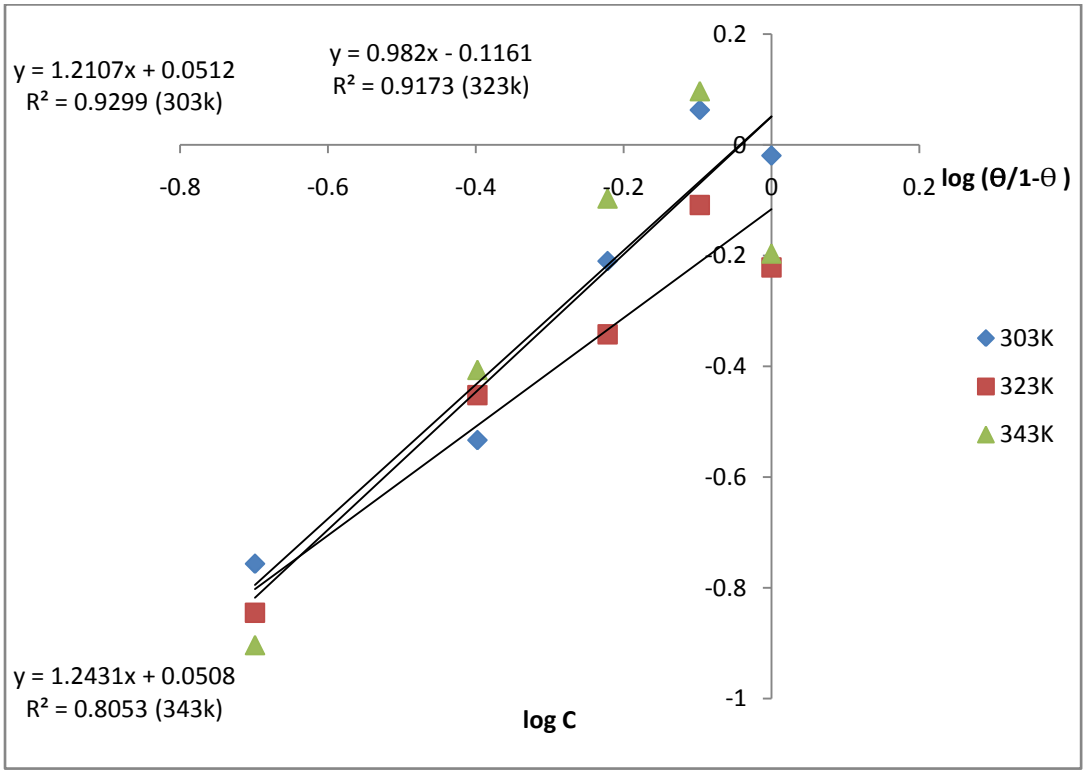

Figure 4.79: El-Awady Isotherm Plots of CM, 1hr

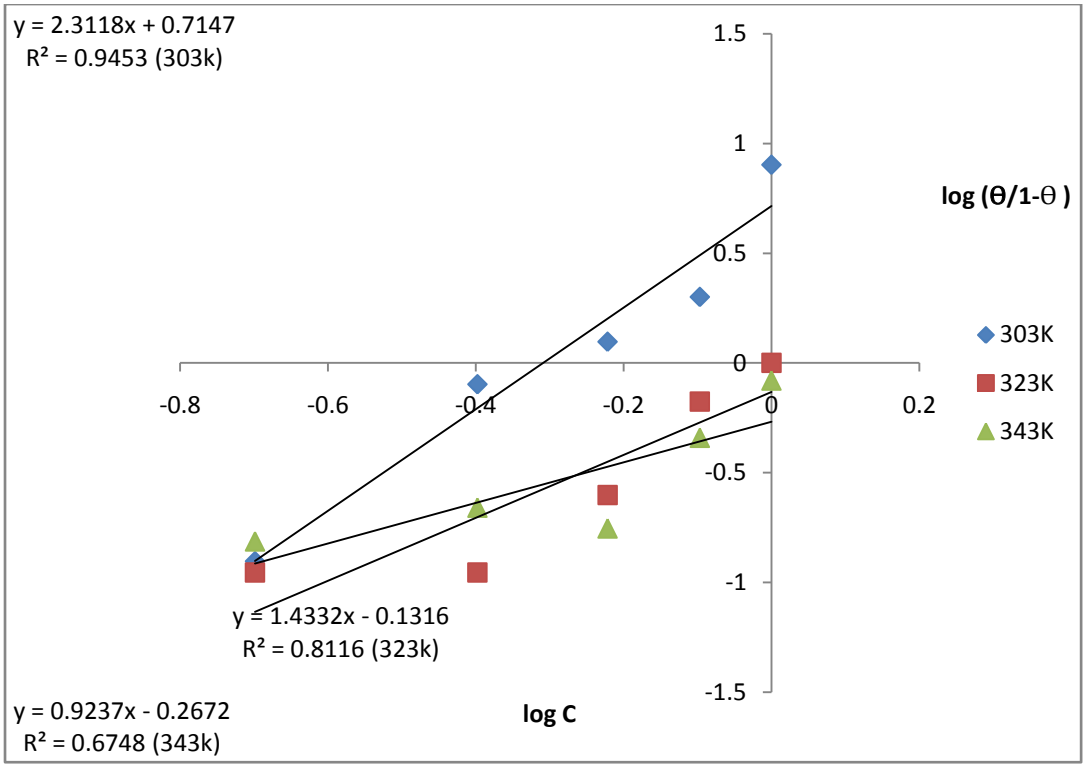

Figure 4.80: El-Awady Isotherm Plots of CG, 1hr.

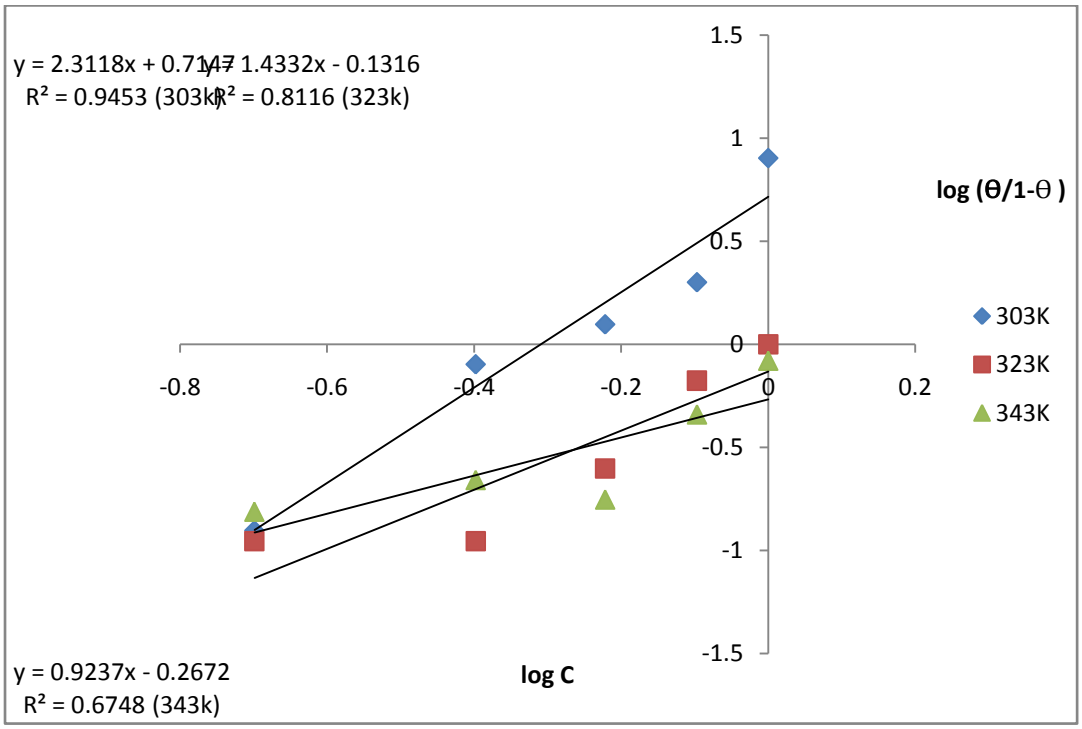

Figure 4.81: El-Awady Isotherm Plots of FP, 1hr.

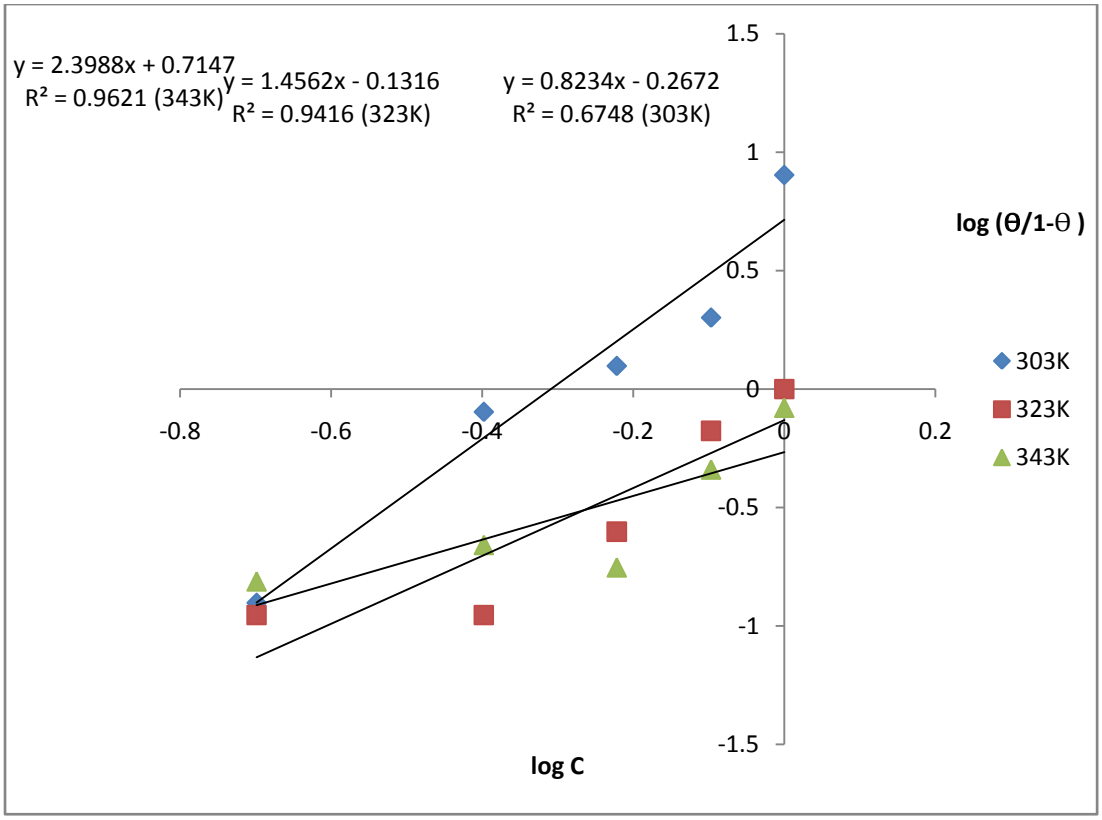

Figure 4.82: El-Awady Isotherm Plots of FE, 1hr.

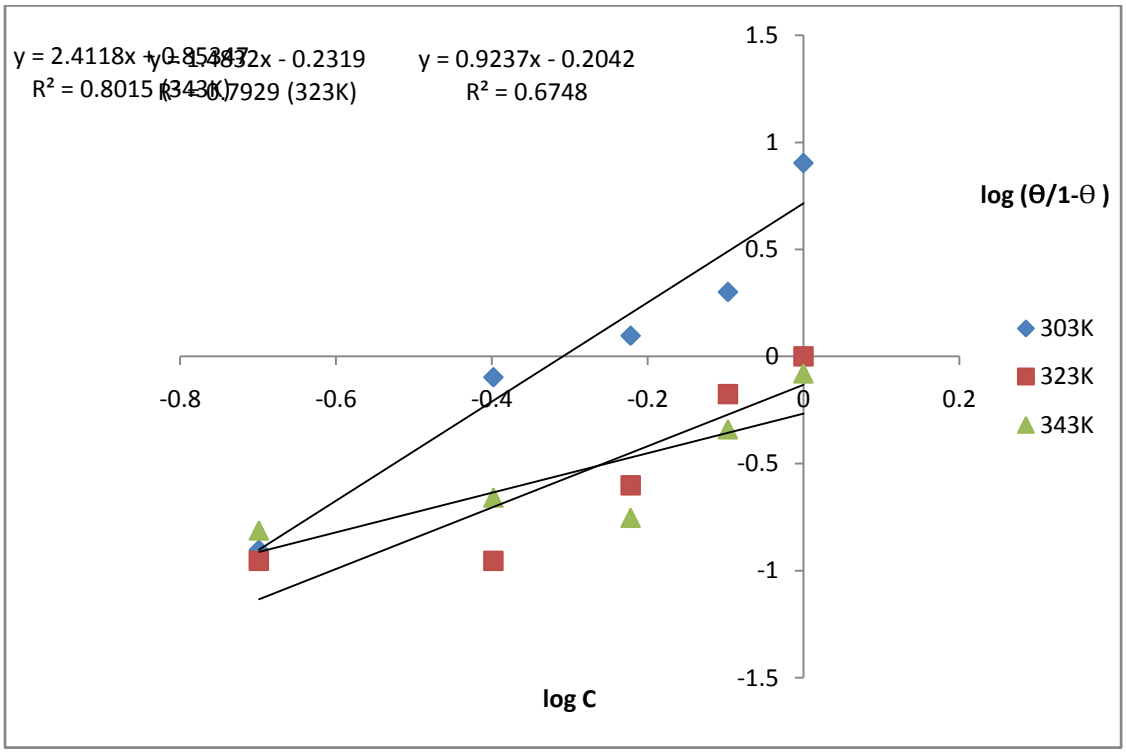

Figure 4.83: El-Awady Isotherm Plots of Sodium Chromate, 1hr. and adsorbent. High values of K_{ads} imply favorable adsorption and hence better inhibitors efficiencies (Joseph *et al*., 2014).

Table 4.5 Adsorption isotherm parameters (Langmuir) for CM, CG, FE, FP, Sodium Chromates at 30^0C, 50^0C and 70^0C, 1 hour in 3.5wt% NaCl Solution.

Extract	**Temperature**	**ΔG_{corr} (kJ/Mol).**	**Slope**	**R^2**	**K_{ads}**
CM	30	-9.56	0.7815	0.2356	0.8017
	50	-10.34	1.2144	0.7217	0.8467
	70	-10.83	0.7030	0.4719	0.8005
CG	30	-9.08	7.5188	0.7361	0.6614
	50	-10.78	6.7793	0.8112	0.9986
	70	-10.45	9.2730	0.9133	0.7033
FE	30	-6.74	15.123	0.6503	0.2614
	50	-10.98	5.5348	0.8307	1.0760
	70	-11.07	8.3957	0.9666	0.8727
FP	30	-11.07	0.3420	0.0215	0.3589
	50	-8.60	0.2162	0.0186	0.4433
	70	-8.53	0.5781	0.9210	1.4577
Sodium Chromate	30	-9.04	0.5253	0.2359	0.6510
	50	-7.66	1.0000	0.1250	0.3125
	70	-9.47	1.9945	0.4699	0.4979

4.2.6 Kinetic/Thermodynamic Consideration

The mode of adsorption of inhibitors which can either be physisorption or chemisorption may be predicted from the knowledge of thermodynamic parameters that govern the adsorption process. The apparent activation energies (E_a) for corrosion process in the absence and presence of leave extracts of CM, CG, FE and FP were calculated using Arrhenius equation (4.2)

$$\text{Log CR} = \text{Log A} + (-Ea/RT) \quad (4.2)$$

where CR is the corrosion rate of Al- Si- Mg alloy, A is the frequency factor and R is the universal gas constant.

The plots of Log (CR/T) versus 1/T shown in Figures 4.84 – 4.88 were used to determine the values of enthalpy and entropy changes of activation for the extracts and the values of the enthalpies were all positive, reflecting endothermic nature of the aluminum dissolution process in the medium. Similarly, plots of Log CR Vs 1/T are presented in Figures 4.89 – 4.93 which give the values of the activation energies of the metal corrosion and were found to increase with increase in inhibitor concentration which is indicative of modification of corrosion process attributable to the interaction of extract chemical constituents with metal surface or corrodent. Similar results have been attributed to physisorption in which inhibition efficiency at normal temperature is high but diminishes at elevated temperatures (Babatunde *et al.,* 2012). In order to have more insight into the mechanism of inhibition of corrosion process, other thermodynamic parameters were calculated using Erying's equation (4.3).

$$\text{Log (CR/T)} = \text{Log (K/h)} + \Delta S^{\circ}/R - \Delta H^{\circ}/RT \quad (4.3)$$

where CR is corrosion rate, K is the Boltzman's constant, h, the plank's constant; ΔS° and ΔH° are changes in entropy and enthalpy of activation respectively.

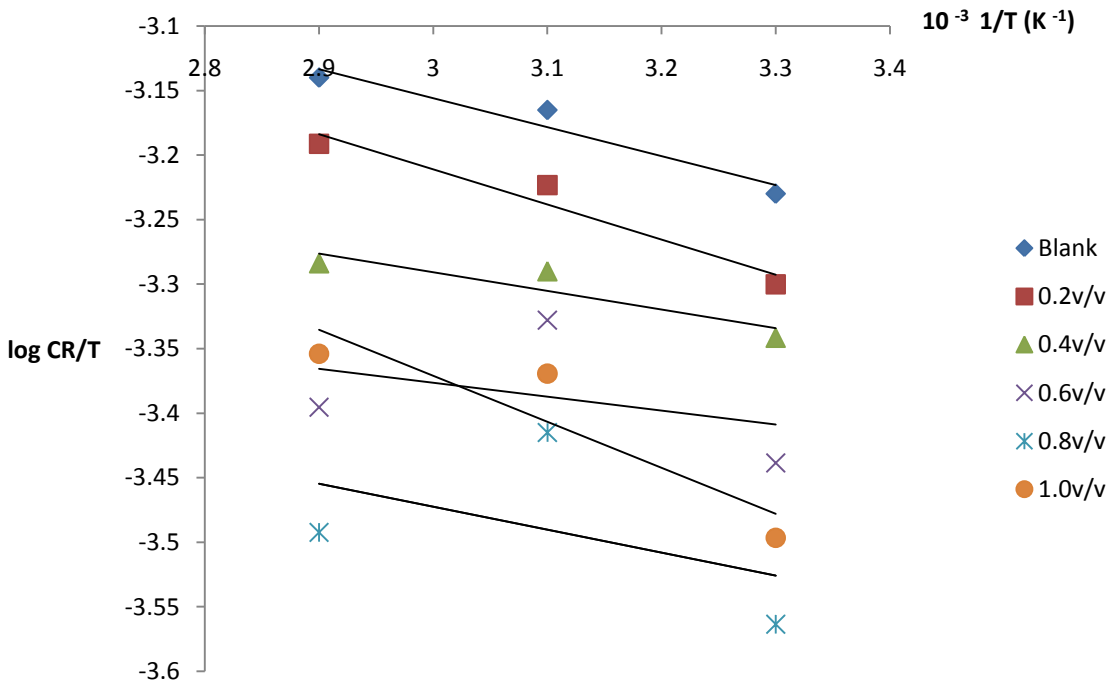

Figure 4.84 Log CR/T versus 1/T of CM in 3.5wt% NaCl of Al-Si-Mg alloy

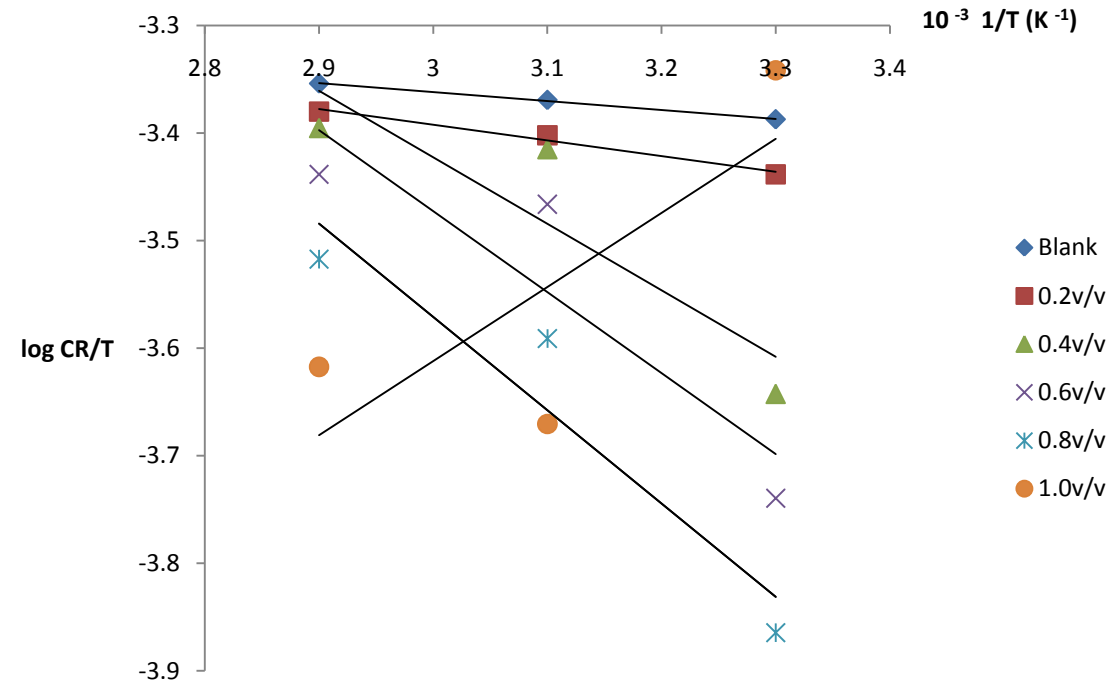

Figure 4.85: Log CR/T versus 1/T of CG in 3.5wt% NaCl of Al-Si-Mg alloy.

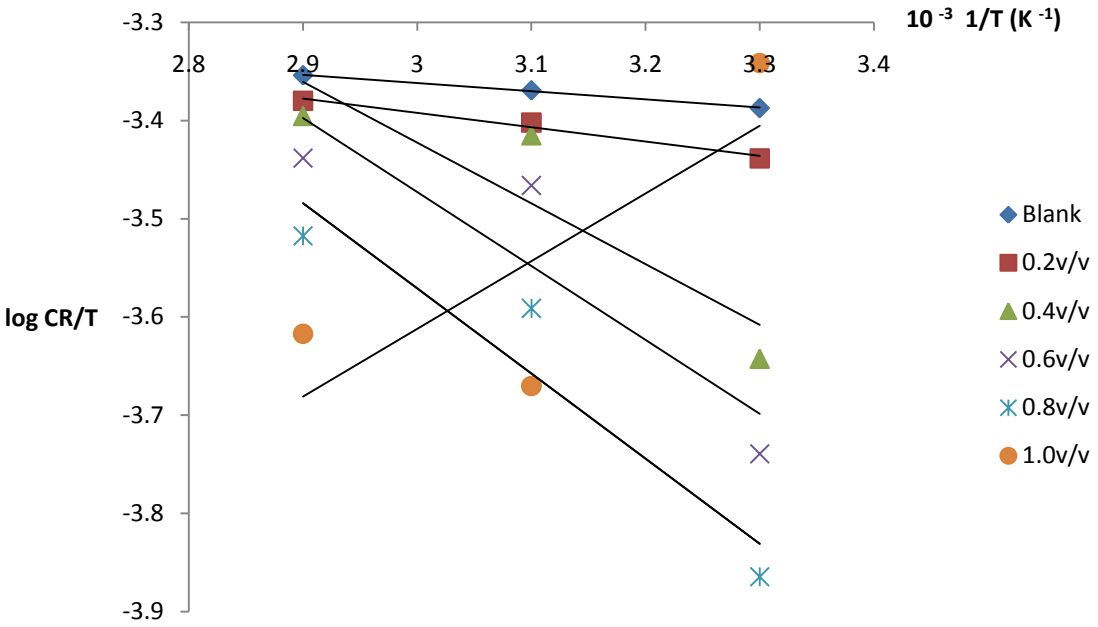

Figure 4.86: Log CR/T versus 1/T of FE in 3.5 wt% NaCl of Al-Si-Mg alloy

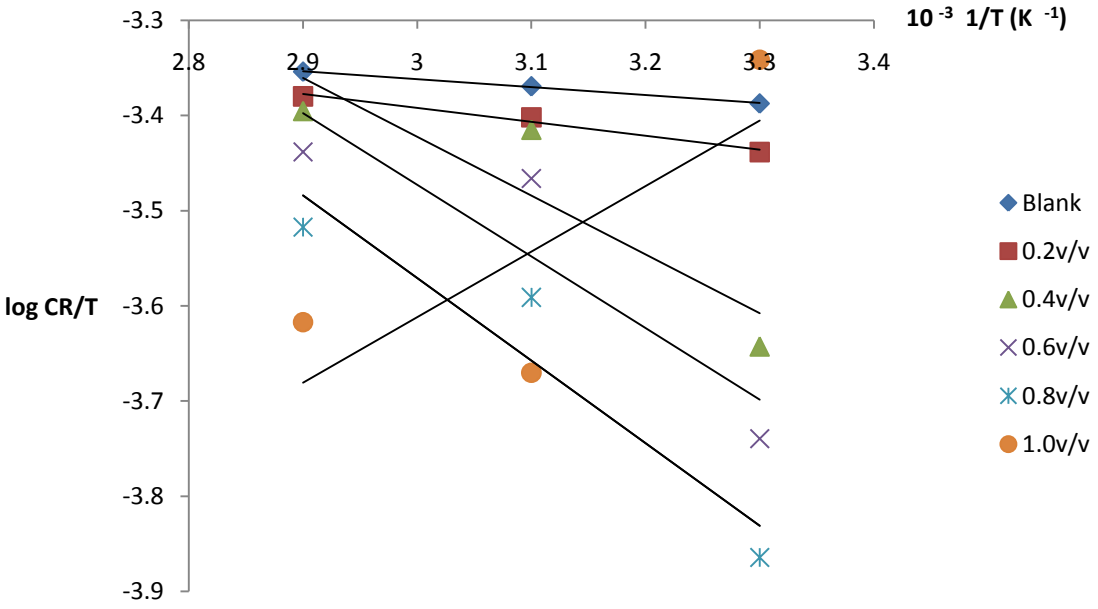

Figure 4.87: Log CR/T versus 1/T of FP in 3.5wt% NaCl of Al-Si-Mg alloy.

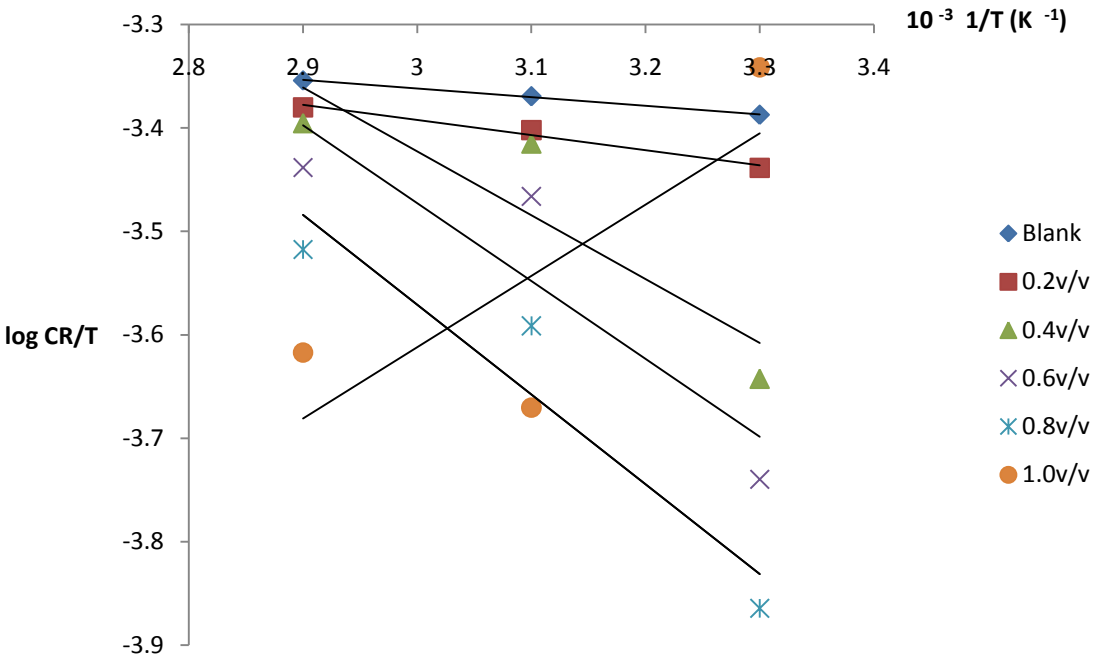

Figure 4.88: Log CR/T versus 1/T of Chromate in 3.5 wt% NaCl of Al-Si-Mg alloy

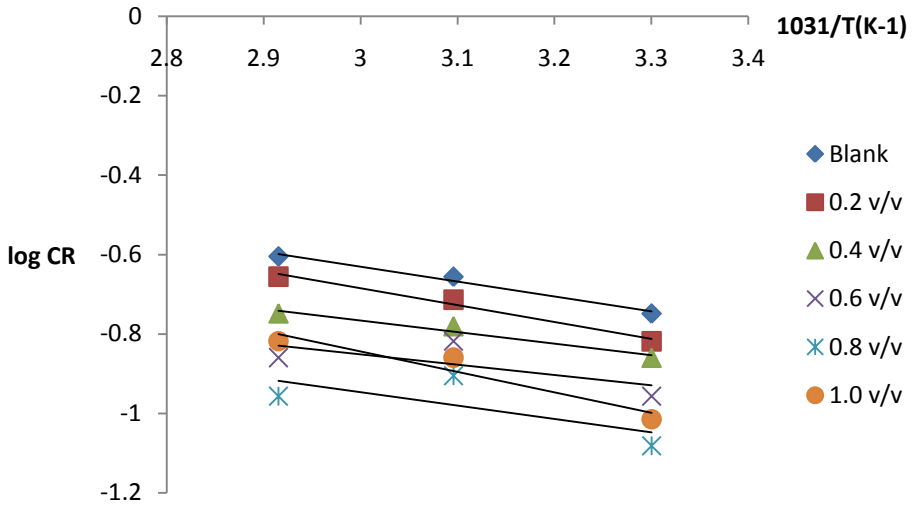

Figure 4.89: Log CR versus 1/T of CM in 3.5wt% NaCl of Al-Si-Mg alloy

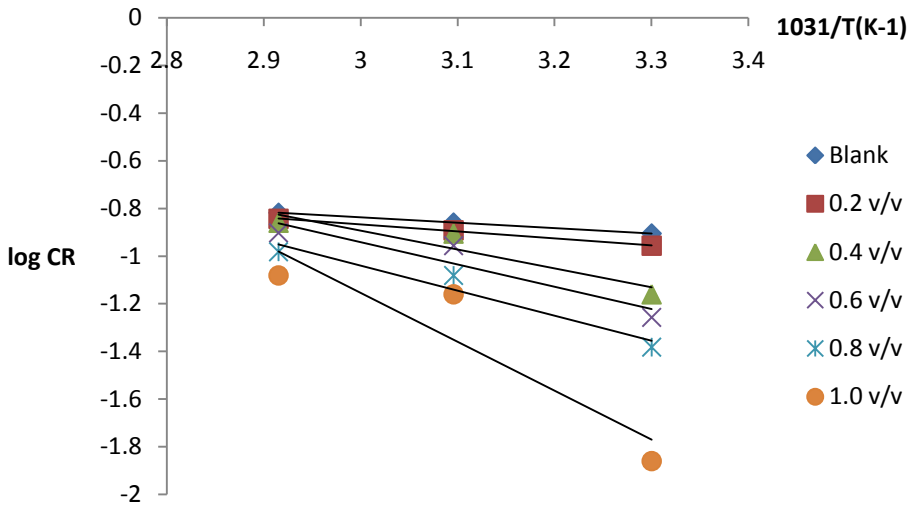

Figure 4.90: Log CR versus 1/T for CG in 3.5wt% NaCl of Al-Si-Mg alloy

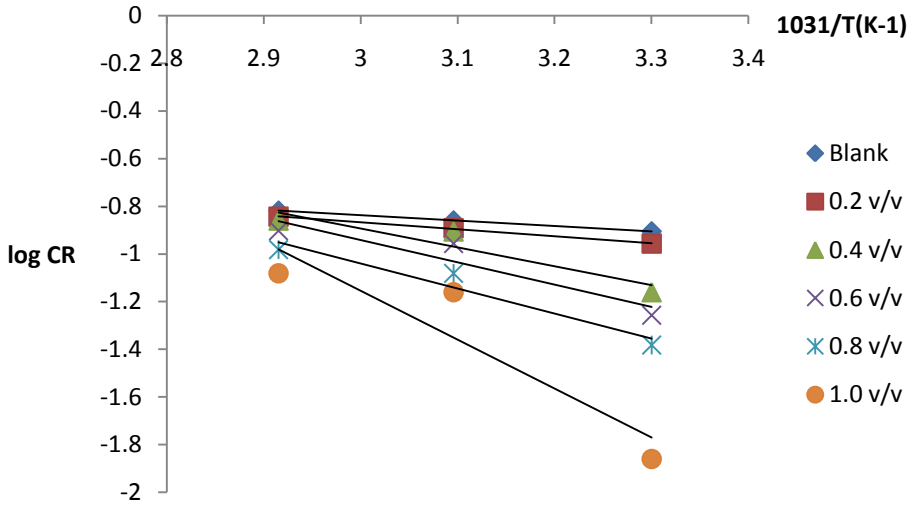

Figure 4.91: Log CR versus 1/T for FE in 3.5wt% NaCl of Al-Si-Mg alloy

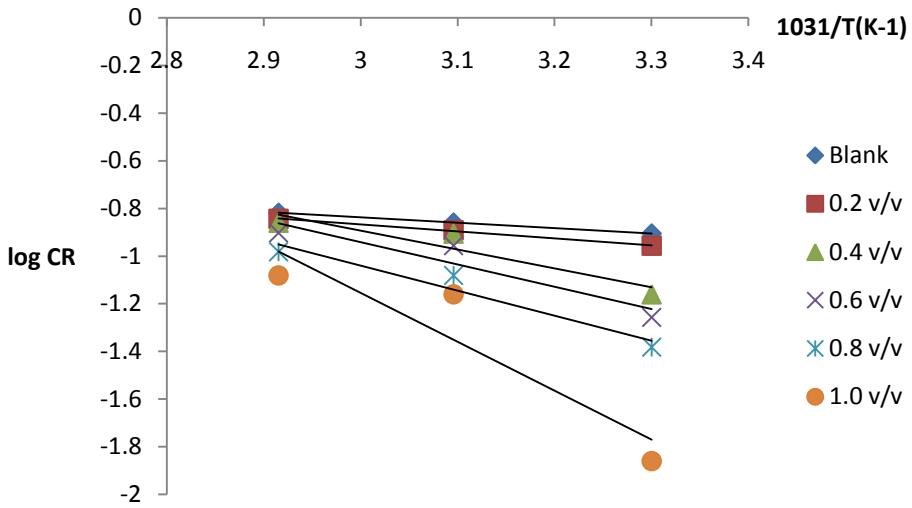

Figure 4.92: Log CR versus 1/T forFP in 3.5wt% NaCl of Al-Si-Mg alloy

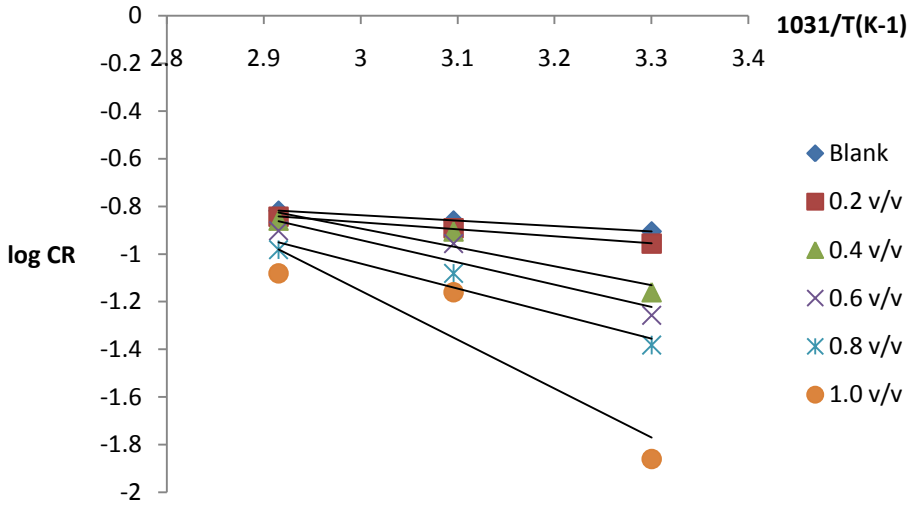

Figure 4.93: Log CR versus 1/T for Sodium Chromates in 3.5wt% NaCl of Al-Si-Mg alloy

The negative values of change in entropy of the reaction, $\Delta S^{\square}$, activation energies, in the presence of the inhibitor as presented in Table 4.6, imply that the activated complex in the rate- determining steps was an association rather than a dissociation step; a decrease in disorderliness took place on going from reactants to the activated complex (Ating *et al*., 2010; Singh *et al*., 2010).

Values of free energy of adsorption of the plant extracts on Al- Si- Mg alloy surface were calculated using equation (4.4) below (Adejo *et al*., 2012; Khadom *et al.*, 2010; Shukla *et al.*, 2011).

$$\Delta G_{ads} = -2.303\ RT\ Log\ (55.5\ k) \qquad (4.4)$$

where $k = \Theta / [(1 - \Theta)\ C]$, C is the inhibitor concentration; Θ is the surface coverage. The values were all negative, a clear indication that adsorption of the inhibitor on to the metal surface is spontaneous and the increase in values with rise in temperature shows that the spontaneity of the adsorption increased as temperature was raised. However, the values were less than -20 kJ/mol, which is the threshold value for physical adsorption mechanism. Generally, when the values of ΔG_{ads} are up to -20 kJ/mol, it was reported to be consistent with electrostatic interaction between charged molecules and a charged metal (which indicates physical adsorption), and when the values were above -40 kJ/mol. it indicates chemisorption (Adejo *et al.*,2013).

4.2.7 Effect of co-inhibition and surfactant addition

The co-inhibition potentials of the plant extracts was evaluated in order to ascertain the effect of one extract in combination with the other. Table 4.7 shows the co-inhibition parameters for the plant extracts. These values were obtained using equation (2.25), where it was reported that if the value of $Sp > 1$ it indicates that there is a synergistic effect, when $Sp < 1$, it indicates the antagonistic interaction between the inhibitors compounds and if Sp approaches unity in implies no interaction (Obot *et al.*, 2011; Umoren *et al.*, 2008).

Table 4.6: Activation Energy Parameters E_a, ΔH_{ads}, ΔS_{ads} for Al-Si-Mg Alloy in 3.5 wt.% NaCl Solution for CM, CG, FE, FP and Sodium Chromate.

Inhibitor Concentration (v/v)		**$-E_{ads}$ (kJ/Mol)**	**ΔH_{ads}.(kJ/Mol)**	**ΔS_{ads} (kJ/Mol. K)**
Blank		7.19	4.30	-0.2452
0.2		8.13	5.21	-0.2435
0.4		5.58	2.76	-0.2524
0.6	CM	4.99	2.06	-0.2562
0.8		6.44	3.40	-0.2539
1.0		9.87	6.82	-0.2435
Blank		4.72	1.94	-0.2536
0.2		5.89	0.90	-0.2579
0.4		6.84	4.05	-0.2503
0.6	CG	6.30	3.53	-0.2510
0.8		5.75	2.99	-0.2519
1.0		4.74	2.03	-0.2541
Blank		1.71	0.98	-0.2649
0.2		2.32	0.39	-0.2637
0.4		2.68	0.20	-0.2646
0.6	FE	2.37	0.13	-0.2645
0.8		2.83	0.22	-0.2629
1.0		1.81	5.74	-0.2810
Blank		3.09	0.40	-0.2581
0.2		7.35	4.42	-0.2468

0.4		14.29	11.00	-0.2277
0.6	FP	17.28	13.82	-0.2210
0.8		20.12	16.50	-0.2138
1.0		23.14	19.58	-0.2066
Blank		4.33	1.59	-0.2573
0.2		5.60	2.80	-0.2542
0.4		15.17	11.83	-0.2277
0.6	Sodium Chromate	17.89	14.19	-0.2216
0.8		20.12	16.61	-0.2162
1.0		39.30	13.20	-0.3064

Table 4.7: Co-inhibition Parameters (Sp) For Different Concentration of Extract at 30^0C in 3.5wt.% NaCl Solution.

Inhibitor Concentration (v/v)		1 hour	5 hour
0.2		1.4079	2.1093
0.4		1.5173	1.9684
0.6	CM with CG	1.2769	1.7247
0.8		0.9427	1.7674
1.0		0.7016	1.5050
0.2		1.9468	2.3653
0.4		1.7385	2.0834
0.6	CM with FP	1.6722	1.9390
0.8		1.5420	2.0464
1.0		1.5101	1.9230
0.2		1.0475	1.7111
0.4		1.4986	1.8534
0.6	CG with FE	0.7918	1.5707
0.8		0.4981	1.4082
1.0		0.2151	1.2700
0.2		2.0472	2.0811
0.4		2.3245	2.0080
0.6	FE with FP	1.6437	1.8057
0.8		1.3269	1.7426
1.0		0.9996	1.6940

Considering CM with CG and CG with FE at 1hr there is synergistic effect at a concentration of 0.2, 0.4, and 0.6 v/v. When the concentration was further increased beyond 0.6 v/v antagonistic interaction prevails. However, at 5hrs, all the values obtained indicated synergy among the extracts.

Considering CM with FP and FE with FP, the values obtained revealed that interaction exists at all concentration and time considered. Considering CM with FP and FE with FP, the values obtained revealed that interaction exists at all concentration and time considered.

Addition of MEA and TEA as surfactants was used to further enhance the corrosion resistance of the Al-Si-Mg alloy. The synergy of the extracts with surfactants show that efficiencies increase with increase in concentration. In the case of FP with MEA and FE with TEA, a maximum efficiency of 84.20 % at 1.0 v/v in 1hr was obtained. Also, the synergy values calculated were greater than unity which shows that the enhanced inhibition efficiency caused by the various additions of the extracts is only due to synergistic effects. This agrees with the report elsewhere (Oguzie 2005; Loto *et al*., 2014). The result obtained also revealed that synergizing two extracts together gave a higher inhibition efficiency of 95.13 % (CG with FE) compared to that of an extract with inhibition efficiency of 94.74 % (FP). This can be attributed to the phytoconstituents present in the extracts (functional groups, aromatic compounds). From the values obtained in Table 4.7, it indicates that the co-inhibition parameters increase with increase in the concentration of the extracts investigated. Finally, with the use of surfactants, it adsorption on to the alloy's surface was found to be responsible for the corrosion inhibition of the alloy and generally related to its capability to aggregate and form micelles (Maqsood *et al.,* 2011). Consequently, a better understanding of the relation between the adsorption of surfactant molecules on to the metal surface and corrosion inhibition is of great importance for both theoretical and experimental reasons. The high affinity of surfactant molecules to adsorb into interfaces to form micelles is likely to be

responsible for their uses. However, the introduction of surfactant did not perform better than plants used singly nor synergized.

4.3 Potentiodynamic Polarization Analysis

The potentiodynamic polarization curves of the corrosion of Al- Si- Mg alloy in 3.5 % NaCl solution (artificial sea water) are shown in Figures 4.94- 4.98. The corrosion parameters such as corrosion potential (E_{corr}), corrosion current (I_{corr}), Tafel slopes (β_a, β_c) for anodic and cathodic slopes, and the linear polarization resistance (LPR) result is presented in Table 4.58. The polarization curves indicated that both anodic and cathodic reactions are inhibited in the presence of CM, CG, FP, FE and Sodium chromate. The values obtained show that the corrosion rates decrease with addition of inhibitors. Similarly, there was a decrease in the corrosion current (I_{corr}) in the presence of extracts as the concentration is increased. This confirms the inhibitive action of the CM, CG, FE, .FP extracts, and sodium chromate in the medium. It was also observed that in the absence of inhibitors, the corrosion potential, E_{corr} is -1.7818V versus Saturated Calomel Electrode (SCE) and in the presence of inhibitors the corrosion potential is shifted to a lower value in all the extracts considered. This suggests that the plant extracts were able to interfere with the anodic and cathodic reaction sites (Sangeetha *et al*, 2012). The R_p values increase and the corrosion current decrease generally. This implies that a protective film was formed on the alloy surface (Saratha and Vasudha, 2010).

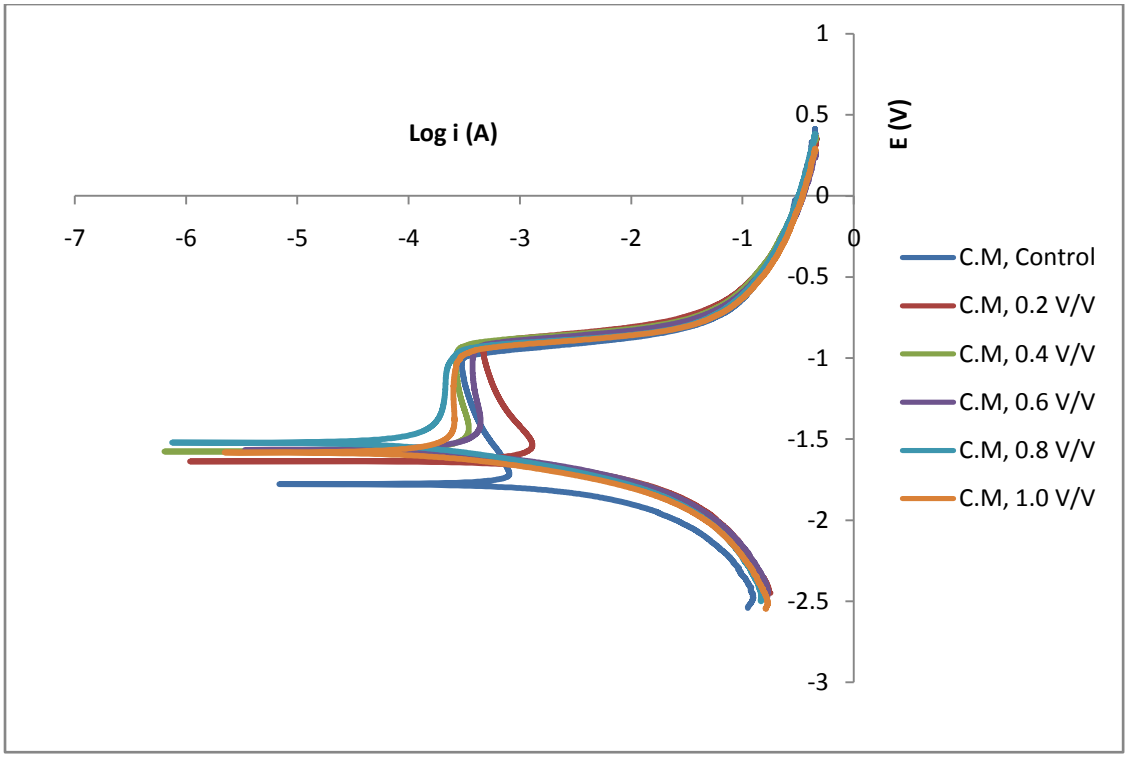

Figure 4.94: Polarization curves for the corrosion of Al-Si-Mg alloy in 3.5 wt.% NaCl Solution in the absence and presence of various concentration of the inhibitor at 303K of CM

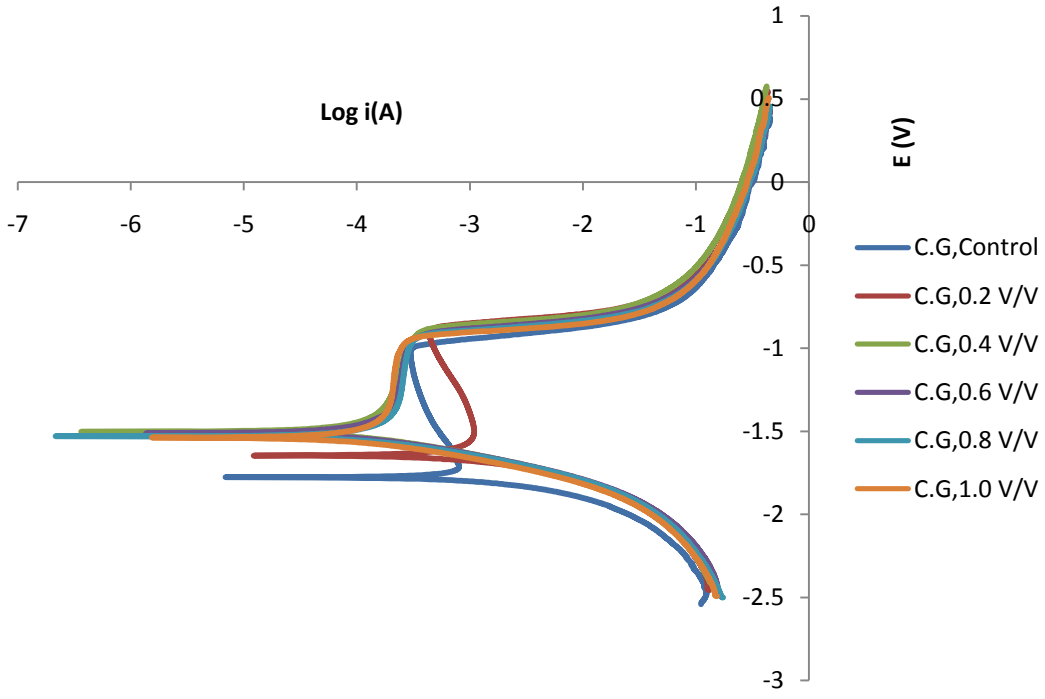

Figure 4.95: Polarization curves for the corrosion of Al-Si-Mg alloy in 3.5 wt.% NaCl Solution in the absence and presence of various concentration to the inhibitor at 303K of CG

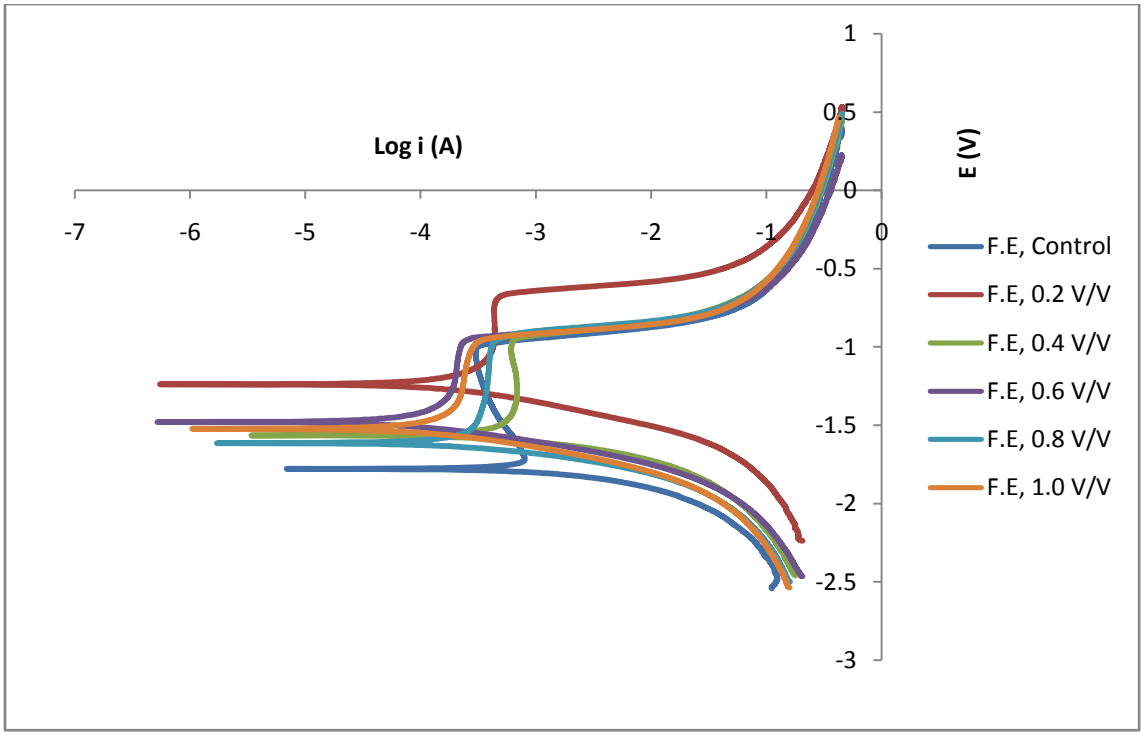

Figure 4.96: Polarization curves for the corrosion of Al-Si-Mg alloy in 3.5 wt.% NaCl Solution in the absence and presence of various concentration of the inhibitor at 303K of FE.

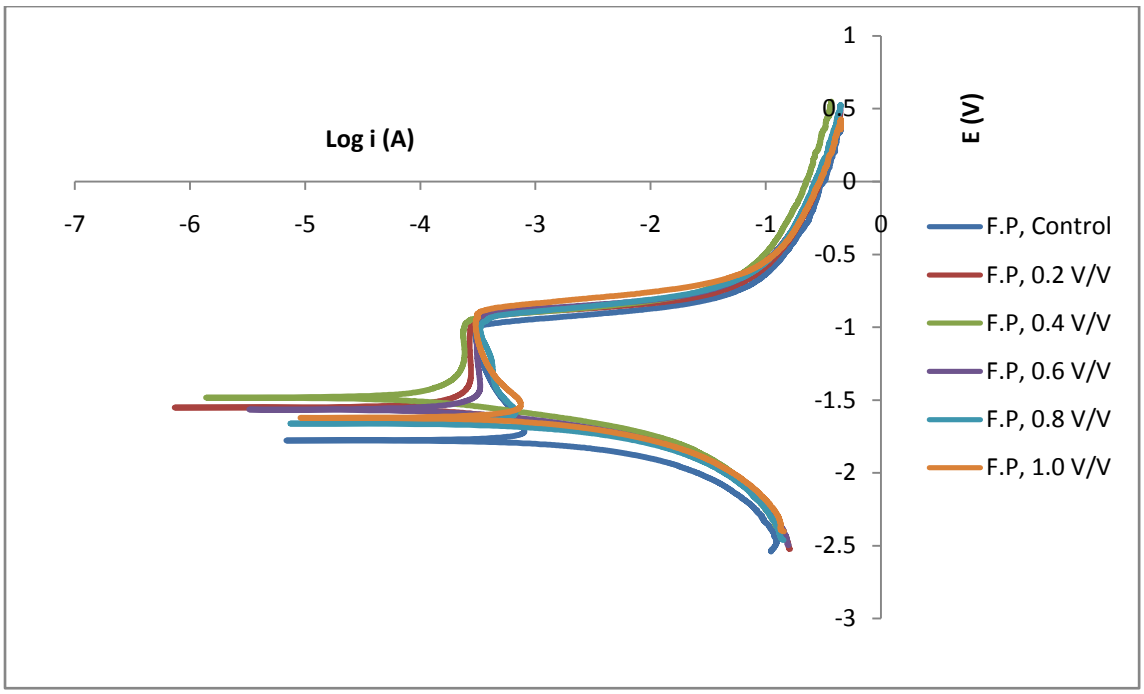

Figure 4.97: Polarization curves for the corrosion of Al-Si-Mg alloy in 3.5 wt.% NaCl Solution in the absence and presence of various concentration of the inhibitor at 303K of FP

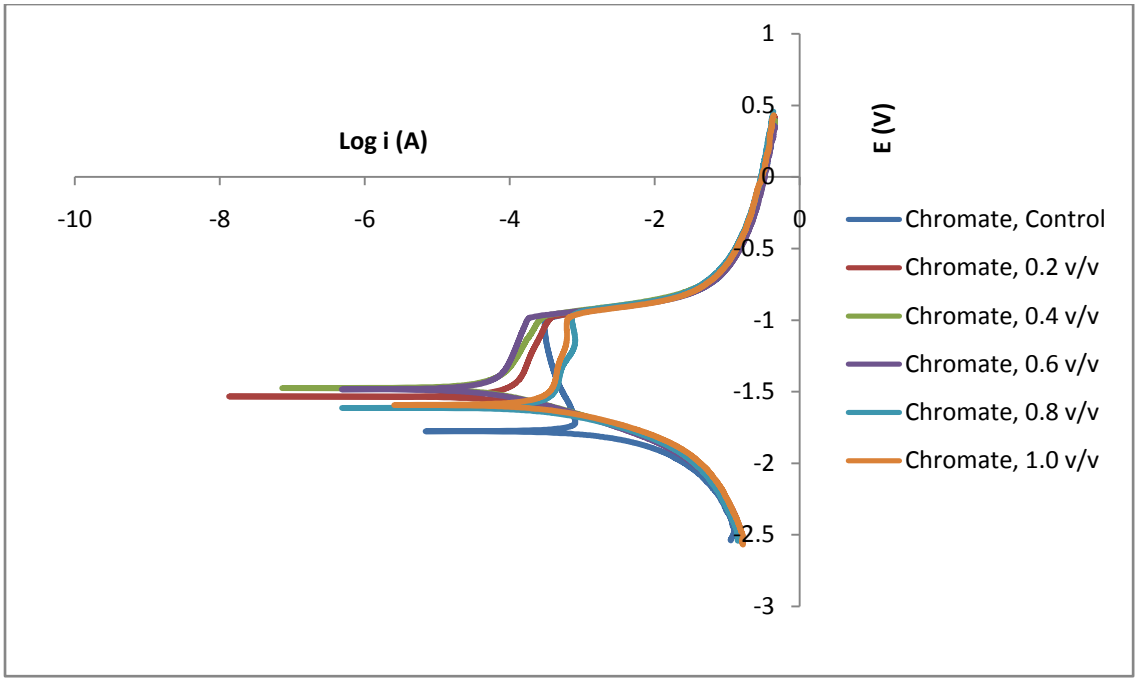

Figure 4.98: Polarization curves for the corrosion of Al-Si-Mg alloy in 3.5 wt.% NaCl Solution in the absence and presence of various concentration of the inhibitor at 303K of Sodium Chromates

Table 4.8: Potentiodynamic Polarization Measurement Parameters of Al-Si-Mg alloy in 3.5wt % NaCl Solution with different Concentration of Extracts.

Extract	I.C (v/v)	Ba	Bc	E_{corr} (v) Calc.	E_{corr} (v) Obs.	I_{corr} (A)	J_{corr} (A/cm^2)	C.R (mm/yr)	P R	I.E (%)
Blank	—	0.1389	-0.2668	-1.7818	-1.7780	0.0040	0.0013	13.02	31.53	—
CM	0.2	0.1378	-0.6926	-1.6418	-1.6372	0.0025	0.000865	8.38	29.10	80.62
	0.4	0.1340	-0.6280	-1.5820	-1.5772	0.00063	0.000211	2.05	117.97	84.33
	0.6	0.1447	-0.8718	-1.5752	-1.5662	0.00068	0.000228	2.21	111.16	83.05
	0.8	0.1251	1.1319	-1.5275	-1.5232	0.00015	0.000517	0.50	318.77	96.15
	1.0	0.1244	11.97	-1.5898	-1.5825	0.00027	0.0000899	0.87	200.38	93.50
CG	0.2	0.0223	0.0606	-1.6577	-1.6459	0.00013	0.0000445	0.43	53.54	96.70
	0.4	0.1387	0.7635	-1.5092	-1.5021	0.000127	0.0000429	0.41	400.23	96.83
	0.6	0.1582	1.4806	-1.5181	-1.5119	0.000174	0.0000586	0.56	356.70	95.65
	0.8	0.1450	2.5183	-1.5334	-1.5302	0.000203	0.0000684	0.66	293.26	94.93
	1.0	0.1500	4.7013	-1.5449	-1.5395	0.000180	0.0000606	0.58	350.75	95.50
FE	0.2	0.2077	2.7129	-1.2493	-1.2391	0.0004	0.0001000	1.22	223.28	90.00
	0.4	0.0921	0.0071	-1.5723	-1.5647	0.000100	0.0000395	0.38	24.69	97.50
	0.6	0.2048	-1.9836	-1.4850	-1.4796	0.000238	0.0000801	0.77	417.03	94.05
	0.8	0.0890	0.6437	-1.6203	-1.6137	0.000290	0.0000770	0.74	148.62	94.28
	1.0	0.2194	-0.7175	-1.5336	-1.5220	0.000433	0.0001460	1.41	317.01	89.18
FP	0.2	0.1315	2.5176	-1.5593	-1.5516	0.000255	0.0000857	0.83	213.34	93.63
	0.4	0.1549	0.8929	-1.4919	-1.4848	0.000181	0.0000609	0.59	316.84	95.48
	0.6	0.1166	2.4489	-1.5749	-1.5657	0.00034	0.0001140	1.10	142.22	91.50
	0.8	0.1279	0.0083	-1.6689	-1.6689	0.000245	0.0000826	0.80	13.87	93.88
	1.0	0.0243	0.0481	-1.6310	-1.6226	0.000103	0.0000348	0.33	67.88	97.43
	0.2	0.1323	0.7688	-1.5441	-1.5367	0.000109	0.0000369	0.3573	448.09	97.28

Chro-mates	0.4	0.1703	0.7553	-1.4868	-1.4767	0.0000730	0.0000246	0.2300	827.33	98.18
	0.6	0.1896	-7.3277	-1.4945	-1.4851	0.0001080	0.0000364	0.3531	781.40	97.30
	0.8	0.1563	-4.5173	-1.6228	-1.6142	0.000557	0.0001870	1.8168	126.31	86.08
	1.0	0.0342	0.0584	-1.6062	-1.5947	0.0000405	0.0000137	0.1323	231.29	98.99

The current densities decrease with increase in the inhibitor concentrations from 0.2 - 1.0 v/v which suggests the resistance of passive layers on the surface of the Al- Si- Mg alloy which was further strengthened in the presence of extracts due to blockage of the active sites on the alloying surface. This observation corresponds to the report elsewhere (Quraish *et al*., 2009).

4.4 Surface Morphology

The surface morphologies of the Al-Si-Mg alloy coupon samples were examined after the corrosion tests using optical microscope and scanning electron microscopy.

4.4.1 Microstructural study of inhibited and uninhibited corroded surfaces using optical microscopy

Plate 4.1 shows the microstructure of Al-Si-Mg alloy consisting of silicon eutectic in the matrix of α- aluminium. In Plate 4.2, the surface indicates less attack by sodium chloride as compared to Plate 4.2 a at a higher volume of inhibitor concentration though at lowest temperature of 30 ^{0}C as expected. While Plate 4.2 b shows the surface morphology at high temperature in which dissolution is expected even with a lower exposure time of 1hour. Plate 4.3 a shows less attack indicating lower corrosion rate as expected while in 4.3 b there is more attack at higher temperature than prolonged exposure time even with higher concentration of inhibitor. Similarly, Plate 4.4 a shows more protected surface at higher exposure time with less corrosion rate compared to Plate 4.4 b. In Plate 4.5, similar result was obtained at lower temperature of 30 ^{O}C for higher concentration of inhibitor (FP) at prolonged exposure time with lower corrosion rate. Although under the same condition with increased temperature, there was dissolution of thin film hence the surface in Plate 4.5 b suffers more degradation or attack as a result of corrosion than Plate 4.5 a. With the addition of sodium chromates in Plate 4.6 a, the alloy was protected at 30 ^{O}C than at 50 ^{O}C as shown in Plate 4.6 b. Generally, the corrosion rates for Al-Si-Mg alloy in 3.5 wt% NaCl solution.

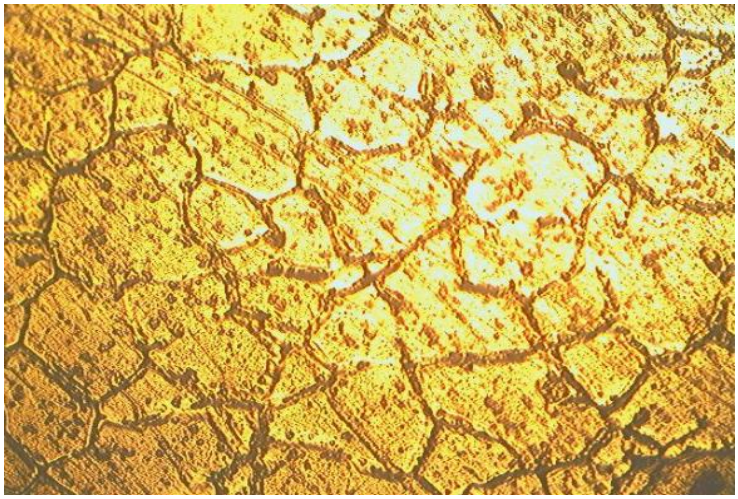

Plate 4.1: Microstructure of Al-Si-Mg alloy, Control x100.

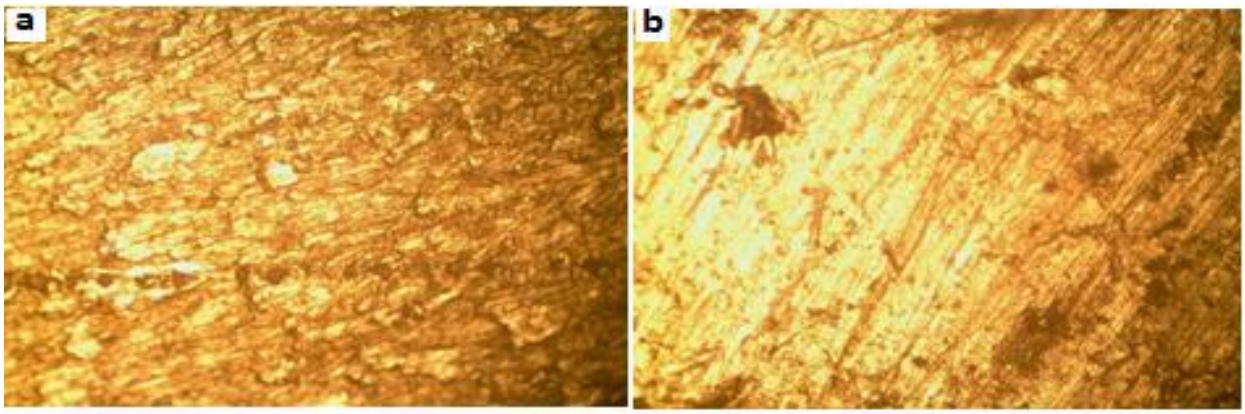

Plate 4.2: Microstructure of Al-Si-Mg alloy in 3.5wt% NaCl solution (a) sample with least corrosion rates at $30^{O}C$ for 5 hrs in the presence of 0.8 v/v C.M (b) sample with highest corrosion rates at $70^{O}C$ for 1 hr in the presence of 0.2 v/v CM X100

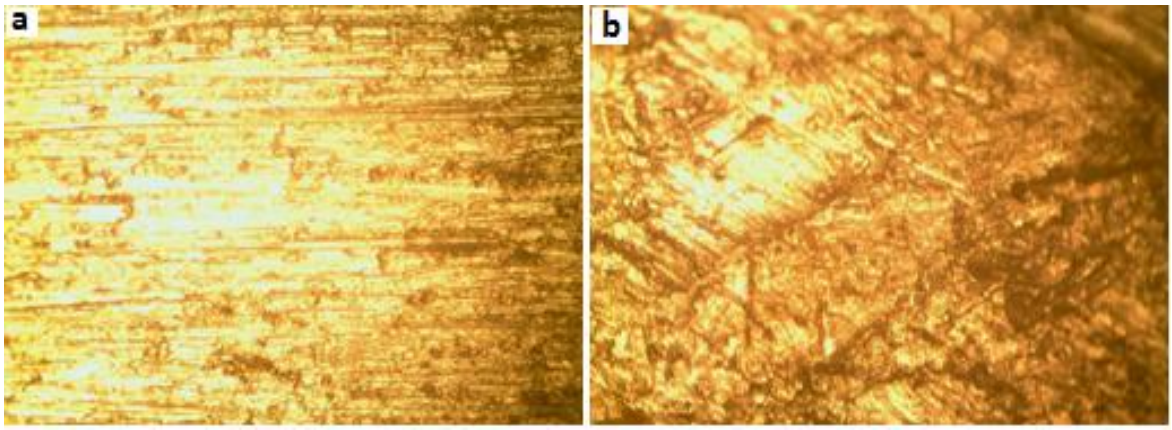

Plate 4.3: Microstructure of Al-Si-Mg alloy in 3.5wt% NaCl solution (a) sample with least corrosion rates at $30^{O}C$ for 5 hrs in the presence of 0.4 v/v CG (b) sample with highest corrosion rate at $70^{O}C$ for 5 hrs in the presence of 0.8 v/v CG X100

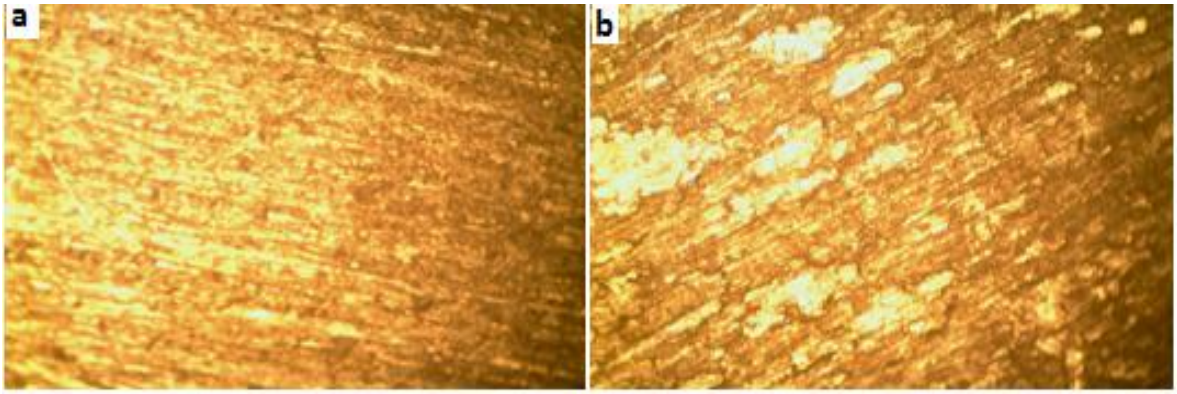

Plate 4.4: Microstructure of Al-Si-Mg alloy in 3.5wt% NaCl solution (a) sample with least corrosion rates at $30^{O}C$ for 5 hrs in the presence of 0.4 v/v FE (b) sample with highest corrosion rate at $70^{O}C$ for 5 hrs in the presence of 0.2 v/v FE X100

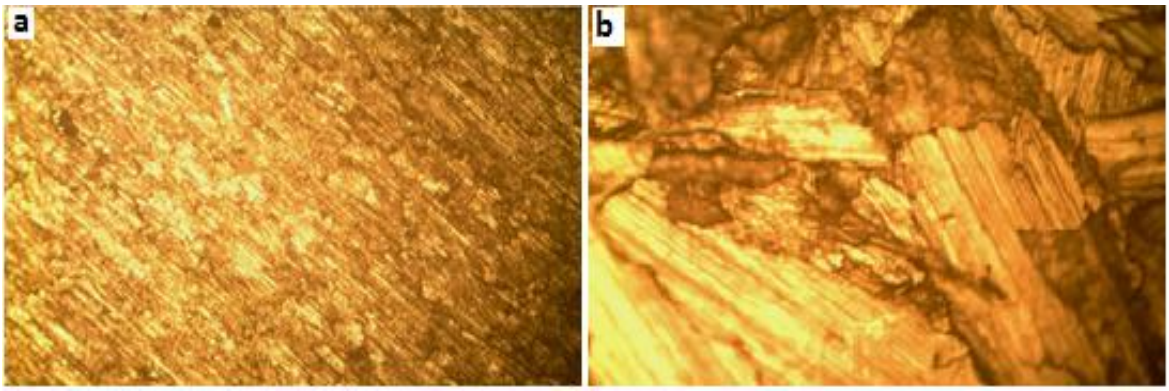

Plate 4.5: Microstructure of Al-Si-Mg alloy in 3.5wt% NaCl solution (a) sample with least corrosion rates at $30^{O}C$ for 5 hrs in the presence of 1.0 v/v FP (b) sample with highest corrosion rate at $70^{O}C$ for 5 hrs in the presence of 1.0 v/v FP X100

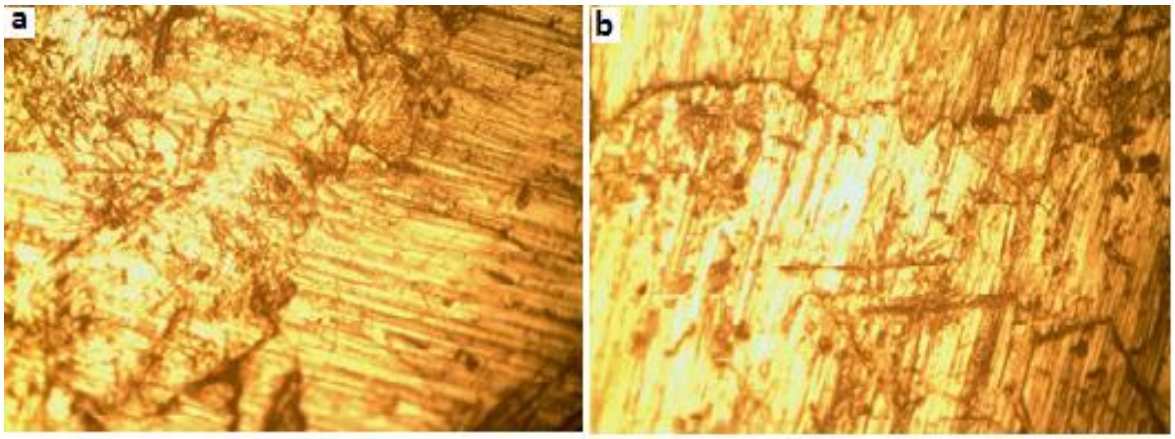

Plate 4.6: Microstructure of Al-Si-Mg alloy in 3.5wt% NaCl solution (a) sample with least corrosion rates at $30^{O}C$ for 5 hrs in the presence of 1.0 v/v Sodium Chromates (b) sample with highest corrosion rate at $50^{O}C$ for 5 hrs in the presence of 1.0 v/v Sodium Chromates. X100

were lower at a lower temperature of30 ^{O}C than higher temperature irrespective of the exposure time and inhibitor concentration

4.4.2. Microstructural study of inhibited and uninhibited corroded surfaces using Scanning Electron Microscopy

Plates 4.7 – 4.12 are the SEM Micrographs of Al- Si- Mg alloy in 3.5 wt% NaCl solution which exhibited the degradation in the absence and presence of inhibitor. Plate 4.7 shows SEM microstructure of the control Al- Si- Mg alloy with the least corrosion rates in the absence of inhibitor. There is evidence of adsorbate on the surface of the alloy and it is more pronounced at x1500 magnification (Plate 4.8). In Plate 4.9, there is similar observation as in the case of Plate 4.7 and 4.8. In plate 4.10, surface appearance of the alloy improved with less degradation that is surface morphology shows improved appearance than the control. Plate 4.11 has a microstructure that indicates a degrading surface due to corrosion attack. Plate 4.12 has the highest corrosion rate in the absence of inhibitor.

4.5 Effects of Varying Parameters on the Corrosion Rates of the Alloy Using ANOVA

Tables 4.9 – 4.13 show the analysis of variance (ANOVA) of CM and the comparison of actual values to the predicted values. It shows the contribution of each parameter (temperature, inhibitor concentration and time) on the response. In Table 4.9 for CM, it was observed that factor B (inhibitor concentration) has a value of 89.74 in the column titled F-value, which was the most significant parameter being the highest statistical influence on the corrosion rates of the alloy. The next was temperature having a value of 60.86. The value of time was 6.67 meaning that it has the least effect on the corrosion rates of the alloy.

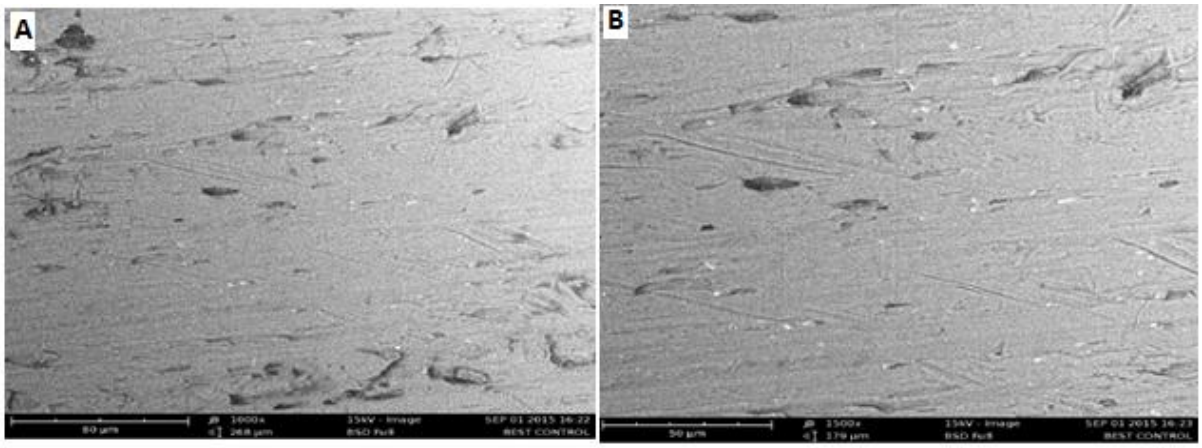

Plate 4.7: SEM micrograph of control Al-Si-Mg alloy with the least corrosion rates without addition of inhibitor using gravimetric method A) x1000 B) x1500

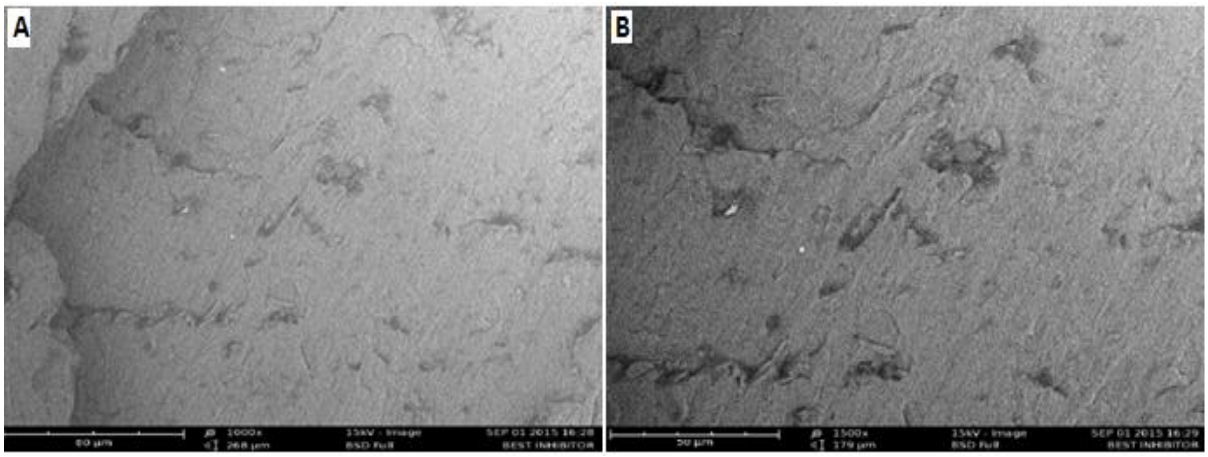

Plate 4.8: SEM micrograph of Al-Si-Mg alloy with the least corrosion rates in the presence of inhibitor using gravimetric method A) x1000 B) x1500

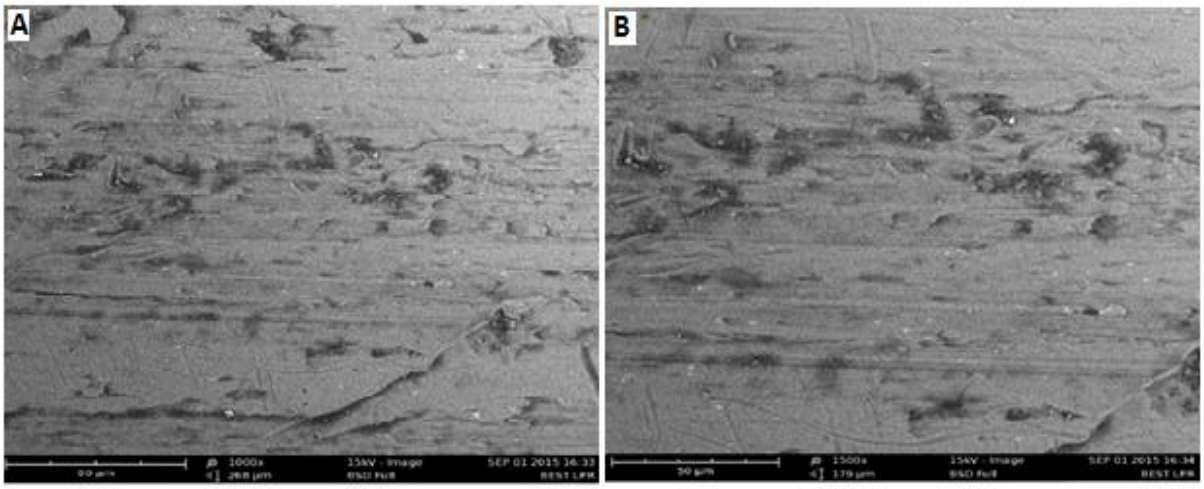

Plate 4.9: SEM micrograph of Al-Si-Mg alloy with the least corrosion rates with addition of inhibitor using LPR method A) x1000 B) x1500

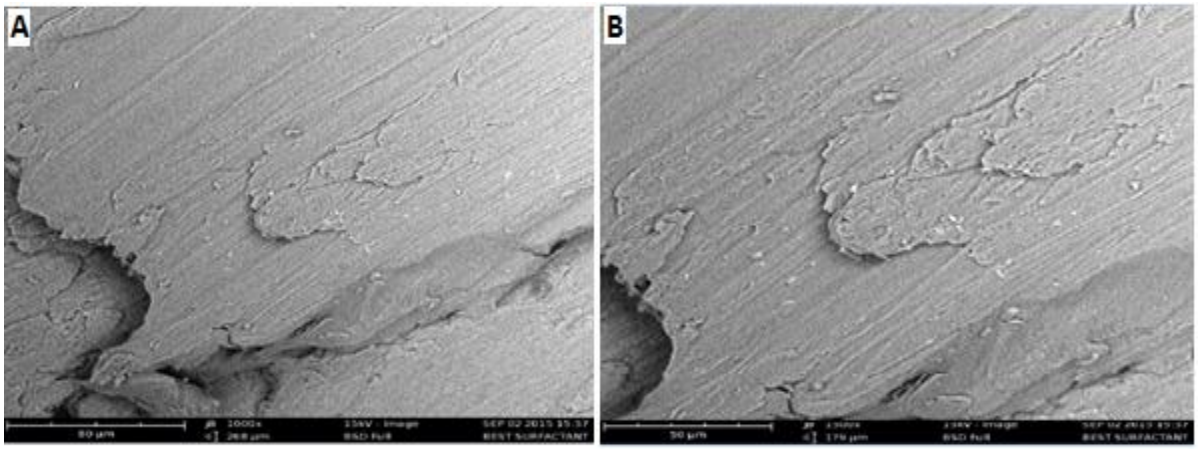

Plate 4.10: SEM micrograph of Al-Si-Mg alloy with the least corrosion rates in the presence of inhibitor/surfactant A) x1000 B) x1500

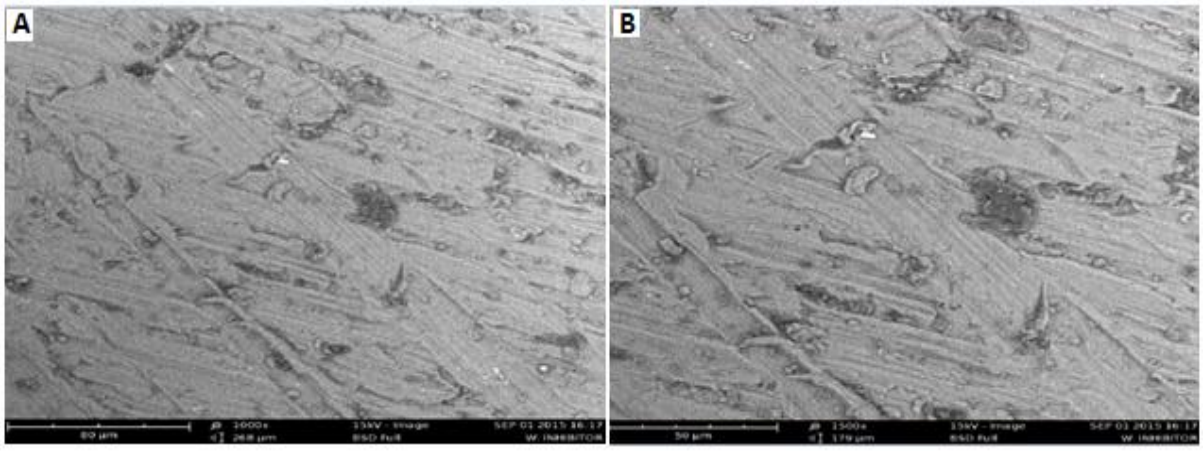

Plate 4.11: SEM micrograph of Al-Si-Mg alloy with the highest corrosion rates in the presence of inhibitor A) x1000 B) x1500

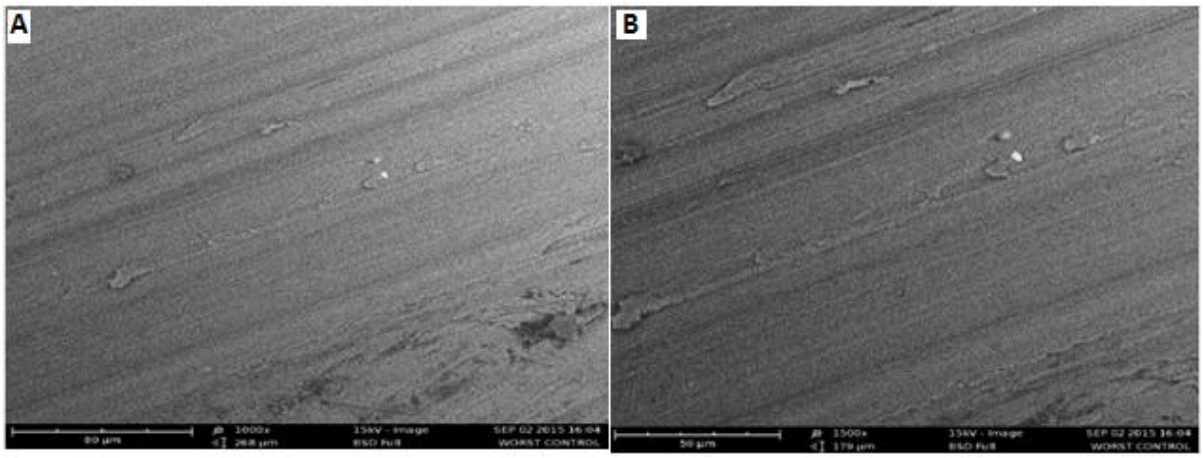

Plate 4.12: SEM micrograph of control Al-Si-Mg alloy with the highest corrosion rate in the absence of inhibitor A) x1000 B) x1500

Table 4.9: Analysis of variance (ANOVA) for corrosion rate in the presence of CM

Source of Variation	Sum of Squares	Degree of freedom (DF)	Means Square	F- Value	Prob > F
Main effect					
A	0.014	1	0.014	60.86	0.0160
B	0.021	1	0.021	89.74	0.0110
C	1.557×10^{-3}	1	1.557×10^{-3}	6.67	0.1229
AB	2.113×10^{-3}	1	2.113×10^{-3}	9.05	0.0951
BC	8.736×10^{-3}	1	8.736×10^{-3}	3.74	0.1928
Residual	4.671×10^{-4}	2	2.335×10^{-4}		
Cor. Total	0.050	7			

Standard Deviation	0.015	R- Squared	0.9907
Mean	0.093	Adj R-Squared	0.9676
C.V	16.51	Pred R-Squared	0.8518
Press	7.473×10^{-3}	Adeq. Precision	17.915

Table 4.10: Analysis of variance (ANOVA) for corrosion rates in the presence of CG

Source of Variation	Sum of Squares	Degree of freedom (DF)	Means Square	F- Value	Prob > F
Main effect					
A	1.625 x 10 -3	1	1.62×10^{-3}	1064.08	< 0.0001
B	0.027	1	0.027	17548.67	< 0.0001
C	1.311×10^{-3}	1	1.311×10^{-3}	858.55	< 0.0001
AB	4.993×10^{-4}	1	4.993×10^{-4}	327.04	0.0004
Residual	4.580×10^{-3}	3	1.527×10^{-6}		
Cor. Total	0.041	7			

Standard Deviation	1.236×10^{-3}	R- Squared	0.9999
Mean	0.10	Adj R-Squared	0.9997
C.V	1.18	Pred R-Squared	0.9992
Press	3.257×10^{-5}	Adeq . Precision	195.943

Table 4.11: Analysis of variance (ANOVA) for corrosion rates in the presence of FE

Source of Variation	Sum of Squares	Degree of freedom (DF)	Means Square	F- Value	Prob > F
Main effect					
A	0.024	1	4.056×10^{-3}	64.13	0.0953
B	0.011	1	0.011	174.31	0.0481
C	4.163×10^{-3}	1	4.163×10^{-3}	65.82	0.0781
AB	5.498×10^{-4}	1	5.498×10^{-4}	8.69	
AC	3.536×10^{-3}	1	3.536×10^{-3}	55.91	0.0846
BC	2.058×10^{-3}	1	2.058×10^{-3}	32.53	0.1105
ABC	2.824×10^{-3}	1	2.824×10^{-3}	44.64	0.0946
Residual	6.325×10^{-5}	1	6.325×10^{-5}		
Cor. Total	0.024	7			

Standard Deviation	7.953×10^{-3}	R- Squared	0.9974
Mean	0.098	Adj R-Squared	0.9819
C.V	8.10	Pred R-Squared	0.5392
Press	0.011	Adeq. Precision	20.551

Table 4.12: Analysis of Variance (ANOVA) for corrosion rates in the presence of FP

Source of Variation	Sum of Squares	Degree of freedom (DF)	Means Square	F- Value	Prob > F
Main effect					
A	0.013	1	0.013	40.63	0.0237
B	0.016	1	0.016	48.02	0.0202
C	1.659×10^{-3}	1	1.659×10^{-3}	5.06	0.1534
AB	1.897×10^{-3}	1	1.897×10^{-3}	5.79	0.1379
BC	1.191×10^{-3}	1	1.191×10^{-3}	3.63	0.1969
Residual	6.555×10^{-4}	2	3.278×10^{-4}		
Cor. Total	0.042	7			

Standard Deviation	0.018	R- Squared	0.9842
Mean	0.084	Adj R-Squared	0.9448
C.V	21.66	Pred R-Squared	0.7475
Press	0.010	Adeq. Precision	13.853

Table 4.13: Analysis of Variance (ANOVA) for corrosion rates in the presence of Sodium Chromates as standard inhibitor

Source of Variation	Sum of Squares	Degree of freedom (DF)	Means Square	F- Value	Prob > F
Main effect					
A	7.236×10^{-3}	1	7.236×10^{-3}	33.66	0.0284
B	7.250×10^{-3}	1	7.250×10^{-3}	33.73	0.0284
C	1.347×10^{-3}	1	1.347×10^{-3}	6.27	0.1294
AB	1.746×10^{-3}	1	1.746×10^{-3}	8.12	0.1042
BC	9.990×10^{-4}	1	9.990×10^{-4}	4.65	0.1639
Residual	4.299×10^{-4}	2	2.150×10^{-4}		
Cor. Total	0.023	7			

Standard Deviation	0.015	R- Squared	0.9810
Mean	0.056	Adj R-Squared	0.9334
C.V	26.03	Pred R-Squared	0.6957
Press	6.879×10^{-3}	Adeq. Precision	12.581

In Table 4.10 for CG, inhibitor concentration has the highest value of 17548.67 followed by temperature with 1064.08 then next is time with 858.55.In this case inhibitor concentration is also the most significant corrosion parameter with the plant extract.

In Table 4.11 for FE as the inhibitor, the inhibitor concentration has the highest value (174.31) followed by time (65.82) and temperature (64.13). This is line with other extracts that has the same trend whereby inhibitor concentration been the most significant parameter influencing the corrosion process followed by time and temperature.

In Table 4.12 for FP, inhibitor concentration has the highest value (48.02) next to temperature (40.63) and then time (5.06). Indicating here that inhibitor concentration also is the most significant parameter as in other extracts in this study.

Table 4.13 for Sodium Chromates, the highest significant value was recorded with inhibitor concentration (33.73) followed by temperature (33.66) and finally time (6.27). It can be said conclusively from the trend of these data generated that the most significant parameter on the corrosion rates of the alloy using these inhibitors was concentration as applicable to all the inhibitors including the standard inhibitor. The next significant parameter is temperature and the least was time with the exception of FE where temperature was the least parameter.

The contribution (P) values are less than 0.0500 which indicate that the model-terms are significant while P values greater than 0.1000 means that the model terms are insignificant. From Tables 4.9, the values of P of extract CM were (0.0160 for temperature, 0.0110 for inhibitor concentration and 0.1229 for time). This indicates that both temperature and inhibitor concentration are models that are significant. In Table 4.10, time, temperature and inhibitor concentration have < 0.0001 values showing that all are significant. In Table 4.11, the temperature has 0.0037, inhibitor concentration has 0.0038 and time has 0.0037. In Table 4.12, the value for temperature is 0.0237, for inhibitor concentration is 0.0202 and for time is

0.1534. Here both temperature and inhibitor concentration are the significant parameters. In Table 4.13, both temperature and inhibitor concentration have 0.0284 values and time has 0.1294. Hence, both temperature and inhibitor concentration are the significant parameters. Similar result had been reported by (Asuke, 2014).

The regression coefficient (R^2) calculated were 0.9907 (99.07 %) for CM, 0.9999 (99.99 %) for CG, 0.9974 (99.74 %) for FE, 0.9842 (98.42 %) for FP and 0.9810 (98.10 %) for sodium chromate. R^2 value is a measure of the degree of fitness. When R^2 approaches unity a better response model results and it fits the actual data.

Therefore, the mathematical equation developed demonstrated feasible and effective way to predict the corrosion rate of the Al – Si – Mg. Thus the developed equations can be used to predict corrosion for any combination of factor levels in the specified range. The actual and predicted corrosion rates values for each inhibitor are presented in the form of histograms in Figures 4.99 - 4.103 and as well in Appendices LI – LV.

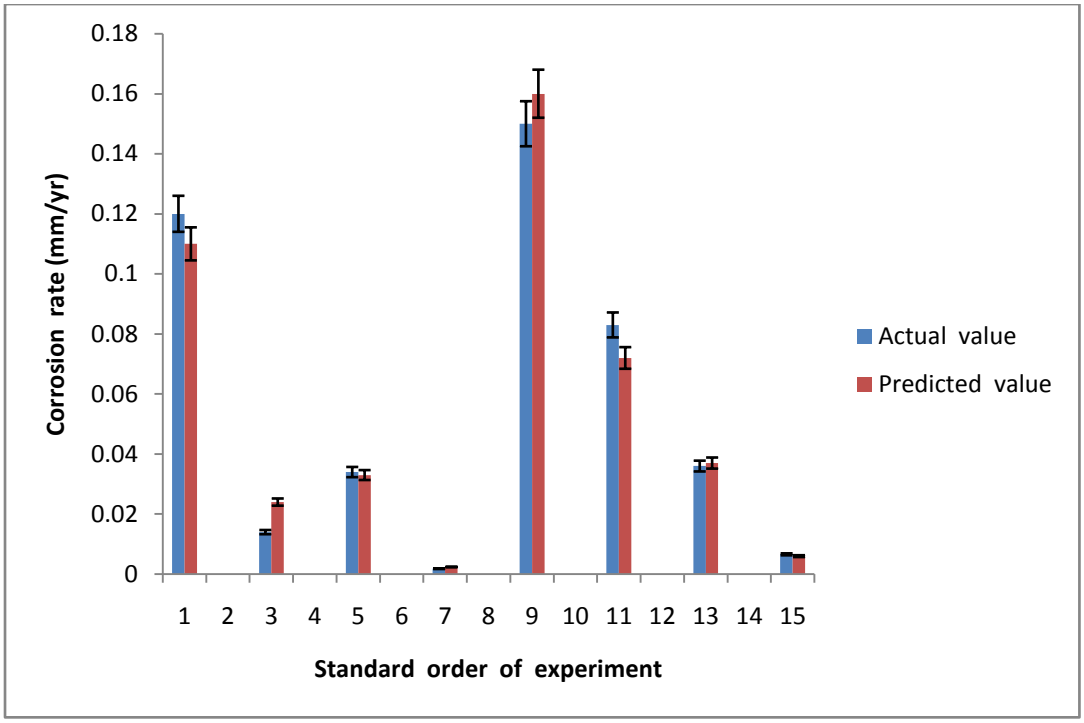

Figure 4.99: Variations of actual and predicted values with standard order of the experiment in presence of CM

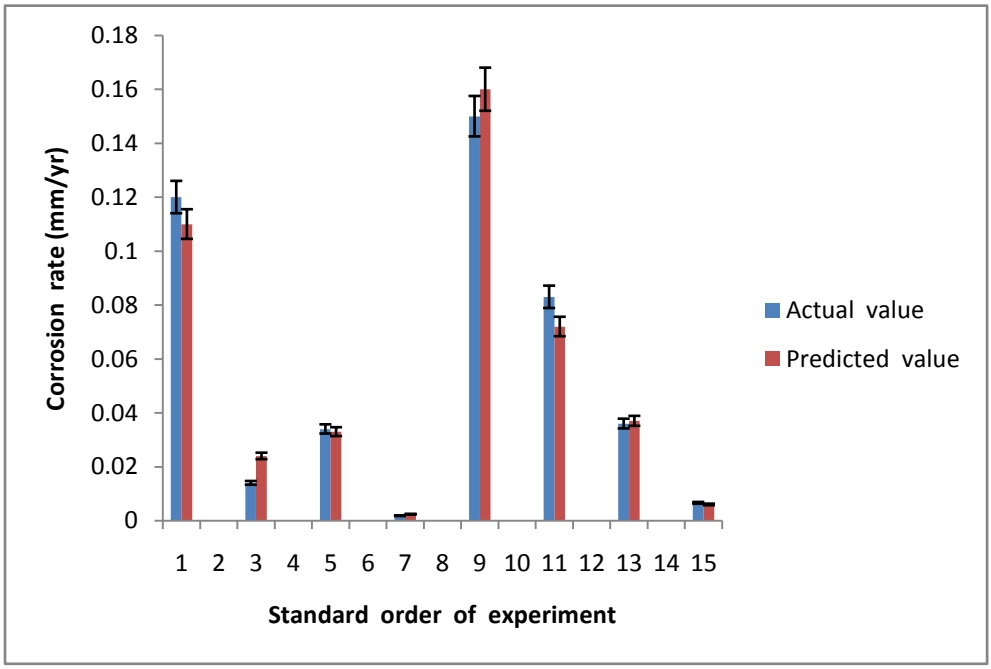

Figure 4.100: Variations of actual and predicted values with standard order of the experiment in presence of CG

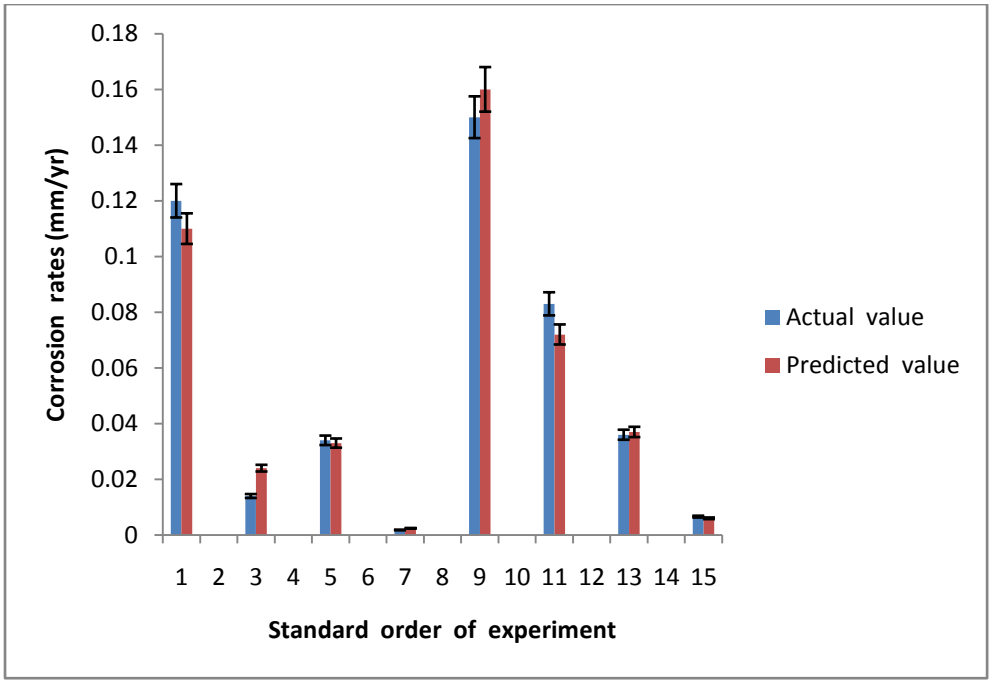

Figure 4.101: Variations of actual and predicted values with standard order of the experiment in presence of FE

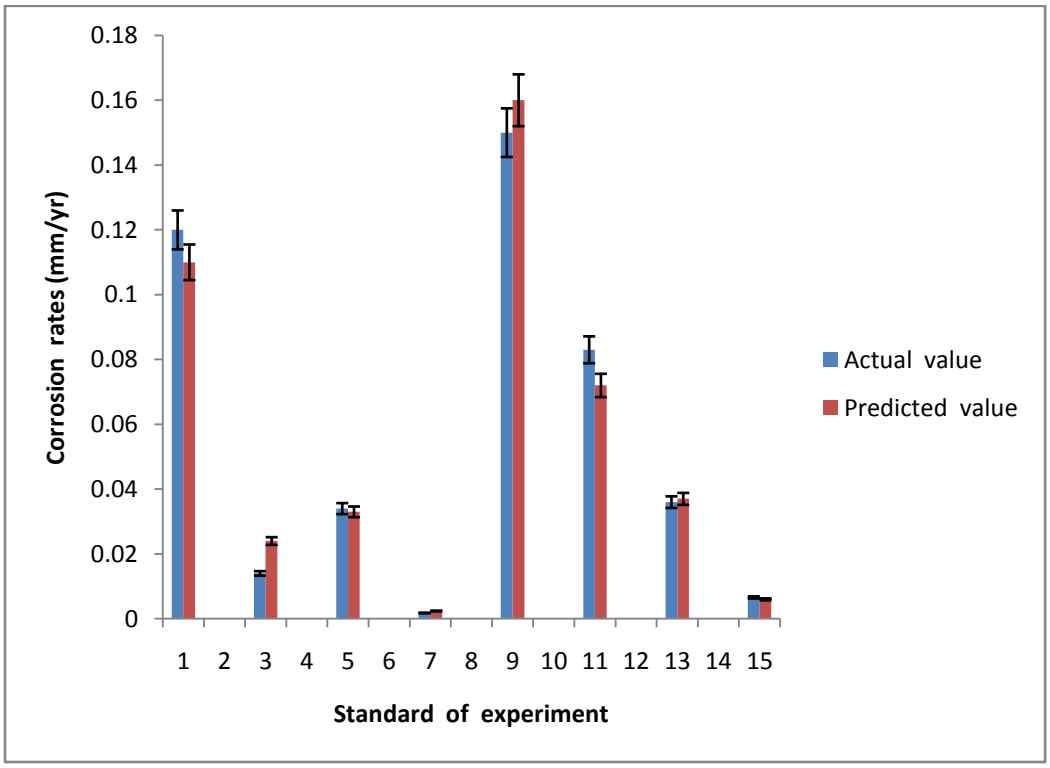

Figure 4.102: Variations of actual and predicted values with standard order of the experiment in presence of FP.

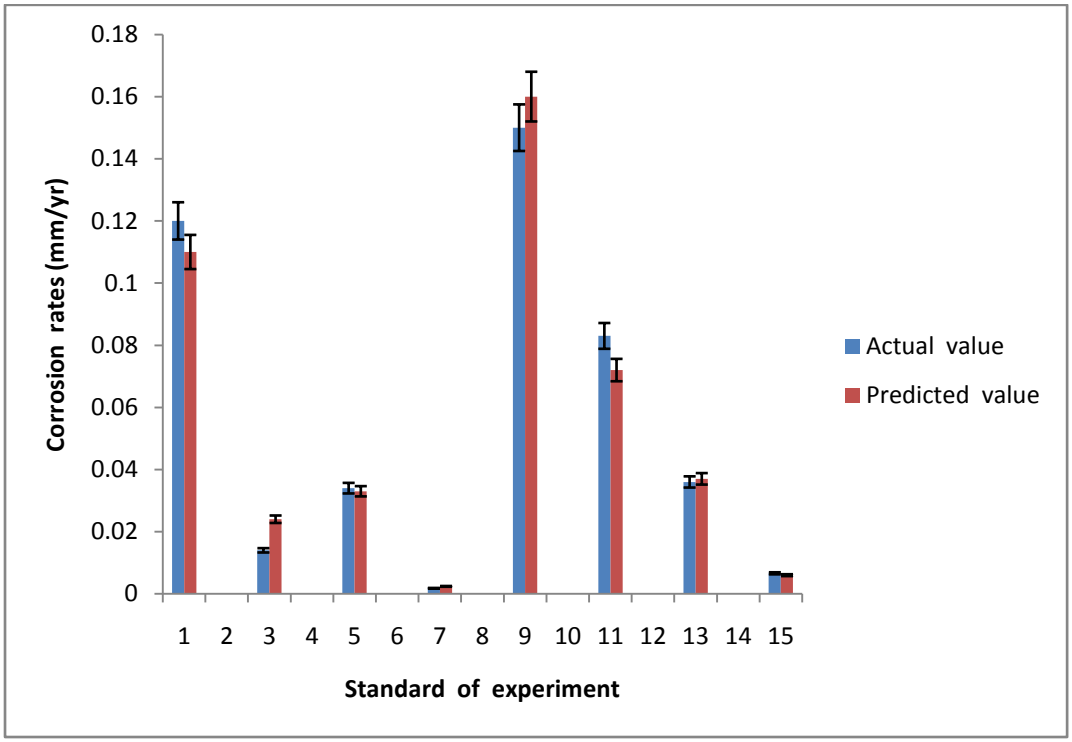

Figure 4.103: Variations of actual and predicted values with standard order of the experiment in presence of sodium chromate.

CHAPTER FIVE

5.0 CONCLUSION AND RECOMMENDATIONS

5.1 Conclusions

From the results and discussion, the following conclusion can be drawn:

1. The characterization of the plant extracts by qualitative and quantitative method, thin layer chromatography TLC, FT-IR, GC-MS revealed the presence of alkaloid, tannins, saponins, flavonoids which showed that the plant extracts have the potential of being used as inhibitors for Al-Si-Mg alloy in the medium.
2. The corrosion rates of the alloy reduced with addition of inhibitors in the average of 91 % CM, 75 % CG, 78 % FE, 90 % FP and 86 % sodium chromates at different experimental conditions considered under this study.
3. The optimum concentrations and inhibitor efficiency attained in this research are as follow: CM has 94.44 % at 0.8 v/v inhibitor concentration, CG with 81.25 % at 0.4 v/v, FE with 84.62 % at 0.4 v/v, FP with 94.74 % at 1.0 v/v and sodium chromates which was the standard has 94.64 % at 1.0 v/v respectively with gravimetric mass-based loss method.
4. Linear polarization result has 96.15 % for CM, 96.83 % for CG, 97.50 % for FE, 97.43 % for FP and 98.99 % for sodium chromates at the same inhibitor concentrations with gravimetric.
5. The Langmuir adsorption isotherm was the best isotherm obtained in this study. However,the adsorption of extracts onto the Al-Si-Mg in 3.5 wt% NaCl solution interface also obeyed the Langmuir, Freundlich and El-Awady adsorption isotherm models.
6. Based on E_a, ΔG_{ads} and ΔS_{ads} values obtained in this work, physical adsorption phenomenon can be proposed for adsorption of the inhibitors, and the adsorption process can be said to be spontaneous.

7. The results obtained using gravimetric measurement and linear polarizations are in good agreement as their efficiencies values were very close.
8. Tafel polarization curves show that the extracts acted as mixed type inhibitor
9. The MEA and TEA surfactants employed did not have efficiency greater than the extract values.

5.2 Recommendations

The followings are recommended for further study:

1. The effect of the extracts *(Combretum Micranthum, Combretum Glutinosum, Ficus Exasperata and Ficus Platyphylla)* on other non-ferrous alloys and metal matrix composites can be study.
2. The use of Electrochemical Impedance Spectroscopy (EIS), Electrochemical Noise (EN) and Electrochemical Frequency Modulation (EFM) techniques to further verify the potential of inhibitors for the same alloy is also recommended.
3. The use of XRD, EDS and Raman Spectroscopy to characterize the surfaces of test coupons after corrosion test in order to identify the complex compounds that are formed by the aluminium alloy and the inhibitors.
4. The use of surfactants in this research is not recommended as it has no impact on the inhibitors.

References

Abdel-Jaber, G.T., Omran, A.M., Seki, M., Yosluda, A.Y., Fujii, M., and K.A. (2010). An Investigation in to Solidification and Mechanical Properties Behavior of Al-Si Casting Alloys. *UMME-UEWS,* 10(4).

Abdulwahab, M., Madugu, I.A., Yaro, S.A., and popoola, A.P.I (2011). Degradation Behavior of High Chrominum Sodium- Modified A356.0 type Al-Si-Mg Alloy in Simulated Seawater Environment. *Journal of minerals of materials characterization of Engineering,* 10(6), 535-551

Abiola, O.K., Oforka, N.C., Ebenso, E.E., and Nwinuka, N.M. (2007). Eco-friendly Corrosion Inhibitors: The Inhibitive Action of Delonix Regia Extract for the Corrosion of Aluminium in Acidic Media. *Anti- Corrosion Methods and Materials,* 54(4), 219 - 224.

Adejo, S.O., Ekwenchi, M.M., Momoh, F., and Odiniya, E. (2012*)*.Adsorption Characterization of Ethanol Extract of Leaves of Portulaca Oleracea as Green Corrosion Inhibitor For Corrosion of Mild Steel in H_2SO_4Medium. *Internatioal Journal Modern Chemistry1*(3), 125 – 134.

Adejo, S.O., Yiase, S.G., Ahile, U.J., Tyohemba, T.G., Gbertyo, J.A.(2013). Inhibitory Effect and Adsorption Parameters of Extract Leaves of Portulaca Oleracea for the Corrosion of Aluminium in H_2SO_4 Solution. *Achieves of Applied Science Research*, 5(1), 25-32.

Aigbodion, V.S., Hassan, S.B., Dauda, E.T., Mohammed, R.A. (2010). The Development of Mathematical Model for the Prediction of Ageing Behaviour for Al-Cu-Mg/ Bagasse Ash Particulate Composites. *Journal ofMinerals and Materials Characterization & Engineering.* 9(10), 907-917.

Ajanaku, K.O., Ajanaku, C.O., Akinsiku, A.A., Falomo, A., Edobor-Osoh, A., and Oluwatosin, M. (2012). Eco-Friendly Impact of Vernonia amygdalina as Corrosion Inhibitor on Aluminium in Acid Media. *Chemistry Journal*, 2(4), 153-157

Akalezi, C.O., Enenebaku, C.K. and Oguzie, E.E. (2012). Application of aqueous extracts of coffee and senna for control of mild steel corrosion in acidic environments. *International Journal of Industrial Chemistry*, 3, 13-25.

Alaneme, K.K. (2011). Corrosion Behaviour of Heat Treated Al-6063/ SiC Composites Immersed in 5 wt% NaCl Solution, *Leonerdo Journal of Science,* 18(5), 5 - 64.

Al-Sehaibani, A. (2000). Evaluation of Extracts of Henna Leaves as Environmentally Friendly Corrosion Inhibitors for Metals. *Material Wissenchaft and Werkstofftechnik,* 12(31), 1060-1063.

Amitha Rani, B.E., and Bharathi Bai J. Basu, (2011). Green Inhibitors for Corrosion Protection of Metals and Alloys: Hindawi Publishing Corporation. *International Journal of Corrosion. 2012, Article ID 380217*, 1-15.

Ambrish Singh; Singh, V.K. Quraishi, M.A (2010). Aqueous Extract of Kalmegh (Andrographis Paniculata) Leaves as Green Inhibitor for Mild Steel in HCl Acid Solution. *International Journal of corrosion,* 1- 10.

Arora, P., Kumar, S., Sharma, M.K. and Mathur, S.P. (2007). Corrosion inhibition by capparis deciduas in acidic media. Electronic Journal of Chemistry, 4(4)**,** 450-456.

Asuke, F. (2014). A Study of the Dephosphorization of Koton Karfe Iron Ore by Acidic Leaching. A ph.d Thesis Unpublished Submitted to the Department of Metallurgical and Materials Engineering, ABU, Zaria.

Asuke, F., Abdulwahab, M., Fayomi, O.S.I., Popoola, A.P.I., Umoru, I.E. (2014). Effect of Avogadro Natural Oil on the Corrosion Inhibition of Mild Steel in Hydrochloric Acid Solution. *Res. Chem. Intermed,* 40, 1115-1123.

Asuke, F., Abdulwahab, M., Fayomi, O.S.I., Aigbodion, V.S., and Popoola, A.P.I. (2015). Inhibitive Action of Potassium Iodide on the Corrosion of Stir-Cast Al-Si/SiC in NaCl-KI Interface. *Journal of Failure Analysis and Prevenention*,doi: 10.1007/s11668-015-0015-8.

ASM International (1992). Properties and Selection, Non-ferrous alloys and special-purpose materials, 2 (10^{th} ed.) pp 619.

ASM International (2004a). Al-Si Casting Alloys Atlas of Microfractographs (#06993G), 1-9.

ASM International (2004b). Metallography and microstructure, 9, 1717.

Ating, E.I., Umoren S.A., Udousoro, I.I., Ebenso, E.E., and Udoh, A.P. (2010). Leaves Extracts of Ananas Sativum as Green Corrosion Inhibitor for Aluminium in Hydrochloric Acid Solutions, *Green Chemistry Letters and Reviews* 3(2), 61-68.

Avwiri, G.O, and Igho, P.O. (2003). Inhibitive Action of Vernonia Amygdalina on the Corrosion of Aluminium Alloys in Acidic Media. *Materials letters,* 57(22-23), 3705-3711.

Awe, F.E., Idris, S.O., Abdulwahab, M., and Oguzie, E.E. (2015). Theoritical and Experimental Inhibitive Properties of Mild Steel in HCl by Ethanolic Extract of Boscia Senegaensis. *Cogent Chemistry*, 1:1112676.

Babatunde A.I, Ogundele O., Oyelola, O.T and Abiola, O.K (2012). The Inhibitive Effect of Irvingia Gabonesis Extract on the Corrosion of Aluminium in 1 M HCl Solution. *Advances in Applied Science Research,Pelagia Research Library*.3 (6), 3944-3949.

Benali, O., Benmehdi, H., Hasnaoui, O., Selles, C., and Balghi, R. (2012). Green Corrosion Inhibitor: Inhibitive Action of Tannin Extract of Chamaerops Humilis Plant for the Corrosion of Mild Steel in 0.5M H_2SO_4. *Journal of Materials. Environmental. Science,*. 4 (1), 127-138.

Chinedu, F.A., Uyai, U., Emezie, A.U. and Utoh-Nedosa, A.U. (2012). Anti-Diarrhoeal, Antispasmodic and Phytochemical Properties of Ethanol Extract of the Leaves of Ficus Exasperate. *Asian Journal of Residence Pharmaceutical Sciences*, 2(1). 26-32

Chowdhury, A.R., and Miltra, C. (1995). Spermatogenic and Steroidogenic Impairment After Chromium Treatment in Rats. *Indian Journal Experimental Biology*,33:480-484.

Denny, J. (2004). Principles and Prevention of Corrosion, Upper Saddle River, New Jersey Printjce Hall. ISBN 0-13-359993-0.

David Talbot and James Talbot (1998).*Corrosion Science and Technology,* CRC Press London. LLC, 2000N.W. Corporate Blvd., Boca Raton, Florida 33431.

Dietrich G. Altenpohl (1998). *Aluminium and aluminium alloys*. The Aluminium Association and TMS.

Ebenso, E. E., and Ekpe, U. J. (1994). Kinetic Study of Corrosion and Corrosion Inhibition of Mild Steel in H_2SO_4, Using Paricapapaya Leave Extract,*West African Journal of Biological and Applied Chemistry,* **37:**13 – 30.

Eddy, N.O. (2008). Inhibition of the Corrosion of Mild Steel in HCl. *International Journal.of Physical. Sciences* 3(11), 275.

Eddy, W.O. (2009). Inhibitive and Adsorption Properties of Ethanol Extract of Colocasia Esculenta Leaves for the Corrosion of Mild Steel in H_2SO_4. *International Journal of Physical Science* 4(4), 165.

Eddy, N.O., Ebenso, E.E., Ibok, U.J. (2010). Adsorption Synergistic Inhibitive Effect and Quantum Chemical Studies of Ampicillin (AMP) and Halides for the Corrosion of Mild Steel in H_2SO_4. *Journal of Applied Electrochemistry,* 40**:**445-456.

Eddy, N.O., and Odiongenyi, A.O. (2010). Corrosion Inhibition and Adsorption Properties of Ethanol Extract of Hernsia Crinata on Mild Steel in H_2SO_4. *Pigment of Resin Technology,* 59(3):288-295.

Eddy, N.O. and Ita, B.I. (2010). Experimental and Theoritical Studies on the Inhibition Potentials of Some Derivatives of Cyclopenta-1,3-diene for the Corrosion of Mild Steel in HCl Solutions. *International journal of Quantum Chemistry,* DOI**:** 104152/pea 200904443.

Eddy, N.O. and Odoemelam, S.A. (2009). Inhibition of the corrosion of mild steel in $H_2SO_4$by ethanol extract of Aloe vera. Resin and Pigment Technology, 38(2), 111-115.

Emmanuel O.A., Kessington O.O. and Mudiakeoghene O.(2009). Biodegradation of Vegetable Oils: A Review. *Scientific Research and Essay,* 4(6), 543-548.

Evans, U. R (1996): *The corrosion and oxidation of metals.* Itodder Arnold London, UK Published (pp 1- 19).

Helen, L.Y.S; Rahim, A.A; Saad, B; Saleh M.I; Bothi R. P. (2014). Aquilaria Crassna Leaves Extracts a Green Corrosion Inhibitor for Mild Steel in 1M HCl Medium. *International Journal of electrochemical Science,*9(2014), 830-846.

Ihebrodike, M.M., Anthony, A.U., Kelechukwu, B.O., and Gregory, A.A. (2010). The Inhibitive Effect of Solanumm Elongena L. Leaf Extract on the Corrosion of Al in H_2SO_4. *African Journal of Pure and Applied Chemistry.* 4(8), 158-165.

Irvine, F.R. (1961). *Woody Plants of Ghana with special reference to their uses*. Oxford University London, U.K. 523-524.

Idawu, Y.S. (2013). *Evaluation of Plant Extracts As Corrosion Inhibitors For Mild Steel in Acidic Environment.* Department of Metallurgical/ Materials Engineering, Ahmadu Bello University, Zaria- Nigeria. Unpublished Ph. D. Thesis.

Jaske, C.F., Beavers, J.A., and Thomson, N.G. (2002). *Corrosion Prevention and Control*. 3(1) 49.

John, E.G., Bernaid, M.(1990). *The treatment of liquid Al-Si alloys.* American Foundry Men Society, Inc.

Johnsirani, V., Sathiyabama, J., Susai, R., Suriya P. A. (2012). Inhibitory Mechanism of Carbon Steel Corrosion in Sea Water by an Aquems Extrac of Henna leaves. *International scholarly Research Network ISRN Corrosion*,2012, Article ID 5744321, 9.

Kasim, A. (2013). *Plant extracts/nanoparticles hybrids as corrosion inhibitors for AA2024 Aluminium Alloy.* Department of Metallurgical/ Materials Engineering, Ahmadu Bello University, Zaria- Nigeria. Unpublished Ph. D. Thesis.

Kelly, L.G., Scully, J.R., Shoessmith, D.W. and Buccheit, R.G. (2003). *Electrochemical techniques in corrosion science*, New York, Morcell Dekker.

Khadom, A.A; Yaro, S.A; and Abdul, A.H (2010). *Journal Chile Chemical. Society, 55, 150 - 152*

Kohl, A.L., Nielsen, R. (1997). *Gas Purification*. 5th edition; Gulf Publishing Company, Houston.ISBN 10: 0884152200.

Lakshman, R.B. (2012). Phytochemical Screening Quantitative Estimation Total Phenolic and Total Flavonoids. Anti Microbial Evaluation of Cyamopsis Tetragonoloba. *International Journal of Research in Pharmaceutical and Biomedical Sciences*, 3(3), 2229-3701.

Lebe A. Nnanna, Onyinyechi, C., Nwadiuko, Nneka D., Ekekwe, Chibueze F., UkabSolomon C., Udensi, Kelechycwu B., Okeoma, Beniah W.,Onwuagba, Ihebrodike M. Majeha,(2011). Adsorption and Inhibitive Properties of Leaf Extract of New Bouldia Leavis as Green Inhibitor for Aluminium Alloy in H_2S0_4. *American Journal of Materials Science*, 1(2), 143- 148Doi: 10. 5923/Journal of materials, 20110102.24.

Lebrini, M., Robert, F., Roos, C. (2011). Alkaloids Extract from *Palicourea guianensis* plant as Corrosion Inhibitor for C38 Steel in 1M HCl acid Medium. *International Journal of Electrochemical Sciences*, 6, 847 – 859.

Loto, C.A., Loto, R.T., Popoola, A.P.I (2011). The Synergistic Effect of Tobacco and Kola Tree Extracts on the Corrosion Inhibition of Mild Steel in Acid Chloride. *International Journal of Electrochemical Sciences, 6, 3830-3843.*

Maqsood Ahmad Malik, Mohammad Ali Hashim, Firdosa Nabi, Shaeel Ahmed Al-Thabaiti, Zaheer Khan (2011). Anti-Corrosion Ability of Surfactants*: A Review International Journal Electrochemical Science,* 6, 1927-1948.

Makrides, A.C., and Hackerman, N. (1954). Action of Polar Organic Inhibitors in Acid Dissolution of Metals. *Indusrial Engineering Chemistry*, 46, 523.

Mercer, A.P. (1990). Chemical Inhibitors for Corrosion Control. Glubley edited, London: *Royal Society of Chemistry.*

Mansfeld, F. (1987). Corrosion Mechanisms. New York: Dekker M.(pp. 102-167).

Maqsood, Ahmad Malik., Mohammad, Ali Hashim., Firdosa, Nabi., Shaeel, Ahmed Al-Thabaiti., Zaheer, Khan (2011). Anti-Corrosion Ability of Surfactants*: A Review International Journal Electrochemical. Science* 6, 1927-1948.

McCafferty, E. (2010). *Introduction to Corrosion Science*. 119-168. ISBN 978-1-4419-0454-6, Springer, New York, 167-169

Mc Graw, I.J., Rabe,T, Sparg, S.G., Jager, A.K., Eloff, J.N., Van, S.J. (2011). An Investigation on the Biological Activity of Combretum Species. *Journal of Ethnopharmacology*, 42, 131- 142.

Millennium Seed Bank Project, MSBP(2008). Seed leaflet No 129 *Combretum Micranthum G.Don*. pp.1 -10.

Miller, I., and Freund, J.E. (2001). *Probability and Statistics for Engineers*. Prentice Hall Publisher, India.

Mohammed, R.A., Abdulwahab, M., Madugu, I.A., Gaminana, J.O. and Asuke, F. (2013). Inhibitive effect by natural Cyperus esculentus L. oil on the corrosion of A356.0-type Al- Si-Mg alloy in simulated seawater environment. Journal Materials Environmental Sciences, 4(1), 93-98.

Monica, W.A., Dubey, A. and Arwind, D. (2005). Inhibiting effect of N-AccetylN,N, Ntrimethylammonium bromide on corrosion of mild steel in acidic medium. *Portugallise Electrochemical Acta*. 23(4):445-455.

Niamen, P.M., Ossonon, D., Trokourey, A., Kouassi, H.A. and Bokra, Y. (2011).Inhibitive Action of Hexa Decyl Trimethyl Ammonium Bromide (HDTAB) on Aluminium Alloy (AA3003) Corrosion in 1M HCl Acid Medium. African Journal of pure and applied chemistry, 5(9): 297-306.

Okafor, P.C., Ebiekpe, V.E., Azike, C.F., Egbung, G.E., Brisibe, E.A. and Ebenso, S.E. (2012). Inhibitory action of Artemisia annua extracts and artemisinin on the corrosion of mild steel in H_2SO_4 solution. Bulletin of Electrochemistry, 22(9): 234-242.

Oguzie, E.E. (2005). Studies of the Inhibitive Effect of Occimum Viridis Extract on the Acid Corrosion of Mild Steel. *Material Chemistry and Physics*, 99**:** 441-446.

Oguzie, E.E, Onuoha, G.N and Ejike, E.N. (2007). Effect of Gongronema Latifolium Extracton Aluminium Corrosion in Acidic and Alkaline Media. *Pigment Resin Technology,* 36(1), 44-49.

Obot, I.B., Obi-Egbedi, N.O., and Umoren, S.A. (2009). The Synergistic Inhibitive Effect of Some Quantum Chemical Parameters of 2, 3- Diaminonapthalene and Iodide Ions on the Hydrochloric Acid Corrosion of Aluminium.*Corrosion Science,* 51(2), 276-282.

Obot, I.B., Obi- Egbedi, N.O. and Eseola, A.O. (2010). Synthesis, Characterization and Corrosion Inhibition Efficiency of 2 (6- methylpyridin -2-yl) –1H- imidazo [4,5,-f] (1, 10) phenanthroline) on Mild Steel in H_2SO_4 Acid. *Arabic Journal of Chemistry,* 7, 197 – 207.

Obot, I. B, Umoren, S. A, and Obi-Egbedi, N. O. (2011). Corrosion Inhibition and Adsorption Behavior for Aluminium by Extract of Aningeria Robusta in HCl Solution: Synergistic Effect of Iodide Ions. *Journal of Materials and Environmental. Science.* 2(1), 60 – 71.

Obot, I.B., Eseola, A.O., Obi-Egbedi, N.O. (2014). Synthesis, Characterization and Corrosion Inhibition Efficiency of 2-(6-Methylpyridin-2-yl)- 1H-imidazo [4,5-1] [1,10] Phenanthroline on Mild Steel in Sulphuric Acid. *Arabian Journal of Chemistry* 7, 197-207.

Oloche, O.B, Yaro, S.A. and Okafor, E.G. (2009). Analytical Correlation Between Varying Corrosion Parameters and Corrosion Rate of Al- 4.5Cu/ 10% $ZrSiO_4$Composites in HCl Acid by Rare Earth Chloride. *Journal of alloys and compounds,* 472, 178-185.

Pourbaix, J. L. (1981). Atias of electrochemical equilibrium in aqueous solution. NACE, London.

Quraishi, M.A; Yadav, D.K; Ahmad, I. (2009). Green Approach to Corrosion Inhibition by Black Pepper Extract in HCl Acid Solution. *Open corrosion Journal,* 2, 56-60.

Rajendran, S., Jeyasundari, J., Usha, P., Selvi, J.A., Narayanasamy, B., Regis, A.P.P. and Rengan, P. (2009). Corrosion Behaviour of Aluminium in the Presence of an Aqueous Extract of Hibiscus Rosa- Sinensis. *Portugaliae Electrochimica Acta,* 27(2), 153-164.

Rajkiran, C., Urvija, G., and Tak, R.K. (2010). Corrosion Inhibition of Aluminium in Acid Media by Citrullus Colocynthis Extract. *Electrochemical Journal of Chemistry,* 8(1), 85-90.

Roberge, P.R. (1999).*Hand book of corrosion Engineering*. McGraw- Hill, 589-591.

Sangeetha, M., Rajendran, S., Sathiyabama. J., and Prabhakar. P. (2012). Eco- Friendly Extract of Banana Peel as Corrosion Inhibitor for Carbon Steel in Sea Water. *Journal of Natural. Product. Plant Resource,* 2 (5), 601- 610.

Saratha, R and Vasudha, V.G (2010). Effect of Launeae Resedifolia Aquerus Extract as Eco Friendly Inhibitor on the Corrosion of Steel in Sulphuric Acid. *E- Journal of Chemistry,* 7(3), 677-684.

Sastri, V.S. (1998). *Chemical aspects of Corrosion Inhibition, Principles and Applications.* England, John Wiley and Sons England.

Sarada, B.N., Srinivasamurthy, P.L. and Swetha (2013). Microstructural Characteristics of Strontium and Sodium Modified Al-Si-Mg Alloy. *International Journal of Innovative Research in Science, Engineering and Technology*. 2(8), 3975-3983.

Sastri, V.S. (2011). *Green Corrosion Inhibitors: Theory and Practice*. John Wiley and Sons, Inc.

Shi, X., Li, Y., Jungwirth, S., Fang, Y., Seeley, N., and Jackson, E. (2013). Identification and Laboratory Assessment of Best Practices to Protect DOT Equipment from the Corrosive Effect of Chemical Deicers, 17.

Shukla, S.K., and Ebenso, E.E. (2011). Corrosion Inhibition Adsorption Behavior and Thermodynamic Properties of Streptomycin on Mild Steel in HCl Acid Medium. *International Journal of Electrochemical Science,* 6(2011), 3277-3291.

Shreir,L.L., Jarman, R.A., and Burstein, G.T. (2000). *Corrosion Metal/Environment Reactions* 1: 4-3

Singh, A; Singh, VR, and Quraishi, M.A (2010). Inhibition Effect of Environmentally Benign Kuchla (Strychnos Nuxvomica) Seed Extract on Corrosion of Mild Steel in HCl Acid Solution. *International. Journal of Corrosion*, 2010, 1, 01 – 10.

Srinivasa , Vadayar, K., and Devaki, Rani, S. (2014). Production and Characterization of Al – 11% Si–3%Cu Alloy. *International Journal of Mechanical and Production Engineering. ISSN 2320-2090.* 2(3), 1-3.

Stephen, G.Y., Sylvester, O.A., Terso, G.T, Ungwanen, J.A. and Joseph, A.G. (2014). Thermodynamic, Kinetic and Adsorptive Parameters of Corrosion Inhibition of Aluminium using Sorghum Bicolor Leaf Extract in H_2SO_4. *International Journal of Advanced Research in Chemical Science,* Vol 1, issue 2, 38-46.

Tarvassoli-Salardini, P. (2004). Inhibition of corrosion of mild steel in aqueous solution. Ph.D. Thesis. University of Sydney.

Tosun,A. , and Ergun, M. (2006). Protection of Corrosion of Carbon Steel by Inhibitors in Chloride Containing Solution..*Journal of science,* 19(3),149-154.

Umoren, S.A., Ebenso, E.E. (2008). Studies of Anti-Corrosive Effect of Raphia Hookeri Exudate Gum and Halide Ions on the Corrosion Inhibition of Al in HCl Solutions. *Pigment Resin Technology,* 37(3), 173-182.

Umoren, S. A., Obot, I. B. and Ebenso, E. E. (2008). Corrosion inhibition of Aluminium using exudate gum from Pacchylobous edulis in the presence of halide ions in HCl. *Electronic Journal of Chemistry,* 5(2), 355-364.

Umoren, S.A., Obot, I.B. and Igwe, I.O. (2009). Synergistic Inhibition between Polyvinylpyrollidone and iodide ions on Corrosion of aluminium in HCl. *The Open Corrosion Journal*, 2, 1-7.

Uwah, I.E., Ugi, B.U., Okafor, P.C. and Ikeuba, A.I. (2013). Comparative Study of the Corrosion Inhibition and Adsorption Characteristics of Ethanol Extracts of *Andrograhis Paniculata* (King bitters) and *Vernonia amygdalina* (Bitter leaf) on Mild steel in HCl solution. International Journal of Applied Chemistry, 9(1), 73-88.

Wan Nik, W.B., Sulaiman, O., Ayob, A.F., Ahmad, M.F., and Rahman, M.M. (2012). Marine Extracts as Corrosion Inhibitor for Aluminium in Seawater Application. *International Journal of Engineering Research and Applications*, 2(1), 455-458. ISSN: 2248-9622.

Winston R R. (2007). *Uhlig's Corrosion Handbook*, 3rd Edition. John Wiley and Sons, Inc. ISBN 0-471-15777-5, 677-690.

Winston, R.R. and Uhlig, H.H. (2008). Corrosion and corrosion control: An introduction to corrosion science and engineering, (4th ed.). pp. 56-70.

Williams, R.J and Bause, D.E. (1996). *A Guide to materials Characterization and chemical Analysis*. 2nd Edition, 115, VCH Publishers, New York.

William, D. (2007).*Materials Science and Engineering: An Introduction* 7th Edition, John Wiley and Sons, Inc.

Yahya, O,Yabefa, J.A.,and Usman , B. (2012). Phytochemical Screening and Antibacterial Activity of Combretum glutinosum Extract Against Some Human Pathogens. *British journal of Pharmacology and Toxicology* 3(5), 233- 236.

Yingchao, Z.,Hongqi, Y., Hui, L., and Kai, H. (2011). Preparation and Characterization of Aluminium Pigment Coated With Silica for Corrosion Protection. *Corrosion science, 53(5), 1694-1699.*

Zhenhua, D., Shunsuke, T., Izumi, M., and Nobuyoshi, H. (2011). Applicability of Constant Dew Point Corrosion Tests for Evaluating Atmospheric Corrosion of Aluminium Alloys. *Journal of corrosion science*, 53(5), 2006-2014.

Zaki, Ahmad (2006).*Principles of Corrosion Engineering and corrosion control*. Elsevier Science and Technology Book, 187-267.

Zhang, L., Eskin, D.G., Miroux, A., and Katgerman, L. (2012). Formation of Microstructure in Al-Si Alloys Under Ultrasonic Melt Treatment. *Light metals (the minerals, metals and materials society) TMS proceedings*, 1-6

Appendices

Appendix I: Prominent Peaks Obtained From Reflectance FTIR Spectroscopy for CM

Frequency (cm^{-1})	Band Assignment
411.82	C – I
596.99	C – Br
1041.60	C = C – CH_2 – OH
2930.93	C – H
3402.54	N – H
3994.71	N – H

Appendix II: Prominent Peaks Obtained From Reflectance FTIR Spectroscopy for CG

Frequency (cm^{-1})	Band Assignment
406.99	C - I
519.83	C – Br
655.82	≡ C – H
1041.60	C = C – CH2 – OH
1452.45	C – H
1509.35	C = C
1640.51	C = O
2932.86	C – H
3402.54	N – H

Appendix III: Prominent Peaks Obtained From Reflectance FTIR Spectroscopy for FE

Frequency (cm^{-1})	Band Assignment
406.99	C – I
453.29	C – I
630.74	C – Br
1134.18	C – O
1527.67	N –N
1643.41	C
3407.37	N – H

Appendix IV:: Prominent Peaks Obtained From Reflectance FTIR Spectroscopy for FP

Frequency (cm^{-1})	Band Assignment
406.99	C – I
772.52	C – H
1091.75	C – O
1518.99	N – H
1628.94	N – H
2929.00	C – H
3393.86	O – H

Appendix V:The Chemical Compounds Identified in the Methanol Distillate of CM Leaves Extract by GC-MS Analysis

Peak	Retention time	Compound Name	Molecular Formula	Molecular Wt. (g/mol.)
1	16.398	Ethylhexyl deaconate	$C_{18}H_{36}O_2$	284
2	19.301	Tridecanoic acid, methylester	$C_{14}H_{28}O_2$	228
3	20.771	Palmitic acid	$C_{16}H_{32}O_2$	256
4	22.454	Linolelaidic acid	$C_{19}H_{34}O_2$	294
5	22.506	Methyl II- Octadecenoate	$C_{19}H_{36}O_2$	296
6	22.83	Heptacosanoic acid, Methyl Ester	$C_{28}H_{56}O_2$	424
7	23.593	Oxacyclotetra decane – 2, II-dione	$C_{14}H_{24}O_3$	240
8	23.809	Stearic acid	$C_{18}H_{36}O_2$	284
9	27.637	Decane, 2,4- dimethyl	$C_{12}H_{24}$	168
10	28.708	Vitamin E acetate	$C_{31}H_{52}O_3$	472

Appendix VI: The Chemical Compounds Identified in the Methanol Distillate of CG Leaves Extract by GC-MS Analysis

Peak	Retention time	Compound Name	Molecular Formula	Molecular Wt. (g/mol)
1	19.057	Methyl Caprinate	$C_{11}H_{22}O_2$	186
2	19.315	Metholene 2216	$C_{17}H_{34}O_2$	270
3	20.500	Ethyl Palmitate	$C_{18}H_{36}O_2$	284
4	20.807	Pentadecane Carboxylic acid	$C_{16}H_{32}O_2$	256
5	22.395	Methyl trans, trans- 9, 12-Octadecadienoic acid	$C_{19}H_{34}O_2$	294
6	22.454	Methyl Cis- 6-Octadecenoate	$C_{19}H_{36}O_2$	296
7	22.794	Eicosanoic acid, methyl ester	$C_{21}H_{42}O_2$	326
8	23.366	9-Octadecenoic acid, ethyl ester	$C_{20}H_{38}O_2$	310
9	23.716	Tridecene	$C_{13}H_{26}$	182
10	23.899	Aqua Cera	$C_{22}H_{44}O_4$	372
11	27.640	Ether, 2- ethylhexyl vinyl	$C_{10}H_{20}O$	156

Appendix VII: The Chemical Compounds Identified in the Methanol Distillate of Ficus Exasperata (FE) Leaves Extract by GC-MS Analysis

Peak	Retention time	Compound Name	Molecular Formula	Molecular Wt. (g/mol)
1	11.376	Butane 2,2 – dimethyl	$C_6 H_{14}$	86
2	13.536	1,3 – Dioxolan-z-one, 4-methyl	$C_4 H_6 O_3$	102
3	17.518	Z-4- Dodecenol	$C_{12} H_{24} O$	184
4	19.301	Methyl 4- methyl valerate	$C_7 H_{14} O_2$	130
5	20.769	Amyl Nitrite	$C_5 H_{11} NO_2$	117
6	22.452	Lineoleoyl Chloride	$C_{18} H_{31} ClO$	298
7	22.500	Methyl Petroselinate	$C_{19} H_{36} O_2$	296
8	22.838	Methyl ester of tridecanoic acid	$C_{14} H_{28} O_2$	228
9	23.610	Oleic acid	$C_{18} H_{34} O_2$	282
10	25.425	Disilane, Pentamethyl	$C_5 H_{16} Si_2$	132
11	26.713	Silane, tetramethyl	$C_4 H_{12} Si$	88
12	27.637	4- methyl- 1- decene	$C_{11} H_{22}$	154
13	27.856	1, 1, 3, 3, 5, 5, 7, 7, 9, 9, 11, 11, 13, 13- tetradecamethyl heptasi loxane	$C_{14} H_{44} 0_6 Si_7$	504
14	29.089	Cyclohexasiloxane,dode camethyl	$C_{12} H_{36} O_6 Si_6$	444

Appendix VIII: The Chemical Compounds Identified in the Methanol Distillate of Ficus Platyphylla (FP) Leaves Extract by GC-MS Analysis

Peak	Retention time	Compound Name	Molecular Formula	Molecular wt. (g/mol)
1	12.477	Phenol, 2- Propyl	$C_9 H_{12} O$	136
2	19.308	Arachidic acid methyl ester	$C_{21} H_{42} O_2$	326
3	20.780	Pelargonic acid	$C_9 H_{18} O_2$	156
4	22.519	Octadec – II- enoic acid, methyl ester	$C_{19} H_{36} O_2$	296
5	22.841	Capric acid methyl ester	$C_{11} H_{22} O_2$	186
6	23.617	Delta (Sup 9)-Cis- Oleic acid	$C_{18} H_{34} O_2$	282
7	29.811	Epoxy- linalooloxide	$C_{10} H_{18} O_3$	186

Appendix IX: Corrosion rates of Al-Si-Mg alloy in 3.5 wt.% NaCl solution in the absence and presence of CM at 30^0C (mm/yr)

Inhibitor Concntration(v/v)	1hr	2hrs	3hrs	4hrs	5hrs
Blank	0.1784	0.1035	0.0690	0.0578	0.0504
0.2	0.1518	0.0621	0.0368	0.0238	0.0168
0.4	0.1380	0.0552	0.0322	0.0204	0.0140
0.6	0.1104	0.0483	0.0276	0.0198	0.0112
0.8	0.0828	0.0345	0.0184	0.0068	0.0028
1.0	0.0966	0.0414	0.0230	0.0136	0.0084

Appendix X: Corrosion rates of Al-Si-Mg alloy in 3.5 wt.% NaCl solution in the absence and presence of CM at 50^0C (mm/yr)

Inhibitor Concentration(v/v)	1hr	2hrs	3hrs	4hrs	5hrs
Blank	0.2208	0.1173	0.0828	0.0646	0.0560
0.2	0.1932	0.0897	0.0506	0.0306	0.0224
0.4	0.1656	0.0690	0.0414	0.0238	0.0168
0.6	0.1518	0.0621	0.0322	0.0170	0.0140
0.8	0.1242	0.0483	0.0276	0.0136	0.0056
1.0	0.1380	0.0552	0.0368	0.0238	0.0188

Appendix XI:Corrosion rates of Al-Si-Mg alloy in 3.5 wt.% NaCl solution in the absence and presence of CM at 70^0C (mm/yr)

Inhibitor Concentration(v/v)	1hr	2hrs	3hrs	4hrs	5hrs
Blank	0.2484	0.1311	0.0920	0.0714	0.0616
0.2	0.2208	0.0966	0.0598	0.0374	0.0280
0.4	0.1784	0.0759	0.0414	0.0272	0.0196
0.6	0.1380	0.0621	0.0368	0.0238	0.0140
0.8	0.1104	0.0483	0.0276	0.0136	0.0056
1.0	0.1518	0.0552	0.0322	0.0224	0.0112

Appendix XII: Corrosion rates of Al-Si-Mg alloy in 3.5 wt.% NaCl solution in the absence and presence of CG at 30^0C (mm/yr)

Inhibitor Concentration(v/v)	1hr	2hrs	3hrs	4hrs	5hrs
Blank	0.1666	0.0897	0.0644	0.0476	0.0448
0.2	0.1518	0.0690	0.0276	0.0170	0.0112
0.4	0.1104	0.0552	0.0230	0.0136	0.0084
0.6	0.1242	0.0621	0.0322	0.0204	0.0140
0.8	0.1380	0.0710	0.0368	0.0238	0.0168
1.0	0.1548	0.0745	0.0414	0.0272	0.0196

Appendix XIII: Corrosion rates of Al-Si-Mg alloy in 3.5 wt.% NaCl solution in the absence and presence of CG at 50^0C (mm/yr)

Inhibitor Concentration(v/v)	1hr	2hrs	3hrs	4hrs	5hrs
Blank	0.1932	0.1104	0.0782	0.0612	0.0532
0.2	0.1666	0.0690	0.0414	0.0238	0.0168
0.4	0.1242	0.0483	0.0276	0.0136	0.0112
0.6	0.1380	0.0621	0.0322	0.0170	0.0140
0.8	0.1518	0.0670	0.0414	0.0238	0.0168
1.0	0.1653	0.0759	0.0460	0.0272	0.0196

Appendix XIV: Corrosion rates of Al-Si-Mg alloy in 3.5 wt.% NaCl solution in the absence and presence of CG at 70^0C (mm/yr)

Inhibitor Concentration(v/v)	1hr	2hrs	3hrs	4hrs	5hrs
Blank	0.2070	0.1173	0.0828	0.0612	0.0560
0.2	0.1794	0.0828	0.0460	0.0367	0.0224
0.4	0.1518	0.0621	0.0368	0.0306	0.0196
0.6	0.1666	0.0759	0.0390	0.0272	0.0234
0.8	0.1804	0.0828	0.0466	0.0340	0.0252
1.0	0.1932	0.0897	0.0552	0.0374	0.0280

Appendix XV: Corrosion rates of Al-Si-Mg alloy in 3.5 wt.% NaCl solution in the absence and presence of FE at 30^0C (mm/yr)

Inhibitor Concentration(v/v)	1hr	2hrs	3hrs	4hrs	5hrs
Blank	0.1380	0.0759	0.0552	0.0442	0.0392
0.2	0.1242	0.0552	0.0322	0.0204	0.0140
0.4	0.0966	0.0414	0.0280	0.0136	0.0084
0.6	0.1104	0.0444	0.0310	0.0170	0.0112
0.8	0.1119	0.0483	0.0340	0.0190	0.0126
1.0	0.1292	0.0512	0.0367	0.0214	0.0140

Appendix XVI: Corrosion rates of Al-Si-Mg alloy in 3.5 wt.% NaCl solution in the absence and presence of FE at 50^0C (mm/yr)

Inhibitor Concentration(v/v)	1hr	2hrs	3hrs	4hrs	5hrs
Blank	0.1518	0.0828	0.0552	0.0442	0.0364
0.2	0.1380	0.0621	0.0368	0.0272	0.0168
0.4	0.0828	0.0414	0.0230	0.0136	0.0056
0.6	0.0966	0.0476	0.0290	0.0170	0.0084
0.8	0.1104	0.0552	0.0322	0.0190	0.0112
1.0	0.1242	0.0581	0.0368	0.0238	0.0148

Appendix XVII: Corrosion rates of Al-Si-Mg alloy in 3.5 wt.% NaCl solution in the absence and presence of FE at 70^0C (mm/yr)

Inhibitor Concentration(v/v)	1hr	2hrs	3hrs	4hrs	5hrs
Blank	0.1490	0.0759	0.0552	0.0442	0.0392
0.2	0.1380	0.0621	0.0368	0.0272	0.0196
0.4	0.1104	0.0414	0.0230	0.0136	0.0112
0.6	0.1242	0.0483	0.0322	0.0204	0.0140
0.8	0.1280	0.0542	0.0378	0.0238	0.0168
1.0	0.1110	0.0653	0.0414	0.0272	0.0196

Appendix XVIII: Corrosion rates of Al-Si-Mg alloy in 3.5 wt.% NaCl solution in the absence and presence of FP at 30^0C (mm/yr)

Inhibitor Concentration(v/v)	1hr	2hrs	3hrs	4hrs	5hrs
Blank	0.1794	0.0916	0.0736	0.0578	0.0532
0.2	0.1380	0.0621	0.0368	0.0238	0.0168
0.4	0.0966	0.0414	0.0276	0.0170	0.0112
0.6	0.0690	0.0276	0.0184	0.0102	0.0086
0.8	0.552	0.0207	0.0138	0.0068	0.0056
1.0	0.0414	0.0138	0.0092	0.0034	0.0028

Appendix XIX: Corrosion rates of Al-Si-Mg alloy in 3.5 wt.% NaCl solution in the absence and presence of FP at 50^0C (mm/yr)

Inhibitor Concentration(v/v)	1hr	2hrs	3hrs	4hrs	5hrs
Blank	0.1932	0.1035	0.0736	0.0612	0.0532
0.2	0.1794	0.0828	0.0506	0.0386	0.0224
0.4	0.1666	0.0759	0.0460	0.0306	0.0196
0.6	0.1380	0.0621	0.0368	0.0238	0.0140
0.8	0.1242	0.0552	0.0322	0.0204	0.0112
1.0	0.0828	0.0345	0.0184	0.0102	0.0056

Appendix XX: Corrosion rates of Al-Si-Mg alloy in 3.5 wt.% NaCl solution in the absence and presence of FP at 70^0C (mm/yr)

Inhibitor Concentration(v/v)	1hr	2hrs	3hrs	4hrs	5hrs
Blank	0.2070	0.1104	0.0782	0.0612	0.0560
0.2	0.1932	0.0897	0.0552	0.0394	0.0280
0.4	0.1856	0.0859	0.0501	0.0366	0.0224
0.6	0.1518	0.0690	0.0468	0.0268	0.0168
0.8	0.1382	0.0598	0.0406	0.0230	0.0142
1.0	0.1202	0.0376	0.0251	0.0108	0.0068

Appendix XXI: Corrosion rates of Al-Si-Mg alloy in 3.5 wt.% NaCl solution in the absence and presence of Sodium Chromate at 30^0C (mm/yr)

Inhibitor Concentration(v/v)	1hr	2hrs	3hrs	4hrs	5hrs
Blank	0.1242	0.0621	0.0460	0.0374	0.0336
0.2	0.1104	0.0414	0.0230	0.0136	0.0084
0.4	0.0690	0.0300	0.0198	0.0102	0.0066
0.6	0.0552	0.0276	0.0138	0.0068	0.0041
0.8	0.0414	0.0138	0.0092	0.0054	0.0030
1.0	0.0138	0.0069	0.0046	0.0034	0.0018

Appendix XXII: Corrosion rates of Al-Si-Mg alloy in 3.5 wt.% NaCl solution in the absence and presence of Sodium Chromate at 50^0C (mm/yr)

Inhibitor Concentration(v/v)	1hr	2hrs	3hrs	4hrs	5hrs
Blank	0.1380	0.0759	0.0506	0.0408	0.0364
0.2	0.1280	0.0621	0.0368	0.0270	0.0220
0.4	0.1242	0.0552	0.0322	0.0204	0.0168
0.6	0.1104	0.0483	0.0276	0.0204	0.0140
0.8	0.0828	0.0414	0.0230	0.0136	0.0112
1.0	0.0690	0.0276	0.0138	0.0068	0.0056

Appendix XXIII: Corrosion rates of Al-Si-Mg alloy in 3.5 wt.% NaCl solution in the absence and presence of Sodium Chromate at 70^0C (mm/yr)

Inhibitor Concentration(v/v)	1hr	2hrs	3hrs	4hrs	5hrs
Blank	0.1518	0.0759	0.0552	0.0408	0.0360
0.2	0.1430	0.0652	0.0422	0.0300	0.0240
0.4	0.1380	0.0583	0.0376	0.0250	0.0200
0.6	0.1250	0.0510	0.0310	0.0220	0.0180
0.8	0.1042	0.0445	0.0294	0.0170	0.0140
1.0	0.0828	0.0295	0.0172	0.0116	0.0066

Appendix XXIV: Corrosion rates of Al-Si-Mg alloy in 3.5 wt.% NaCl solution in the absence and presence of CM with CG at 30^0C (mm/yr)

inhibitor Concentration (v/v)	1hr	2hrs	3hrs	4hrs	5hrs
Blank	0.1104	0.0621	0.0414	0.0340	0.0260
0.2	0.0828	0.0345	0.0184	0.0152	0.0084
0.4	0.0690	0.0276	0.0138	0.0108	0.0056
0.6	0.0552	0.0207	0.0092	0.0068	0.0038
0.8	0.0276	0.0138	0.0062	0.0044	0.0028
1.0	0.0138	0.0069	0.0046	0.0034	0.0018

Appendix XXV: Corrosion rates of Al-Si-Mg alloy in 3.5 wt.% NaCl solution in the absence and presence of CM with FP at 30^0C (mm/yr)

Inhibitor Concentration (v/v)	1hr	2hrs	3hrs	4hrs	5hrs
Blank	0.0690	0.0414	0.0322	0.0272	0.0260
0.2	0.0552	0.0276	0.0138	0.0130	0.0110
0.4	0.0414	0.0207	0.0092	0.0085	0.0070
0.6	0.0276	0.0138	0.0056	0.0064	0.0040
0.8	0.0138	0.0069	0.0040	0.0035	0.0025
1.0	0.0113	0.0042	0.0025	0.0024	0.0018

Appendix XXVI: Corrosion rates of Al-Si-Mg alloy in 3.5 wt.% NaCl solution in the absence and presence of CG with FE at 30^0C (mm/yr)

Inhibitor Concentration (v/v)	1hr	2hrs	3hrs	4hrs	5hrs
Blank	0.0966	0.0552	0.0414	0.0340	0.0308
0.2	0.0690	0.0276	0.0138	0.0102	0.0056
0.4	0.0552	0.0207	0.0092	0.0068	0.0041
0.6	0.0414	0.0138	0.0072	0.0050	0.0032
0.8	0.0276	0.0069	0.0040	0.0030	0.0022
1.0	0.0138	0.0051	0.0029	0.0019	0.0015

Appendix XXVII: Corrosion rates of Al-Si-Mg alloy in 3.5 wt.% NaCl solution in the absence and presence of FP with FE at 30^0C (mm/yr)

Inhibitor Concentration(v/v)	1hr	2hrs	3hrs	4hrs	5hrs
Blank	0.0828	0.0483	0.0363	0.0306	0.0280
0.2	0.0690	0.0276	0.0138	0.0112	0.0100
0.4	0.0552	0.0207	0.0092	0.0071	0.0055
0.6	0.0414	0.0138	0.0076	0.0054	0.0038
0.8	0.0276	0.0115	0.0050	0.0039	0.0026
1.0	0.0138	0.0069	0.0046	0.0024	0.0016

Appendix XXVIII: Corrosion rates of Al-Si-Mg alloy in 3.5 wt.% NaCl solution in the absence and presence of Extract and Surfactant at 30^0C (mm/yr)

Inhibitor Concentration (v/v)	CM + MEA	CG + TEA	FP + MEA	FE + TEA
Blank	0.2076	0.2076	0.2076	0.2076
0.2	0.1092	0.0983	0.1311	0.0874
0.4	0.0874	0.0874	0.1092	0.0765
0.6	0.0655	0.0655	0.0983	0.0655
0.8	0.0765	0.0874	0.0765	0.0437
1.0	0.0983	0.0983	0.0546	0.0328

Appendix XXIX: Inhibition Efficiency of CM at 30^0C

Inhibitor Concentration(v/v)	1hr	2hrs	3hrs	4hrs	5hrs
0.2	14.91	40.00	46.67	58.82	66.67
0.4	22.65	46.67	53.33	64.71	72.22
0.6	38.12	53.33	60.00	65.74	77.78
0.8	53.59	66.67	73.33	88.24	94.44
1.0	48.85	60.00	66.67	70.93	83.33

Appendix XXX: Inhibition Efficiency of CM at 50^0C

Inhibitor Concentration(v/v)	1hr	2hrs	3hrs	4hrs	5hrs
0.2	12.50	23.53	38.89	52.63	60.00
0.4	26.09	41.18	50.00	63.16	70.00
0.6	31.25	47.06	61.11	73.68	75.00
0.8	43.75	58.82	66.67	78.95	90.00
1.0	37.50	52.94	55.56	63.16	66.43

Appendix XXXI: Inhibition Efficiency of CM at 70 ^{0}C

Inhibitor Concentration(v/v)	1hr	2hrs	3hrs	4hrs	5hrs
0.2	11.11	26.32	35.00	47.62	54.55
0.4	28.18	42.11	55.00	61.90	68.18
0.6	44.44	52.63	60.00	66.67	77.27
0.8	55.56	63.16	70.00	80.95	90.91
1.0	38.89	57.89	65.00	71.43	81.82

Appendix XXXII: Inhibition Efficiency of CG at 30^0C

Inhibitor Concentration(v/v)	1hr	2hrs	3hrs	4hrs	5hrs
0.2	19.88	23.08	57.14	64.29	75.00
0.4	33.73	38.46	64.29	71.43	81.25
0.6	25.45	30.77	50.00	57.14	68.75
0.8	17.17	20.85	42.86	50.00	62.50
1.0	12.84	16.95	35.71	42.86	56.25

Appendix XXXIII: Inhibition Efficiency of CG at 50^0C

Inhibitor Concentration(v/v)	1hr	2hrs	3hrs	4hrs	5hrs
0.2	13.77	37.50	47.06	61.11	68.42
0.4	35.71	56.25	64.71	77.78	78.95
0.6	28.57	43.75	58.82	72.22	73.68
0.8	21.43	39.31	47.06	61.11	66.54
1.0	14.44	31.25	41.18	55.56	63.16

Appendix XXXIV: Inhibition Efficiency of CG at 70^0C

Inhibitor Concentration(v/v)	1hr	2hrs	3hrs	4hrs	5hrs
0.2	13.33	29.41	44.44	50.00	60.00
0.4	26.67	47.06	55.56	66.67	65.00
0.6	19.52	35.29	52.90	55.56	58.21
0.8	12.85	29.41	43.72	44.44	55.00
1.0	11.89	23.53	33.33	38.89	50.00

Appendix XXXV: Inhibition Efficiency of FE at 30^0C

Inhibitor Concentration(v/v)	1hr	2hrs	3hrs	4hrs	5hrs
0.2	10.00	27.27	41.67	53.85	64.29
0.4	30.00	45.45	49.28	69.23	78.57
0.6	20.00	41.50	43.84	61.54	71.43
0.8	18.91	36.36	38.41	57.01	67.86
1.0	6.38	32.54	33.51	51.58	64.29

Appendix XXXVI: Inhibition Efficiency of FE at 50^0C

Inhibitor Concentration(v/v)	1hr	2hrs	3hrs	4hrs	5hrs
0.2	20.15	25.00	33.33	38.46	53.85
0.4	45.45	50.00	58.33	69.23	84.62
0.6	36.36	42.51	47.46	61.54	76.92
0.8	27.27	33.33	41.67	57.01	69.23
1.0	18.18	29.83	33.33	46.15	59.34

Appendix XXXVII: Inhibition Efficiency of FE at 70^0C

Inhibitor Concentration(v/v)	1hr	2hrs	3hrs	4hrs	5hrs
0.2	17.38	18.18	33.33	38.46	50.00
0.4	25.91	45.45	58.33	69.23	71.43
0.6	16.64	36.36	41.67	53.85	64.29
0.8	14.09	28.59	31.52	46.15	57.14
1.0	13.37	13.97	25.00	38.46	50.00

Appendix XXXVIII: Inhibition Efficiency of FP at 30^0C

Inhibitor Concentration(v/v)	1hr	2hrs	3hrs	4hrs	5hrs
0.2	23.08	32.21	50.00	58.82	68.42
0.4	46.15	54.80	62.50	70.59	78.95
0.6	61.54	69.87	75.00	82.35	83.83
0.8	69.23	77.40	81.25	88.24	89.47
1.0	76.92	84.93	87.50	94.12	94.74

Appendix XXXIX: Inhibition Efficiency of FP at 50 ^{0}C

Inhibitor Concentration(v/v)	1hr	2hrs	3hrs	4hrs	5hrs
0.2	12.24	20.00	31.25	36.93	57.89
0.4	13.77	26.67	37.50	50.00	63.16
0.6	28.57	40.00	50.00	61.11	73.68
0.8	35.71	46.67	56.26	66.67	78.95
1.0	57.14	66.67	75.00	83.33	89.47

Appendix XL: Inhibition Efficiency of FP at 70^0C

Inhibitor Concentration(v/v)	1hr	2hrs	3hrs	4hrs	5hrs
0.2	10.02	18.75	29.41	35.62	50.00
0.4	10.34	22.19	35.93	40.19	60.00
0.6	26.67	37.50	40.15	56.21	70.00
0.8	33.24	45.83	48.08	62.42	74.00
1.0	41.93	65.94	67.90	82.35	87.86

Appendix XLI: Inhibition Efficiency of Sodium Chromate at 30^0C

Inhibitor Concentration(v/v)	1hr	2hrs	3hrs	4hrs	5hrs
0.2	11.11	33.33	50.00	63.64	75.00
0.4	44.44	51.69	56.96	72.73	80.36
0.6	55.56	55.56	70.00	81.82	87.80
0.8	66.67	77.78	80.00	85.56	91.07
1.0	88.89	88.89	90.00	90.91	94.64

Appendix XLII: Inhibition Efficiency of Sodium Chromate.at 50^0C

Inhibitor Concentration(v/v)	1hr	2hrs	3hrs	4hrs	5hrs
0.2	10.00	18.18	27.27	33.82	39.56
0.4	10.00	27.27	36.36	41.67	53.85
0.6	20.00	36.37	45.45	50.00	61.54
0.8	40.00	45.46	54.55	66.67	69.23
1.0	50.00	63.64	72.73	83.33	84.62

Appendix XLIII: Inhibition Efficiency of Sodium Chromate at 70^0C

Inhibitor Concentration(v/v)	1hr	2hrs	3hrs	4hrs	5hrs
0.2	13.35	14.10	23.55	34.07	34.07
0.4	18.00	23.19	31.88	45.05	45.05
0.6	17.65	32.81	43.84	50.55	50.55
0.8	31.36	41.37	46.08	61.54	61.54
1.0	45.45	61.13	68.84	71.57	81.87

Appendix XLIV: Inhibition Efficiency of CM with CG at 30^0C

Inhibitor Concentration(v/v)	1hr	2hrs	3hrs	4hrs	5hrs
0.2	25.00	44.44	55.56	55.88	67.69
0.4	37.50	55.56	66.67	68.24	78.46
0.6	50.00	66.67	77.78	80.00	85.38
0.8	75.00	77.78	85.02	87.06	89.23
1.0	87.50	88.89	88.89	90.00	93.08

Appendix XLV: Inhibition Efficiency of CM with FP at 30^0C

Inhibitor Concentration(v/v)	1hr	2hrs	3hrs	4hrs	5hrs
0.2	20.00	33.33	52.21	57.14	57.69
0.4	40.00	50.00	68.75	71.43	73.08
0.6	60.00	66.67	76.47	82.61	84.62
0.8	80.00	83.33	87.13	87.58	90.38
1.0	83.62	89.86	91.18	92.24	93.08

Appendix XLVI: Inhibition Efficiency of CG with FE at 30 ^{0}C

Inhibitor Concentration(v/v)	1hr	2hrs	3hrs	4hrs	5hrs
0.2	28.57	50.00	66.67	70.00	81.82
0.4	42.86	62.50	77.78	80.00	86.69
0.6	57.14	75.00	82.61	85.29	89.61
0.8	71.43	87.50	90.34	91.18	92.86
1.0	85.71	90.76	92.99	94.41	95.13

Appendix XLVII: Inhibition Efficiency of FE with FP at 30 ^{0}C

Inhibitor Concentration(v/v)	1hr	2hrs	3hrs	4hrs	5hrs
0.2	16.67	42.86	62.50	63.40	64.29
0.4	33.33	57.14	75.00	76.80	80.36
0.6	50.00	71.43	79.35	82.35	86.43
0.8	66.67	76.19	86.41	87.25	90.71
1.0	83.33	85.71	87.50	92.16	94.29

Appendix XLVIII: Inhibition Efficiency of Extracts with surfactants at 30 ^{0}C

Inhibitor Concentration(v/v)	CM + MEA	CG + TEA	FP + MEA	FE + TEA
0.2	47.40	27.72	36.85	57.90
0.4	57.90	57.90	47.40	63.15
0.6	64.45	64.45	52.65	64.45
0.8	63.15	58.00	63.15	78.95
1.0	27.72	27.72	73.70	84.20

Appendix XLIX: Comparing Maximum Inhibition Efficiency (IE %) and Maximum Concentrations of all the Extracts, Sodium Chromate, Synergy at 30 ^{0}C

Plant Extracts/ IC	Inhibition Efficiency (I.E%) Exposure Time (Hours)				
	1hr	2hrs	3hrs	4hrs	5hrs
0.8 v/v CM	53.59	66.67	73.33	88.24	94.44
0.4 v/v CG	33.73	38.46	64.29	71.43	81.25
0.4 v/v FE	30.00	45.45	49.28	69.23	78.57
1.0 v/v FP	76.72	84.93	87.50	94.12	94.74
1.0v/v sodium Chromate	88.89	88.89	90.00	90.91	94.64
1.0 v/v CM with C.G	87.50	88.89	88.89	90.00	93.08
1.0 v/v CM with FP	83.62	89.86	91.18	92.24	93.08
1.0 v/v CG with FE	85.71	90.76	92.99	94.41	95.13
1.0 v/v FE with FP	83.33	85.71	87.50	92.16	94.29

Appendix L: Comparing the Variation of Inhibition Efficiencies of all Extracts with Inhibitor Concentration after 5 hrs of exposure at different temperatures.

Plant Extract / I.C (v/v)	30 ^{0}C	50 ^{0}C	70 ^{0}C
CM			
0.2	66.67	60.00	54.55
0.4	72.22	70.00	68.18
0.6	77.78	75.00	72.27
0.8	94.44	90.00	90.91
1.0	83.33	66.43	81.82
CG			
0.2	75.00	68.42	60.00
0.4	81.25	78.95	65.00
0.6	68.75	73.68	58.21
0.8	62.50	66.54	55.00
1.0	56.25	63.16	50.00
FE			
0.2	64.29	53.85	50.00
0.4	78.57	84.62	71.43
0.6	71.43	76.92	64.29
0.8	67.86	69.23	57.14
1.0	64.29	59.34	50.00
FP			
0.2	68.42	57.89	50.00
0.4	78.95	63.16	60.00
0.6	83.83	73.68	70.00
0.8	89.47	78.95	74.00
1.0	94.74	89.47	87.86
Sodium Chromate			
0.2	75.00	39.56	34.07
0.4	80.36	53.85	45.05
.6	87.80	61.54	50.55
0.8	91.07	69.23	61.54
1.0	94.64	84.62	81.87

Appendix LI: Comparison of the Actual Value with the Predicted Value for Al-Si- Mg alloy Using CM

Standard Order	Temp. (^oC)	Inhibitor (% v/v)	Time (Min.)	Corrosion rates (mm/yr) Actual value	Predicted value	Residual
1	-1	-1	-1	0.18	0.19	-0.011
2	+1	-1	-1	0.083	0.072	0.011
3	-1	+1	-1	0.050	0.052	-2.100×10^{-3}
4	+1	+1	-1	2.800×10^{-3}	7.000×10^{-3}	2.100×10^{-3}
5	-1	-1	+1	0.25	0.24	0.011
6	+1	-1	+1	0.11	0,12	-0.011
7	-1	+1	+1	0.062	0.060	2.100×10^{-3}
8	+1	+1	+1	5.600×10^{-3}	7.700×10^{-3}	-2.100×10^{-3}

Appendix LII: Comparison of the Actual Value with the Predicted Value for Al-Si- Mg alloy Using CG

Standard Order	Temp. (^oC)	Inhibitor (% v/v)	Time (Min.)	Corrosion rates (mm/yr) Actual value	Predicted value	Residual
1	-1	-1	-1	0.17	0.17	5000×10^{-5}
2	+1	-1	-1	0.14	0.14	-5.000×10^{-5}
3	-1	+1	-1	0.045	0.045	-2.500×10^{-4}
4	+1	+1	-1	0.017	0.017	2.500×10^{-4}
5	-1	-1	+1	0.21	0.21	-9.500×10^{-4}
6	+1	-1	+1	0.18	0.81	9.500×10^{-4}
7	-1	+1	+1	0.056	0.055	1.150×10^{-3}
8	+1	+1	+1	0.025	0.026	-1.150×10^{-3}

Appendix LIII: Comparison of the Actual Value with the Predicted Value for Al-Si- Mg alloy Using FE

Standard Order	Temp. (^oC)	Inhibitor (% v/v)	Time (Min.)	Corrosion rates (mm/yr) Actual value	Predicted value	Residual
1	-1	-1	-1	0.14	0.13	3.772×10^{-3}
2	+1	-1	-1	0.11	0.12	-3.773×10^{-3}
3	-1	+1	-1	0.039	0.035	3.772×10^{-3}
4	+1	+1	-1	0.013	0.016	-3.773×10^{-3}
5	-1	-1	+1	0.15	0.15	1.257×10^{-3}
6	+1	-1	+1	0.13	0,13	-1.25×10^{-3}
7	-1	+1	+1	0.039	0.038	1.258×10^{-3}
8	+1	+1	+1	0.17	0.17	-1.258×10^{-3}

Appendix LIV: Comparison of the Actual Value with the Predicted Value for Al-Si- Mg alloy Using FP

Standard Order	Temp. (^oC)	Inhibitor (% v/v)	Time (Min.)	Corrosion rates (mm/yr) Actual value	Predicted value	Residual
1	-1	-1	-1	0.18	0.17	0.013
2	+1	-1	-1	0.041	0.054	-0.013
3	-1	+1	-1	0.053	0.053	-2.000×10^{-4}
4	+1	+1	-1	2.800 x10 -3	2.600 x10 -3	2.000×10^{-4}
5	-1	-1	+1	0.21	0.22	-0.013
6	+1	-1	+1	0.12	0,11	0.013
7	-1	+1	+1	0.058	0.058	2.000×10^{-4}
8	+1	+1	+1	6.800 x10 -3	7.000 x 10 -3	-2.000×10^{-4}

Appendix LV: Comparison of the Actual Value with the Predicted Value for Al-Si- Mg alloy Using Sodium Chromate as standard inhibitor

Standard Order	Temp. (^oC)	Inhibitor (% v/v)	Time (Min.)	Corrosion rates (mm/yr) Actual value	Predicted value	Residual
1	-1	-1	-1	0.12	0.11	0.010
2	+1	-1	-1	0.014	0.024	-0.010
3	-1	+1	-1	0.034	0.033	6.000×10^{-4}
4	+1	+1	-1	1.800×10^{-3}	2.400×10^{-3}	-6.000×10^{-4}
5	-1	-1	+1	0.15	0.16	-0.010
6	+1	-1	+1	0.083	0.072	0.010
7	-1	+1	+1	0.036	0.037	-6.000×10^{-4}
8	+1	+1	+1	6.600×10^{-3}	6.000×10^{-3}	6.000×10^{-4}